Observer-based Fault Detection in Nonlinear Systems

Von der Fakultät für Ingenieurwissenschaften der
Universität Duisburg-Essen
Abteilung Elektrotechnik und Informationstechnik
zur Erlangung des akademischen Grades eines

Doktor-Ingenieurs (Dr.-Ing.)

genehmigte Dissertation

von

Abdul Qayyum Khan

aus

Mardan, I. R. Pakistan

1. Gutachter: Prof. Dr.-Ing. Steven X. Ding
2. Gutachter: Prof. Dr. Dominique Sauter

Tag der mündlichen Prüfung: December 13, 2010

Acknowledge

This work is carried out during my stay at the Institute of Automatic Control and Complex Systems (AKS), University of Duisburg-Essen for acquiring my Ph.D degree under the joint grant of Higher Education Commission (HEC) of Pakistan and German Academic Exchange Program (DAAD) Germany.

Besides every doctoral thesis lie years of hard work. Looking back over the last three and half years, I can see many people who have given me support and encouragement during this period. It is, therefore, my pleasure to thank all of them.

First and foremost, I would like to express my deepest gratitude to my thesis supervisor Prof. Dr.-Ing. Steven X. Ding. His unique view of fault detection theory and mathematical discipline taught me to see nonlinear fault detection problems from a new perspective that enhanced my understanding of what constitutes an acceptable solution for certain fundamental issues in nonlinear fault detection. I can never thank him enough for giving me the freedom to choose the theoretical fields of my interest and helping me to pursue my goals. I have always valued his advice greatly. With out his immense help and cooperation, it was very difficult to achieve this very important milestone of my professional career. His behavior as supervisor and as colleague was outstanding. I am also greatly indebted to Prof. Dr. Dominique Sauter for his interest in my work. His valuable suggestions and constructive remarks added to the quality of this thesis.

I would like to thank my friends and groupmates Dr. Muhammad Abid and M.Sc. Wei Chen for their support and long hour discussion on the basic as well as advanced concepts on nonlinear observers and fault diagnosis. I am also greatly obliged to my senior colleagues Dr.-Ing. Ibrahim Al-Salami who not only helped me in my research but also in solving social problems in my initial days in Duisburg, and Dr. Y. Q. Wang who helped me to understand basic concepts of fault diagnosis theory during the beginning of my research. Many thanks to all of my colleagues at AKS for creating an inspiring, conducive, and friendly atmosphere for research.

I would like to appreciate the great efforts and support provided by my wife and kids. Staying away from family for such a long period is not an easy job, but many thanks to my wife and kids who not only gave me this opportunity but also encouraged me to achieve my goals. I am also grateful to my parents for their ever increasing encouragement throughout my career.

Finally, I wish to acknowledge Higher Education Commission (HEC) of Pakistan and German Academic Exchange Program (DAAD) Germany for providing me financial support to carry out this research.

Abdul Qayyum Khan
Duisburg, December 2010

To my Parents, Wife
&
Maria, Iqra and M. Saad (Children)

Contents

List of Symbols x

Abstract xiii

1 Introduction 1
- 1.1 Motivation . . . 1
- 1.2 Objectives . . . 3
- 1.3 Thesis outline and contributions . . . 5

2 Review of fault detection techniques 8
- 2.1 Basic concepts of faults, disturbances, and fault diagnosis technique . . . 8
- 2.2 Desirable features of an FD scheme . . . 9
- 2.3 Classification of FD techniques . . . 9
  - 2.3.1 Hardware redundancy based FD . . . 9
  - 2.3.2 Plausibility test . . . 10
  - 2.3.3 Signal-based FD . . . 10
  - 2.3.4 Model-based FD . . . 11
- 2.4 Comparison of FD schemes . . . 16
- 2.5 FD in nonlinear systems . . . 16
  - 2.5.1 Nonlinear observer-based residual generation schemes . . . 17
- 2.6 Residual evaluation and threshold setting . . . 20
- 2.7 Summary . . . 21

3 Nonlinear systems, unknown inputs, and faults representation 22
- 3.1 State-space representation of nonlinear systems . . . 22
  - 3.1.1 Lipschitz equivalent model of nonlinear systems . . . 23
- 3.2 Representation of disturbances and uncertainties . . . 25
- 3.3 Representation of faults in nonlinear systems . . . 27
  - 3.3.1 Types of faults . . . 27
- 3.4 An example: A nonlinear three-tank system subject to faults and disturbances 31
  - 3.4.1 Description of faults and disturbances . . . 33
- 3.5 Summary . . . 33

4 Optimal residual generation 34
- 4.1 Problem formulation . . . 36
- 4.2 Finite-horizon FDF . . . 39
  - 4.2.1 FDF design based on $\mathscr{H}_-$–index (HminNLFDF) . . . 39
  - 4.2.2 FDF design based on $\mathscr{H}_\infty$-norm (HinfNLFDF) . . . 42

4.2.3 FDF design based on the mixed $\mathscr{H}_-/\mathscr{H}_\infty-$ optimization 46
4.2.4 A discrete-time LTI case 47
4.3 Infinite-horizon FDF 48
4.3.1 FDF design based on $\mathscr{H}_-$–index 49
4.3.2 FDF design based on $\mathscr{H}_\infty$-norm 49
4.3.3 FDF design based on the mixed $\mathscr{H}_-/\mathscr{H}_\infty$–optimization 50
4.3.4 A discrete-time LTI case 51
4.4 A design example 52
4.4.1 Computation of parameters for $\mathscr{H}_-$–FDF 54
4.4.2 Computation of parameters for $\mathscr{H}_\infty$–FDF 54
4.4.3 Computation of parameters for $\mathscr{H}_-/\mathscr{H}_\infty$–FDF 55
4.5 Summary 56

5 Optimal residual generation for Lipschitz systems 57
5.1 Discrete-time FDF 58
5.1.1 Preliminaries and Problem formulation 58
5.1.2 Design of FDF based on $\mathscr{H}_-/\mathscr{H}_\infty-$ optimization 59
5.2 Continuous-time FDF 64
5.2.1 Problem formulation 64
5.2.2 Design of FDF based on $\mathscr{H}_-/\mathscr{H}_\infty-$ optimization 66
5.3 A design example 68
5.4 Summary 69

6 Threshold computation for Lipschitz nonlinear systems 70
6.1 Evaluation functions 73
6.2 Constant threshold for discrete-time case 75
6.2.1 Problem formulation 75
6.2.2 Computation of $J_{th,RMS,2}$ 77
6.2.3 Computation of $J_{th,Peak,Peak}$ 79
6.2.4 Computation of $J_{th,Peak,2}$ 82
6.2.5 A design example 85
6.3 Constant threshold for continuous-time case 88
6.3.1 Problem formulation 88
6.3.2 Computation of $J_{th,RMS,2}$ 89
6.3.3 Computation of $J_{th,Peak,Peak}$ 90
6.3.4 Computation of $J_{th,Peak,2}$ 91
6.3.5 A design example 92
6.4 Adaptive threshold generation 93
6.4.1 A design example 96
6.5 Dynamic threshold generation for discrete-time case 96
6.5.1 Notations and preliminaries 98
6.5.2 Problem formulation 99
6.5.3 Computation of dynamic threshold 99
6.5.4 A design example 103
6.6 Dynamic threshold for continuous-time case 104

6.7 A comparison . . . 106
6.8 Summary . . . 107

7 Application to benchmark problems 108
7.1 Three-tank system . . . 108
7.1.1 Fault detection for three-tank system . . . 110
7.1.2 Simulation results and discussion . . . 113
7.2 Inverted pendulum control system . . . 116
7.2.1 Nonlinear model . . . 119
7.2.2 Simulation results and discussion . . . 122
7.3 Summary . . . 124

8 Conclusions and recommendations 127
8.1 Conclusions . . . 127
8.2 Future directions . . . 130

A Important mathematical tools 132
A.1 Implicit function theorem . . . 132
A.2 Two-player, zero-sum differential game . . . 132
A.3 Some useful Lemmas . . . 132

B Proofs 134
B.1 Proof of Theorem 6.3.1 . . . 134
B.2 Proof of Theorem 6.3.2 . . . 136
B.3 Proof of Theorem 6.3.3 . . . 136
B.4 Proof of Theorem 6.6.1 . . . 137

C Technical data for benchmark systems 139
C.1 Parameters of the three-tank system (DTS200) . . . 139
C.2 Parameters of the inverted pendulum control system (LIP100) . . . 139

Bibliography 140

List of Figures

2.1 Schematic description of the hardware redundancy scheme [1] 10
2.2 Schematic depiction of the plausibility test scheme 10
2.3 Schematic description of signal-based FD scheme 11
2.4 Schematic description of model-based FD scheme 12
2.5 Schematic description of parity space approach 13
2.6 Schematic description of observer-based residual generation 14
2.7 Schematic description of parameter identification scheme [1] 15
2.8 Residual evaluation scheme 20

3.1 Graphical depiction of common types of actuator faults 28
3.2 Graphical view of different sensor faults 29
3.3 Graphical view of faults based on their time-domain representation 30
3.4 Three-tank system (DTS 200) 31

4.1 Schematic description of optimal residual generation scheme 35
4.2 Residual signal with $f_k = 0.2$ at $k = 100[s]$ 54
4.3 Residual signal with $f_k = 0.2$ at $k = 100[s]$ 55
4.4 Residual signal with $f_k = 0.2$ at $k = 100[s]$ 56

5.1 Evaluated residual with f = 0.2 69

6.1 Schematic depiction of a complete FD scheme 71
6.2 Comparison of constant and variable threshold 72
6.3 Evaluated residual (RMS) and threshold $J_{th,RMS,2}$ 87
6.4 Evaluated residual(Peak) and thresholds $J_{th,Peak,Peak}$,$J_{th,Peak,2}$ 87
6.5 Evaluated residual(RMS) and thresholds $J_{th,RMS,2}$ 94
6.6 Evaluated residual(Peak) and thresholds $J_{th,Peak,Peak}$,$J_{th,Peak,2}$ 94
6.7 Generated sensor fault 96
6.8 Adaptive threshold using RMS framework 97
6.9 Adaptive threshold using Peak-to-Peak framework 97
6.10 Adaptive threshold using Peak-to-2 framework 98
6.11 Detection of sensor fault using dynamic threshold framework 105

7.1 Three-tank system 109
7.2 Open Loop FD System 114
7.3 Fault in the water level sensor of Tank 1 115
7.4 Fault in the water level sensor of Tank 2 115
7.5 Fault in the incoming water flows in Pump 1 116

7.6 Fault in the incoming water flows in Pump 2 117
7.7 Leakage detection in Tank 1 under open loop FD 117
7.8 Leakage detection in Tank 2 under open loop FD 117
7.9 The inverted pendulum: LIP100 118
7.10 Closed loop FD for LIP100 123
7.11 Detection of offset of magnitude 5 V in actuator 124
7.12 Detection of fault in position sensor of the cart 125
7.13 Detection of fault in angle sensor of the pendulum 125
7.14 Detection of fault in velocity sensor of the cart 126

List of Symbols

Abbreviations

Abbreviation	Meaning
FD	Fault detection
FDI	Fault detection and isolation
FDF	Fault detection filter
LMI	Linear matrix inequality
HJIE	Hamilton-Jacobi-Isaac's equation
HJI	Hamilton-Jacobi inequality
HOT	Higher order terms
LTI	Linear time invariant
RMS	Root mean square

General notations

Symbols	Description
$a(\cdot)$	a vector system function
c	an output function
A	a system matrix
C	an output matrix
$B(\cdot)$ & $D(\cdot)$	a distribution matrix for input vectors
B & D	a distribution matrix for input vectors
$E_w(\cdot)$ & $F_w(\cdot)$	a distribution matrix for the vector unknown inputs
E_w & F_w	a distribution matrix for the vector unknown inputs
$E_f(\cdot)$ & $F_f(\cdot)$	a distribution matrix for the vector faults
E_f & F_f	a distribution matrix for the vector faults
$L(\cdot)$	the filter gain which is a function of some arguments
L	filter gain
V	post-filter gain
x	state-vector
u	input-vector
w	unknown input vector
f	fault vector
y	output vector
r	vector of residual signals

e	vector of error signal, i.e., $x - \hat{x}$
ζ_0	initial conditions
δ_w	upper bound on the modulus of unknown inputs
$\delta_{w,2}$	upper bound on $\mathscr{L}_2$ norm of unknown inputs
$\delta_{w,\infty}$	upper bound on Peak norm of unknown inputs
$\delta_{u,2}$	upper bound on $\mathscr{L}_2$ norm of control input
$\delta_{u,\infty}$	upper bound on Peak norm of control input
J_e	Evaluated residual
J_{th}	Threshold
$J_{th,Peak,Peak}$	Peak-to-Peak threshold
$J_{th,RMS,2}$	RMS-to-2 threshold
$J_{th,Peak,2}$	Peak-to-2 threshold
f_a	actuator fault
f_s	sensor fault
α	attenuation level for unknown inputs
β	sensitivity level for the faults
γ	Lipschitz constant
Δ	model uncertainty
$\bar{\sigma}(\cdot)$	the maximum (the largest) singular value
$diag(\cdot)$	diagonal matrix
a^T	transpose of a vector a
A^T	transpose of a matrix A
Σ	a dynamic system
$P > 0 (P \geq 0)$	the matrix P is symmetric and positive (semi) definite
$P < 0 (P \leq 0)$	the matrix P is symmetric and negative (semi) definite
$V > 0 (V \geq 0)$	the function V is symmetric and positive (semi) definite
$V < 0 (V \leq 0)$	the function V is symmetric negative (semi) definite
$I_n\,(0_n)$	identity matrix (null matrix) of dimensions $n \times n$
$I_{n\times m}\,(0_{n\times m})$	identity matrix (null matrix) of dimensions $n \times m$
iff	if and only if
sgn	sign or signum function
k	sample point
t	time
T_s	sampling time interval
T or N	length of observation window
$\leqq$	element-wise less than or equal to
$=$	equal to
$\neq$	not equal to
$\triangleq$	equal by definition
$\in$	belongs to
$\subseteq$	is subset of
$\Rightarrow$	implies
$\otimes$	Kroneker product
$\mathfrak{R}^n$	space of real valued n-dimensional Euclidean space
$\mathfrak{R}^{n\times m}$	space of real valued $n \times m$ matrices

$\mathscr{L}_2^m[0,\infty)$	The space of functions in $\mathfrak{R}^m$ that are square integrable and absolutely bounded over $[0,\infty)$
$\mathscr{L}_2^m[0,K)$	The space of functions in $\mathfrak{R}^m$ that are square integrable and absolutely bounded over $[0,K)$
inf	infimum
min	minimum
sup	supremum

Abstract

Interests in fault detection and isolation for nonlinear systems have grown significantly in recent years due to the fact that most of the systems, we face in practice, are nonlinear in nature. There exists a number of techniques for fault detection, among them, the so-called observer-based fault detection is widely studied. In addition, this technique has been proven efficient in detecting faults. In a typical observer-based scheme, the process of fault detection is carried out in two steps: residual generation and residual evaluation. The purpose of residual generation is to produce the so-called residual signal by comparing the process outputs with their estimates generated by the observer. Roughly speaking, the residual signal, thus generated, carries the information of faults only. It means that under fault-free operation, the residual should go to zero and deviates only in the presence of fault. However, due to model uncertainties and unknown inputs (process disturbances, measurement noises, and faults of no interest), the residual signal is non-zero even in the fault-free operation of the process. In order to extract the information of faults in the presence of model uncertainties and unknown inputs, additional efforts need to be done. The process of residual evaluation serves this purpose. In this step, some function of the residual signal (evaluation function) is compared with a bound, the so-called threshold, regarding all possible unknown inputs and model uncertainties. An alarm is generated if the former exceeds the later which shows the presence of fault. Selection of a suitable threshold is very critical task in fault detection. The performance of a typical fault detection system can be evolved by a threshold. If it is selected too low, some unknown inputs may cause the evaluated residual to cross it which results into a false alarm. Conversely, selecting it too high may result into a missed detection, which means some set of faults may remain undetected.

This thesis presents novel methods for designing observer-based residual generator (fault detection filters) and threshold computation scheme for nonlinear uncertain systems subject to unknown inputs. The objective of designing fault detection filter is to generate a residual signal which is robust against unknown inputs and sensitive to faults. Exploiting the tools of game theory and dissipation inequality, three kinds of fault detection filters are proposed. These filters are designed with the objectives: to enhance sensitivity of the residual signal to faults, to improve robustness of the residual signal against unknown inputs, and to simultaneously provide sensitivity to faults and robustness against the unknown inputs. Similarly, the objective of designing a threshold computation scheme is to eliminate the possibility of false alarms and ensures the detectability of small faults so that the performance of fault detection system can be improved. For this purpose, various kinds of thresholds for nonlinear systems are proposed. These thresholds include constant thresholds, adaptive thresholds, and dynamic threshold. For designing constant thresholds, a framework based on signal norms is proposed. Utilizing the tools from robust control theory and linear matrix inequality, algorithms are derived for different kinds of

thresholds. The framework for adaptive threshold is also proposed using signal norms. In this scheme, the resultant threshold is a function of the instantaneous energies of the control inputs. This threshold is very sensitive to the variations in fault-free residual. For designing dynamic threshold, a dynamic system is proposed based on deriving an inequality on the modulus of the residual signals. This dynamic system takes the information of the instantaneous values of the control input, a bound on model uncertainties and unknown inputs and generates a variable threshold accordingly. The threshold, thus generated, fits as close to the residual signal as possible under fault-free operation.

The fault detection methodologies proposed in this thesis are expressed in the form of algorithms that can be directly implemented. This shows that the proposed schemes are computationally tractable and user oriented. These algorithms are tested with the numerical examples in the respective chapters and with the benchmark problems; that is, three-tank system (DTS200) and the inverted pendulum control system (LIP100) to demonstrate their applicability and use.

Chapter 1

Introduction

This chapter briefly describes the motivation and objectives of the present study. The outline of the thesis and its contributions are also presented in this chapter.

1.1 Motivation

The research interest of this dissertation is observer-based fault detection in nonlinear systems. The motivating objectives for embarking on this research are explained in the following lines:

Why fault detection / process monitoring ?

The most critical issues in the design of an automated system include higher performance, cost efficiency, production of a quality product, reliability[1], and safety. In order to achieve these objectives, a traditional way is to improve the quality, reliability, and robustness of individual process components such as sensors, actuators, plant equipments, and controllers. Even then, the fault-free operation of the plant can not be guaranteed. Faults in the process may arise due to the minor equipment damage, process abnormalities, bad tuning of the controller parameters, and sensor or actuator malfunctions, etc.

Faults may cause the process to operate far away from the desired operating points and as a result degrades the performance of the process, which, in turn, affect the operation cost and quality of the final product. For instance, recent reports [2] show that industries lose billion of dollars due to various faults in plant. In most cases, (minor) faults may lead to the unplanned shut-down of the plant which, in turn, result in the major production loss and two to three fold repair cost. Nowadays the term "higher performance" cover the environmental issues as well. With the growing concerns about the water/air/earth contaminations, environment protection and global warming, industries are urged to monitor the process and product quality. Governments also impose substantial fines on violations of environmental protection regulations [2]. In order to avoid equipment damage, production loss, and unplanned shutdown on one side and to improve efficiency, reliability on the other side, the role of process monitoring and fault diagnostic systems is inevitable.

[1] It is the ability of a system or component to perform its required functions under the stated conditions for a specified period of time

Another and probably the most important reason for fault diagnosis and process monitoring is safety. Sometimes a fault is developed slowly within the process, if care is not taken in the early stages, might have disastrous implications on the plant, which not only causes economic loss but also results into human casualties. According to the Abnormal Situation Management (ASM), operations practices can lead to costs of 3-8 percent of plant capacity due to unexpected events. Moreover, an estimated loss of approx. $10 billion is observed in the U.S. petrochemical industries annually[3, 4]. In addition, survey conducted in [3] shows that petrochemical plants on average suffer a major incident every three years which not only results into economic loss but also human casualties. In safety-critical systems, for instance, in nuclear reactors, aircrafts, etc., faults result in big loss of human lives as well. A few of the catastrophic incidents are given below:

- Crash of Japan Air lines B-747, Flight 123, August 12, 1985 [520 casualties] [5]
- Explosion of Chernobyl nuclear power plant, Ukraine, April 26, 1986 [more than 4000 deaths] [6]
- Explosion in Piper Alpha Oil Rig, North Sea oil production platform, July 6, 1988 [167 deaths toll] [7]

Surprisingly, these incidents did not occur due to major problems in the plant, but rather due to some minor and simple faults. Later investigations and research reports on these incidents showed that many of them could have been avoided if there was a suitable monitoring system. Due to the above mentioned reasons, the discipline of fault detection and isolation (FDI) and fault tolerant control (FTC) are receiving a considerable attention in both academia and industry and are quite often prescribed by the authorities. Its significance can be viewed from the recent published monographs, for instance, [1, 8–13] to name a few.

Why observer-based fault detection ?

One way to design an FDI system is to install additional hardware (redundant) known as *Hardware redundancy* in parallel with the process itself. The presence of fault is inferred from the deviation between the actual process output and the output of redundant process component. Apart from the high reliability and direct fault isolation, hardware redundancy require additional cost, weight, and space to install the redundant components [8]. Another way to achieve FDI for a system is the analytical model-based. The model-based FDI techniques make explicit use of process model and deduce the information of a fault by comparing the process output with their estimates. The model-based FDI methods have been proven efficient in detecting faults and are also demonstrated by a large number of real-time applications. Due to efficient fault detection and on-line implementation capability on one hand, technological and economic demands on the other hand, model-based FDI has been proven as a powerful tool to solve fault diagnosis problems in technical processes [1].

Among all the model-based FDI techniques, the so-called observer-based FDI has received a considerable interest over the past three decades. The use of observer-based FD

can be justified by a number of reasons. Firstly, this technique has been used in the framework of the well-established advanced control theory, where powerful tools for designing observers, efficient and reliable algorithms for data processing in order to reconstruct process variables, are available. Secondly, due to the associated advantages of observer-based FD methods; that is, quick detection, easy on-line implementation, etc. Thirdly, it has been proven in a number of publications that all other model-based FDI schemes are only a special form of observer-based approach.

Why fault detection for nonlinear systems?

Fault detection for linear systems is a relatively mature subject with a variety of powerful tools and its successful applications in industry. Thus, it is natural for one to wonder why so many researchers have recently showed a very active interest in studying and developing nonlinear fault detection techniques. The reasons could be as follows: (i) most of the systems are nonlinear in nature. If the operating point of a system is not deviating too wide, the well established linear techniques can be employed by linearizing the system at that particular operating point. However, if the operating point is deviating too much, the conventional linear methods are not suitable to work with. Consequently, there is a need to study fault detection for nonlinear systems. (ii) Another assumption of linear FDI is that the system is linearizable. However, sometimes the process has hard nonlinearities whose discontinuous nature does not allow the process to be linearized. The linear methods can not be applied to compensate their effects. Nonlinear FD methods must be developed to detect faults in the presence of these nonlinearities.

Why fault detection for discrete-time nonlinear systems?

Nowadays most of the systems are controlled using digital devices. In such a situations, the actual process is continuous-time while the controllers and FD systems are implemented on digital computers. One approach to handle these situations is, discretize the process, and design an FD system based on that, then apply it to the real-time process. It is, thus, very important to understand these theoretical developments in digital (sampled-data) settings. Thus studying a discrete-time FD problem is of great importance and a natural candidate for digital implementation.

1.2 Objectives

Inspired by the motivations mentioned in the last section, this thesis is primarily concerned with the development of observer-based fault detection (FD) technology for nonlinear systems in the presence of model uncertainties and exogenous disturbances. The major focus is devoted to develop novel FD methods for both continuous- and discrete-time settings which are computationally tractable.

The observer-based FD aims to deliver estimates of the process outputs, and compare these estimates with the actual measurements from the process in order to generate the so-called residual signal. The procedure of generating a residual signal is known as *residual generation*. A fault detection filter (FDF) is one of the widely studied observer-based

residual generator. The residual signal, thus generated, carries the information of faults. In ideal situations, the residual signal should be sensitive to faults only, that is,

$$\textbf{if residual} \neq 0 \ \ \textbf{fault}; \ \ \textbf{otherwise, no fault}$$

However, the influence of the unknown inputs (model uncertainties, process disturbances, and measurement noises) on the process make the residual signal corrupted, and as a result, it does not go to zero even if there is no fault in the system. In order to extract the information of faults from the non-zero residual signal, extra efforts need to be done; that is, post processing of the residual signal. This procedure is referred to as *residual evaluation*. The process of residual evaluation can be evolved in two steps; that is, selection of a proper threshold and decision logic. In residual evaluation, some function of the residual signal (evaluation function) is compared with the threshold, and if the former exceeds the latter an alarm is generated which indicates the presence of fault in the system. Selection of a proper threshold is very critical task in process monitoring and fault diagnosis. If a threshold is selected too low, the unknown inputs may cause the residual signal to cross the threshold which results into a false alarm. In which case the FD system indicates a fault; however in reality, there is no fault in the system. Conversely, if it is selected too high, some of the faults will not be able the residual to cross threshold, and hence will result into a missed detection, which means that a set of faults remains undetected. It is, therefore, required to devise a systematic strategy which can be used for the design of a proper threshold. With this background, the objective of an FD system is to design an optimal residual generator which simultaneously produces robustness against the unknown inputs and sensitivity to faults, and to design a threshold so that false alarms are precluded and detection of faults is ensured. The research objective of the present thesis lies in the development of optimal residual generation and threshold computation schemes for nonlinear systems in both discrete-time and continuous-time settings. In addition, it is particularly focused on the applicability and computational tractability of the proposed schemes and algorithms. These objectives are formulated as follows:

- Design of an observer-based residual generator which produces robustness against process disturbances, measurement noises, and model uncertainties and enhances sensitivity to faults.

  To achieve robustness, worst case scenario of unknown inputs; that is, the unknown inputs which have maximum influence on the residual signal, is considered. Similarly, to achieve sensitivity, the "*best-case*" fault; that is, the fault which has minimum influence on the residual signal, is considered. Note that the reason for calling this fault as "*the best-case fault*" is stated in Chapter 4.

- Design a threshold so that faults can be distinguished from unknown inputs. Further objectives in the threshold design lies in the reduction of false alarms together with missed detection.

  Different kinds of thresholds are proposed and compared. The proposed thresholds include constant threshold, adaptive threshold, and dynamic threshold. Thereby providing a complete design of an alarm system. With the help of these thresholds,

the performance of the FD system is improved by eliminating false alarms as well as missed detection which, in turn, result into enhancing fault detection capability.

From a global point of view, this thesis provides optimal fault detection schemes for nonlinear systems which are computationally tractable, user oriented, and applicable to a large class of practical FD problems.

1.3 Thesis outline and contributions

The following overview displays an outline of this thesis and briefly summarizes its major contributions.

Chapter 2: Review of fault detection techniques - introduces to the basic terminology used in FDI and presents an overview of fault detection techniques for dynamical systems. Fundamental concepts, such as faults, failure, unknown inputs, fault diagnosis, fault detection, fault isolation, and fault identification are defined according to the IFAC[2] technical committee on SAFEPROCESS[3]. A widely accepted classification of fault detection techniques is presented with a particular focus on model-based techniques. A comparison among different FD schemes, and among various model-based approaches is presented. A comprehensive survey on observer-based methods for linear and nonlinear systems is given. A detailed study on most commonly used observers for residual generators is presented. At the end of this chapter, residual evaluation and threshold setting techniques are briefly described.

Chapter 3: Nonlinear systems, unknown inputs, and fault representation - presents the basic concepts of modeling of faults and disturbances in nonlinear systems. The state-space models of nonlinear systems are provided. The associated fault models including actuator faults, sensor faults, and components faults are introduced. In addition, the disturbance and uncertainty models are also presented. The transformation of nonlinear systems into their Lipschitz equivalent models are introduced. Moreover, different classification of faults, for instance, with respect to the sources of faults, with regards to the time-domain behavior, and with reference to process models, are described. An example of nonlinear three-tank system is presented at the end of this chapter in order to illustrate the underlying philosophy.

Chapter 4: Optimal residual generation: $\mathscr{H}_-$, $\mathscr{H}_\infty$, and $\mathscr{H}_-/\mathscr{H}_\infty$– optimization - contributes to the design of fault detection filter (FDF) for discrete-time input-affine nonlinear systems using $\mathscr{H}_-$–index, $\mathscr{H}_\infty$–norm, and mixed $\mathscr{H}_-/\mathscr{H}_\infty$– optimization. In order to facilitate the study on optimal fault detection in nonlinear systems, the time domain definition of $\mathscr{H}_-$–index is proposed and the definition of $\mathscr{H}_\infty$–norm is obtained from the literature on robust control theory of nonlinear systems. Based on the above optimization indices, three problems of designing FDF are formulated. These are: $\mathscr{H}_-$–FDF which is used to design an FDF in order to acquire maximum possible sensitivity of the residual to the *best-case fault* present in the system, $\mathscr{H}_\infty$–FDF which results into an FDF attaining robustness of the residual against the unknown inputs to a pre-defined level,

[2]International Federation of Automatic Control
[3]Fault Detection, Supervision, and Safety of Technical Processes

and the mixed $\mathscr{H}_-/\mathscr{H}_\infty$–FDF which simultaneously provide robustness against the worst case unknown inputs and sensitivity to the *best-case fault*. Using the theory of differential games and dissipation inequalities, sufficient conditions are derived in the form of Hamilton-Jacobi-inequalities. All of these problems are studied over the finite-horizon as well as over infinite-horizon. It is also shown that the generalized results obtained can be used to study the problem of fault detection in discrete-time linear system both in finite-horizon as well as over infinite-horizon. Finally, a design example is given which illustrates the theory, proposed in this chapter. Parts of this chapter are based on [14, 15]

Chapter 5: Optimal residual generation for Lipschitz nonlinear systems: $\mathscr{H}_-/\mathscr{H}_\infty$– optimization - addresses the problem of designing $\mathscr{H}_-/\mathscr{H}_\infty$-FDF for nonlinear systems with Lipschitz nonlinearities using convex optimization. Since Lipschitz nonlinear systems cover a wide range of nonlinear systems as described in Chapter 3, it is focused on designing an optimal FDF for this very important class of nonlinear systems. Sufficient conditions for the solution of the $\mathscr{H}_-/\mathscr{H}_\infty$-FDF are derived in the form of linear matrix inequalities (LMIs) for both discrete- as well as continuous-time settings. Two algorithms are presented which ease the design of optimal FDF for both cases. An illustrative example is provided in order to elaborate the design procedure for continuous-time systems.

Chapter 6: Computation of thresholds for Lipschitz nonlinear uncertain systems - proposes methods for the computation of thresholds for Lipschitz nonlinear uncertain systems in the presence of unknown inputs. Different kind of thresholds are studied in this chapter. These include constant threshold, adaptive threshold, and dynamic threshold. For constant threshold, a generalized framework based on signal norms is developed. Different kinds of constant thresholds; which include $J_{th,RMS,2}$, $J_{th,Peak,Peak}$, and $J_{th,Peak,2}$, are studied with the proposed framework. The threshold computation problem is formulated as an optimization problem and using LMI tools, algorithms are derived for the computation of these thresholds. The adaptive threshold is proposed based on the similar framework developed for constant thresholds. In this scheme, the instantaneous values of the energies of u is used instead of using a bound on it. This scheme considerably reduces the size of the constant threshold and as a result improves the fault detection capability. For dynamic threshold, an inequality on the upper bound of the solution of the Lipschitz nonlinear systems is derived. This inequality has been proven to be an efficient tool for the computation of dynamic threshold. All of these thresholds are studied for both continuous- and discrete-time settings. Algorithms are proposed for the computation of these thresholds. The usefulness of the proposed methodologies is shown by numerical examples given at the end of each section. A comparative analysis of the proposed schemes is provided at the end of the chapter. Parts of this chapter are based on [16–18].

Chapter 7: Application to benchmark problems - presents the application of proposed FD methods and algorithms to benchmark problems. The first one is a **Three-tank system: DTS200** consisting of three circular tanks coupled via interconnecting pipes showing a typical characteristics of tanks, pipelines, etc., often used in chemical industry. The nonlinear dynamics of three-tank system make it a handsome example for testing and validating the nonlinear FD algorithms. The second chosen benchmark is **The inverted pendulum control system: LIP100**. This application is also dynamically nonlinear and unstable. It shows a typical characteristics of electromechanical systems. Due to its highly nonlinear behavior and open loop instability in nature, it becomes an

excellent candidate for illustrating the usefulness of the closed loop FD techniques for nonlinear systems. Part of this chapter is based on [19].

Chapter 8: Conclusions and recommendations - provides a summary of the dissertation, discusses the achievements, and gives recommendations for possible further developments of the proposed techniques.

Chapter 2

Review of fault detection techniques

This chapter introduces to the basic terminology used in FDI and presents a review of fault detection techniques for dynamical systems. Fundamental terminology, such as faults, failure, unknown inputs, fault diagnosis, fault detection, fault isolation, and fault identification are defined. A widely accepted classification of fault detection techniques is presented with a particular focus on model-based techniques. Observer-based fault detection for nonlinear systems is the focus of the present work, therefore, a particular attention has been given to the state-of-the art methods for observer-based residual generation for nonlinear systems. Finally, a brief description of the residual evaluation and threshold setting is provided. Most commonly used evaluation functions are described.

2.1 Basic concepts of faults, disturbances, and fault diagnosis technique

The terminology used in this thesis is fairly standard and is based on the recommendation of IFAC technical committee SAFEPROCESS. Below, some basic definitions of faults, failure, disturbances and uncertainties, fault detection, fault isolation, fault identification, and fault diagnosis are given. The interested reader is referred to [1, 12, 20] for the detailed explanation of the above mentioned terminology.

A *fault* is an un-permitted deviation of at least one characteristic property or parameter of the system from the acceptable (standard condition). A very close term *failure* is regarded as a permanent interruption of a system's ability to perform a required function under specified operating conditions. A failure is used for complete breakdown of a system, while fault is used to indicate a deviation from the normal characteristics. As far as detection is concerned, both faults and failures can be treated alike. Moreover, a *fault* can be treated as an external input or as parameter deviation which changes the system characteristics. Similar to faults; disturbances, uncertainties, and noises can also be treated as external inputs. In fault detection and isolation (FDI) terminology, these are termed as unknown inputs. Unlike faults, these unknown inputs are uncontrolled and unavoidable and are present during the normal process operation. The effect of the unknown inputs can be incorporated in the controller design and process can perform well even in the presence of them. Faults, on the other hand, have very severe effects on the

process and should be detected.

The process *fault diagnosis* is referred to as determination of the size, location, time of detection and type of fault in the process. Based on the performance, a *fault diagnosis system* is regarded as *fault detection (FD)* or *fault detection and isolation (FDI)* or *fault detection, isolation and analysis (FDIA)* [1]. An FD is the process of determinating the fault in the process and its time of occurrence. An FDI, besides detection also determine the kind and location of a fault present in the system. Similarly, an FDIA, together with detection and isolation also aims to determine the size and time behavior of the fault. It is worth noting that the existence conditions for fault isolation are more stringent than for fault detection, and even more harder to hold in case of fault identification. Consequently, it is difficult to isolate or identify faults in most of the situations.

2.2 Desirable features of an FD scheme

A fault detection system system should ideally meet some general requirement. The most important desirable features are given below:

- early detection of faults (incipient and abrupt)
- successful detection of actuator, component, and sensor faults
- robustness against unknown inputs (external disturbances, measurement noises, model uncertainties)
- differentiating faults from the unknown inputs so that false alarms are avoided
- should use less on-line computation so that it can be integrated into large scale systems easily

Besides the above mentioned very important attributes, the design procedure of an FD scheme should be as simple as possible.

2.3 Classification of FD techniques

There exists a number of techniques used for fault detection in technical process. In sequel, the widely accepted classification of these techniques is presented.

2.3.1 Hardware redundancy based FD

The crux of this scheme is the reconstruction of the process component using the identical hardware component. Figure 2.1 shows the schematic description of the hardware redundancy. The information of the fault is extracted if there is any deviation of the output of the process component from its redundancy. The high reliability and ability of direct fault isolation are the main advantages of this scheme. However, the major problems encountered with this scheme are the extra components, increased maintenance cost and additional space required to accommodate the equipment. Thus, its use is limited to a

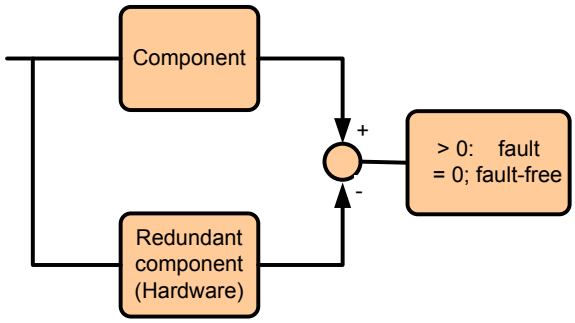

Figure 2.1: Schematic description of the hardware redundancy scheme [1]

number of key applications, for example, nuclear power plants, flight control systems, etc. [1, 8]

2.3.2 Plausibility test

Figure 2.2 shows the schematic depiction of the plausibility test. The basic idea of this technique is to evaluate the measured process variable with regard to credible, convincing values and their compatibility among each other. On the assumption that a fault leads to the loss of plausibility, the information about the presence of a fault in a certain variable can be extracted using plausibility check. It can be performed by simple rules with binary logic. The plausibility test is also a kind of limit checking but with a wider tolerance. This test can be viewed as a first step to model-based FD method. However, it is limited in its efficiency for detecting faults in a complex process [1, 12].

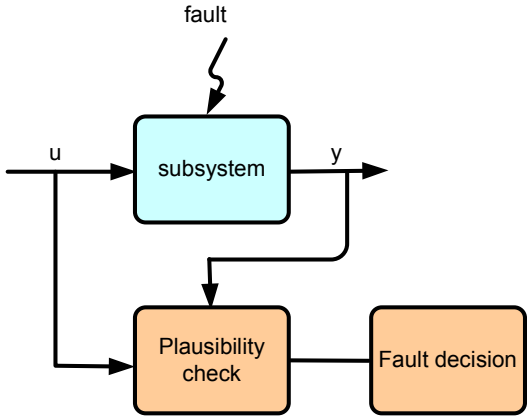

Figure 2.2: Schematic depiction of the plausibility test scheme

2.3.3 Signal-based FD

Figure 2.3 shows the conceptual depiction of signal-based FD technique. The central idea of this scheme is to extract the fault information from the process signals. For this purpose,

some signal properties (symptoms) are analyzed. These symptoms are generally divided into time domain characteristics and frequency domain characteristics of the process signal. The time domain characteristics comprises of magnitude, mean (arithmetic or quadratic), limit values, trends, and statistical moments of the amplitude distributions, etc., while the frequency domain characteristics include spectral power densities, frequency spectral lines, to list a few. The signal-based FD is used under steady-state operation of the process. The efficiency of this scheme is limited when the process is operating in a wide range due to the possible variation of input signals [1].

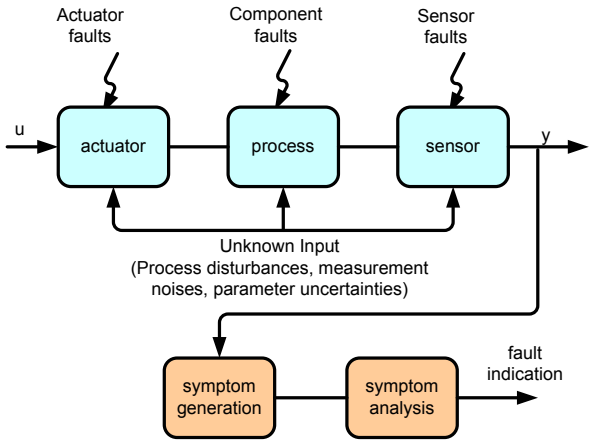

Figure 2.3: Schematic description of signal-based FD scheme

2.3.4 Model-based FD

The intuitive idea of the model-based FD technique is to replace the hardware redundancy by a process model which is implemented in software. The process model runs in parallel with process itself and is driven by the same process inputs. In this way, the process behavior can be reconstructed on-line. Analogous to hardware redundancy, it is called software redundancy or analytical redundancy [1]. It is well-known that the model-based FD techniques are more powerful than signal-based FD schemes [21, 22] because it uses more information about the process.

Figure 2.4 shows a typical model-based FD scheme. It consists of two stages: residual generation and residual evaluation. In residual generation, the so-called residual signal is generated by comparing the process outputs with their estimates. The residual signal carries the information for the faults. Since the residual signal, in real process, is affected by the faults, disturbances, and measurement noises simultaneously, it is required to process the residual signal further for the possible information of faults. This is done in the residual evaluation stage.

Note that the process model represents the qualitative and quantitative behavior of the process, which can be obtained by utilizing the well-established techniques from system modeling. The quantitative or analytical model of the process can be represented by a set of differential or difference equations while the qualitative model is expressed in terms

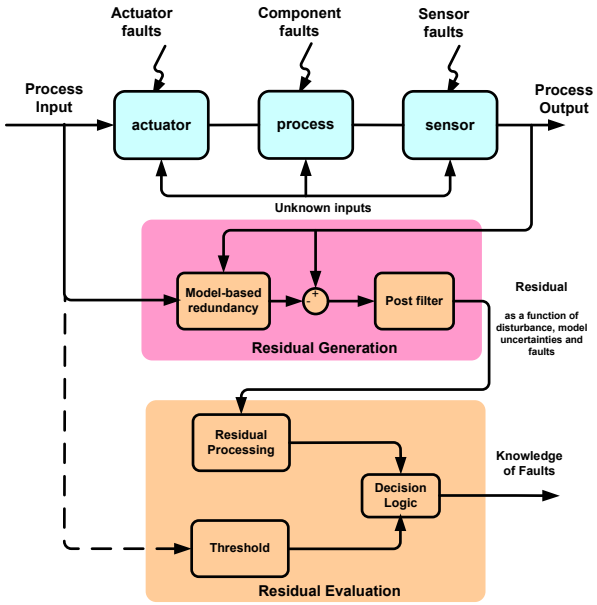

Figure 2.4: Schematic description of model-based FD scheme

of qualitative functions centered around different units in the process. The qualitative models are also called as knowledge-based models which include neural networks, petri nets, expert systems, fuzzy logic etc. [21, 22]. Based on these arguments, the model-based FD schemes can be divided into two classes; that is, analytical model-based and knowledge-based. The knowledge-based FD techniques are useful where the precise model is not available or very hard to obtain. The examples include the large scale chemical process and nuclear reactors. An extensive study on knowledge-based FD methods can be found in [21, 23, 24] and some recent books [10, 25]. The analytical model-based FD techniques, on the other hand, make use of the analytical models for the purpose of residual generation. These can broadly be classified into: (i) parity space FD (ii) observer-based FD (iii) parameter identification based FD. These approaches are described in the sequel.

Parity space approach

Figure 2.5 shows the conceptual diagram of parity space based approach for residual generation. The parity space approach, initiated in [26], makes use of the parity check on the consistency of parity equation. In this approach, a set of properly modified system equations (also called parity relations) is derived based on the measured signals from the process. These parity relations decouple the residuals from the system states and also among each other. This enhances the fault detectability. The inconsistency in the parity relations indicates the presence of fault. Chow and Willsky derived the parity relations based on state-space model of the system in their pioneering work in [26] which were, later, derived using system transfer function in [27–30].

As mentioned in [1, 22, 31], there exists a close relationship between parity space based

and observer-based approach. An extensive study on parity space FD has been presented in [1], where it has been shown that there exists a one-to-one mapping between the design parameters of observer and parity space based residual generation. Thus given a set of parity relations, a diagnostic observer can be designed and vice versa.

Parity space approach has also been used to study the problem of fault detection in nonlinear systems. For instance, in [32], a relation between high-gain observers and nonlinear parity space residuals has been studied. The work in [33, 34] extended the parity space approach to a class of nonlinear systems using TS fuzzy models and linear matrix inequality (LMI) techniques. Recently the parity space approach has also been utilized to study the problem of robust fault detection in nonlinear systems with application to mobile robots in [35–38]. A comprehensive study on parity equations for nonlinear systems using TS fuzzy models has also been carried out in [12].

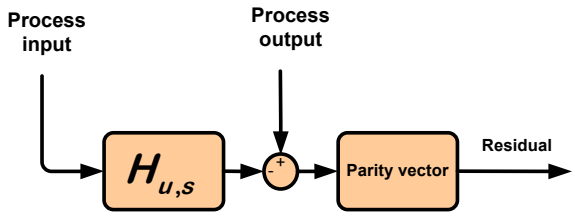

Figure 2.5: Schematic description of parity space approach

Observer-based approach

Observer-based technique is one of the mostly applied model-based scheme for detection of faults in a system. In this scheme, the residual signal is obtained by comparing the process outputs with their estimates. It is worth noting that the observers are mainly used by the control community in order to estimate the unmeasured states in the process, while the FDI community are using it for diagnostic purposes. The existence conditions for diagnostic observers are more relaxed than for a state observer, however one particular class of diagnostic observer; that is, fault detection filter (FDF), which can be used for state estimation as well as diagnostic purposes.

The idea of using observer for diagnosis purposes was stimulated in the early 70's, when Beard developed the first fault detection filter which was later redefined by Jones in 1973 in geometric framework. This was named as *Beared-Jones Fault Detection filter*. Parallel to this development, the statistical approaches were also developed, where Mehra and Peschon introduced a fault detection scheme based on Kalman filter [8]. Since then, observer-based fault detection is the focus of immense research. The motivation that a detection filter should be robust against disturbances and measurement noises led the researchers to the area of robust fault detection and isolation (FDI). Frank [39] used the first robust observer-based fault detection schemes for instrument faults. Later robust unknown input observers (UIO) were introduced in the mid 80's with the pioneering work of Wünnenberg and Frank in [40] and then considerable contribution was made in [41–46].

The main idea of UIO was to make the residual signal independent of the unknown inputs. This was achieved by decoupling the disturbances from the residual signal. It was later observed that the existence condition for the unknown input observer are very hard, which were then relaxed by introducing the so-called matrix pencil approach. In this approach, attempts were made to make the residual signal insensitive to unknown inputs instead of making the decoupling of estimated states from the unknown inputs [31, 47, 48]. An elegant solution to the problem of unknown input observer using the so-called geometric approach was proposed by Massoumnia [49]. The requirement on deep mathematical knowledge of geometric theory limited the use of this technique for fault detection, however, a modified form of this technique has been adopted in [1]. Most of the results on geometric approach presented in [1] are the dual of the results on decoupling control which can be found in [50]. Different algorithms for the full order, reduced order and minimum order detection filters have recently been proposed in [1, 51]. A geometric-based approach has also been used for fault detection in interval systems in [52]. It is worth noting that the

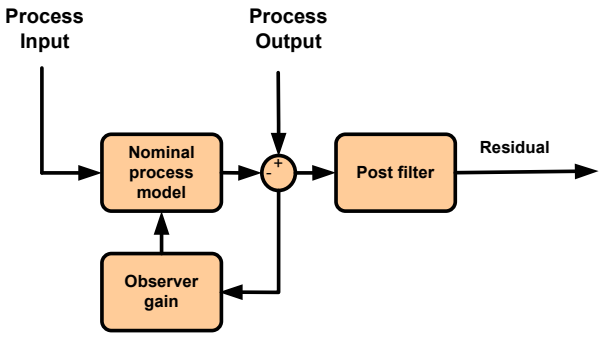

Figure 2.6: Schematic description of observer-based residual generation

approaches described above; that is, unknown input observers, matrix pencil approaches and geometric approaches, are based on the decoupling of unknown inputs. Further, these approaches are not well suited to handle the uncertain systems. One solution may be to model the uncertainties as unknown inputs and used the prescribed approaches. Another problem in these approaches is if the fault lies in the same subspace of the disturbances, then upon decoupling the disturbances, the residual will also be insensitive to fault, which is obviously not the objective of a detection filter. Moreover, the existence conditions for decoupling the unknown inputs are quite strict, which limits the use of these approaches.

A frequency domain approach for the design of robust detection filters has also been proposed in [1, 45, 53–62], to list a few. In this approach, a solution is proposed for improving robustness to unknown inputs instead of decoupling them completely. Various techniques have been introduced from the well-established control theory. These include $\mathscr{H}_\infty$ and $\mathscr{H}_2$ based fault detection filter design [1, 45, 53–57]. Further efforts have also been made to address the robustness against the unknown inputs and sensitivity to faults. To this end, various optimization indices, that is, $\mathscr{H}_\infty/\mathscr{H}_\infty$, $\mathscr{H}_2/\mathscr{H}_2$, $\mathscr{H}_-/\mathscr{H}_\infty$ have been proposed in [1, 8, 56, 58–66] to list a few. The works in [65] and [1] have proposed a unified solution for the design of optimal FDF, which solves the problem of $\mathscr{H}_i/\mathscr{H}_\infty$ with $i \in (-, \infty)$ over the whole frequency range and in all directions in the measurement

subspace. In addition, it requires a solution of one algebraic Riccati equation which saves the processing time and computational effort. The traditional approach, that is, the fault alarm should be released in case of nonzero residual signal, does not hold while addressing the problem in $\mathscr{H}_\infty$, $\mathscr{H}_2$ $\mathscr{H}_\infty/\mathscr{H}_\infty$, $\mathscr{H}_2/\mathscr{H}_2$ or $\mathscr{H}_-/\mathscr{H}_\infty$ settings. The main source of nonzero residual signal in fault-free operation is the unknown inputs and model uncertainties. For this purpose, residual evaluation is used for extracting the information of faults. The problem of residual evaluation for linear systems has also been addressed in literature, for instance, see [1, 11, 67–73] and the references therein.

Since observer-based fault detection for nonlinear system is the focus of this thesis, a survey on residual generation techniques for nonlinear systems will be presented in Section 2.5. Further, a more detailed explanation of evaluation functions for the purpose of residual evaluation will be provided in Section 2.6.

Parameter identification based approach

Parameter identification based approach is also one of the important FDI techniques and mostly addressed in [12, 74, 75]. In this approach, fault detection is performed based on the on-line parameter estimation. The information of the fault can be extracted by comparing the estimated parameter with the nominal process parameter. Any discrepancy between the two gives the indication of fault. Figure 2.7 shows the schematic description of parameter identification based FD scheme. The advantages of this scheme are: i) several parameters can be estimated with less number of input and output of the process [12], ii) it yields the size of the discrepancy which is useful for fault analysis [21]. The disadvantage is that an excitation signal is necessary in order to estimate the parameter which may cause problems in the case of processes running at stationary operating point. Further, the determination of physical parameter from its mathematical model may not, in general, give a unique result and only feasible if system order is low [21]. There are several parameter estimation techniques available in literature, among them, are the least square (LS) method, recursive least square (RLS) method, extended least squares (ELS) method, etc.

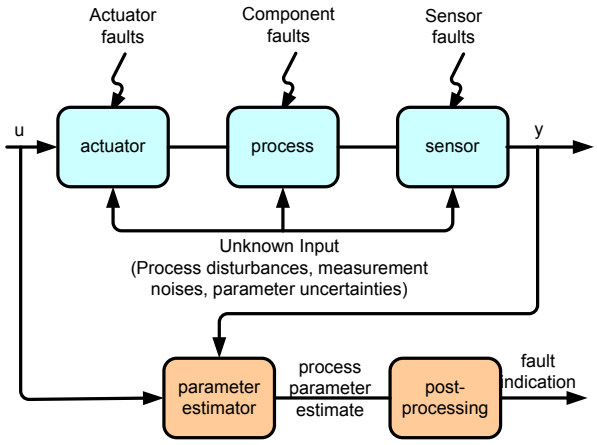

Figure 2.7: Schematic description of parameter identification scheme [1]

Parameter estimation techniques have also been utilized for fault detection in nonlinear systems. Isermann [12] used this techniques for single input and single output nonlinear systems. Recently, the work in [76] presented an application of this approach to fault detection in nonlinear satellite model.

2.4 Comparison of FD schemes

It is quite difficult to compare different FD schemes. The choice of a particular FD scheme to be used depends upon several factors, for instance, information about the process itself (linear or nonlinear, time-varying or time-invariant), the availability of the process model, types of the unknown inputs, open-loop or close-loop, the application sensitivity, for example how much safety is required, typical applications include, nuclear power plants, air bus systems, to list a few. The situations where process model is available or easy to model the process, the model-based approaches are preferred. The example include electrical and mechanical systems. In contrast to electrical and mechanical system, it is difficult to obtain an analytical model for chemical or industrial process or sometimes a mathematical model is too complex to handle. In such situations, qualitative model-based approaches or signal-based approaches are employed. It is worth noting that analytical model-based approaches are efficient in detecting faults and their on-line implementation is easier and simple.

Among the analytical model-based approaches, an interesting comparison is given in [12] where the author showed advantages and disadvantages of each approach. For instance, parameter estimation requires the structure of the model to be known where as parity space and observer-based approaches assumes that the model and its parameters to be known. Parameter estimation approach requires input excitation while the other two schemes do not admit such limitations. For the detection of multiplicative faults, parameter estimation approach is a better choice. A further essential difference is that fault isolation can be made based on the single output information in parameter estimation approach while in the other two approaches, it is not possible. Parity space approaches are more sensitive to measurement noises as compared to observer-based and parameter estimation approaches. Making the long story short, it can be concluded that different methods works well in different scenarios. Hence, it is possible to combine different approaches to enjoy the advantages of each approach. Some combining strategies are given in [12].

2.5 FD in nonlinear systems

Most of the real time systems are nonlinear in nature. If these systems are running at fixed operating point, the well-established techniques for linear FDI can be utilized by considering their linearized model. However, when the nonlinear system is not running at a fixed operating point, the linear FDI techniques can not be employed. Further, in particular, even due to the occurrence of fault, the operating point deviates too much and as a result the linear FDI scheme is submitted to increased modeling errors and runs out of its valid range of operation, which, in turn, generates false alarms instead of detecting

faults [77]. Owing to this reason, a great deal of attention has been attracted the research in FD for nonlinear systems.

To this end, several approaches for fault detection in nonlinear systems have been proposed. These include nonlinear observer-based approaches [8, 78, 79], parity space approaches [33, 35, 36], neural networks [80, 81], fuzzy nets [21, 33, 82] etc. Since the nonlinear observer-based fault detection is the major interest of this thesis, an overview of some state-of-the art methods for observer-based residual generation in nonlinear systems is given in the following subsection.

2.5.1 Nonlinear observer-based residual generation schemes

Nonlinear observer-based residual generation has been the topic of intensive research over the past three decades. Various approaches have been proposed in literature. Some of them are described below:

Extended Luenberger observer

The basic idea of extended Luenberger observer is to linearize the nonlinear model around the current estimated state, instead of a fixed point, for instance, the origin. The detailed study on this class of observers can be found in [83]. For the purpose of fault detection, a similar approach has been used in [84]. The discrete time version of this observer is studied in [79]. Sometimes due to the time varying nature and the linearization errors, it is difficult to obtain a proper filter gain matrix, and hence limits its use in practice [79].

Nonlinear identity observer approach

The idea of nonlinear identity observer based fault detection was initiated in [85]. Later, it was presented with more details in various survey papers, for instance, see [78, 86–88]. The basic idea behind the design is to linearize the observer error dynamics at the estimated state and neglect the higher order terms. A filter gain is determined in such a way that the equilibrium point of the error dynamics, that is, $e = 0$ is asymptotically stable. A solution to this problem was first proposed in [84] by assuming that the measurements are linear.

Unknown input observer approach

The intuitive idea of unknown input observer (UIO) to design an observer for the purpose of fault detection in such a way that the effect of the unknown inputs on the residual signal is completely eliminated. A direct extension of this approach to nonlinear case was made in [31]. This approach takes the advantage of the structure of the system model which is in observable form while admits a difficulty to transform the general nonlinear systems into the form suitable for this approach. Further, even for linear case, the existence condition for UIO are also restrictive [87].

The disturbance decoupling nonlinear observer approach

The disturbance decoupling nonlinear observer for fault detection was first proposed in [89, 90], which relaxed the existence conditions of nonlinear UIO. The basic idea of disturbance decoupling nonlinear observer is the same as UIO but a more general class of nonlinear systems is used. Further, a nonlinear transformation instead of the linear one is used. The transformation required to be necessarily state-transformation and is used in such away that the disturbances are decoupled from the faults. A difficulty arises when the disturbances distribution matrix depends explicitly on the input. Some solutions were proposed in [89, 90] to avoid this difficulty. After achieving the required transformation, the observer can be designed using any observer design method, for instance, nonlinear UIO method etc.

Adaptive nonlinear observer approach

As mentioned in [22], the conventional observer-based methods have poor performance in detecting slowly developing faults in nonlinear uncertain systems, especially when the uncertainties are dominant. To overcome this difficulty, one solution is the use of adaptive observer. This class of observers has been widely utilized for detecting faults in nonlinear systems in the presence of model uncertainties, for instance, see [91, 92] to list a few. Another advantage of this approach is that some uncertain parameters may be estimated on-line which can be used for improving robustness against model uncertainties.

High-gain observer approach

The high gain observers, initially proposed in [93], are usually designed with the objective of handling the model uncertainties. It has also been applied to fault detection in nonlinear systems in [32, 94–97]. An intrinsic feature of any high gain observer is the peaking phenomenon, however, it has also been addressed in literature. Reference [98] is of particular interest for this solution.

Sliding mode observer approach

Sliding mode observers have been widely applied to fault detection in nonlinear systems [99–101]. The inherent property of sliding mode observers of being robust to uncertainties and disturbances, makes them suitable for state estimation and fault detection.

Geometric approach

The nonlinear geometric approach for fault detection has been proposed in [102]. The basic idea is based on the detection filter design for linear systems using geometric approach proposed by Massoumnia [49]. In this approach, the residual generator is designed in such a way that the obtained residual signal depends trivially on fault and non-trivially on disturbances in its decoupled form. The associated shortcoming of this method is the requirement of deep understanding of the geometric theory. Further, the disturbance decoupling process may lead to the undetectability of the faults which lie in the same

subspace of the disturbances. This approach has also been applied for fault detection in bilinear systems in [103, 104].

Game-theoretic approach

Game theory has been utilized in designing observers for linear systems [105–107] and for nonlinear systems [108–111]. It has also been utilized in the context of fault detection [54, 102, 112]. The advantages of game-theoretic based design are two fold; that is, extreme case scenarios for disturbances and filter gains can be treated very easily and that it can be applied to more general class of nonlinear systems. De Persis and Isidori [113] used the game-theoretic based approach for fault detection in continuous-time nonlinear systems. They proposed a fault detection filter which attenuates the effect of measurement noises while keeping the minimal effect of fault on the "innovation signal" (which is called as residual signal). They exploited the tools of geometric techniques in order to get a special form of nonlinear systems in which case the disturbance subspace is decoupled. The residual generator thus designed depends non-trivially on fault and trivially on disturbances (in decoupled form). It can be noted from the the proposed design scheme that the filter provides disturbance attenuation to the desired level in the presence of fault which has minimal effect on the innovation signal. However, it does not address the problem of $\mathscr{H}_-$–index[1] based design which is often demanded in the design. In addition, the proposed approach considered the innovation signal as a residual signal. However, in real FD problems the residual signal is the difference between the actual output of the process and their estimates. To the optimal design of FD systems, the residual signal (not the innovation signal) should be considered in the design.

Observers for Lipschitz Nonlinear systems

Lipschitz nonlinear systems cover a wide range of nonlinear systems. In these systems, the nonlinear function is assumed to be bounded by some constant. Nonlinear systems involving sinusoidal nonlinearities are always bounded and can be considered as globally Lipschitz nonlinear systems. Similarly, systems having nonlinearities other than sinusoidal can be bounded for a particular range of process operation and hence are regarded as locally Lipschitz nonlinear systems. Lipschitz nonlinear systems is an active field of research in the context of control, observers and FDI. Some of the reasons are as follows

- Any type of nonlinearity can be transformed into Lipschitz nonlinear systems, at least locally
- Analytical solutions can be presented for nonlinear problems involving Lipschitz nonlinearities
- A well-established LMI techniques can be utilized to formulate the nonlinear problems involving Lipschitz nonlinearities. These LMIs can then be solved using standard computer softwares, for instance, MATLAB etc.

[1] It is the measure of that fault which has minimum influence on the residual. See Chapter 4 for the detailed discussion

Observer design for Lipschitz nonlinear systems, initiated in [114], has received a considerable attention in recent years, for instance, [115–124]. Many of these contributions proposed LMI based framework to solve robustness problems for their proposed observers.

In parallel with the observer design, study on fault detection of Lipschitz nonlinear systems has also been the focus of extensive research in recent years. To have a flavor of these results, see some references, for instance [58, 79, 94, 125–131].

2.6 Residual evaluation and threshold setting

After a successful design of residual generator, the remaining task in the FD scheme is the evaluation of residuals. A typical model-based fault detection system consists of two steps; that is, residual generation and residual evaluation. In ideal situation, the residual signal should be affected by the faults only. It means that the residual signal should deviate from zero only when there is a fault. However, such an ideal situation seldom arises in practice and the residual signal is influenced by the process disturbance, measurement noises, and model uncertainties. These factors make the residual signal nonzero even if in the fault-free case. If care for these factors is not taken in the design, the FD scheme may generate false alarms. In order to infer the presence of fault, the process of residual evaluation and threshold setting is used. Different techniques have been reported in literature for designing thresholds for fault detection in linear systems (see [1, 11, 67–73] and the references therein), however, very little attention has been devoted to nonlinear system, for instance [92, 132, 133].

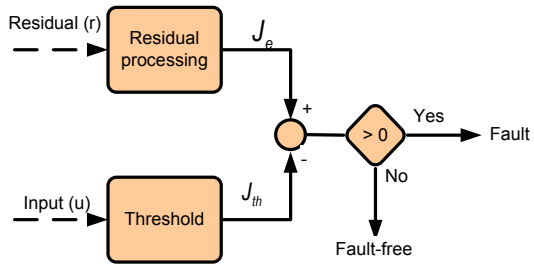

Figure 2.8: Residual evaluation scheme

Figure 2.8 shows a typical residual evaluation scheme. In this scheme, the residual signal is processed through some function, known as evaluation function and the resultant residual is referred to as evaluated residual. This evaluated residual is then compared with a threshold and if the former exceeds the later, a fault alarm is released. Based on the type of system under consideration, there exist two evaluation strategies, that is, statistical-based and norm-based. For stochastic systems, the so-called statistical-based evaluation is used. In stochastic framework, mean, variance, likelihood ratio (LR), generalized likelihood ratio (GLR) are frequently used for the evaluation of residuals. For the detailed study on residual evaluation in stochastic framework, the interested reader is referred to [1, 134, 135]. On the other hand, the norm-based residual evaluation is employed when a deterministic system is under consideration. This scheme, besides requiring less

on-line computation, allows a systematic way for threshold computation. The so-called *Peak* and *Root Mean Square (RMS)* norm of the residual signal are widely used for the purpose of evaluation. Another evaluation operator which is mostly used for evaluation is the weighted norm of the residual signal. These evaluation functions will be described in details in Chapter 6. Note that in all of these evaluation strategies, the common thing is to create a bound, the so-called threshold, regarding to all possible model uncertainties, unknown inputs, and faults of no interest. Exceeding the threshold indicates a fault and will release an alarm signal. Since this thesis considers only deterministic nonlinear systems, the analysis is restricted to norm-based settings.

2.7 Summary

In this chapter, basic concepts of FD techniques were introduced. Definitions of basic terminology used in FDI such as fault, failure, unknown inputs, fault diagnosis, fault detection, fault isolation, and fault identification were presented. A detailed review of FD techniques evolved over the last three decade was presented. The main features of each technique were described by elaborating their merits and demerits. A particular attention has been given to observer-based approaches. A detailed survey of these approaches in the context of robustness issues has also been presented. Observer-based residual generation techniques in nonlinear systems were also presented in detail. Commonly used observers and their limitations were discussed. Finally, a brief description of the residual evaluation and threshold setting techniques was presented.

Chapter 3

Nonlinear systems, unknown inputs, and faults representation

The objective of this chapter is to introduce the basic concepts of modeling of faults and disturbances in nonlinear systems. The state-space models of nonlinear systems are provided. The associated fault models including actuator, sensor, and components faults are introduced. In addition, the disturbance and uncertainty models are also presented. The transformation of nonlinear systems into their Lipschitz equivalent models is introduced. Moreover, different classification of faults, for instance, with respect to the sources of faults, with regards to the time-domain behavior, and with reference to process models, are described. Finally, a realistic example of nonlinear three-tank system is presented in order to illustrate the underlying philosophy.

3.1 State-space representation of nonlinear systems

Depending on the process dynamics and modeling objectives, there exist a number of ways to represent process behavior. Among them, the state-space representation is most widely used. To this end, consider a nonlinear system governed by the following set of differential equations

$$\dot{x}(t) = g(x(t), u(t)), \qquad x(0) = \zeta_0 \tag{3.1}$$
$$y(t) = h(x(t), u(t)) \tag{3.2}$$

An input-affine version of the above system is

$$\begin{aligned} \dot{x}(t) &= f(x(t)) + G(x(t))u(t), \qquad x(0) = \zeta_0 \\ y(t) &= h(x(t)) + H(x(t))u(t) \end{aligned} \tag{3.3}$$

In order to get a discrete model of (3.3), Euler discretization is used. Note that exact discretization of nonlinear systems is very hard to obtain or even sometimes impossible. The so-called Euler discretization are used because it is very easy to derive and it preserves the structure of the original nonlinear model. To this end, a discrete-time counter part of

the process (3.3) can be obtained using the well-known Euler discretization as follows

$$\begin{aligned}\frac{x(k+1)-x(k)}{T_s} &= f(x(k)) + G(x(k))u(k)\\ x(k+1) &= x(k) + T_s f(x(k)) + T_s G(x(k))u(k)\\ &= a(x(k)) + B(x(k))u(k)\\ y(k) &= c(x(k)) + D(x(k))u(k)\end{aligned}$$

or

$$\begin{aligned}x(k+1) &= a(x(k)) + B(x(k))u(k)\\ y(k) &= c(x(k)) + D(x(k))u(k)\end{aligned} \tag{3.4}$$

where T_s is sampling time at which the discretization is performed, ζ_0 denotes the initial conditions, $x(\cdot) \in \mathfrak{R}^n$ represents the state vector, $u(\cdot) \in \mathfrak{R}^p$ is the input vector, and $y(\cdot) \in \mathfrak{R}^m$ denotes the vector of measured outputs. Furthermore, $a(x(k)) = x(k) + T_s f(x(k))$ is the system function, $B(x(k)) = T_s G(x(k))$ represents the matrix function which couples the inputs to the process, $c(x(k)) = h(x(k))$ is the system output function, and $D(x(k)) = H(x(k))$ is the input distribution matrix function which couples the input to the output. Moreover, the following assumptions are made throughout this thesis:

A1. The functions $f(\cdot)$, $G(\cdot)$, $h(\cdot)$, $H(\cdot)$, $a(\cdot)$, $c(\cdot)$, $B(\cdot)$ and $D(\cdot)$ are smooth in their arguments and having appropriate dimensions.

A2. The origin $x_{eq} = 0$ is assumed to be the equilibrium point.

A3. $f(0) = 0$, $h(0) = 0$ and $a(0) = 0$, $c(0) = 0$

A4. The system (3.3) (or the vector field $f(\cdot)$) and (3.4)(or the vector field $a(\cdot)$) is locally asymptotically stable around $x = 0$

Remark 3.1.1. *In the remainder of this thesis, the variable t in the function arguments given in* (3.3) *is dropped for brevity. Furthermore, the time instant k in function arguments given in* (3.4) *is modified as, for example, $x(k) = x_k$.*

3.1.1 Lipschitz equivalent model of nonlinear systems

A Lipschitz nonlinear system can be described as follows

$$\dot{x} = Ax + Bu + \phi(x, u) \tag{3.5}$$

where the nonlinear function $\phi(x, u)$ satisfies the following condition:

$$\|\phi(x_1, u) - \phi(x_2, u)\| \leq \gamma \|x_1 - x_2\| \quad \forall x_1, x_2 \in \mathscr{D} \subset \mathfrak{R}^n, \forall u \in \mathfrak{R}^p \tag{3.6}$$

with γ is known as Lipschitz constant.

Lipschitz nonlinear systems cover a wide range of nonlinear systems. A nonlinear system can be regarded as Lipschitz locally or globally, depending on the domain over which the

Lipschitz condition (3.6) holds. A function $\phi : \mathscr{D}_x \times \mathscr{D}_u \longrightarrow \mathfrak{R}^n$ is said to be Lipschitz locally on a domain (open and connected set) $\mathscr{D} \subset \mathfrak{R}^n$ if each point of $\mathscr{D}$ has a neighborhood $\mathscr{D}_0$ such that ϕ satisfies the Lipschitz conditions (3.6) for all points in $\mathscr{D}_0$ with some Lipschitz constant γ_0. A locally Lipschitz function on a domain $\mathscr{D}$ is not necessarily Lipschitz on $\mathscr{D}$, since the Lipschitz condition may not hold uniformly for all points on $\mathscr{D}$. However, a locally Lipschitz function on a domain $\mathscr{D}$ is Lipschitz on every compact (closed and bounded) subset of $\mathscr{D}$. The function $\phi(x, u)$ is said to be globally Lipschitz if it is Lipschitz on $\mathfrak{R}^n$[98]. The systems involving the sinusoidal nonlinearities are classified as globally Lipschitz nonlinear systems. Similarly, some nonlinearities, for instance polynomial nonlinearities, are termed as locally Lipschitz for a bounded range of system operation.

As mentioned in [136, 137], any nonlinear system of the form $\dot{x} = g(x, u)$ which is smooth in its arguments and having the origin as an equilibrium point for the unforced system, can be transformed into the form given in (3.5), provided the condition (3.6) together with

$$\phi(0, u) = 0 \quad \forall u \in \mathfrak{R}^p \tag{3.7}$$

are satisfied in a local region arround the origin. Pertew et al. [136] mentioned a method which shows that how a nonlinear system can be transformed into its Lipschitz equivalent model in a local region around the origin. This method is elaborated in the following lines.

Let us consider the linearization of (3.1) around the operating point (x^*, u^*) by using Taylor series expansion

$$\dot{x} = \frac{\partial g}{\partial x}\Big|_{x=x^*,u=u^*} x + \frac{\partial g}{\partial u}\Big|_{x=x^*,u=u^*} u + HOT$$

setting $\frac{\partial g}{\partial x}|_{x=x^*,u=u^*} = A$ and $\frac{\partial g}{\partial u}|_{x=x^*,u=u^*} = B$ and ignoring the higher order terms (HOT), then

$$\dot{x} = Ax + Bu \tag{3.8}$$

is referred to as the linearized model of the process (3.1). Note that this is an approximate model for the nonlinear process (3.1). Now taking the nonlinear model (3.1) and the corresponding linearized model (3.8), then

$$\begin{aligned} \dot{x} &= Ax + Bu + \{g(x(t), u(t)) - Ax - Bu\} \\ &= Ax + Bu + \phi(x, u) \end{aligned} \tag{3.9}$$

Note that the system (3.9) is the exact replica of the nonlinear system (3.1). The nonlinear function $\phi(x, u)$ can be regarded as Lipschitz, at least locally. The only assumption needed in this transformation is the linearization. If a system is linearizable at some operating point, then it can be easily transformed into Lipschitz nonlinear system of the form (3.9) for an operating region. Now the question arises that how to compute the Lipschitz constant for a nonlinear function $\phi(x, u)$? A Lipschitz constant can computed in number of ways, for instance, see the reference [136–138]. In this thesis, the method proposed in [136, 137] will be adopted; that is, the Lipschitz constant can be found by computing $\max\{\|\frac{\partial \phi}{\partial x}\|\}$ over the operating range. Since the Lipschitz nonlinear model (3.9) is the exact representation of the nonlinear model (3.1), it can be used for the design of fault

detection schemes for benchmark problems (Chapter 7) whose dynamics are represented by a general nonlinear models (3.1).

In order to get a discrete model of (3.9), Euler discretization is used. To this end, the following approximate discrete-time model for (3.9) is obtained

$$x_{k+1} = A_T x_k + B_T u_k + \phi_T(x_k, u_k) \tag{3.10}$$

where $A_T = I + T_s A$, $B_T = T_s B$ and $\phi_T = T_s \phi$ with T_s is the sampling time. It is worth mentioning that while dealing with Lipschitz nonlinear system, the measurements are assumed linear in this thesis. To this end, the following mathematical model will be used for the analysis:

$$\begin{aligned} \dot{x} &= Ax + Bu + \phi(x, u) \\ y &= Cx + Du \end{aligned} \tag{3.11}$$

for continuous-time, and

$$\begin{aligned} x_{k+1} &= Ax_k + Bu_k + \phi(x_k, u_k) \\ y_k &= Cx_k + Du_k \end{aligned} \tag{3.12}$$

for discrete-time case. Moreover, assume that the unforced systems (3.11) and (3.12) are asymptotically stable in their equilibrium points, that is, $x = 0$ and $x_k = 0$.

Remark 3.1.2. *In the remainder of this chapter, the discrete-time model will be focused. The continuous-time systems can be modeled in a similar way. To this end, the following set of difference equations will be used for an input-affine discrete-time nonlinear systems*

$$\begin{aligned} x_{k+1} &= a(x_k) + B(x_k)u_k \\ y_k &= c(x_k) + D(x_k)u_k \end{aligned} \tag{3.13}$$

Similarly, a discrete-time Lipschitz nonlinear systems will be described as follows:

$$\begin{aligned} x_{k+1} &= Ax_k + Bu_k + \phi(x_k, u_k) \\ y_k &= Cx_k + Du_k \end{aligned} \tag{3.14}$$

3.2 Representation of disturbances and uncertainties

In practice, a technical system is always prone to environmental disturbances, measurement and process noises as well as unexpected changes within the technical process itself. All these factors are often modeled as unknown input vector, in particular, in the FDI framework. These unknown inputs can be denoted by $w \in \mathfrak{R}^q$. w will also be called as disturbance vector. The same terminology is adopted throughout this work. The system (3.13) can be extended as

$$\begin{aligned} x_{k+1} &= a(x_k) + B(x_k)u_k + E_w(x_k)w_k \\ y_k &= c(x_k) + D(x_k)u_k + F_w(x_k)w_k \end{aligned} \tag{3.15}$$

and for Lipschitz nonlinear systems (3.14) as

$$\begin{aligned} x_{k+1} &= Ax_k + \phi(x_k, u_k) + Bu_k + E_w w_k \\ y_k &= Cx_k + Du_k + F_w w_k \end{aligned} \tag{3.16}$$

where E_w and F_w are the disturbance distribution matrices of compatible dimensions. It is worth noting that modeling of a system is very involved task and further, it is very hard to model a system perfectly. A few reasons are: the unknown changes within the process, external environment, multiple coupling between different process components etc. The difference between the nominal model and the reality always exist, which is represented by model uncertainty. There exist a number of ways to represent model uncertainty in the process models. It can be norm-bounded or polytopic type of uncertainties, structured or unstructured. The interested reader is referred to [1] for the detailed description of uncertainty representation in FDI framework. For this analysis and synthesis, the norm-bounded uncertainty will be used in this thesis. To this end, the system (3.15) is given as follows

$$\begin{aligned} x_{k+1} &= a(x_k) + B(x_k)u_k + E_w(x_k)w_k + \eta_1(x_k, u_k, k) \\ y_k &= c(x_k) + D(x_k)u_k + F_w(x_k)w_k + \eta_2(x_k, u_k, k) \end{aligned} \tag{3.17}$$

and the Lipschitz nonlinear model (3.16) is represented as

$$\begin{aligned} x_{k+1} &= Ax_k + \phi(x_k, u_k) + Bu_k + E_w w_k + \eta_1(x_k, u_k, w_k, k) \\ y_k &= Cx_k + Du_k + F_w w_k + \eta_2(x_k, u_k, w_k, k) \end{aligned} \tag{3.18}$$

where η_1 and η_2 represents the model uncertainties. For the process (3.18), the uncertainties η_1 and η_2 are represented as

$$\begin{aligned} \eta_1(x_k, u_k, w_k, k) &= \Delta A x_k + \Delta B u_k + \Delta E_w w_k \\ \eta_2(x_k, u_k, w_k, k) &= \Delta C x_k + \Delta D u_k + \Delta F_w w_k \end{aligned}$$

The resultant system model can be expressed as

$$\begin{aligned} x_{k+1} &= \bar{A}x_k + \phi(x_k, u_k) + \bar{B}u_k + \bar{E}_w w_k \\ y_k &= \bar{C}x_k + \bar{D}u_k + \bar{F}_w w_k \end{aligned} \tag{3.19}$$

with
$\bar{A} = A + \Delta A$, $\bar{B} = B + \Delta B$, $\bar{C} = C + \Delta C$, $\bar{D} = D + \Delta D$, $\bar{E}_w = E_w + \Delta E_w$ and $\bar{F}_w = F_w + \Delta F_w$.
where

$$\begin{bmatrix} \Delta A & \Delta B & \Delta E_w \\ \Delta C & \Delta D & \Delta F_w \end{bmatrix} = \begin{bmatrix} E \\ F \end{bmatrix} \Delta(k) \begin{bmatrix} G & H & J \end{bmatrix}$$

with E,F, G, H and J are known matrices having appropriate dimension and $\Delta(k)$ is bounded in the sense

$$\Delta^T(k)\Delta(k) \leq I \tag{3.20}$$

3.3 Representation of faults in nonlinear systems

A *fault* is regarded as an unacceptable (un-permitted) deviation of at least one characteristic property or parameter of the process from its acceptable standard and healthy operation. Faults may arise in sensors, actuators, or in the process components. There exist a number of ways to model faults. The following model is adopted in this thesis:

$$\begin{aligned} x_{k+1} &= a(x_k) + \Delta a(x_k, f_k) + B(x_k)u_k + E_w(x_k)w_k + \eta_1(x_k, u_k, k) + E_f(x_k)f_a \\ y_k &= c(x_k) + \Delta c(x_k, f_k) + D(x_k)u_k + F_w(x_k)w_k + \eta_2(x_k, u_k, k) + F_f(x_k)f_s \end{aligned} \tag{3.21}$$

for input-affine nonlinear systems, and

$$\begin{aligned} x_{k+1} &= (\bar{A} + \Delta A_F)x_k + \phi(x_k, u_k) + \bar{B}u_k + \bar{E}_w w_k + E_f f_k \\ y_k &= (\bar{C} + \Delta C_F)x_k + \bar{D}u_k + \bar{F}_w w_k + F_f f_k \end{aligned} \tag{3.22}$$

for Lipschitz nonlinear systems. Where $\Delta a(x_k, f_k)$,$\Delta c(x_k, f_k)$, ΔA_F, ΔC_F, $E_f(\cdot)$, $F_f(\cdot)$, E_f and F_f indicate the place where a fault occurs and its influence on the system components. It is worth noting that both faults and unknown inputs are introduced as exogenous inputs acting on the system (3.21) and (3.22). Thus, from the system theoretic view point, there is no difference between faults and unknown inputs. The difference between the two is rather subjective; that is, fault belongs to set of those external inputs which is required to be detected while unknown inputs are those inputs whose effects are compensated and tolerated. The unknown inputs are present from the beginning of the process operation and their influence on the system is distributed throughout the process operation while fault does not necessarily to be present in the beginning. Further, the following assumptions on fault and unknown inputs will be made throughout this thesis:

(i) Both faults and unknown inputs are assumed to be deterministic time functions

(ii) Both fault and unknown inputs are $\mathscr{L}_2$−norm bounded.

In the following, different sources of the faults and their types are described.

3.3.1 Types of faults

Faults can be classified in a number of ways, for instance, based on the sources of faults, the time domain behavior, or with regards to the process models. The following lines describes these categories in a bit detail:

Types of faults based on their sources

Faults in the process arises due actuator abnormalities, sensor malfunctioning, or abnormalities in the process components. Based on these sources, faults can mainly be divided into the following three categories [1]:

- **actuator fault (f_a):** These can be regarded as abnormal changes in the actuator. In many technical systems, the output of a control system can not be directly applied to

a process. Actuators transform the control signal to a signal suitable for a particular system, for example, torque, force, etc. Faults in the actuators affect not only the system performance but sometimes may lead to a complete system breakdown [139]. These faults, in general, include stuck-open, stuck-close, and abnormal leakage in control valve, faults in pumps [139, 140]. Figure 3.1 shows the graphical depiction of some types of actuator faults.

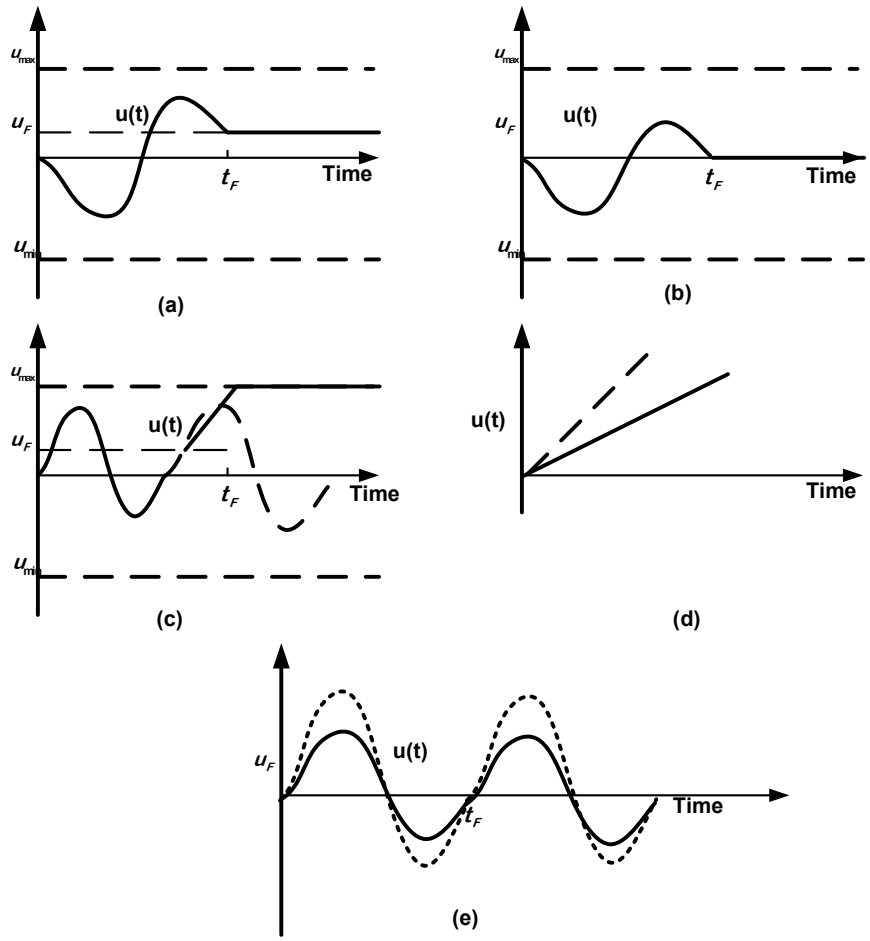

Figure 3.1: Graphical depiction of common types of actuator faults. Dotted lines show the desired value of actuator and the solid lines show actual value. (a)Lock-in-place (b) Float (c) Hard-over (d) Loss of effectiveness [139, 140] (e) scaling fault

- **sensor fault** (f_s)**:** These are the abnormal changes occurred in the process measurement due to the sensor malfunctioning. Sensors are basically the output interface of a system to the external world, and convey information about a system's behavior and its internal states. Therefore sensor faults may cause substantial performance degradation of a system. These faults may cause severe effect, especially when the sensor measurements are used for control purposes. In which case, sensor fault some-

times cause complete system breakdown, when not handled at very early stage[13]. Typical sensor faults include: bias, drift, performance degradation (or loss of accuracy), sensor freezing and calibration error (or scaling) [1, 139, 140]. Figure 3.2 shows the graphical representation of various kinds of sensor faults.

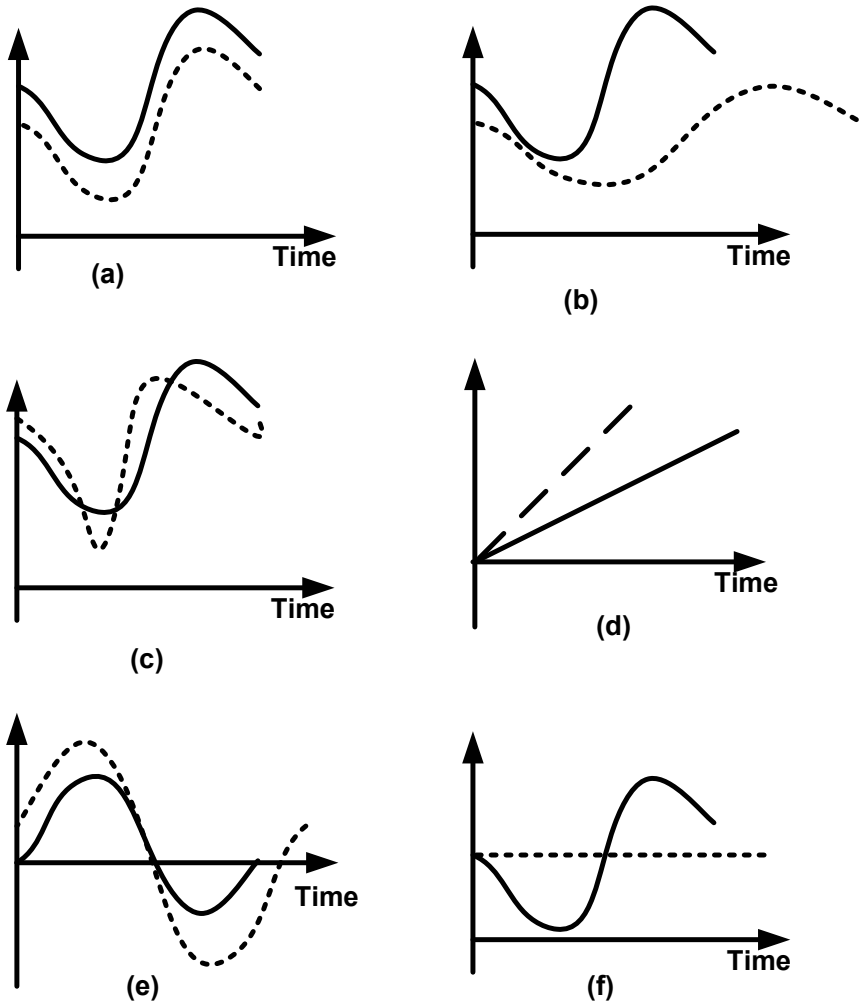

Figure 3.2: Graphical view of different sensor faults; Dotted line shows the measured value and the solid line shows the actual value (a) Bias (b) Drift (c) Loss of accuracy (d) Calibration error [139] (e) Scaling (f) sensor freezing

- **process fault:** These faults describes the malfunctions with in the process itself. It can also be regarded as component fault which shows the fault in the process component. Wear and tear, aging of a components are the main causes of these faults. Some example include leakage in tanks in a chemical process; body damage faults in aerial vehicles (damage of control surfaces); breaks and/or cracks in the gearbox in vehicles; friction faults due to lubricant deterioration; bearing faults in

rotational equipments [139].

Types of faults based on their time-domain behavior

Faults can also be described based on the time domain interpretation. A fault which arises suddenly like a step-up or step-down functions is regarded as *abrupt fault*. Similarly, a fault which develops slowly with time is called *incipient fault*. In practice, both the constant slope and variable slope incipient faults can be observed. Further, fault which appears at discrete interval is known as *intermittent fault*. Figure 3.3 shows the pictorial representation of such faults. It is wroth noting that abrupt faults and intermittent faults have a severe effect on the component of process, but luckily, these can be easily detected. On the other hand, incipient fault doest not affect the system instantly and due to the slowly growing nature, it can not be detected quickly, but in a long process operation, these has also severe effect.

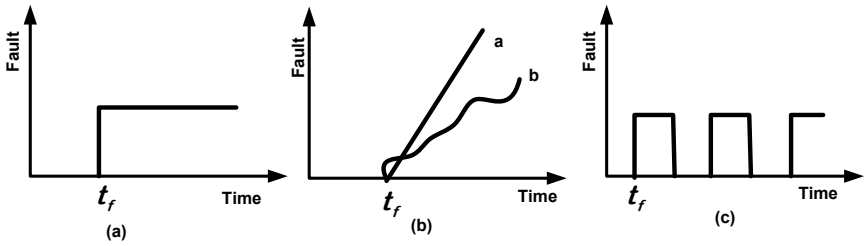

Figure 3.3: Graphical view of faults based on their time-domain representation; (a) Abrupt fault (b) Incipient fault of constant as well as variable slop (c) Intermittent fault

Types of faults with regards to the process models

With regards to process models, faults can be described as additive fault or multiplicative faults. Faults shown in the system model (3.22), which influence the process through E_f and F_f are termed as additive faults. The faults shown by $E_f(x_k)$, $F_f(x_k)$, $\Delta a(x_k, f_k)$, $\Delta c(x_k, f_k)$, ΔA_F and ΔC_F in the system models (3.21) and (3.22) are called multiplicative faults. Generally speaking, additive faults do not affect the system stability, irrespective of if the feedback control loop is integrated into the system under observation [1], however, it is not the case for nonlinear systems represented by (3.21). In this model, the faults f_a and f_s seem to appear in additive way, however due to the coupling with the system states, it will affect the system stability. On the other hand, E_f does not depend on the system states in the system model (3.22),, and therefore, fault (f_a) will not affect the stability of the system. The multiplicative faults cause changes in the model parameters, independent of if a sensor fault, actuator fault, or components fault, and generally modeled as parameter changes. Since multiplicative faults directly influence the parameters of the system, it affects the system stability. Note that as mentioned in [1], the multiplicative faults can be modeled as additive faults.

For the purpose of designing fault detection scheme for nonlinear systems, the following system models will be used in the subsequent chapters

$$\begin{aligned} x_{k+1} &= a(x_k) + B(x_k)u_k + E_w(x_k)w_k + \eta_1(x_k, u_k, k) + E_f(x_k)f_k \\ y_k &= c(x_k) + D(x_k)u_k + F_w(x_k)w_k + \eta_2(x_k, u_k, k) + F_f(x_k)f_k \end{aligned} \tag{3.23}$$

for input affine discrete-time nonlinear systems, and

$$\begin{aligned} x_{k+1} &= \bar{A}x_k + \phi(x_k, u_k) + \bar{B}u_k + \bar{E}_w w_k + E_f f_k \\ y_k &= \bar{C}x_k + \bar{D}u_k + \bar{F}_w w_k + F_f f_k \end{aligned} \tag{3.24}$$

for Lipschitz nonlinear systems.

3.4 An example: A nonlinear three-tank system subject to faults and disturbances

A three-tank system, as shown in Figure 3.4, is utilized to illustrate the discussion carried out in this chapter. Since all types of faults can possibly be observed in this system and furthermore, the disturbances are also available, it is a nice candidate for elaborating the theory developed in this chapter. This example will also serve for demonstrating subsequently developed methods for residual generation and threshold computation.

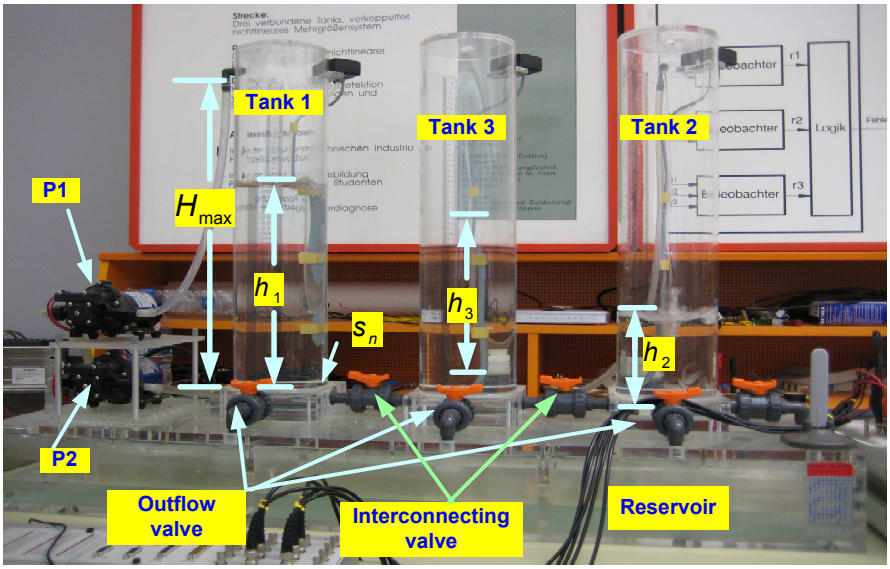

Figure 3.4: Three-tank system (DTS 200)

The three-tank system consists of three cylindrical tanks T_1, T_2, and T_3 each of cross sectional area A_c. These tanks are connected to each other through cylindrical pipes of cross sectional area s_n. There is a valve in tank T_2 for the water outflow. The outflow water goes to the reservoir. The water from the reservoir can be pumped into T_1 and

T_2 with the the help of two pumps P_1 and P_2 having mass flow-rate $Q_1(t)$ and $Q_2(t)$ respectively. The water level in a tank T_i is represented by $h_i(t)$ which can be measured by piezoresistive pressure meter. The maximum water level in any tank can be denoted by H_{max}. For our purpose, the following nonlinear model is used which has been derived using the incoming and outgoing mass flows under consideration of Torricellies law [141]

$$\begin{aligned} A_c\dot{h_1} &= Q_1 - Q_{13} \\ A_c\dot{h_2} &= Q_2 + Q_{32} - Q_{20} \\ A_c\dot{h_3} &= Q_{13} - Q_{32} \end{aligned} \tag{3.25}$$

where

$$\begin{aligned} Q_{13} &= a_1 s_{13}\text{sgn}(h_1 - h_3)\sqrt{2g|h_1 - h_3|} \\ Q_{32} &= a_3 s_{23}\text{sgn}(h_3 - h_2)\sqrt{2g|h_3 - h_2|} \\ Q_{20} &= a_2 s_0\sqrt{2gh_2} \end{aligned}$$

and sgn is known as signum functions which is defined as

$$sgn(x) = \begin{cases} -1 & \text{if } x < 0 \\ 0 & \text{if } x = 0 \\ 1 & \text{if } x > 0 \end{cases}$$

The incoming mass flows $Q_1(t)$, $Q_2(t)$ are considered as process input and the water levels $h_1(t)$ and $h_2(t)$ in Tanks 1 and 2 are the process output. The three circular tanks have the same cross section A_c and are interconnected via circular pipes with cross sections s_{13}, s_{23}. The outlet pipe is also circular with cross section s_0. a_1,a_2, and a_3 are scaling constants and g is the gravity constant. All the technical data for DTS200 is given in appendix C.1.

Defining $\begin{bmatrix} x_1^T & x_2^T & x_3^T \end{bmatrix}^T = \begin{bmatrix} h_1^T & h_2^T & h_3^T \end{bmatrix}^T$ and $\begin{bmatrix} u_1^T & u_2^T \end{bmatrix}^T = \begin{bmatrix} Q_1^T(t) & Q_2^T(t) \end{bmatrix}^T$, then (3.25) can be represented as

$$\begin{aligned} \dot{x} &= f(x) + G(x)u \\ y &= h(x) \end{aligned} \tag{3.26}$$

where

$$f(x) = \frac{1}{A_c}\begin{bmatrix} -a_1 s_{13}\text{sgn}(x_1 - x_3)\sqrt{2g|x_1 - x_3|} \\ a_3 s_{23}\text{sgn}(x_3 - x_2)\sqrt{2g|x_3 - x_2|} - a_2 s_0\sqrt{2gx_2} \\ a_1 s_{13}\text{sgn}(x_1 - x_3)\sqrt{2g|x_1 - x_3|} - a_3 s_{23}\text{sgn}(x_3 - x_2)\sqrt{2g|x_3 - x_2|} \end{bmatrix},$$

$$G(x) = \frac{1}{A_c}\begin{bmatrix} 1 & 0 \\ 0 & 1 \\ 0 & 0 \end{bmatrix} \quad \text{and} \quad h(x) = \begin{bmatrix} x_1 \\ x_2 \end{bmatrix} = Cx$$

A discrete-time version of the above model is described by the following difference equations

$$\begin{aligned} x_{k+1} &= a(x_k) + Bu_k \\ y_k &= Cx_k \end{aligned} \tag{3.27}$$

where $a(x_k) = x_k + Tf(x_k)$, $B = TG$, and $C = I_2$.

3.4.1 Description of faults and disturbances

In three-tank system, both additive and multiplicative faults can be realized. The additive faults include the faults in the pumps and faults in the sensors measuring the water levels in different tanks. The multiplicative faults are leaks in a particular tank to the reservoir and leakage between the tanks. These leakage faults are regarded as component faults or process fault. Since multiplicative faults can be modeled as additive faults, the leakage faults in three-tanks system will be treated as additive faults in this thesis. A more detail about these faults, for instance, how they arises and what are their effects, will be described in Chapter 7.

The source of disturbances in DTS200 is the water bubbles due to the fall of water from the each pump and measurement noises in sensors measuring the water level. These disturbances are modeled as output disturbances. The faults and disturbances described above may be incorporated in the state-space realization of three-tank system (3.27) as follows:

$$\begin{aligned} x_{k+1} &= a(x_k) + Bu_k + E_f f_k \\ y_k &= Cx_k + F_w w_k + F_f f_k \end{aligned} \tag{3.28}$$

$$E_f = [0_{3\times 2}\ B\ I_{3\times 2}] \in \mathfrak{R}^{3\times 6},\ F_f = [I_2\ 0_{2\times 4}] \in \mathfrak{R}^{2\times 6}; F_w = I_2;$$
$$f_k = [f_1\ f_2\ f_3\ f_4\ f_5\ f_6]^T, w_k = [w_1\ w_2]^T$$

3.5 Summary

In this chapter, the state-space models of nonlinear systems and their transformation to Lipschitz equivalent models were introduced. It was also illustrated that how faults, unknown inputs, and model uncertainties can be incorporated into input-affine nonlinear systems and in Lipschitz nonlinear systems. A framework for discrete-time Lipschitz nonlinear systems and input affine nonlinear systems was developed while a road-map for continuous-time nonlinear system was also provided. A classification of faults based on their source, time-domain behavior, and with regards to process models was introduced. The effects of various types of faults on system performance has also bee discussed. Finally, the concepts of faults and disturbance modeling in nonlinear systems was illustrated with the help of a realistic example; that is, nonlinear three-tank system subject to faults and disturbances.

Chapter 4

Optimal residual generation: $\mathscr{H}_-$, $\mathscr{H}_\infty$, and $\mathscr{H}_-/\mathscr{H}_\infty-$ optimization

The objective of this chapter is to design fault detection filter (FDF) for input-affine discrete-time nonlinear systems using $\mathscr{H}_-$−index, $\mathscr{H}_\infty$−norm, and mixed $\mathscr{H}_-/\mathscr{H}_\infty-$ optimization. In order to facilitate the study on optimal fault detection of nonlinear systems, the time domain definitions of $\mathscr{H}_-$−index is proposed and that of $\mathscr{H}_\infty$−norm is obtained from the literature on robust control theory of nonlinear systems. Based on the above optimization indices, three problems are formulated. These include: $\mathscr{H}_-$−FDF which is used to design an FDF in order to acquire maximum possible sensitivity of the residual to the best-case fault in the system, $\mathscr{H}_\infty$−FDF which results into an FDF attaining robustness of the residual against the unknown inputs to a pre-defined level, and the mixed $\mathscr{H}_-/\mathscr{H}_\infty$−FDF which simultaneously provide robustness against unknown inputs and sensitivity to the best-case fault. Using the theory of differential games and dissipation inequalities, sufficient conditions are provided in the form of Hamilton-Jacobi-inequalities. All of these problems are studied, both in finite- and infinite-horizon. It is also shown that the generalized results obtained can be used to study the problem of fault detection for discrete-time linear systems both in finite-horizon as well as over infinite-horizon. Finally, a design example is introduced which illustrates the theory proposed in this chapter.

A residual generator is considered to be a central part in any fault detection scheme. Among all the model-based FD techniques, an observer-based fault detection is one of the most common way of generating residuals. As shown in Figure 4.1, the residual signal is not only affected by faults but also by unknown inputs which include disturbances, measurement noises, and model uncertainties.

It is a widely accepted fact that a fault detection filter (FDF) should be designed in the framework of improving robustness against unknown inputs and sensitivity to faults. To measure robustness against the unknown inputs, $\mathscr{H}_\infty$ norm is extensively used. The $\mathscr{H}_\infty$ norm measures the effect of those unknown inputs which have maximum influence on the residual signal. The disturbance which has maximum effect on the residual signal, is regarded as worst-case disturbance[1]. For LTI systems, it is interpreted by the largest

[1]Since the unknown inputs are modeled as exogenous disturbances in Chapter 3, the term disturbances and unknown inputs will be alternatively used in this study to represent the same meaning.

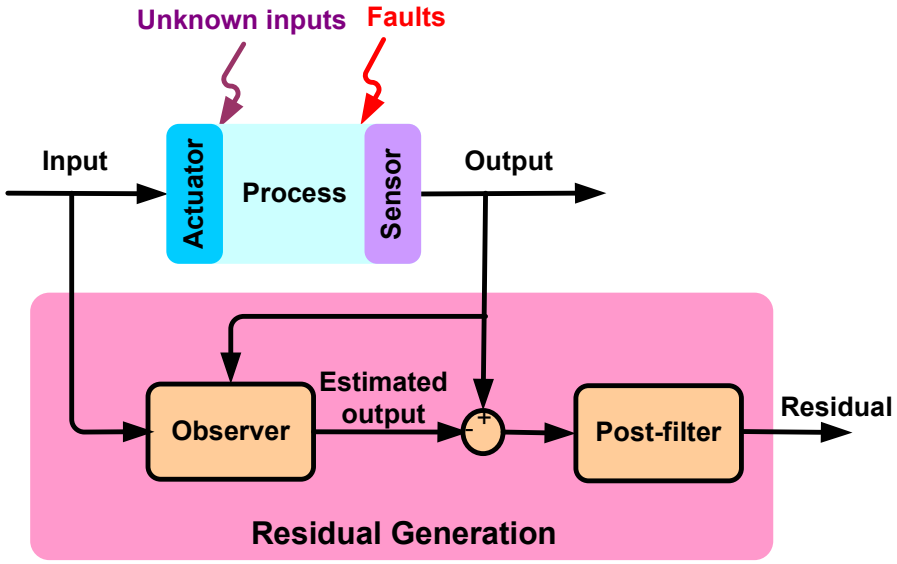

Figure 4.1: Schematic description of optimal residual generation scheme

singular value of the transfer function of the unknown inputs to the residual. Likewise, the sensitivity to faults is measured by the so-called $\mathscr{H}_-$–index. It is the measure of the minimum influence of the fault on the residual signal. In the present thesis, this fault is named as the *best-case fault*. The reason for calling it as a *best-case fault* is rather subjective. Since the influence of such a fault is minimal on the residual signal, it is likely to have minimum effect on the system as well. Due to this reason, this fault has the best effect on the process among all the possible faults. It is, hence, named as the *best-case fault* in this dissertation. From the FD system design view point, the *best-case fault* is of particular interest. The intuitive objective of an FD system is to enhance the effect of such fault on the residual signal so that the detection of the remaining faults become easy. For LTI system, the $\mathscr{H}_-$–index is interpreted by the smallest singular value of the fault to the residual transfer function.

There has been extensive research to address the problem of FDF design using $\mathscr{H}_\infty$– and $\mathscr{H}_-/\mathscr{H}_\infty$, in the context of LTI systems. In particular, the optimal design using $\mathscr{H}_-/\mathscr{H}_\infty$ optimization, initiated in [63] and [64], has received a considerable attention in the recent years, for instance, see [1, 56, 59, 61, 66, 142] and the references therein. Different from LTI systems, most of the research has been focused on designing robust FDF for nonlinear systems, see for instance [58, 113, 131, 133, 143, 144] to list a few. To our knowledge, the problem of designing FDF for nonlinear systems using $\mathscr{H}_-$–index and $\mathscr{H}_-/\mathscr{H}_\infty$ has not been studied. Further, the use of these approaches and even in the context of $\mathscr{H}_\infty$– norm based FDF (besides a very limited contributions in the literature) has not been employed for discrete-time nonlinear systems.

In this chapter, the problem of designing FDF using $\mathscr{H}_-$–, $\mathscr{H}_\infty$–, and $\mathscr{H}_-/\mathscr{H}_\infty$ optimization is studied. Based on these optimization indices, three problems are formulated which include; $\mathscr{H}_-$–FDF, $\mathscr{H}_\infty$– FDF, and the mixed $\mathscr{H}_-/\mathscr{H}_\infty$– FDF. The $\mathscr{H}_-$–index based FDF, addressed in Section 4.2.1 and 4.3.1, aims to enhance sensitivity of the FD system

to the best-case fault, while robustness against unknown inputs is not the primary objective. The $\mathscr{H}_\infty$−norm based FDF, presented in Section 4.2.2 and 4.3.2, admits robustness against the worst-case unknown inputs to the desired level while sensitivity to fault is not the main concern of this scheme. In the mixed $\mathscr{H}_-/\mathscr{H}_\infty$ FDF, presented in Section 4.2.3 and 4.3.3, the objective is to design an FDF which improves robustness against unknown inputs in the sense of $\mathscr{H}_\infty$ and sensitivity to faults in the sense of $\mathscr{H}_-$.

The theory of differential games and dissipation inequalities has been exploited to derive solutions for these problems. Sufficient conditions for the solvability of these problems are derived in the form of Hamilton-Jacobi inequalities together with some side conditions. Note that the optimization indices, $\mathscr{H}_-$−index and $\mathscr{H}_\infty$−norm are initially defined in frequency domain in literature. It is worth noting that the frequency domain analysis can not be extended to nonlinear systems. Another important issue in a typical FD system, is the operation over finite-time (finite-horizon). It is also very difficult to carry out the frequency domain analysis over finite-horizon. Therefore, in order to facilitate the analysis and synthesis of nonlinear FDF design using these optimization indices, the time domain definition of $\mathscr{H}_-$−index and $\mathscr{H}_\infty$−norm have been provided in Section 4.1. This has, in turn, eased the study of FDF design for nonlinear systems.

4.1 Problem formulation

Consider an input-affine discrete-time nonlinear system governed by the following equations

$$\Sigma_{\mathscr{P}}: \begin{cases} x_{k+1} & = a(x_k) + B(x_k)u_k + E_w(x_k)w_k + E_f(x_k)f_k \\ y_k & = c(x_x) + F_w(x_k)w_k + F_f(x_k)f_k \end{cases} \tag{4.1}$$

where $x_k \in \mathfrak{R}^n$ is the state vector, $u_k \in \mathscr{U} \subset \mathfrak{R}^p$ is the vector of admissible inputs, $y_k \in \mathfrak{R}^m$ is the vector of measured outputs, $w_k \in \mathfrak{R}^q$ is the vector of unknown inputs which includes disturbances and measurement noises, $f_k \in \mathfrak{R}^\ell$ is the fault vector which can be sensor, actuator, or component faults. The following assumptions will be used frequently in the remainder of this chapter:

A1. A,B,C,E_f,E_w,F_f, and F_w are smooth functions in x.

A2. w_k and f_k are $\mathscr{L}_2$−norm bounded.

A3. The nonlinear process (4.1) under fault-free operation is finite gain $\mathscr{L}_2$− stable.

For the purpose of fault detection, the following form of a nonlinear fault detection filter (FDF) is employed

$$\Sigma_{\mathscr{F}}: \begin{cases} \hat{x}_{k+1} & = a(\hat{x}_k) + B(\hat{x}_k)u_k + L(\cdot)r_k \\ r_k & = y_k - c(\hat{x}_k) \end{cases} \tag{4.2}$$

where $\hat{x}_k \in \mathfrak{R}^n$ is the estimated state vector, $L(\cdot) \in \mathfrak{R}^{n\times m}$ is the filter (observer) gain matrix which is smooth and has to be determined and $r_k \in \mathfrak{R}^m$ is the vector of residuals. Note that the argument of the filter gain is not specified intentionally, as it will be determined

later. Defining the observation error as $e_k = x_k - \hat{x}_k$, the filter error dynamics can then be represented as follows

$$\begin{aligned} e_{k+1} &= a(x_k, e_k, L) + B(x_k, e_k, L)u_k + E_w(x_k, L)w_k + E_f(x_k, L)f_k \\ r_k &= c(x_k, e_k) + F_w(x_k)w_k + F_f(x_k)f_k \end{aligned} \tag{4.3}$$

where

$$\begin{aligned} a(x_k, e_k, L) &= a(x_k) - a(x_k - e_k) - L(\cdot)c(x_k, e_k), \quad c(x_k, e_k) = c(x_k) - c(x_k - e_k), \\ B(x_k, e_k, L) &= B(x_k) - B(x_k - e_k), \quad E_w(x_k, L) = E_w(x_k) - L(\cdot)F_w(x_k), \\ E_f(x_k, L) &= E_f(x_k) - L(\cdot)F_f(x_k), \end{aligned}$$

Combining the system (4.1) and filter error system (4.3), the following augmented form of the residual generator is obtained

$$\Sigma_{\mathscr{R}} : \begin{cases} x_{0,k+1} & = g_0(x_{0,k}, w_{0,k}, f_{0,k}) \\ & = a_0(x_{0,k}) + E_{0,w_0}(x_{0,k})w_{0,k} + E_{0,f_0}(x_{0,k})f_{0,k} \\ r_{0,w_0,f_0,k} & = c_0(x_{0,k}) + F_{0,w_0}(x_{0,k})w_{0,k} + F_{0,f_0}(x_{0,k})f_{0,k} \end{cases} \tag{4.4}$$

where $x_{0,k} = \begin{bmatrix} x_k^T & e_k^T \end{bmatrix}^T$, $w_{0,k} = \begin{bmatrix} u_k^T & w_k^T \end{bmatrix}^T$, $f_{0,k} = f_k$,

$$a_0(x_{0,k}) = \begin{bmatrix} a(x_k) \\ a(x_k, e_k, L) \end{bmatrix}, E_{0,w_0}(x_{0,k}) = \begin{bmatrix} B(x_k) & E_w(x_k) \\ B(x_k, e_k, L) & E_w(x_k, L) \end{bmatrix},$$

$$E_{0,f_0}(x_{0,k}) = \begin{bmatrix} E_f(x_k) \\ E_f(x_k, L) \end{bmatrix}, F_{0,f_0}(x_{0,k}) = F_f(x_k),$$

$$c_0(x_{0,k}) = c(x_k, e_k), F_{0,w_0}(x_{0,k}) = \begin{bmatrix} 0 & F_w(x_k) \end{bmatrix}$$

Recall that the robustness against the worst-case disturbance is defined in terms of $\mathscr{H}_\infty$ norm while sensitivity to best-case fault is interpreted in terms of $\mathscr{H}_-$−index. Note that these indices are defined in frequency domain for LTI systems which can not be used while studying the FD problem in nonlinear systems. Furthermore, looking from a practical view point, it is more reasonable to study the system performance over a finite-horizon. In such a situation, the frequency domain analysis can not be used. Therefore, the time-domain definitions of these indices are provided. Due to which the problem of fault detection in nonlinear systems using $\mathscr{H}_\infty$, $\mathscr{H}_-$, and $\mathscr{H}_-/\mathscr{H}_\infty$-optimizations, can be easily handled. The definitions are provided based on the residual generator (4.4), however, it can be generalized to any nonlinear system.

Definition 4.1.1. *Given the discrete-time nonlinear system $\Sigma_{\mathscr{R}}$ (4.4), the $\mathscr{H}_-$−index is defined as*

$$||\Sigma_{\mathscr{R}}||_- = \inf_{f_{0,k} \neq 0} \frac{||r_{0,f_0,k}||_2}{||f_{0,k}||_2}$$

For finite-horizon, that is, $[0, K]$*, it is defined as*

$$\|\Sigma_{\mathscr{R}}\|_{-,[0,K]} = \inf_{f_{0,k}\neq 0} \frac{\|r_{0,f_0,k}\|_{2,[0,K]}}{\|f_{0,k}\|_{2,[0,K]}}$$

Moreover, the $\mathscr{H}_-$*−index is said to be larger than some positive number* β *over finite-horizon, if the following condition holds*

$$\sum_{k=0}^{K} \|r_{0,f_0,k}\|^2 \geq \beta^2 \sum_{k=0}^{K} \|f_{0,k}\|^2 \quad \forall f_{0,k} \neq 0 \tag{4.5}$$

where $r_{0,f_0,k}$ *is the residual affected by faults only, while the disturbances are assumed to be zero.*

Definition 4.1.2. *Given the discrete-time nonlinear system* $\Sigma_{\mathscr{R}}$ (4.4)*, the* $\mathscr{H}_\infty$ *norm is defined as*

$$\|\Sigma_{\mathscr{R}}\|_\infty = \sup_{w_{0,k}\neq 0} \frac{\|r_{0,w_0,k}\|_2}{\|w_{0,k}\|_2}$$

For finite-horizon case, that is, $[0, K]$*, it is defined as*

$$\|\Sigma_{\mathscr{R}}\|_{\infty,[0,K]} = \sup_{w_{0,k}\neq 0} \frac{\|r_{0,w_0,k}\|_{2,[0,K]}}{\|w_{0,k}\|_{2,[0,K]}}$$

Further, the $\mathscr{H}_\infty$ *norm for a given scalar* $\alpha > 0$ *over finite-horizon is defined as*

$$\sum_{k=0}^{K} \|r_{0,w_0,k}\|^2 \leq \alpha^2 \sum_{k=0}^{K} \|w_{0,k}\|^2 \quad \forall w_{0,k} \neq 0 \tag{4.6}$$

where $r_{0,w_0,k}$ *is the residual signal affected by disturbances under fault-free condition.*

In the following lines, the optimization problems; i.e., $\mathscr{H}_-$–FDF, $\mathscr{H}_\infty$–FDF, and mixed $\mathscr{H}_-/\mathscr{H}_\infty$–FDF, are formulated:

Problem 4.1.1. $\mathscr{H}_-$**– FDF [(sub-) optimal] design**
Given the input-affine discrete-time nonlinear system (4.1)*, the FDF* (4.2)*, a scalar* $\beta > 0$*, find the filter gain* $L(\cdot)$ *such that the* $\mathscr{H}_-$*– gain of the residual generator* $\Sigma_{\mathscr{R}}$ (4.4) *is greater than or equal to* β*; that is, the condition* (4.5) *holds.*

Problem 4.1.2. $\mathscr{H}_\infty$**– FDF [(sub-) optimal] design**
Given the input-affine discrete-time nonlinear system (4.1)*, the FDF* (4.2)*, a scalar* $\alpha > 0$*, find the filter gain* $L(\cdot)$ *such that the* $\mathscr{H}_\infty$*– norm of the residual generator* $\Sigma_{\mathscr{R}}$ (4.4) *is less than or equal to* α*; that is, the condition* (4.6) *holds.*

Problem 4.1.3. $\mathscr{H}_-/\mathscr{H}_\infty$**– FDF [(sub-) optimal] design**
Given the input-affine discrete-time nonlinear system (4.1)*, the FDF* (4.2)*, and two scalars* $\alpha > 0$ *and* $\beta > 0$*, find the filter gain* $L(\cdot)$ *such that the following constraints are simultaneously satisfied,*

(i) the $\mathscr{H}_\infty-$ norm of the residual generator $\Sigma_{\mathscr{R}}$ (4.4) is less than or equal to α, that is,

$$\sum_{k=0}^{K} \|r_{0,w_0,k}\|^2 \leq \alpha^2 \sum_{k=0}^{K} \|w_{0,k}\|^2 \tag{4.7}$$

(ii) the $\mathscr{H}_-$ gain of the residual generator $\Sigma_{\mathscr{R}}$ (4.4) is greater than or equal to β, that is,

$$\sum_{k=0}^{K} \|r_{0,f_0,k}\|^2 \geq \beta^2 \sum_{k=0}^{K} \|f_{0,k}\|^2 \tag{4.8}$$

the FDF (4.2) simultaneously satisfying the above constraints is regarded as mixed $\mathscr{H}_-/\mathscr{H}_\infty$ FDF and is said to be (sub-) optimal in the sense of $\mathscr{H}_-/\mathscr{H}_\infty$.

Remark 4.1.1. *The above problems are the finite-horizon problems. It become infinite-horizon problems if $K \to \infty$.*

4.2 Solution to optimal FDF for finite-horizon

In this section, the problem of optimal FDF design for discrete-time nonlinear systems over finite-horizon is studied. First, sufficient conditions for the solvability of $\mathscr{H}_-$–FDF are given. Then, a solution to the problem of $\mathscr{H}_\infty-$ FDF is presented. Both of the above problems are formulated in the framework of zero-sum differential games. Note that the theory of differential games is advantageous in the sense that extreme values can be handled very easily. The interested reader is referred to [145, 146] for acquiring knowledge about differential games and their different formulations in control and filtering problems. Next, sufficient conditions for the solvability of $\mathscr{H}_-/\mathscr{H}_\infty$–FDF are given. Finally, the proposed approach is shown to be useful to study optimal FD problem for LTI systems.

4.2.1 FDF design based on $\mathscr{H}_-$–index (HminNLFDF)

Consider the the sensitivity constraints defined in (4.5). In view of game theory, a game is described by the residual generator (4.4) with the following finite-horizon cost functional

$$\mathcal{J}_1(L(\cdot), f_{0,k}) = \sum_{k=0}^{K} \left\{ \|r_{0,f_0,k}\|^2 - \beta^2 \|f_{0,k}\|^2 \right\} \tag{4.9}$$

Note that (4.5) holds if $\mathcal{J}_1 \geq 0$. This may be viewed as a two-player zero-sum differential game. A filter gain $L(\cdot)$ desires to maximize $\mathcal{J}_1$ while fault wishes to minimize it. In other words, the objective is to design a filter which maximizes the minimal effect of fault on the residual signal. An equilibrium point solution for the game (4.9) and (4.4) is said to be existing if it is possible to find a pair $(L^*_{\hat{x}_k,k}, f^*_{0,k})$ such that

$$\mathcal{J}_1(L^*(\cdot), f_{0,k}) \leq \mathcal{J}_1(L^*(\cdot), f^*_{0,k}) \leq \mathcal{J}_1(L(\cdot), f^*_{0,k}) \quad \forall L(\cdot) \in \mathfrak{R}^{n\times m}, f_{0,k} \in \mathfrak{R}^{\ell} \tag{4.10}$$

In order to arrive at a solution to this problem, sufficient conditions are given in the form of discrete-time Hamilton-Jacobi-Isaacs equation (HJIE) as

$$\begin{aligned} Y_k(x_{0,k}) &= \sup_{L_{\hat{x}_k,k}\in\mathfrak{R}^{n\times m}} \inf_{f_{0,k}\in\mathfrak{R}^q} \left\{ Y_{k+1}(x_{0,k+1}) + \frac{1}{2}(\|r_{0,f_{0,k}}\|^2 - \beta^2\|f_{0,k}\|^2) \right\} \\ Y_k(x_{0,k}) &= \frac{1}{2}(\|r_{0,f_0^*,k}\|^2 - \beta^2\|f_{0,k}^*\|_2^2) + Y_{k+1}(g_0(x_{0,k}, f_{0,k}^*)) \end{aligned} \tag{4.11}$$

where a function $Y_k(\cdot) : [0, N] \times \mathfrak{R}^n$ is the solution of the above discrete-time HJIE. The following lemma gives a solution for the desired filter.

Lemma 4.2.1. *Consider the input-affine discrete-time nonlinear system* (4.1)*, the FDF* (4.2)*, and the residual generator* (4.4)*. Assume, there exists a negative definite function* $Y_k(\cdot)$[2]*, a smooth function* $L(\cdot)$ *and a scalar* $\beta > 0$ *satisfying the following discrete-time Hamilton-Jacobi-Isaac's equation (HJIE)*

$$\mathcal{H}_1(x_{0,k}, f_{0,k}^*, L^*(\cdot), Y) = Y_{k+1}(g_0(x_{0,k}, f_{0,k}^*)) - Y_k(x_{0,k}) + \frac{1}{2}(\|r_{0,f_0^*,k}\|^2 - \beta^2\|f_{0,k}^*\|^2) = 0 \tag{4.12}$$

together with the following side conditions

$$f_0^* = -\left(F_{0,f_0}^T F_{0,f_0} - \beta^2 I\right)^{-1} \left\{ E_{0,f_0}^T \left.\frac{\partial Y}{\partial \eta}(\eta)\right|_{\eta=g_0(x_{0,k},f_{0,k})} + F_{0,f_0}^T C_0 \right\} \tag{4.13}$$

$$E_{0,f_0}^T \left.\frac{\partial^2 Y}{\partial \eta^2}(\eta)\right|_{\eta=g_0(x_{0,k},f_{0,k})} E_{0,f_0} + F_{0,f_0}^T F_{0,f_0} - \beta^2 I \Big|_{x_0=0;f_0=0} > 0 \tag{4.14}$$

$$L^*(\cdot) = \arg\max_L \mathcal{H}_1(x_{0,k}, f_{0,k}^*, L(\cdot), Y) \tag{4.15}$$

$$\left.\frac{\partial^2 \mathcal{H}_1}{\partial L^2}(x_{0,k}, f_{0,k}^*, L(\cdot), Y)\right|_{x_{0,k}=0} < 0 \tag{4.16}$$

then

(i) there exists a unique equilibrium solution $(f_0^*, L^*(\cdot))$ *for the game* (4.9) *and* (4.4)

(ii) the FDF with filter gain $L(\cdot)$ *that satisfies* (4.15)*, solves the sensitivity problem* (4.5)*.*

Proof. Define a Hamiltonian function

$$\mathcal{H}_1(x_{0,k}, f_{0,k}, L(\cdot), Y) = Y_{k+1}(g_0(x_{0,k}, f_{0,k})) - Y_k(x_{0,k}) + \frac{1}{2}(\|r_{0,f_0,k}\|^2 - \beta^2\|f_{0,k}\|^2) \tag{4.17}$$

[2] $Y_k(\cdot) = Y(\cdot, k)$

then using some straightforward calculations, necessary conditions for optimality[3] are given as

$$\left.\frac{\partial \mathcal{H}_1}{\partial f_0}\right|_{f_0=f_0^*} = \left.\frac{\partial Y}{\partial \eta}\right|_{\eta=g_0(x_0,f_0)} E_{0,f_0} + C_0^T F_{0,f_0} + f_0^{*T}\left(F_{0,f_0}^T F_{0,f_0} - \beta^2 I\right) = 0 \tag{4.18}$$

$$f_0^* = -\left(F_{0,f_0}^T F_{0,f_0} - \beta^2 I\right)^{-1}\left\{E_{0,f_0}^T \left.\frac{\partial Y^T(\eta)}{\partial \eta}\right|_{\eta=g_0(x_0,f_0^*)} + F_{0,f_0}^T C_0\right\} = \lambda(x_0, f_0^*) \tag{4.19}$$

Further,

$$\frac{\partial^2 \mathcal{H}_1}{\partial f_0^2} = E_{0,f_0}^T \left.\frac{\partial Y}{\partial \eta}\right|_{\eta=g_0(x_0,f_0^*)} E_{0,f_0} + F_{0,f_0}^T F_{0,f_0} - \beta^2 I$$

is nonsingular at $(x_0, f_0) = (0, 0)$. It is worth noting that f_0^* is an implicit function. By implicit function theorem A.1, there exists an open neighborhood $\mathscr{N} \subset \mathfrak{R}^n$ of $x_0 = 0$ and an open neighborhood $\mathcal{L} \subset \mathfrak{R}^\ell$ of $f_0 = 0$ and a unique mapping $\lambda : \mathscr{N} \to \mathcal{L}$ such that (4.18) has a unique solution $f_{0,k} = \lambda(x_{0,k})$. Now using Taylor series, expanding the Hamiltonian function $\mathcal{H}_1$ around $f_0^* = \lambda(x_0)$

$$\mathcal{H}_1(\cdot, f_0, L(\cdot), \cdot) = \mathcal{H}_1(\cdot, f_0^*, L(\cdot), \cdot) + \frac{1}{2}(f_0 - f_0^*)^T \frac{\partial^2 \mathcal{H}_1}{\partial f_0^2}(f_0 - f_0^*) + O(\|f_0 - f_0^*\|^3) \tag{4.20}$$

Considering the condition (4.14), equation (4.20) implies that

$$\mathcal{H}_1(., f_0, L(\cdot), .) \geq \mathcal{H}_1(., f_0^*, L(\cdot), .) \tag{4.21}$$

Similarly, expanding $\mathcal{H}_1(\cdot, f_0^*, L(\cdot), \cdot)$ around $L^*(\cdot)$, assuming condition (4.15) to hold, then

$$\begin{aligned}\mathcal{H}_1(\cdot, f_0^*, L(\cdot), \cdot) \;=\; & \mathcal{H}_1(\cdot, f_0^*, L^*(\cdot), \cdot) + \frac{1}{2} Tr\left\{\left[I_n \otimes (L(\cdot) - L^*(\cdot))^T\right] \frac{\partial^2 \mathcal{H}_1}{\partial L^2} \times \right. \\ & \left. \left\{\left[I_m \otimes (L(\cdot) - L^*(\cdot))^T\right]\right\}\right\} + O(\|L(\cdot) - L^*(\cdot)\|^3)\end{aligned}$$

using the condition (4.16), it can be seen that

$$\mathcal{H}_1(f_0^*, L^*(\cdot)) \geq \mathcal{H}_1(f_0^*, L(\cdot)) \tag{4.22}$$

Condition (4.21) and (4.22) together implies that

$$\mathcal{H}_1(f_0^*, L(\cdot)) \leq \mathcal{H}_1(f_0^*, L^*(\cdot)) \leq \mathcal{H}_1(f_0, L^*(\cdot)) \tag{4.23}$$

which shows that $(f_0^*, L^*(\cdot))$ is the equilibrium solution for the game (4.9) and (4.4). Substituting $(f_0^*, L^*(\cdot))$ in (4.17), discrete-time HJIE (4.12) is obtained. Thus, the FDF (4.2) with filter gain $L^*(\cdot)$ solves the sensitivity problem (4.5).
This completes the proof. □

[3]The arguments in functions are dropped for notational simplicity, for instance, $E_{0,f} = E_{0,f}(x_{0,k})$. In the remainder of this thesis, this convention will be followed wherever it does not cause ambiguity.

4.2.2 FDF design based on $\mathscr{H}_\infty$-norm (HinfNLFDF)

The robustness requirements of the residual generator (4.4) in terms of $\mathscr{H}_\infty$- constraints can be givens as

$$\sum_{k=0}^{K} \|r_{0,w_0,k}\|^2 \leq \alpha^2 \sum_{k=0}^{K} \|w_{0,k}\|^2 \tag{4.24}$$

which is a typical disturbance attenuation problem. For our purpose, consider the residual generator (4.4) and a finite-horizon cost function given as

$$\mathcal{J}_2(L_{\hat{x}_k,k}, w_{0,k}) = \sum_{k=0}^{K} \left\{ \|r_{0,w_0,k}\|^2 - \alpha^2 \|w_{0,k}\|^2 \right\} \tag{4.25}$$

Note that the $\mathscr{H}_\infty$- constraints (4.24) holds if the cost function (4.25) is made non-positive; that is, $\mathcal{J}_2(L(\cdot), w_{0,k}) \leq 0$. In game theoretic framework, the game is devised between the two opposing players; that is, $L_{\hat{x}_k,k}$ and $w_{0,k}$. In which case player 1 ($w_{0,k}$) wishes to maximize $\mathcal{J}_2$ while player 2 ($L^*(\cdot)$) tries to minimize it. An equilibrium solution is said to exist and admissible if it is possible to find a pair $(L^*(\cdot), w^*_{0,k})$ such that

$$\mathcal{J}_2(L^*(\cdot), w_{0,k}) \leq \mathcal{J}_2(L^*(\cdot), w^*_{0,k}) \leq \mathcal{J}_2(L(\cdot), w^*_{0,k}) \quad \forall L(\cdot) \in \mathfrak{R}^{n\times m}, w_{0,k} \in \mathfrak{R}^{p+q}$$

Sufficient conditions for the solvability of the above game are given in the form of the following discrete-time HJIE

$$\begin{aligned} V_k(x_{0,k}) &= \inf_{L(\cdot)\in\mathfrak{R}^{n\times m}} \sup_{w_{0,k}\in\mathfrak{R}^r} \left\{ \frac{1}{2}\|r_{0,w_0,k}\|^2 - \frac{1}{2}\alpha^2\|w_{0,k}\|^2 + V_{k+1}(x_{0,k+1}) \right\} \\ V_k(x_{0,k}) &= \frac{1}{2}(\|r_{0,w^*_0,k}\|^2 - \alpha^2\|w^*_{0,k}\|^2) + V_{k+1}(g_0(x_{0,k}, w^*_{0,k})) \end{aligned} \tag{4.26}$$

where the function $V(\cdot) : [0, N] \times \mathfrak{R}^n \to \mathfrak{R}$ is the solution of (4.26) and is assumed to be positive (semi-) definite function. It is to be noted that the discrete-time HJIE (4.26) is a necessary and sufficient condition for the existence of (4.25) and hence for (4.24). To this end, the next lemma is useful.

Lemma 4.2.2. *Consider an input-affine nonlinear system of the form* (4.1)*, FDF of the form* (4.2)*, and the residual generator dynamics* (4.4)*. Assume, there exists a positive (semi-) definite function $V_k(\cdot)$, and smooth matrix function $L(\cdot) \in \mathfrak{R}^{n\times m}$ called filter gain satisfying the following discrete-time HJIE*

$$\mathcal{H}_2(x_{0,k}, w^*_{0,k}, L^*(\cdot), V) = V_{k+1}(g_0(x_{0,k}, w^*_{0,k})) - V_k(x_{0,k}) + \frac{1}{2}(\|r_{0,w^*_0,k}\|^2 - \alpha^2\|w^*_{0,k}\|^2) = 0 \tag{4.27}$$

with

$$w^*_0 = -\left(F^T_{0,w_0}F_{0,w_0} - \alpha^2 I\right)^{-1} \times \left\{ E^T_{0,w_0} \left.\frac{\partial V}{\partial \eta}(\eta)\right|_{\eta=g_0(x_{0,k},w^*_{0,k})} + F^T_{0,w_0}C_0 \right\} \tag{4.28}$$

$$\left\{ E_{0,w_0}^T \frac{\partial^2 V}{\partial \eta^2}(\eta)\Big|_{\eta=g_0(x_{0,k},w_{0,k})} E_{0,w_0} + F_{0,w_0}^T F_{0,w_0} - \alpha^2 I \right\}\Big|_{x_{0,k}=0;w_{0,k}=0} < 0 \tag{4.29}$$

$$L^*(\cdot) = \arg\min_L \mathcal{H}_2(x_{0,k}, w_{0,k}^*, L(\cdot), V) \tag{4.30}$$

$$\frac{\partial^2 \mathcal{H}_2}{\partial L^2}(x_{0,k}, w_{0,k}^*, L(\cdot), V)\Big|_{x_{0,k}=0} > 0 \tag{4.31}$$

then

(i) there exist a unique equilibrium solution $\left(w_k^*, L^*(\cdot)\right)$ *for the game* (4.25) *and* (4.4)*;*

(ii) the residual generator (4.4) *has* $\mathscr{L}_2$*−gain less than or equal to* α*;*

(iii) the FDF of the form (4.2) *with filter gain* $L(\cdot)$ *that satisfies* (4.30) *and* (4.25)*, solves the robustness problem with the attenuation level* α*.*

Proof. (i) Define a Hamiltonian function as

$$\mathcal{H}_2(x_{0,k}, w_{0,k}, L(\cdot), V) = V(g_0(x_{0,k}, w_{0,k})) - V(x_{0,k}) + \frac{1}{2}(\|r_{0,w_0,k}\|^2 - \alpha^2 \|w_{0,k}\|^2) \tag{4.32}$$

using a simple calculations yield

$$\frac{\partial \mathcal{H}_2}{\partial w_{0,k}} = \frac{\partial V}{\partial \eta}(\eta)\Big|_{\eta=g_0(x_{0,k},w_{0,k})} E_{0,w_0} + C_0^T F_{0,w_0} + w_{0,k}^T F_{0,w_0}^T F_{0,w_0} - \alpha^2 w_{0,k}^T = 0$$

the worst-case value of the disturbance is

$$w_{0,k}^* = -\left(F_{0,w_0}^T F_{0,w_0} - \alpha^2 I\right)^{-1} \times \left\{ E_{0,w_0}^T \frac{\partial V^T}{\partial \eta^T}(\eta)\Big|_{\eta=g_0(x_{0,k},w_{0,k}^*)} + F_{0,w_0}^T C_0 \right\} = \lambda(x_{0,k}, w_{0,k}^*) \tag{4.33}$$

which shows that $w_{0,k}^*$ is an implicit function. Similarly

$$\frac{\partial^2 \mathcal{H}_2}{\partial w^2} = E_{0,w_0}^T \frac{\partial V}{\partial \eta}\Big|_{\eta=g_0(k,x_{0,k},w_{0,k})} E_{0,w_0} + F_{0,w_0}^T F_{0,w_0} - \alpha^2 I$$

is nonsingular at $(x_0, w_0) = (0, 0)$, which, further, shows that $w_{0,k}^*$ defined in (4.28), is the worst-case disturbance. By the implicit function theorem A.1, there exists an open neighborhood $\mathscr{N} \subset \mathfrak{R}^n$ of $x_0 = 0$, an open neighborhood of $\mathscr{Q} \subset \mathfrak{R}^q$ of $w_{0,k} = 0$ and a unique mapping $\lambda : \mathscr{N} \to \mathscr{Q}$ such that (4.33) has a unique solution $w_k^* = \lambda(x_{0,k})$. Now expanding $\mathcal{H}_2(x_{0,k}, w_{0,k})$ around $w_{0,k}^*$ using Taylor expansion

$$\begin{aligned}\mathcal{H}_2(x_{0,k}, w_{0,k}, L(\cdot), V) &= \mathcal{H}_2(x_{0,k}, w_{0,k}^*, L(\cdot), V) \\ &+ \frac{1}{2}(w_{0,k} - w_{0,k}^*)^T \frac{\partial^2 \mathcal{H}_2}{\partial w^2}(w_{0,k} - w_{0,k}^*) + O(\|w_{0,k} - w_{0,k}^*\|^3)\end{aligned}$$

Considering $w^*_{0,k}$ as in (4.33) and the condition (4.29), $\mathcal{H}_2(x_k, w^*_{0,k}, L(\cdot), V)$ constitutes a local maximum in $w^*_{0,k}$. Now considering equation (4.32), after $w^*_{0,k}$,

$$\mathcal{H}_2(x_{0,k}, w^*_k, L(\cdot), V) = V(g_0(x_{0,k}, w^*_k) - V(x_{0,k}) + \frac{1}{2}(||r_{0,w^*_0,k}||^2 - \alpha^2||w^*_k||^2)$$

Let

$$L^*(\cdot) = \arg\min_L \mathcal{H}_2(x_{0,k}, w^*_{0,k}, L(\cdot), V) \tag{4.34}$$

considering the condition (4.31) to hold, then expanding $\mathcal{H}_2(x_{0,k}, w^*_{0,k}, L(\cdot))$ about $L^*(\cdot)$ using Taylor series approximation as

$$\begin{aligned}\mathcal{H}_2(\cdot, w^*_{0,k}, L(\cdot), \cdot) = \mathcal{H}_2(\cdot, w^*_{0,k}, L^*(\cdot), \cdot) + \\ \frac{1}{2}Tr\Big\{ \left[I_n \otimes (L(\cdot) - L^*(\cdot))^T\right] \times \frac{\partial^2 \mathcal{H}_2}{\partial L^2} \\ \times \left\{[I_m \otimes (L(\cdot) - L^*(\cdot))^T]\right\} \Big\} + O(||L(\cdot) - L^*(\cdot)||^3)\end{aligned}$$

Thus taking $L^*(\cdot)$ as in (4.30) and if the condition (4.31) holds then $\mathcal{H}_2(\cdot, w^*_{0,k}, L(\cdot), \cdot)$ is minimized and the equilibrium condition

$$\mathcal{H}_2(w_{0,k}, L^*(\cdot)) \le \mathcal{H}_2(w^*_{0,k}, L^*(\cdot)) \le \mathcal{H}_2(w^*_{0,k}, L(\cdot)) \tag{4.35}$$

Hence it is proved that $(L^*(\cdot), w^*_{0,k})$ constitutes the equilibrium condition for the game (4.4) and (4.25). Also substituting $(L^*(\cdot), w^*_{0,k})$ in (4.32), discrete time Hamiltonian Jacobi equation (4.27) is obtained.
(ii) Consider the conditions (4.35)

$$\mathcal{H}_2(w_{0,k}, L^*(\cdot)) \le \mathcal{H}_2(w^*_{0,k}, L^*(\cdot)) = 0$$

or

$$\begin{aligned}V(g_0(x_{0,k}, w_{0,k})) - V(x_{0,k}) + \frac{1}{2}(||r_{0,w_0,k}||^2 - \alpha^2||w_{0,k}||^2) \le 0 \\ \Delta V(x_{0,k}) + \frac{1}{2}(||r_{0,w_0,k}||^2 - \alpha^2||w_{0,k}||^2) \le 0\end{aligned}$$

Taking the summation from $k = 0$ to $k = K$, it implies that

$$\begin{aligned}\sum_{k=0}^{K}\left\{\Delta V(x_{0,k}) + \frac{1}{2}(||r_{0,w_0,k}||^2 - \alpha^2||w_{0,k}||^2)\right\} \le 0 \\ V(x_{0,K+1}, K+1) - V(x_{0,0}) + \sum_{k=0}^{K}\left\{\frac{1}{2}(||r_{0,w_0,k}||^2 - \alpha^2||w_{0,k}||^2)\right\} \le 0\end{aligned}$$

For $V(x_{K+1}, K+1) > 0$, then

$$\begin{aligned}- V(x_{0,0}) + \sum_{k=0}^{K}\left\{\frac{1}{2}(||r_{0,w_0,k}||^2 - \alpha^2||w_{0,k}||^2)\right\} \\ \sum_{k=0}^{K}\left\{||r_{0,w_0,k}||^2\right\} \le \alpha^2 \sum_{k=0}^{K}\left\{||w_{0,k}||^2\right\} + 2V(x_{0,0})\end{aligned}$$

Assuming zero initial conditions, then $V(x_{0,0}) = 0$ and taking the square roots of the above equation

$$\sqrt{\sum_{k=0}^{K} ||r_{0,w_0,k}||^2} \leq \alpha \sqrt{\sum_{k=0}^{K} ||w_{0,k}||^2}$$
$$||r_{0,w_0,k}||_{2,K} \leq \alpha ||w_{0,k}||_{2,K}$$

Hence, it is proved that the $\mathscr{L}_2$–gain of the residual generator (4.4) is less than or equal to α. Finally, (iii) can be proven by combining (i) and (ii). This completes the proof. □

Remark 4.2.1. *It is worth noting that the condition* (4.15) *and* (4.30) *show that the filter gain $L(\cdot)$ may depend on the original states of the system which are generally not available. These constraints make the filter impractical. However, for some kind of non-linear systems, the filter gain can be obtained independent of the system states. Further, it also makes sense to search for a sub-optimal solution in which case the filter gain is independent of the states of the systems. To this end, the next remark is useful.*

Remark 4.2.2. *With out loss of generality, Lemma 4.2.1 and 4.2.2 remain true if the HJIE* (4.12) *and* (4.27) *are replaced by*

$$\mathcal{H}_1(x_{0,k}, f^*_{0,k}, L^*(\cdot), Y) \geq 0 \tag{4.36}$$
$$\mathcal{H}_2(x_{0,k}, w^*_{0,k}, L^*(\cdot), V) \leq 0 \tag{4.37}$$

This helps us to obtain a sub-optimal solution for $L^*(\cdot)$ which may be independent of the system states. Let us consider the sensitivity problem as

$$\sum_{k=0}^{K} ||r_{0,f_0,k}||^2 - \beta^2 \sum_{k=0}^{K} ||f_{0,k}||^2 \geq 0 \tag{4.38}$$

A sufficient condition for minimum sensitivity to hold is given in the form of the following Hamilton-Jacobi inequality (HJI),

$$\begin{aligned}
&\sum_{k=0}^{K} ||r_{0,f_0,k}||^2 - \beta^2 \sum_{k=0}^{K} ||f_{0,k}||^2 + Y_k(x_{0,k}) \geq 0 \Rightarrow \\
&\sum_{k=0}^{K} \left\{ ||r_{0,f_0,k}||^2 - \beta^2 ||f_{0,k}||^2 + \Delta Y_k(x_{0,k}) \right\} \geq 0 \Rightarrow \\
&||r_{0,f_0,k}||^2 - \beta^2 ||f_{0,k}||^2 + Y_{k+1}(x_{0,k+1}) - Y_k(x_{0,k}) \geq 0
\end{aligned} \tag{4.39}$$

where $Y_k(x_{0,k})$ is a negative definite function. Likewise, the robustness problem (4.24) *can be satisfied if there exists a positive (semi-) definite function $V_k(x_{0,k})$ such that the following HJI holds*

$$\begin{aligned}
&\sum_{k=0}^{K} ||r_{0,w_0,k}||^2 - \alpha^2 \sum_{k=0}^{K} ||w_{0,k}||^2 + V_k(x_{0,K}) \leq 0 \Rightarrow \\
&\sum_{k=0}^{K} \left\{ ||r_{0,w_0,k}||^2 - \alpha^2 |w_{0,k}||^2 + \Delta V_k(x_{0,k}) \right\} \leq 0 \Rightarrow \\
&||r_{0,w_0,k}||^2 - \alpha^2 ||w_{0,k}||^2 + V_{k+1}(x_{0,k+1}) - V_k(x_{0,k}) \leq 0
\end{aligned} \tag{4.40}$$

Note that the HJIs (4.39) *and* (4.40) *are similar to the HJIEs* (4.12) *and* (4.27) *except the inequality sign.*

To this end, the filter gain is fixed as $L(\cdot) = L(\hat{x}_k, k)$ and the condition (4.15) and (4.30) is omitted in Lemma 4.2.1 and 4.2.2, respectively. Consequently, any filter gain $L_{\hat{x}_k,k} = L(\hat{x}_k, k)$ that satisfies (4.39) and/or (4.40) for maximum possible value of sensitivity level β and/or robustness level α is the desired filter gain.

4.2.3 FDF design based on the mixed $\mathscr{H}_-/\mathscr{H}_\infty$– optimization

The problem addressed in Lemma 4.2.1 provides an FDF which has fault sensitivity level greater than or equal to some given constant while it does not necessarily guarantee the disturbance attenuation level to the desired value. On the other hand, the problem addressed in Lemma 4.2.2 ensures a disturbance attenuation level to the pre-defined value but it does not necessarily produce fault sensitivity to the intended value. Since the two problems are different, the filter gain may also be most likely different. In the mixed $\mathscr{H}_-/\mathscr{H}_\infty$–FDF, the aim is to simultaneously attain robustness against unknown inputs and sensitivity to faults to the desired levels. The following theorem gives sufficient conditions for the solvability of $\mathscr{H}_-/\mathscr{H}_\infty$–FDF.

Theorem 4.2.1. *Consider the input-affine discrete-time nonlinear system* (4.1)*, the FDF* (4.2)*, and the residual generator* (4.4)*. Further, assume that there exists a pair of positive and negative definite functions $V_k(\cdot)$ and $Y_k(\cdot)$ respectively and a matrix function $L_{\hat{x}_k,k}$ satisfying the following coupled discrete-time Hamilton-Jacobi inequalities (HJIs)*

$$Y_{k+1}(g_0(x_{0,k}, f^*_{0,k})) - Y_k(x_{0,k}) + \frac{1}{2}(\|r_{0,f^*_0,k}\|^2 - \beta^2\|f^*_{0,k}\|^2) \geq 0 \tag{4.41}$$

$$V_{k+1}(g_0(x_{0,k}, w^*_{0,k})) - V_k(x_{0,k}) + \frac{1}{2}(\|r_{0,w^*_0,k}\|^2 - \alpha^2\|w^*_{0,k}\|^2) \leq 0 \tag{4.42}$$

with the side conditions

$$w^*_0 = -\left(F^T_{0,w_0}F_{0,w_0} - \alpha^2 I\right)^{-1}\left\{E^T_{0,w_0}\left.\frac{\partial V}{\partial \eta}(\eta)\right|_{\eta=g_0(x_{0,k},w^*_{0,k})} + F^T_{0,w_0}C_0\right\} \tag{4.43}$$

$$f^*_0 = -\left(F^T_{0,f_0}F_{0,f_0} - \beta^2 I\right)^{-1}\left\{E^T_{0,f_0}\left.\frac{\partial Y}{\partial \eta}(\eta)\right|_{\eta=g_0(x_{0,k},f_{0,k})} + F^T_{0,f_0}C_0\right\} \tag{4.44}$$

$$\left\{E^T_{0,w_0}\left.\frac{\partial^2 V}{\partial \eta^2}(\eta)\right|_{\eta=g_0(x_{0,k},w_{0,k})} E_{0,w_0} + F^T_{0,w_0}F_{0,w_0} - \alpha^2 I\right\}\Big|_{x_0=0;w_0=0} < 0 \tag{4.45}$$

$$\left\{E^T_{0,f_0}\left.\frac{\partial^2 Y}{\partial \eta^2}(\eta)\right|_{\eta=g_0(x_{0,k},f_{0,k})} E_{0,f_0} + F^T_{0,f_0}F_{0,f_0} - \beta^2 I\right\}\Big|_{x_0=0;f_0=0} > 0 \tag{4.46}$$

then the FDF of the form (4.2) *with filter gain $L_{\hat{x}_k,k}$ solves the problem of $\mathscr{H}_-/\mathscr{H}_\infty$-FDF for the given scalars α and β over the finite horizon.*

Proof. (Sketch) Choose two Hamiltonian functions as

$$\mathscr{H}_1 = Y_{k+1}(g_0(x_{0,k}, f_{0,k})) - Y_k(x_{0,k}) + \frac{1}{2}(\|r_{0,f_0,k}\|^2 - \beta^2\|f_{0,k}\|^2) \tag{4.47}$$

$$\mathscr{H}_2 = V_{k+1}(g_0(x_{0,k}, w_{0,k})) - V_k(x_{0,k}) + \frac{1}{2}(\|r_{0,w_0,k}\|^2 - \alpha^2\|w_{0,k}\|^2) \tag{4.48}$$

and follow the similar procedure as the one adopted in the proof of Lemma 4.2.1 and 4.2.2 to complete the proof. □

4.2.4 A discrete-time LTI case

It is worth noting that the results presented in Theorem 4.2.1 can be used to study solvability of mixed $\mathscr{H}_-/\mathscr{H}_\infty$-FDF for linear discrete-time systems over a finite-horizon. As mentioned, the problems over finite-horizon result in time varying solutions independent of whether the system under consideration is time varying or not. This fact is elaborated with the help of linear discrete-time LTI system in the following lines. To this end, consider a discrete-time LTI system

$$\Sigma_{\mathscr{P}} : \begin{cases} x_{k+1} &= Ax_k + Bu_k + E_w w_k + E_f f_k \\ y_k &= Cx_k + Du_k + F_w w_k + F_f f_k \end{cases} \tag{4.49}$$

and an FDF

$$\Sigma_{\mathscr{F}} : \begin{cases} \hat{x}_{k+1} &= A\hat{x}_k + Bu_k + L(y_k - \hat{y}_k) \\ r_k &= y_k - \hat{y}_k = y_k - C\hat{x}_k - Du_k \\ &= C(x_k - \hat{x}_k) + F_w w_k + F_f f_k \end{cases} \tag{4.50}$$

The compact form of the residual generator is as

$$\Sigma_{\mathscr{R}} : \begin{cases} x_{0,k+1} &= A_0 x_{0,k} + E_{0,w} w_k + E_{0,f} f_k \\ r_{0,k} &= C_0 x_{0,k} + F_{0,w} w_k + F_{0,f} f_k \end{cases} \tag{4.51}$$

where $x_{0,k} = (x_k - \hat{x}_k)$, $A_0 = A - LC$, $E_{0,w} = E_w - LF_w$, $E_{0,f} = E_f - LF_f$, $C_0 = C$, $F_{0,w} = F$, and $F_{0,f} = F_f$. The above system is a linear version of the residual generator (4.4). Based on Theorem 4.2.1, the following Corollary is presented.

Corollary 4.2.1. *Given a discrete-time LTI system $\Sigma_{\mathscr{P}}$ (4.49), an FDF $\Sigma_{\mathscr{F}}$ (4.50) and the residual generator $\Sigma_{\mathscr{R}}$ (4.51). Assume, there exists a pair of symmetric positive and negative (semi-) definite matrices $P(k)$ and $Q(k)$ and filter gain L that satisfy the following coupled inequalities*

$$\begin{aligned} &A_0^T P_{k+1} A_0 - P_k + C_0^T C_0 - \left(A_0^T P_{k+1} E_{0,w} + C_0^T F_{0,w}\right) \times \\ &\left(E_{0,w}^T P_{k+1} E_{0,w} + F_{0,w}^T F_{0,w} - \alpha^2 I\right)^{-1} \left(A_0^T P_{k+1} E_{0,w} + C_0^T F_{0,w}\right)^T \leq 0 \end{aligned} \tag{4.52}$$

$$\begin{aligned} &A_0^T Q_{k+1} A_0 - Q_k + C_0^T C_0 - \left(A_0^T Q_{k+1} E_{0,f} + C_0^T F_{0,f}\right) \times \\ &\left(E_{0,f}^T Q_{k+1} E_{0,f} + F_{0,f}^T F_{0,f} - \beta^2 I\right)^{-1} \times \left(A_0^T Q_{k+1} E_{0,f} + C_0^T F_{0,f}\right)^T \geq 0 \end{aligned} \tag{4.53}$$

Then, the FDF $\Sigma_{\mathscr{F}}$ solves the mixed $\mathscr{H}_-/\mathscr{H}_\infty$-FDF problem for discrete-time LTI systems $\Sigma_{\mathscr{P}}$ (4.49).

Proof. Considering $V_k(x_{0,k}) = \frac{1}{2}x_{0,k}^T P_k x_{0,k}, P_k = P_k^T > 0$, the discrete-time HJI (4.42) is reduced to

$$x_{0,k+1}^T P_{k+1} x_{0,k+1} - x_{0,k}^T P_k x_{0,k} + \|C_0 x_{0,k} + F_{0,w} w_k^*\|^2 - \alpha^2 \|w_k^*\|^2 \leq 0 \tag{4.54}$$

The condition (4.43) implies

$$w_k^* = -\left(E_{0,w}^T P_{k+1} E_{0,w} + F_{0,w}^T F_{0,w} - \alpha^2 I\right)^{-1} \times \left(E_{0,w}^T P_{k+1} A_0 + F_{0,w} C_0\right) x_{0,k} \tag{4.55}$$

and the condition (4.45) is reduced to

$$E_{0,w}^T P_{k+1} E_{0,w} + F_{0,w}^T F_{0,w} - \alpha^2 I < 0 \tag{4.56}$$

Considering (4.56) and combining (4.55) and (4.54), the inequality (4.52) is obtained which provides sufficient conditions for the robustness constraints (4.24) to hold over finite-horizon. Similarly, considering $Y_k(x_{0,k}) = \frac{1}{2}x_{0,k}^T Q_k x_{0,k}, Q_k = Q_k^T$, the discrete-time HJI (4.41) is reduced to

$$x_{0,k+1}^T Q_{k+1} x_{0,k+1} - x_{0,k}^T Q_{k+1} x_{0,k} - \beta^2 \|f_k^*\|^2 + \|C_0 x_{0,k} + F_{0,f} f_k^*\|^2 \geq 0 \tag{4.57}$$

The condition (4.44) is reduced to

$$f_k^* = -\left(E_{0,f}^T Q_{k+1} E_{0,f} + F_{0,f}^T F_{0,f} - \beta^2 I\right)^{-1} \times \left(E_{0,f}^T Q_{k+1} A_0 + F_{0,f} C_0\right) x_{0,k} \tag{4.58}$$

and the condition (4.46) is reduced to

$$E_{0,f}^T Q_{k+1} E_{0,f} + F_{0,f}^T F_{0,f} - \beta^2 I > 0 \tag{4.59}$$

Considering (4.59), and combining the (4.58) and (4.57), the inequality (4.53) is obtained which provides sufficient conditions for sensitivity constraints (4.5) to hold over a finite-horizon.
This completes the proof. □

Remark 4.2.3. *It is evident from the inequalities* (4.52) *and* (4.53) *that the solution for the filter gain* $L(\cdot)$ *depends on the time instant* k *due to the time dependency of* P *and* Q *matrices.*

4.3 Solution of the problem of optimal FDF design over infinite-horizon

In this section, the Problems 4.1.1, 4.1.2, and 4.1.3 are studied over infinite-horizon, in which case $K \to \infty$. Since a time-invariant filter $L_{\hat{x}_k} = L(\hat{x}_k)$ is the major interest in this study, the goal is to find time-independent functions Y and V in order to solve the desired objectives. In the sequel, three propositions addressing the problems of $\mathscr{H}_-$–FDF, $\mathscr{H}_\infty$–FDF and the mixed $\mathscr{H}_-/\mathscr{H}_\infty$–FDF over infinite-horizon are given. Finally, it is shown that the proposed framework can be successfully utilized for studying the problem of mixed $\mathscr{H}_-/\mathscr{H}_\infty$– FDF for LTI systems.

4.3.1 FDF design based on $\mathscr{H}_-$–index

The following proposition gives sufficient conditions for the solvability of $\mathscr{H}_-$–FDF over infinite-horizon.

Proposition 4.3.1. *Consider the input-affine discrete-time nonlinear system* (4.1)*, the FDF* (4.2)*, residual generator* (4.4)*, and infinite-horizon problem. Suppose, there exists a negative definite function $Y(\cdot)$ and filter gain $L_{\hat{x}_k}$ satisfying the following discrete-time HJI*

$$\mathcal{H}_1(x_{0,k}, f^*_{0,k}, L^*_{\hat{x}_k}, Y) := Y(g_0(x_{0,k}, f^*_{0,k})) - Y(x_{0,k}) + \frac{1}{2}(\|r_{0,f^*_0,k}\|^2 - \beta^2\|f^*_{0,k}\|^2) \geq 0 \quad (4.60)$$

together with the side conditions

$$f^*_0 = -\left(F^T_{0,f_0}F_{0,f_0} - \beta^2 I\right)^{-1} \times \left\{E^T_{0,f_0}\left.\frac{\partial Y}{\partial \eta}(\eta)\right|_{\eta=g_0(x_{0,k},f_{0,k})} + F^T_{0,f_0}C_0\right\} \quad (4.61)$$

$$E^T_{0,f_0}\left.\frac{\partial^2 Y}{\partial \eta^2}(\eta)\right|_{\eta=g_0(x_{0,k},f_{0,k})} E_{0,f_0} + F^T_{0,f_0}F_{0,f_0} - \beta^2 I\Big|_{x_0=0,f_0=0} > 0 \quad (4.62)$$

then the FDF (4.2) *with $L_{\hat{x}_k}$ solves the sensitivity problem* (4.5) *for a given sensitivity level β over infinite-horizon.*

Proof. The proof follows the similar lines of the proof of Lemma 4.2.1. □

4.3.2 FDF design based on $\mathscr{H}_\infty$-norm

Sufficient conditions for the solution of $\mathscr{H}_\infty$-FDF can be obtained from the following proposition.

Proposition 4.3.2. *Consider an input-affine discrete-time nonlinear system* (4.1)*, FDF* (4.2)*, the residual generator dynamics* (4.4)*, and infinite-horizon problem. Suppose, there exists a positive (semi-) definite function $V(\cdot)$ and a filter gain $L_{\hat{x}_k} \in \mathfrak{R}^{n\times m}$ satisfying the following discrete-time HJI*

$$\mathcal{H}_2(x_{0,k}, w^*_{0,k}, L^*_{\hat{x}_k}, V) := V(g_0(x_{0,k}, w^*_{0,k})) - V(x_{0,k}) + \frac{1}{2}(\|r_{0,w^*_0,k}\|^2 - \alpha^2\|w^*_{0,k}\|^2) \leq 0 \quad (4.63)$$

together with the following side conditions

$$w^*_0 = -\left(F^T_{0,w_0}F_{0,w_0} - \alpha^2 I\right)^{-1} \times \left\{E^T_{0,w_0}\left.\frac{\partial V}{\partial \eta}(\eta)\right|_{\eta=g_0(x_{0,k},w^*_{0,k})} + F^T_{0,w_0}C_0\right\} \quad (4.64)$$

$$\left\{E^T_{0,w_0}\left.\frac{\partial^2 V}{\partial \eta^2}(\eta)\right|_{\eta=g_0(x_{0,k},w_{0,k})} E_{0,w_0} + F^T_{0,w_0}F_{0,w_0} - \alpha^2 I\right\}\Big|_{x_0=0} < 0 \quad (4.65)$$

then

(i) the residual generator (4.4) *has finite* $\mathscr{L}_2-$*gain less than or equal to* α*, and*

(ii) the FDF of the form (4.2) *with filter gain* $L_{\hat{x_k}}$ *solves the robustness problem* (4.24) *with the attenuation level* α *over infinite-horizon.*

Proof. The proof follows the similar lines in the proof of of item (ii) and (iii) in Lemma 4.2.2.

□

4.3.3 FDF design based on the mixed $\mathscr{H}_-/\mathscr{H}_\infty$–optimization

The following proposition provides sufficient conditions for the solvability of the mixed $\mathscr{H}_-/\mathscr{H}_\infty-$ FDF over infinite-horizon.

Proposition 4.3.3. *Consider the input-affine discrete-time nonlinear system* (4.1)*, the FDF* (4.2)*, the residual generator* (4.4)*, and infinite-horizon problem. Suppose, there exists a pair of positive and negative definite functions* V *and* Y *respectively and a filter gain* $L(\hat{x}_k)$ *satisfying the following coupled discrete-time HJIs*

$$V(g_0(x_{0,k}, w^*_{0,k})) - V(x_{0,k}) + \frac{1}{2}(\|r_{0,w^*_0,k}\|^2 - \alpha^2\|w^*_{0,k}\|^2) \leq 0 \tag{4.66}$$

$$Y(g_0(x_{0,k}, f^*_{0,k})) - Y(x_{0,k}) + \frac{1}{2}(\|r_{0,f^*_0,k}\|^2 - \beta^2\|f^*_{0,k}\|^2) \geq 0 \tag{4.67}$$

together with the side conditions given as follows

$$w^*_0 = -\left(F^T_{0,w_0}F_{0,w_0} - \alpha^2 I\right)^{-1}\left\{E^T_{0,w_0}\,\frac{\partial V}{\partial \eta}(\eta)\Big|_{\eta=g_0(x_{0,k},w_{0,k})} + F^T_{0,w_0}C_0\right\} \tag{4.68}$$

$$f^*_0 = -\left(F^T_{0,f_0}F_{0,f_0} - \beta^2 I\right)^{-1}\left\{E^T_{0,f_0}\,\frac{\partial Y}{\partial \eta}(\eta)\Big|_{\eta=g_0(x_{0,k},f_{0,k})} + F^T_{0,f_0}C_0\right\} \tag{4.69}$$

$$\left\{E^T_{0,w_0}\,\frac{\partial^2 V}{\partial \eta^2}(\eta)\Big|_{\eta=g_0(x_{0,k},w_{0,k})} E_{0,w_0} + F^T_{0,w_0}F_{0,w_0} - \alpha^2 I\right\}\Big|_{x_0=0,w_0=0} < 0 \tag{4.70}$$

$$\left\{E^T_{0,f_0}\,\frac{\partial^2 Y}{\partial \eta^2}(\eta)\Big|_{\eta=g_0(x_{0,k},f_{0,k})} E_{0,f_0} + F^T_{0,f_0}F_{0,f_0} - \beta^2 I\right\}\Big|_{x_0=0,f_0=0} > 0 \tag{4.71}$$

then

(i) residual generator (4.4) *has finite* $\mathscr{L}_2-$*gain less than or equal to* α*, and*

(ii) the FDF (4.2) *with* $L_{\hat{x}_k}$ *solves the problem of* $\mathscr{H}_-/\mathscr{H}_\infty-$*FDF for infinite-horizon with the given sensitivity and robustness levels* β *and* α*.*

Proof. (i) The finite $\mathscr{L}_2-$ gain stability can be proven along the similar lines of the proof of Proposition 4.3.2
(ii) The proof of this part follows from the similar lines as in Theorem 4.2.1
This completes the proof. □

Theorem 4.2.1 and Proposition 4.3.3 provide sufficient conditions for the solution of mixed $\mathscr{H}_-/\mathscr{H}_\infty$-FDF for discrete-time nonlinear systems over finite and infinite-horizon respectively. Obtaining an explicit relation for suitable filter gain $L_{\hat{x}_k,k}$ or $L_{\hat{x}_k}$ is a challenging task. One may obtain an explicit relation for the filter gain in case of $\mathscr{H}_-$–FDF design with a suitable linearization of HJI (4.39) or HJI (4.60) by following the similar arguments given in [147] for $\mathscr{H}_\infty$ filtering. Further, a suboptimal solution may also be obtained using Lemma 4.2.1 together with Remark 4.2.2 for finite-horizon and using Proposition 4.3.1 for infinite-horizon. Likewise, following the similar lines, an explicit relation for the filter gain in case of $\mathscr{H}_\infty$–FDF can also be obtained. However, since it is difficult to derive an explicit relation for the filter gain in case of the mixed $\mathscr{H}_-/\mathscr{H}_\infty$–FDF, any solution for L satisfying the HJIs (4.41) and (4.42) or HJIs (4.66) and (4.67) for given scalars α and β would be the desired filter gain.

4.3.4 A discrete-time LTI case

This subsection shows that the results presented in Proposition 4.3.3 can be deduced to the well-established results for the mixed $\mathscr{H}_-/\mathscr{H}_\infty$-FDF for discrete-time LTI systems given in [1]. Since the problem is solved over infinite-horizon, the filter gain is also time-invariant. To this end, consider the same discrete-time system, FDF and the residual generator as the one considered in Section 4.3.4; that is, $\Sigma_{\mathscr{P}}$ (4.49), $\Sigma_{\mathscr{F}}$ (4.50), and $\Sigma_{\mathscr{R}}$ (4.51) respectively. The following Corollary describes the results for the mixed $\mathscr{H}_-/\mathscr{H}_\infty$-FDF for discrete-time LTI systems over infinite-horizon.

Corollary 4.3.1. *Given a discrete-time LTI system $\Sigma_{\mathscr{P}}$ (4.49), an FDF $\Sigma_{\mathscr{F}}$ (4.50), the residual generator $\Sigma_{\mathscr{R}}$ (4.51), and infinite-horizon problem. Assume, there exists a pair of symmetric positive and negative (semi-) definite matrices P and Q and filter gain L that satisfy the following coupled LMIs*

$$\begin{bmatrix} -P & P(A-LC) & P(E_w-LF_w) & 0 \\ * & -P & 0 & C^T \\ * & * & -\alpha^2 I & F_w^T \\ * & * & * & -I \end{bmatrix} \leq 0 \tag{4.72}$$

$$\begin{bmatrix} -Q & Q(A-LC) & Q(E_f-LF_f) \\ * & -Q+C^TC & C^TF_f \\ * & * & F_f^TF_f-\beta^2 I \end{bmatrix} \geq 0 \tag{4.73}$$

Then, the FDF $\Sigma_{\mathscr{F}}$ solves the mixed $\mathscr{H}_-/\mathscr{H}_\infty$-FDF problem for discrete-time LTI systems over infinite-horizon.

Proof. Considering $V(x_{0,k}) = \frac{1}{2}x_{0,k}^T P x_{0,k}, P = P^T > 0$, the discrete-time HJI (4.66) is reduced to (4.74).

$$x_{0,k+1}^T P x_{0,k+1} - x_{0,k}^T P x_{0,k} + \|C_0 x_{0,k} + F_{0,w} w_k^*\|^2 - \alpha^2 \|w_k^*\|_2^2 \leq 0 \tag{4.74}$$

The condition (4.68) is reduced to

$$w_k^* = -\left(E_{0,w}^T P E_{0,w} + F_{0,w}^T F_{0,w} - \alpha^2 I\right)^{-1} \times \left(E_{0,w}^T P A_0 + F_{0,w} C_0\right) x_{0,k} \tag{4.75}$$

Further, the condition (4.70) implies

$$E_{0,w}^T P E_{0,w} + F_{0,w}^T F_{0,w} - \alpha^2 I < 0 \tag{4.76}$$

Similarly, using the condition (4.55) together with (4.54), the following necessary and sufficient condition for robustness constraints (4.24) for $K \to \infty$ can be obtained

$$\begin{aligned} &A_0^T P A_0 - P + C_0^T C_0 - \left(A_0^T P E_{0,w} + C_0^T F_{0,w}\right) \times \\ &\left(E_{0,w}^T P E_{0,w} + F_{0,w}^T F_{0,w} - \alpha^2 I\right)^{-1} \left(A_0^T P E_{0,w} + C_0^T F_{0,w}\right)^T \leq 0 \end{aligned} \tag{4.77}$$

which can be transformed to LMI (4.72) by using the well known Schur complements.

Similarly, considering $Y_k(x_{0,k}) = \frac{1}{2}x_{0,k}^T Q x_{0,k}, Q = Q^T$, the discrete-time HJI (4.67) is reduced to

$$x_{0,k+1}^T Q x_{0,k+1} - x_{0,k}^T Q x_{0,k} - \beta^2 \|f_k^*\|_2^2 + \|C_0 x_{0,k} + F_{0,f} f_k^*\|^2 \geq 0 \tag{4.78}$$

The condition (4.69) is reduced to

$$f_k^* = -\left(E_{0,f}^T Q E_{0,f} + F_{0,f}^T F_{0,f} - \beta^2 I\right)^{-1} \times \left(E_{0,f}^T Q A_0 + F_{0,f} C_0\right) x_{0,k} \tag{4.79}$$

and the condition (4.71) implies that

$$E_{0,f}^T Q E_{0,f} + F_{0,f}^T F_{0,f} - \beta^2 I > 0 \tag{4.80}$$

Combining the condition (4.58) and (4.78), a necessary and sufficient condition for sensitivity constraints (4.5) for $K \to \infty$, is obtained as

$$\begin{aligned} &A_0^T Q A_0 - Q + C_0^T C_0 - \left(A_0^T Q E_{0,f} + C_0^T F_{0,f}\right) \times \\ &\left(E_{0,f}^T Q E_{0,f} + F_{0,f}^T F_{0,f} - \beta^2 I\right)^{-1} \times \left(A_0^T Q E_{0,f} + C_0^T F_{0,f}\right)^T \geq 0 \end{aligned} \tag{4.81}$$

which can be easily converted into the LMI (4.73) by using the Schur complements. This completes the proof. □

4.4 A design example

In order to demonstrate the use of the proposed approach, a discrete-time nonlinear system governed by the following set of difference equations is considered

$$\begin{aligned} x_{1,k+1} &= 0.456 x_{2,k} \\ x_{2,k+1} &= -0.762 x_{1,k} + 0.19 x_{2,k} + 0.12 sin(x_{1,k}) + 0.5 u_k + 0.5 w_k + 0.5 f_k \\ y_k &= x_{2,k} + 0.2 w_k + f_k \end{aligned} \tag{4.82}$$

where

$$a(x_k) = A_1 x_k + \phi(x_k) = \begin{bmatrix} 0 & 0.456 \\ -0.762 & 0.19 \end{bmatrix}\begin{bmatrix} x_{1,k} \\ x_{2,k} \end{bmatrix} + \begin{bmatrix} 0 \\ 0.12sin(x_{1,k}) \end{bmatrix}; F_w(x_k) = 0.2$$

$$B(x_k) = E_w(x_k) = E_f(x_k) = \begin{bmatrix} 0 \\ 0.5 \end{bmatrix}; c(x_k) = [0 \;\; 1]\, x_k; \quad F_f(x_k) = 1$$

Consider the residual generator (4.4) for the system (4.82), and assume $V(x_{0,k}) = x_{0,k}^T P x_{0,k}$, $P = P^T > 0$, the HJI (4.66) in Proposition 4.3.3 with the worst-case disturbance (4.68) is reduced to

$$\begin{aligned} & x_{0,k}^T \left(\bar{A}_0^T P \bar{A}_0 + C_0^T C_0 - P\right) x_{0,k} + 2x_{0,k}^T \bar{A}_0^T P \Psi_{k,x_0} + \Psi_{k,x_0}^T P \Psi_{k,x_0} \\ & - \Big\{ \left(x_{0,k}^T [\bar{A}_0^T P E_{0,w} + C_0^T F_{0,w}] + \Psi_{k,x_0}^T P E_{0,w}\right) \left(E_{0,w}^T P E_{0,w} + F_{0,w}^T F_{0,w} - \alpha^2 I\right)^{-1} \times \\ & \left(x_{0,k}^T [\bar{A}_0^T P E_{0,w} + C_0^T F_{0,w}] + \Psi_{k,x_0}^T P E_{0,w}\right)^T \Big\} \le 0 \end{aligned} \tag{4.83}$$

where

$$A_0 = \bar{A}_0 x_{0,k} + \Psi_{k,x_0} = \begin{bmatrix} A_1 & 0 \\ 0 & A_1 - LC \end{bmatrix}\begin{bmatrix} x_k \\ e_k \end{bmatrix} + \begin{bmatrix} \phi(x_k) \\ \phi(x_k) - \phi(\hat{x}_k) \end{bmatrix};$$

Similarly, considering $Y(x_{0,k}) = x_{0,k}^T Q x_{0,k} = -x_{0,k}^T P x_{0,k}$ with $Q = -P$ the HJI (4.67) with the best-case fault (4.69) is reduced to

$$\begin{aligned} & x_{0,k}^T \left(\bar{A}_0^T P \bar{A}_0 - C_0^T C_0 - P\right) x_{0,k} + 2x_{0,k}^T \bar{A}_0^T P \Psi_{k,x_0} + \Psi_{k,x_0}^T P \Psi_{k,x_0} \\ & - \Big\{ \left(x_{0,k}^T [\bar{A}_0^T P E_{0,f} - C_0^T F_{0,f}] + \Psi_{k,x_0}^T P E_{0,f}\right) \times \left(E_{0,f}^T P E_{0,f} - F_{0,f}^T F_{0,f} + \beta^2 I\right)^{-1} \\ & \times \left(x_{0,k}^T [\bar{A}_0^T P E_{0,f} - C_0^T F_{0,f}] + \Psi_{k,x_0}^T P E_{0,f}\right)^T \Big\} \le 0 \end{aligned} \tag{4.84}$$

Treating the terms involving nonlinearity in (4.83) and (4.84) as

$$\begin{aligned} & 2x_{0,k}^T \bar{A}_{0,k}^T P \Psi_{k,x_0} \le 0.24 x_{0,k}^T \bar{A}_0^T P P_0 x_{0,k}, \quad \Psi_{k,x_0}^T P \Psi_{k,x_0} \le 0.0144 x_{0,k}^T P_0^T P P_0 x_{0,k}, \\ & E_{0,w}^T P \Psi_{k,x_0} \le 0.12 E_{0,w}^T P P_0 x_{0,k}, \quad E_{0,f}^T P \Psi_{k,x_0} \le 0.12 E_{0,f}^T P P_0 x_{0,k} \end{aligned}$$

where $P_0 = \begin{bmatrix} \bar{P} & 0 \\ 0 & \bar{P} \end{bmatrix}$ and $\bar{P} = \begin{bmatrix} 0 & 0 \\ 1 & 0 \end{bmatrix}$. Based on the above analysis, the HJI (4.83) is represented as follows

$$\begin{aligned} & \left(\bar{A}_0^T P \bar{A}_0 + C_0^T C_0 - P\right) + 0.24 \bar{A}_0^T P P_0 + 0.144 P_0^T P P_0 \\ & - \Big\{ \left(\bar{A}_0^T P E_{0,w} + C_0^T F_{0,w} + 0.12 P_0^T P E_{0,w}\right) \times \left(E_{0,w}^T P E_{0,w} + F_{0,w}^T F_{0,w} - \alpha^2 I\right)^{-1} \\ & \times \left(\bar{A}_0^T P E_{0,w} + C_0^T F_{0,w} + 0.12 P_0^T P E_{0,w}\right)^T \Big\} \le 0 \end{aligned} \tag{4.85}$$

and the HJI (4.84) is

$$\begin{aligned} & \left(\bar{A}_0^T P \bar{A}_0 - C_0^T C_0 - P\right) + 0.24 \bar{A}_0^T P P_0 + 0.144 P_0^T P P_0 \\ & - \Big\{ \left(\bar{A}_0^T P E_{0,f} - C_0^T F_{0,f} + 0.12 P_0^T P E_{0,f}\right) \times \left(E_{0,f}^T P E_{0,f} - F_{0,f}^T F_{0,f} + \beta^2 I\right)^{-1} \\ & \times \left(\bar{A}_0^T P E_{0,f} - C_0^T F_{0,f} + 0.12 P_0^T P E_{0,f}\right)^T \Big\} \le 0 \end{aligned} \tag{4.86}$$

4.4.1 Computation of parameters for $\mathscr{H}_-$–FDF

Using the well-known Schur complements, the inequality (4.86) is transformed into LMI and solved using LMI toolbox in MATLAB® in order to compute filter gain L so that the maximum possible sensitivity level is achieved. The following parameters of the $\mathscr{H}_-$–FDF has been computed:

$$\beta = 1.0000; \quad P_1 = 10^{-5} \times \begin{bmatrix} 0.1849 & -0.0147 \\ -0.0147 & 0.0527 \end{bmatrix};$$
$$P_2 = 10^{7} \times \begin{bmatrix} 6.3520 & 0.8188 \\ 0.8188 & 5.9024 \end{bmatrix}; \quad L = \begin{bmatrix} -0.0000 \\ 0.5000 \end{bmatrix}$$

Figure 4.2 shows the residual generated using the $\mathscr{H}_-$–FDF. Note that in the design

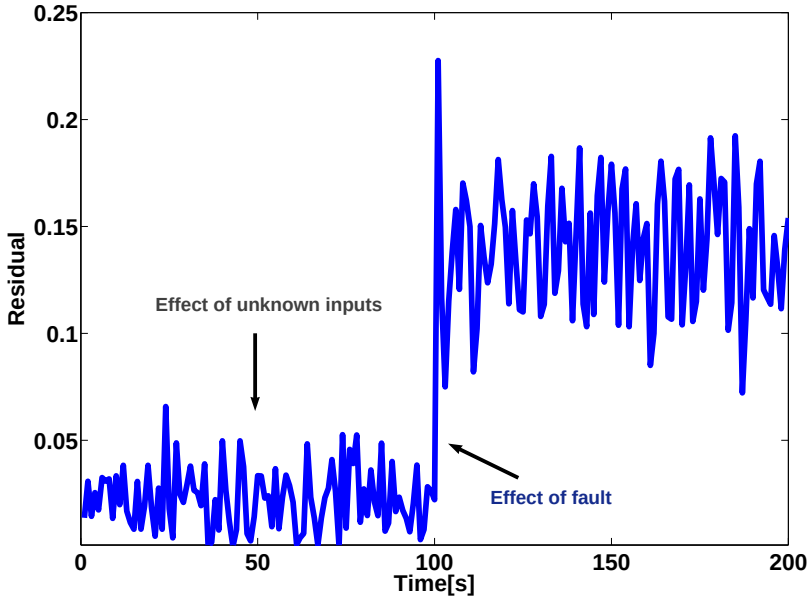

Figure 4.2: Residual signal with $f_k = 0.2$ at $k = 100[s]$

of $\mathscr{H}_-$–FDF, attaining a maximum possible sensitivity to the best-case fault is primary objective while robustness against unknown inputs is not addressed.

4.4.2 Computation of parameters for $\mathscr{H}_\infty$–FDF

In order to compute the parameters of the $\mathscr{H}_\infty$–FDF, the inequality (4.85) is also transformed into LMI using the well-known Schur complements and solved using LMI toolbox in MATLAB®. The following parameters are obtained:

$$\alpha = 0.8; \quad P_1 = \begin{bmatrix} 2.7719 & -0.2110 \\ -0.2110 & 0.7424 \end{bmatrix};$$
$$P_2 = \begin{bmatrix} 10.7228 & 2.3317 \\ 2.3317 & 2.2773 \end{bmatrix}; \quad L = \begin{bmatrix} 0.3183 \\ 0.8187 \end{bmatrix}$$

It is evident that in the design of $\mathscr{H}_\infty$–FDF, the primary concern in the design is to achieve

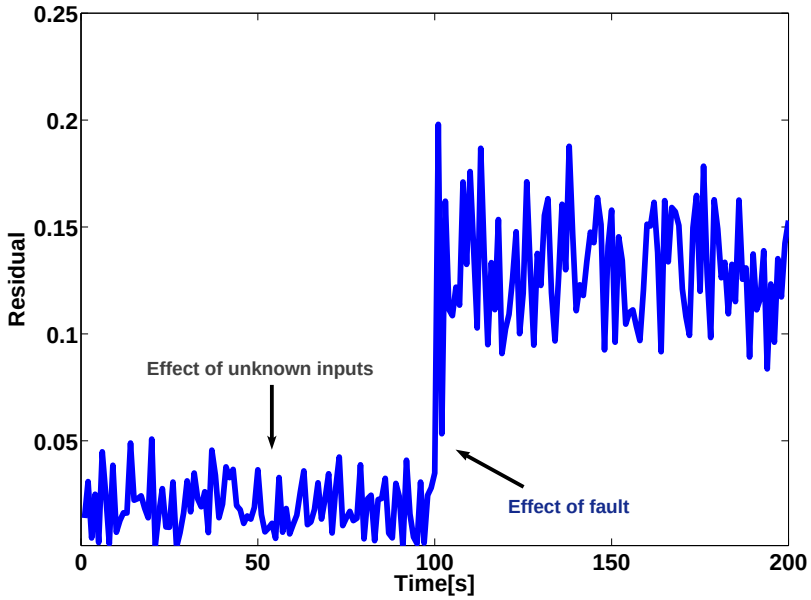

Figure 4.3: Residual signal with $f_k = 0.2$ at $k = 100[s]$

robustness against the unknown inputs to the desired level while attaining a sensitivity to the best-case fault is not the subject of the design. Figure 4.3 shows the residual generated using the $\mathscr{H}_\infty$–FDF.

4.4.3 Computation of parameters for $\mathscr{H}_-/\mathscr{H}_\infty$–FDF

For the design of the mixed $\mathscr{H}_-/\mathscr{H}_\infty$–FDF, the inequalities (4.85) and (4.86) have to be simultaneously solved. To this end, these inequalities are first transformed into LMIs and are then simultaneously solved using LMI toolbox in MATLAB® in order to compute filter gain L so that the sensitivity level β is maximized while keeping the disturbances attenuation below a prescribed level α. The following parameters are computed for a predefined attenuation level $\alpha = 0.8$:

$$\beta = 0.8630; \quad P = \begin{bmatrix} P_1 & 0 \\ 0 & P_2 \end{bmatrix}; \quad P_1 = 10^{-4} \times \begin{bmatrix} 0.2565 & -0.0200 \\ -0.0200 & 0.0696 \end{bmatrix};$$

$$P_2 = \begin{bmatrix} 5.6640 & 0.7602 \\ 0.7602 & 3.1004 \end{bmatrix}; \quad L = \begin{bmatrix} -0.1276 \\ 0.6015 \end{bmatrix}$$

Fig. 4.4 shows the residual signal generated by the proposed filter. It is evident from the simulation that the residual generated with the proposed filter is much sensitive to faults for a given disturbance attenuation level. Note that all of the above simulations are carried out for $200[s]$. The unknown disturbance is simulated as a uniform random number in the range $\{-0.1, 0.1\}$. A bias sensor fault is generated at $k = 100[s]$ as step function of magnitude equals to 0.2.

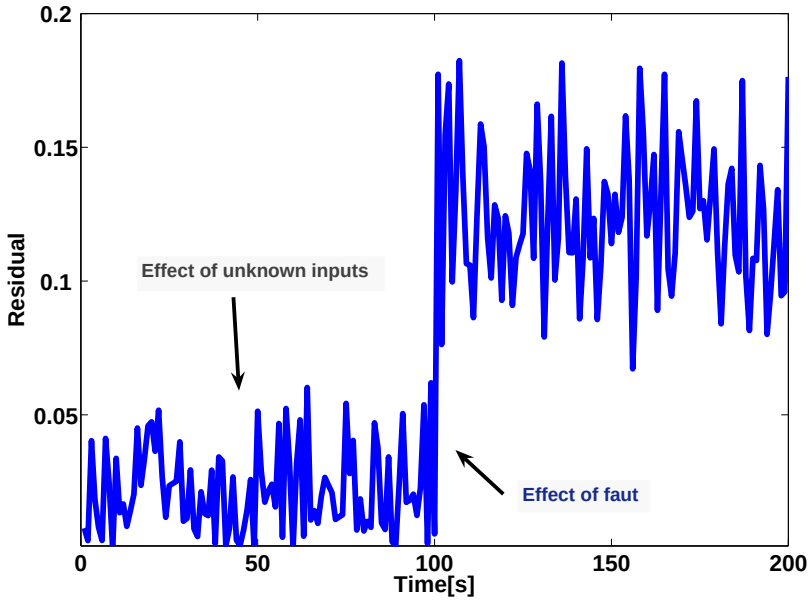

Figure 4.4: Residual signal with $f_k = 0.2$ at $k = 100[s]$

4.5 Summary

This chapter has introduced the problem of designing an FDF for input affine discrete-time nonlinear systems using $\mathscr{H}_-$–index, $\mathscr{H}_\infty$–norm, and mixed $\mathscr{H}_-/\mathscr{H}_\infty$– optimization. The time domain definitions of $\mathscr{H}_-$–index and $\mathscr{H}_\infty$–norm were presented in order to facilitate the study regarding the problems of optimal fault detection in nonlinear systems. Exploiting the theory of differential games and dissipation inequalities, three different problems were formulated and sufficient conditions for their solvability were also provided. These problems include; $\mathscr{H}_-$–FDF which aimed to design an FDF in order to acquire maximum possible sensitivity to the best-case fault in the system, $\mathscr{H}_\infty$–FDF which is used to design an FDF in order to attain robustness against the unknown inputs to a pre-defined level, and the mixed $\mathscr{H}_-/\mathscr{H}_\infty$–FDF which simultaneously provide robustness against unknown inputs and sensitivity to the best-case fault. These problems were studied for both finite- and infinite-horizon. It was also shown that the generalized results obtained for nonlinear systems can also be used to study the problem of FDF design in linear discrete-time systems. Finally, a design example was incorporated to elaborate the theory developed in this chapter.

Chapter 5

Optimal residual generation for Lipschitz nonlinear systems: $\mathscr{H}_-/\mathscr{H}_\infty-$ optimization

The major objective of this chapter is to formulate the problem of designing $\mathscr{H}_-/\mathscr{H}_\infty$-FDF for nonlinear systems with Lipschitz nonlinearities using convex optimization. Sufficient conditions for the existence of such a filter are derived in the form of linear matrix inequalities (LMIs) for both discrete-time and continuous-time Lipschitz nonlinear systems. Two algorithms (for discrete- and continuous-time settings respectively)are presented which ease the design of mixed $\mathscr{H}_-/\mathscr{H}_\infty$-FDF for each case. An illustrative example is provided in order to elaborate the design procedure for continuous-time systems.

Lipschitz nonlinear systems cover a wide range of nonlinear systems. As mentioned in Chapter 3, any type of nonlinear function which is smooth in its arguments can be transformed into Lipschitz nonlinear systems. In this type of nonlinear systems, the change in the nonlinear function with respect to its arguments is always bounded by a constant number. This constant number is referred to as Lipschitz constant. Depending on the type of nonlinearity, a Lipschitz nonlinear system can be regarded as locally Lipschitz or globally Lipschitz. For instance, the sinusoidal type of nonlinearities are termed as globally Lipschitz while the polynomial nonlinearities are regarded as locally Lipschitz.

Observer-design and observer-based fault detection filter design for Lipschitz nonlinear systems have been received a considerable attention over the past two decades; for instance, see [79, 94, 119, 122, 126, 129, 131, 148–151] to list a few. In addition, the LMI formulation of these problems are extensively appeared in various contributions and monographs published in recent years [79, 121, 122, 126, 152] etc. There exist a few motivating reasons behind the LMI formulations of these problem. A few of them are: (i) A variety of design specifications and constraints can be expressed as LMI, (ii) the problem casted into LMIs, can be exactly solved by the efficient convex optimization algorithms available in the LMI toolbox in MTALAB, (iii) problems involving multiple constraints or objectives can be easily handled using LMIs.

In this chapter, the problem of designing mixed $\mathscr{H}_-/\mathscr{H}_\infty$-FDF for Lipschitz nonlinear systems has been formulated as a convex optimization problem and sufficient conditions have been provided in the framework of LMIs. Section 5.1.1 presents the problem formulation for discrete-time while Section 5.2.1 for continuous-time Lipschitz nonlinear systems.

Similarly, sufficient conditions in the form of coupled LMIs are provided in Section 5.1.2 for discrete-time and in Section 5.2.2 for continuous-time Lipschitz nonlinear systems. Finally, an illustrative example is provided for continuous-time Lipschitz nonlinear systems while for discrete-time counter part, a similar procedure can be followed to design $\mathscr{H}_-/\mathscr{H}_\infty$-FDF.

5.1 Residual generation for discrete-time Lipschitz nonlinear systems

5.1.1 Preliminaries and Problem formulation

Consider the following discrete-time Lipschitz nonlinear systems

$$\begin{aligned} x_{k+1} &= Ax_k + \phi(x_k, u_k) + Bu_k + E_w w_k + E_f f_k \\ y_k &= Cx_k + Du_k + F_w w_k + F_f f_k \end{aligned} \tag{5.1}$$

where $x \in \mathfrak{R}^n$ is the state vector, $u \in \mathscr{U} \subset \mathfrak{R}^p$ is the set of admissible control input, $y \in \mathfrak{R}^m$ is the measurement output vector, $w \in \mathfrak{R}^q$ is the unknown input vector, $f \in \mathfrak{R}^\ell$ is the fault vector to be detected. $A, B, C, D, E_w, E_f, F_w, F_f$ are known matrices with appropriate dimensions. The following assumptions will be used frequently in the remainder of this chapter.

A1. The pair (C, A) is detectable.

A2. w and f are $\mathscr{L}_2-$ norm bounded.

A3. The nonlinear function $\phi(x_k, u_k)$ is assumed to be Lipschitz in x with a Lipschitz constant γ:

$$\|\phi(x_1, u_k) - \phi(x_2, u_k)\| \leq \gamma \|x_1 - x_2\| \quad \forall x_1, x_2, u_k \in \mathscr{U} \subset \mathfrak{R}^p$$

The fault detection filter (FDF) based on nonlinear observer is

$$\begin{aligned} \hat{x}_{k+1} &= A\hat{x}_k + \phi(\hat{x}_k, u_k) + Bu_k + L(y_k - C\hat{x}_k - Du_k) \\ r_k &= W(y_k - C\hat{x}_k - Du_k) \end{aligned} \tag{5.2}$$

where r_k is the residual signal, L the filter gain and W is the post filter. Denoting the estimation error $e_k = x_k - \hat{x}_k$, the following error dynamics can be obtained

$$\begin{aligned} e_{k+1} &= (A - LC)e_k + \phi(x_k, u_k) - \phi(\hat{x}_k, u_k) + (E_w - LF_w)w_k + (E_f - LF_f)f_k \\ r_k &= W(Ce_k + F_w w_k + F_f f_k) \end{aligned} \tag{5.3}$$

The residual generator dynamics for the system (5.1) can finally be represented as follows

$$\begin{aligned} x_{0,k+1} &= A_0 x_{0,k} + \Psi_{0,k} + E_0 w_{0,k} + E_{0,f} f_{0,k} \\ r_{0,k} &= C_0 x_{0,k} + F_0 w_{0,k} + F_{0,f} f_{0,k} \end{aligned} \tag{5.4}$$

where

$$\begin{aligned} x_{0,k} &= e_k; \quad w_{0,k} = w_k; \quad f_{0,k} = f_k; \quad A_0 = A - LC; \\ E_0 &= E_w - LF_w; \quad E_{0,f} = E_f - LF_f \\ C_0 &= WC; \quad F_0 = WF_w; \quad F_{0,f} = WF_f; \\ \Psi_{0,k}: &= \Psi_0(x_k, \hat{x_k}, u_k) = \phi(x_k, u_k) - \phi(\hat{x_k}, u_k) \end{aligned}$$

In order to analyze the effect of unknown inputs on the residual signal, the fault-free operation is assumed; that is, $f_{0,k} = 0$. To this end, the following state-space model of the residual generator (5.4) is used

$$\begin{aligned} x_{0,k+1} &= A_0 x_{0,k} + \Psi_{0,k} + E_0 w_{0,k} \\ r_{0,w} &= C_0 x_{0,k} + F_0 w_{0,k} \end{aligned} \tag{5.5}$$

and the associated $\mathscr{H}_\infty$−norm is defined as

$$\sum_{k=0}^{\infty} \|r_{0,w}\|^2 \leq \alpha^2 \sum_{k=0}^{\infty} \|w_{0,k}\|^2 \tag{5.6}$$

Similarly, studying the effect of faults alone on the residual signal, the unknown inputs are set equal to zero; that is, $w_{0,k} = 0$, so that a clear picture about the sensitivity of the residual signal to the best-case fault is achieved. For this purpose, the following state-space model for the residual generator (5.4) is used

$$\begin{aligned} x_{0,k+1} &= A_0 x_{0,k} + \Psi_{0,k} + E_{0,f} f_{0,k} \\ r_{0,f} &= C_0 x_{0,k} + F_{0,f} f_{0,k} \end{aligned} \tag{5.7}$$

and the associated $\mathscr{H}_-$ index is given by

$$\sum_{k=0}^{\infty} \|r_{0,f}\|^2 \geq \beta^2 \sum_{k=0}^{\infty} \|f_{0,w}\|^2 \tag{5.8}$$

In the next section, sufficient conditions for the existence of mixed $\mathscr{H}_-/\mathscr{H}_\infty$ FDF are derived, which simultaneously solves the constraints given in (5.8) and (5.6).

5.1.2 Design of FDF based on $\mathscr{H}_-/\mathscr{H}_\infty$− optimization

Theorem 5.1.1. *Consider the Lipschitz nonlinear system* (5.1)*, the FDF* (5.2) *with the filter gain L and post filter W, the associated residual generator* (5.4)*, and given scalars $\alpha > 0$ and $\beta > 0$. Further, suppose that there exist symmetric positive definite matrices P, Q, and nonnegative scalars $\epsilon_i|_{i=1,\cdots,4} > 0$, $\eta_i|_{1,2} > 0$ satisfying the following set of LMIs*

$$\mathscr{L}_1 := \begin{bmatrix} \eta_1 I & P \\ * & \eta_1 I \end{bmatrix} > 0 \tag{5.9}$$

$$\mathscr{L}_2 := \begin{bmatrix} -P & PA_0 & 0 & PE_0 & 0 \\ * & \Omega_1 & A_0^T P & 0 & C_0^T F_{0,w} \\ * & * & -\frac{1}{\epsilon_1} P & 0 & 0 \\ * & * & * & -\alpha^2 I + F_0^T F_0 & E_0^T P \\ * & * & * & * & -\frac{1}{\epsilon_2} P \end{bmatrix} < 0 \tag{5.10}$$

$$\mathscr{L}_3 := \begin{bmatrix} \eta_2 I & Q \\ * & \eta_2 I \end{bmatrix} > 0 \tag{5.11}$$

$$\mathscr{L}_4 := \begin{bmatrix} -Q & QA_0 & 0 & QE_f & 0 \\ * & \Omega_2 & A_0^T P & 0 & -C_0^T F_f \\ * & * & \beta^2 I - F_f^T F_f & 0 & 0 \\ * & * & * & -\frac{1}{\epsilon_3} Q & E_f^T Q \\ * & * & * & * & -\frac{1}{\epsilon_4} Q \end{bmatrix} < 0 \tag{5.12}$$

where $\Omega_1 = -P + C_0^T C_0 + (1 + \frac{1}{\epsilon_1} + \frac{1}{\epsilon_2})\gamma^2 \eta_1 I$, $\Omega_2 = -Q - C_0^T C_0 + (1 + \frac{1}{\epsilon_3} + \frac{1}{\epsilon_4})\gamma^2 \eta_2 I$. *Then, the residual generator is stable and the FDF* (5.2) *is considered to solve the following constraints simultaneously*

$$\|r_{0,w}\|_2 \leq \alpha \|w_{0,k}\|_2 \tag{5.13}$$
$$\|r_{0,f}\|_2 \geq \beta \|f_{0,k}\|_2 \tag{5.14}$$

Proof. Let us consider a quadratic Lyapunov function

$$V_k = x_{0,k}^T P x_{0,k}; \quad V_{k+1} = x_{0,k+1}^T P x_{0,k+1}$$

taking the difference along the trajectory of the residual generator (5.5)

$$\Delta V_k = V_{k+1} - V_k = x_{0,k+1}^T P x_{0,k+1} - x_{0,k}^T P x_{0,k}$$

$$\begin{aligned} \Rightarrow \Delta V_k = (A_0 x_{0,k} + E_0 w_{0,k})^T P (A_0 w_{0,k} + E_0 w_{0,k}) - x_{0,k}^T P x_{0,k} \\ + \underbrace{2x_{0,k}^T A_0^T P \Psi_k + 2w_{0,k}^T E_0^T P \Psi_k + \Psi_k^T P \Psi_k} \end{aligned} \tag{5.15}$$

Notice that the last three terms (indicated with under-braced) contain the nonlinear part of (5.5). Using Lemma (A.3.2), the above terms are expanded as follows

$$\begin{aligned} 2x_{0,k}^T A_0^T P \Psi_k &\leq x_{0,k}^T \epsilon_1 A_0^T P A_0 x_{0,k} + \frac{1}{\epsilon_1} \Psi_k^T P \Psi_k \\ 2w_{0,k}^T E_0^T P \Psi_k &\leq w_{0,k}^T \epsilon_2 E_0^T P E_0 w_{0,k} + \frac{1}{\epsilon_2} \Psi_k^T P \Psi_k \end{aligned} \tag{5.16}$$

using Cashy-Schwarz inequality

$$\Psi_k^T P \Psi_k \leq \gamma^2 \bar{\sigma}(P) x_{0,k}^T x_{0,k} \tag{5.17}$$

using equation (5.17), (5.16) becomes

$$\begin{aligned} 2w_{0,k}^T A_0^T P \Psi_k &\leq x_{0,k}^T \epsilon_1 A_0^T P A_0 x_{0,k} + \frac{1}{\epsilon_1} \gamma^2 \bar{\sigma}(P) x_{0,k}^T x_{0,k} \\ 2w_{0,k}^T E_0^T P \Psi_k &\leq w_{0,k}^T \epsilon_2 E_0^T P E_0 w_{0,k} + \frac{1}{\epsilon_2} \gamma^2 \bar{\sigma}(P) x_{0,k}^T x_{0,k} \end{aligned} \tag{5.18}$$

using (5.18) and (5.17), (5.15) can be represented as

$$\Delta V_k \leq (A_0x_{0,k} + E_0w_{0,k})^T P(A_0x_{0,k} + E_0w_{0,k}) - x_{0,k}^T Px_{0,k} + x_{0,k}^T\epsilon_1 A_0^T PA_0x_{0,k} + w_{0,k}^T\epsilon_2 E_0^T PE_0w_{0,k} + (1 + \frac{1}{\epsilon_1} + \frac{1}{\epsilon_2})\gamma^2\bar{\sigma}(P)x_{0,k}^T x_{0,k}$$

Let $\bar{\sigma}(P) < \eta_1$, with $\eta_1 > 0$. It is equivalent to $0 < \eta_1 I - \eta_1^{-1}PP$ which can be represented by LMI $\mathscr{L}_1$ of Theorem 5.1.1. Now (5.16) implies that

$$\Delta V_k \leq (A_0x_{0,k} + E_0w_{0,k})^T P(A_0x_{0,k} + E_0w_{0,k}) - x_{0,k}^T Px_{0,k} + x_{0,k}^T\epsilon_1 A_0^T PA_0x_{0,k} + w_{0,k}^T\epsilon_2 E_0^T PE_0w_{0,k} + (1 + \frac{1}{\epsilon_1} + \frac{1}{\epsilon_2})\gamma^2\beta I x_{0,k}^T x_{0,k}$$

Also considering

$$\|r_{0,w}\|_2 \leq \alpha\|w_{0,k}\|_2$$
$$\Rightarrow \sum_{k=0}^{\infty}\left[r_{0,k}^T r_{0,k} - \alpha^2 w_{0,k}^T w_{0,k}\right]$$

and defining

$$\mathscr{J} = \sum_{k=0}^{\infty}\left[r_{0,k}^T r_{0,k} - \alpha^2 w_{0,k}^T w_{0,k}\right] \tag{5.19}$$

under zero-initial conditions

$$\mathscr{J} = \sum_{k=0}^{\infty}\left[r_{0,k}^T r_{0,k} - \alpha^2 w_{0,k}^T w_{0,k} + \Delta V_k\right]$$

A sufficient condition for $\mathscr{J} \leq 0$ can thus be given as

$$r_{0,w}^T r_{0,w} - \alpha^2 w_{0,k}^T w_{0,k} + \Delta V_k < 0 \Rightarrow \tag{5.20}$$

It turns out

$$r_{0,w}^T r_{0,w} - \eta^2 w_{0,k}^T w_{0,k} + \Delta V_k \leq (C_0x_{0,k} + F_0w_{0,k})^T(C_0x_{0,k} + F_0w_{0,k}) - \alpha^2 w_{0,k}^T w_{0,k} + (A_0x_{0,k} + E_0w_{0,k})^T P(A_0x_{0,k} + E_0w_{0,k}) - x_{0,k}^T Px_{0,k} + x_{0,k}^T\epsilon_1 A_0^T PA_0x_{0,k} + w_{0,k}^T\epsilon_2 E_0^T PE_0w_{0,k} + (1 + \frac{1}{\epsilon_1} + \frac{1}{\epsilon_2})\gamma^2\beta I x_{0,k}^T x_{0,k}$$

in order to ensure $\mathscr{J} \leq 0$; the right hand side (RHS) of the above inequality must be negative, that is,

$$\begin{bmatrix} x_{0,k}^T \\ w_{0,k}^T \end{bmatrix}^T \left(\begin{bmatrix} A_0^T & C_0^T \\ E_0^T & F_0^T \end{bmatrix}\begin{bmatrix} P & 0 \\ 0 & I \end{bmatrix}\begin{bmatrix} A_0 & E_0 \\ C_0 & F_0 \end{bmatrix} + \begin{bmatrix} \zeta_1 & 0 \\ 0 & \zeta_2 \end{bmatrix}\right)\begin{bmatrix} x_{0,k} \\ w_{0,k} \end{bmatrix} < 0 \tag{5.21}$$

where $\zeta_1 = -P + \epsilon_1 A_0^T PA_0 + (1 + \frac{1}{\epsilon_1} + \frac{1}{\epsilon_2})\gamma^2\beta I$, $\zeta_2 = \epsilon_2 E_0^T PE_0 - \alpha^2 I$. Using Schur complement, the inequality (5.21) can be transformed into LMI $\mathscr{L}_2$ of Theorem 5.1.1.

Now consider another quadratic Lyapunov function, that is $Y_k = x_{0,k}^T Q x_{0,k}$, $Q^T = Q > 0$ and taking the difference along the trajectories of the residual generator (5.7) as

$$\Delta Y_k = Y_{k+1} - Y_k = x_{0,k+1}^T Q x_{0,k+1} - x_{0,k}^T Q x_{0,k}$$

$$\begin{aligned} \Rightarrow \Delta Y_k = (A_0 x_{0,k} + E_{0,f} f_{0,k})^T Q (A_0 f_{0,k} + E_{0,f} f_{0,k}) - f_{0,k}^T Q f_{0,k} \\ + \underbrace{2 f_{0,k}^T A_0^T Q \Psi_k + 2 f_{0,k}^T E_{0,f}^T P \Psi_k + \Psi_k^T Q \Psi_k} \end{aligned} \tag{5.22}$$

The nonlinear terms are shown under-braced. Using Cashy-Schwarz inequality

$$\Psi_k^T Q \Psi_k \leq \gamma^2 \bar{\sigma}(Q) x_{0,k}^T x_{0,k} \tag{5.23}$$

together with Lemma (A.3.2) implies

$$\begin{aligned} 2 x_{0,k}^T A_0^T Q \Psi_k &\leq x_{0,k}^T \epsilon_1 A_0^T Q A_0 x_{0,k} + \frac{1}{\epsilon_1} \gamma^2 \bar{\sigma}(Q) x_{0,k}^T x_{0,k} \\ 2 f_{0,k}^T E_{0,f}^T Q \Psi_k &\leq f_{0,k}^T \epsilon_2 E_{0,f}^T Q E_{0,f} f_{0,k} + \frac{1}{\epsilon_2} \gamma^2 \bar{\sigma}(Q) x_{0,k}^T x_{0,k} \end{aligned} \tag{5.24}$$

using (5.24) and (5.23), (5.22) can be represented as

$$\begin{aligned} \Delta Y_k \leq & (A_0 x_{0,k} + E_0 f_{0,k})^T Q (A_0 x_{0,k} + E_0 f_{0,k}) - x_{0,k}^T Q x_{0,k} + x_{0,k}^T \epsilon_3 A_0^T Q A_0 x_{0,k} + \\ & f_{0,k}^T \epsilon_4 E_0^T Q E_0 f_{0,k} + (1 + \frac{1}{\epsilon_1} + \frac{1}{\epsilon_2}) \gamma^2 \bar{\sigma}(Q) x_{0,k}^T x_{0,k} \end{aligned} \tag{5.25}$$

Let $\bar{\sigma}(Q) < \eta_2$, with $\eta_2 > 0$. It is equivalent to $0 < \beta_2 I - \beta_2^{-1} Q Q$ which can be represented by LMI $\mathscr{L}_3$ of Theorem 5.1.1. Now (5.25) implies that

$$\begin{aligned} \Delta V_k \leq & (A_0 x_{0,k} + E_0 f_{0,k})^T Q (A_0 x_{0,k} + E_0 f_{0,k}) - x_{0,k}^T Q x_{0,k} + x_{0,k}^T \epsilon_3 A_0^T Q A_0 x_{0,k} \\ & + f_{0,k}^T \epsilon_4 E_0^T Q E_0 f_{0,k} + (1 + \frac{1}{\epsilon_3} + \frac{1}{\epsilon_4}) \gamma^2 \beta I x_{0,k}^T x_{0,k} \end{aligned} \tag{5.26}$$

Also considering

$$\begin{aligned} \|r_{0,f}\|_2 \geq \beta \|f_{0,k}\|_2 \\ \Rightarrow \sum_{k=0}^{\infty} \left[r_{0,k}^T r_{0,k} - \beta^2 f_{0,k}^T f_{0,k} \right] \geq 0 \end{aligned}$$

and defining

$$\mathscr{J} = \sum_{k=0}^{\infty} \left[r_{0,k}^T r_{0,k} - \beta^2 f_{0,k}^T f_{0,k} \right] \tag{5.27}$$

under zero-initial conditions

$$\mathscr{J} < \sum_{k=0}^{\infty} \left[-r_{0,k}^T r_{0,k} + \beta^2 f_{0,k}^T f_{0,k} + \Delta V_k \right] \tag{5.28}$$

A sufficient condition for $\mathscr{J} \leq 0$ can thus be given as

$$-r_{0,f}^T r_{0,f} + \beta^2 f_{0,k}^T f_{0,k} + \Delta V_k < 0 \tag{5.29}$$

It turns out

$$\begin{aligned}-r_{0,f}^T r_{0,f} + \beta^2 f_{0,k}^T f_{0,k} + \Delta V_k \leq & -(C_0 x_{0,k} + F_0 f_{0,k})^T (C_0 x_{0,k} + F_0 f_{0,k}) + \beta^2 f_{0,k}^T f_{0,k} \\ & + (A_0 x_{0,k} + E_0 f_{0,k})^T Q (A_0 x_{0,k} + E_0 f_{0,k}) - x_{0,k}^T Q x_{0,k} \\ & + x_{0,k}^T \epsilon_3 A_0^T Q A_0 x_{0,k} + f_{0,k}^T \epsilon_4 E_0^T Q E_0 f_{0,k} + \\ & (1 + \frac{1}{\epsilon_3} + \frac{1}{\epsilon_4}) \gamma^2 \beta I x_{0,k}^T x_{0,k}\end{aligned}$$

making the right hand side (RHS) of the above inequality negative ensures $\mathscr{J} \leq 0$; that is,

$$\begin{bmatrix} x_{0,k}^T \\ f_{0,k}^T \end{bmatrix}^T \left(\begin{bmatrix} A_0^T \\ E_{0,f}^T \end{bmatrix} Q \begin{bmatrix} A_0 & E_{0,f} \end{bmatrix} + \begin{bmatrix} \zeta_1 & -C_0^T F_{0,f} \\ -F_{0,f}^T C_0 & \zeta_2 \end{bmatrix} \right) \begin{bmatrix} x_{0,k} \\ f_{0,k} \end{bmatrix} < 0$$

where $\zeta_1 = -Q - C_0^T C_0 + \epsilon_3 A_0^T Q A_0 + (1 + \frac{1}{\epsilon_3} + \frac{1}{\epsilon_4}) \gamma^2 \beta I; \zeta_2 = \epsilon_4 E_{0,f}^T Q E_{0,f} - F_{0,f}^T F_{0,f} + \beta^2 I$ using Schur complement, the LMI $\mathscr{L}_4$ of Theorem 5.1.1 can be obtained.
For the stability analysis, rewriting the conditions (4.34) as

$$\Delta V_k < -r_{0,w}^T r_{0,w} + \alpha^2 w_0^T w_0 \tag{5.30}$$

which shows the residual generator (5.5) is dissipative with $V(.)$ and with respect to supply rate $\mathscr{S} = -r_{0,w}^T r_{0,w} + \alpha^2 w_0^T w_0$. Now substituting $w_{0,k} = 0$, the above inequality becomes

$$\Delta V_k < -r_0^T r_0 \tag{5.31}$$

which shows the (global) asymptotic stability of the origin; that is, $x_{0,k} = 0$ of the nominal form of the residual generator (5.5). The inequality (5.31) can be expressed as

$$\begin{bmatrix} \eta_1 I & P \\ * & \eta_1 I \end{bmatrix} > 0 \tag{5.32}$$

$$\begin{bmatrix} -P & & P A_0 & 0 \\ * & -P + C_0^T C_0 + \left(1 + \frac{1}{\epsilon_1}\right) \gamma^2 \eta_1 & A_0^T P \\ * & & * & -\frac{1}{\epsilon_1} P \end{bmatrix} < 0 \tag{5.33}$$

Note that the LMIs (5.32) and (5.33) can also be obtained directly from LMIs (5.9) and (5.10) by substituting $w_{0,k} = 0$. Consequently, the feasibility of LMIs (5.9) and (5.10) imply the feasibility of LMIs (5.32) and (5.33). This shows that the stability of the residual generator can be ensured from the feasibility of the LMIs (5.9) and (5.10) and hence, it is not needed to satisfy LMIs (5.30) and (5.31) additionally.
This completes the proof. □

Remark 5.1.1. *Note that both P and Q matrices are defined as positive definite matrices in the above Theorem. Declaring $Q = P$, the filter gain L can also be obtained by solving the LMIs $\mathscr{L}_1$-$\mathscr{L}_4$. In that case, a matrix Y of appropriate dimensions has to be defined as an additional LMI variable and then by setting $PA_0 = PA - YC$, the filter gain L will be determined using the relation; that is, $L = P^{-1}Y$. Furthermore, the post filter W is usually chosen before hand. However it can also be computed from the above LMIs. To this end, a new LMI variable $Z = W^TW \geq \eta_3 I$ has to be defined. The limit $\eta_3 > 0$ is introduced in order to avoid the trivial solution; that is, $Z = 0$. The post filter can then be computed as $W = \sqrt{Z}$*[1]

Based on the above discussion, the following algorithm is proposed:

Algorithm 5.1.1. *Computation of the mixed $\mathscr{H}_-/\mathscr{H}_\infty-$ FDF for discrete-time Lipschitz nonlinear systems*

Step I. *Set the disturbance attenuation level α to some value*

Step II. *Choose $P = Q$, and set $Y = PL$. Also define $Z = W^TW$, if the post filter is to be computed on-line, otherwise, set it to some constant value of appropriate dimensions.*

Step III. *Solve the LMIs* (5.9),(5.10), (5.12) *so that the sensitivity level β is maximized for some nonnegative scalars $\epsilon_i|_{i=1,\cdots,4}$ and $\eta_i|_{1,2}$, a matrix Y, Z (if W is not pre-chosen) and positive definite matrix P.*

Step IV. *Once the problem is solved, then for the desired filter gain set $L = P^{-1}Y$ and for the post filter $W = \sqrt{Z}$*

5.2 Residual generation for continuous-time Lipschitz nonlinear systems

5.2.1 Problem formulation

Consider a continuous-time Lipschitz nonlinear system governed by the following differential equations

$$\begin{aligned} \dot{x} &= Ax + Bu + \phi(x,u) + E_w w + E_f f \\ y &= Cx + Du + F_w w + F_f f \end{aligned} \tag{5.34}$$

The nonlinear function satisfies the Lipschitz conditions (3.6) with a Lipschitz constant γ. In addition, the pair (C, A) is assumed to be detectable and the w, f are $\mathscr{L}_2-$ norm

[1] This is, indeed, a matrix square root

bounded. Moreover, consider the following nonlinear observer-based fault detection filter

$$\Sigma_O : \begin{cases} \dot{\hat{x}} = A\hat{x} + Bu + \phi(\hat{x}, u) + L(y - C\hat{x} - Du) \\ r = W(y - C\hat{x} - Du) \end{cases} \tag{5.35}$$

where the signals x, u, w, f, y, r and the matrices $A, B, C, D, E_w, F_w, E_f, F_f, L, W$ serve the same purpose as introduced in Section 5.1.1 but in continuous-time. Denoting the estimation error $e = x - \hat{x}$, the error dynamics can be obtained as follows

$$\Sigma_\xi : \begin{cases} \dot{e} = (A - LC)e + (E_w - LF_w)\, w + \phi(x, u) - \phi(\hat{x}, u) + (E_f - LF_f)f \\ r = W(Ce + F_w w + F_f f) \end{cases} \tag{5.36}$$

Analogous to the discrete-time residual generator (5.4), the following residual generator is used for continuous-time case

$$\Sigma_{\mathscr{R}} : \begin{cases} \dot{x}_0 = A_0 x_0 + E_0 w_0 + \Psi_0 + E_{0,f} f_0 \\ r_0 = C_0 x_0 + F_0 w_0 + F_{0,f} f_0 \end{cases} \tag{5.37}$$

where

$$\begin{aligned} x_0 &= e; \quad w_0 = w; \quad f_0 = f \quad A_0 = A - LC; \\ E_0 &= E_w - LF_w; \quad E_{0,f} = E_f - LF_f \\ C_0 &= WC; \quad F_0 = WF_w; \quad F_{0,f} = WF_f; \end{aligned}$$

$$\Psi_0 \coloneqq \Psi_0(x, \hat{x}, u) = \phi(x, u) - \phi(\hat{x}, u)$$

In order to analyse the effect of unknown inputs on the residual signal, assume $f = 0$. The following state-space model of the residual generator (5.37) will be used

$$\begin{aligned} \dot{x}_0 &= A_0 x_0 + \Psi_0 + E_0 w_0 \\ r_{0,w} &= C_0 x_0 + F_0 w_0 \end{aligned} \tag{5.38}$$

The associated $\mathscr{H}_\infty$−norm is defined as

$$\int_0^\infty \|r_{0,w}\|^2 dt \le \alpha^2 \int_0^\infty \|w_0\|^2 dt \tag{5.39}$$

Similarly, studying the effect of faults alone on the residual signal, putting $w = 0$, the following state-space model for the residual generator (5.37) will be used

$$\begin{aligned} \dot{x}_0 &= A_0 x_0 + \Psi_0 + E_{0,f} f_0 \\ r_{0,f} &= C_0 x_0 + F_{0,f} f_0 \end{aligned} \tag{5.40}$$

and the associated $\mathscr{H}_-$ index is given by

$$\int_0^\infty \|r_{0,f}\|^2 dt \ge \beta^2 \int_0^\infty \|f_0\|^2 dt \tag{5.41}$$

5.2.2 Design of FDF based on $\mathscr{H}_-/\mathscr{H}_\infty-$ optimization

The following theorem presents sufficient conditions for the existence of $\mathscr{H}_-/\mathscr{H}_\infty-$ for continuous-time Lipschitz nonlinear systems.

Theorem 5.2.1. *Given the Lipschitz nonlinear system* (5.34)*, the FDF* (5.35)*, the associated residual generator* (5.36) *and scalars* $\alpha > 0$ *and* $\beta > 0$*. Further, suppose there exist nonnegative constants* ϵ_1, ϵ_2*, symmetric positive (semi) definite matrices* P*,* Q*, matrices* L *and* W *called filter gain and post filter gain respectively, satisfying the following set of LMIs*

$$\mathscr{L}_1 := \begin{bmatrix} \Omega_1 & P(E_w - LF_w) + C^T Z F_w & P \\ * & -\alpha^2 I + F_w^T Z F_w & 0 \\ * & * & -\epsilon_1 I \end{bmatrix} < 0 \tag{5.42}$$

$$\mathscr{L}_2 := \begin{bmatrix} \Omega_2 & Q(E_f - LF_f) - C^T Z F_f & Q \\ * & -\beta^2 I + F_f^T Z F_f & 0 \\ * & * & -\epsilon_2 I \end{bmatrix} < 0 \tag{5.43}$$

where $\Omega_1 = P(A - LC) + (A - LC)^T P + C^T Z C + \epsilon_1 \gamma^2 I$*,* $\Omega_2 = Q(A - LC) + (A - LC)^T Q - C^T Z C + \epsilon_2 \gamma^2 I$*,* $W = \sqrt{Z}$*.*
Then, the residual generator is stable and the FDF (5.35) *solves the following mixed constraints simultaneously*

$$\|r_{0,w}\|_2 \le \alpha \|w_0\|_2 \tag{5.44}$$

$$\|r_{0,f}\|_2 \ge \beta \|f_0\|_2 \tag{5.45}$$

Proof. Consider a quadratic Lyapunov function

$$V = x_0^T P x_0 \qquad P = P^T > 0$$

Differentiating it along the trajectory of the residual generator (5.38), then

$$\begin{aligned} \dot{V} &= \dot{x}_0^T P x_0 + x_0^T P \dot{x}_0 \\ &= (A_0 x_0 + \Psi_0 + E_0 w_0)^T P x_0 + x_0^T P (A_0 x_0 + \Psi_0 + E_0 w_0) \end{aligned}$$

or

$$\dot{V} = x_0^T \left(A_0^T P + P A_0\right) x_0 + x_0^T P E_0 w_0 + w_0^T E_0^T P x_0 + \underbrace{\Psi_0^T P x_0 + x_0^T P \Psi_0} \tag{5.46}$$

The nonlinear terms shown under the braces are bounded in the following sense

$$\Psi_0^T P x_0 + x_0^T P \Psi_0 \le x_0^T \epsilon_1 P P x_0 + \frac{1}{\epsilon_1} \Psi_0^T \Psi_0$$

where $\epsilon_1 > 0$. Using the Lipschitz conditions, the above bound can be obtained as

$$\Psi_0^T P x_0 + x_0^T P \Psi_0 \le x_0^T \epsilon_1 P P x_0 + \frac{1}{\epsilon_1} \gamma^2 x_0^T x_0 \tag{5.47}$$

using (5.47), equation (5.46) is given as

$$\begin{aligned}\dot{V} \leq x_0^T \left(A_0^T P + P A_0\right) x_0 + x_0^T P E_0 w_0 \\ + w_0^T E_0^T P x_0 + x_0^T \epsilon_1 P P x_0 + \frac{1}{\epsilon_1}\gamma^2 x_0^T x_0\end{aligned} \tag{5.48}$$

Now considering the constraints (5.44)

$$\|r_{0,w}\|_2 \leq \alpha \|w_0\|_2$$

Defining an index $\mathscr{J}_1$ as

$$\mathscr{J}_1 = \int_0^\infty \left[r_{0,w}^T r_{0,w} - \alpha^2 w_0^T w_0\right] dt \tag{5.49}$$

Under zero initial conditions

$$\mathscr{J}_1 < \int_0^\infty \left[r_{0,w}^T r_{0,w} - \alpha^2 w_0^T w_0 + \dot{V}\right] dt$$

Therefore

$$r_{0,w}^T r_{0,w} - \alpha^2 w_0^T w_0 + \dot{V} < 0 \tag{5.50}$$

for $\mathscr{J}_1 \leq 0$. Now using (5.48), inequality (5.50) is obtained as

$$\begin{aligned}x_0^T \left(A_0^T P + P A_0\right) x_0 + x_0^T A_0^T P E_0 w_0 + w_0^T E_0^T P A_0 x_0 + x_0^T \epsilon_1 P P x_0 + \frac{1}{\epsilon_1}\gamma^2 x_0^T x_0 \\ x_0^T C_0^T F_0 w_0 + w_0^T F_w C_0 x_0 + x_0^T C_0^T C_0 x_0 + w_0^T (F_w F_w - \alpha^2 I) w_0 < 0\end{aligned} \tag{5.51}$$

using Schur complements together with simple mathematical manipulations, the above inequality can be transformed into LMI $\mathscr{L}_1$. Similarly, considering a Lyapunov function $Y = x_0^T Q x_0$ and defining the index

$$\mathscr{J}_2 = \int_0^\infty \left[r_{0,f}^T r_{0,f} - \beta^2 f_0^T f_0\right] dt$$

under zero initial conditions

$$\mathscr{J}_2 < \int_0^\infty \left[\beta^2 f_0^T f_0 - r_{0,f}^T r_{0,f} + \dot{Y}\right] dt$$

Proceeding in the similar way as above, the following inequality should hold which provide sufficient condition for the sensitivity constrains (5.45)

$$\begin{aligned}x_0^T \left(A_0^T Q + Q A_0\right) x_0 + x_0^T Q E_{0,f} f_0 + f_0^T E_{0,f}^T Q x_0 + x_0^T \epsilon_2 Q Q x_0 + \frac{1}{\epsilon_2}\gamma^2 x_0^T x_0 \\ -x_0^T C_0^T F_{0,f} f_0 - f_0^T F_{0,f} C_0 x_0 - x_0^T C_0^T C_0 x_0 - f_0^T (F_{0,f} F_{0,f} - \beta^2 I) f_0 < 0\end{aligned} \tag{5.52}$$

which together with Schur complements and some mathematical manipulation yields the LMI $\mathscr{L}_2$.
Furthermore, the stability analysis of the proposed filter can be performed along the similar lines of the proof of Theorem 5.1.1.
This completes the proof. □

Remark 5.2.1. *The $\mathscr{H}_-$−index does not guarantee the stability of the residual generator. However, sufficient conditions for the stability is provided by the LMI* (5.42) *in the mixed problem. Once it is feasible, stability can be achieved.*

Following the similar arguments established in Remark 5.1.1, LMIs (5.42) and (5.43) can be used to determine the filter gain L. This can be done by choosing $P = Q$. Similarly the post filter gain can also be computed from these LMIs by introducing Z as LMI variable. In what follows, an algorithm is proposed which is useful in solving the problem of mixed FDF design for nonlinear systems.

Algorithm 5.2.1. *Computation of the mixed $\mathscr{H}_-/\mathscr{H}_\infty-$ FDF for continuous-time Lipschitz nonlinear systems*

Step I. *Set the disturbance attenuation level α to pre-defined value*

Step II. *Choose $P = Q$, and set $Y = PL$. Also define $Z = W^TW$, if the post filter has to be computed on-line.*

Step III. *Solve the LMIs* (5.42) *and*(5.43) *so that the sensitivity level β is maximized for some nonnegative constants ϵ_1, ϵ_2 and positive definite matrix P.*

Step IV. *Once the problem is solved, then for the desired filter gain set $L = P^{-1}Y$ and for the post filter $W = \sqrt{Z}$*

5.3 A design example

In order to illustrate the theory developed in this chapter, a continuous-time Lipschitz nonlinear systems governed by (5.34) with the following coefficient matrices is considered

$$A = \begin{bmatrix} 0 & 1 \\ -0.6 & -1.5 \end{bmatrix}; B = E_w = E_f = \begin{bmatrix} 1 \\ 1 \end{bmatrix}; C = [1 \;\; 0]; \;\; D = F_w = 0.2; F_f = 1;$$
$$\phi(x) = 0.21 sin(x_2); \;\; \text{with} \;\; \gamma = 0.21.$$

Using algorithm 5.2.1, for the a given disturbance attenuation level $\alpha = 0.9$ and post filter $W = 1.5$, the parameter for the mixed FDF are computed and are given as follows:

$$\beta = 0.9070; \;\; P = \begin{bmatrix} 1.3947 & 0.5620 \\ 0.5620 & 1.2393 \end{bmatrix}$$
$$Y = \begin{bmatrix} 3.2483 \\ 2.9738 \end{bmatrix}; \;\; L = \begin{bmatrix} 1.6666 \\ 1.6438 \end{bmatrix};$$

Note that the LMIs are solved using LMI toolbox in MATLAB®.

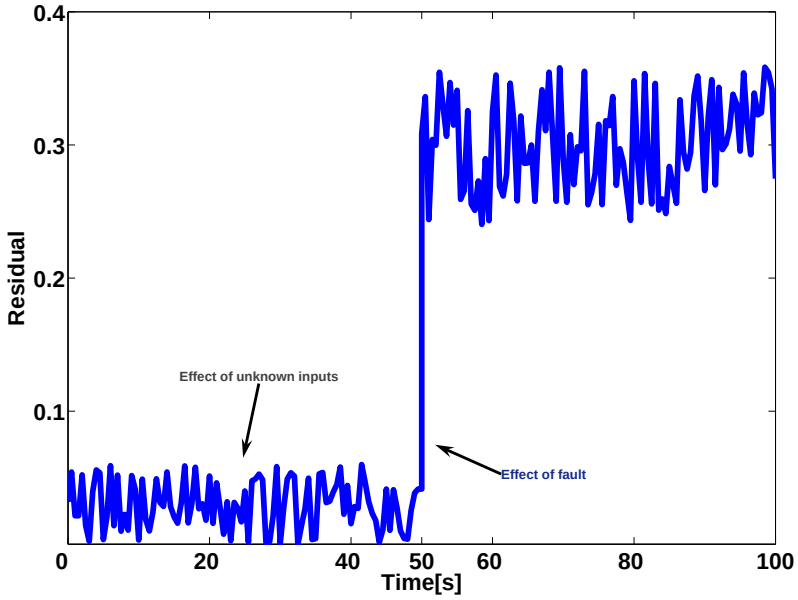

Figure 5.1: Evaluated residual with f = 0.2

Figure 5.1 shows the generated residual signal with the proposed filter having filter gain L and post filter V computed above. The unknown disturbance is assumed to have a uniform random distribution over the interval $\{-0.2, 0.2\}$. The fault is simulated with a step function of magnitude 0.2 which is appeared at time $50[s]$. The quick response of the residual signal to the fault at time $50[s]$ shows its sensitivity to fault.

5.4 Summary

In this chapter, the problem of mixed $\mathscr{H}_-/\mathscr{H}_\infty$[sub-optimal]-FDF design for Lipschitz nonlinear systems is formulated using convex optimization. Sufficient conditions for the solvability of optimal filter has been provided for discrete-time and continuous-time settings in the form of coupled LMIs. The design procedure of proposed filter were elaborated with the help of two algorithms, one for each case. Finally, an illustrative example was provided in order to elaborate the design procedure of the the mixed $\mathscr{H}_-/\mathscr{H}_\infty$–FDF for continuous-time Lipschitz nonlinear systems.

Chapter 6

Computation of thresholds for Lipschitz nonlinear uncertain systems

This chapter presents methods for the computation of thresholds for Lipschitz nonlinear uncertain systems in the presence of unknown inputs. Different types of thresholds are studied. These include constant threshold, adaptive threshold, and dynamic threshold. For constant threshold, a generalized framework based on signal norms is developed. Different kinds of constant thresholds are studied with the framework proposed. The threshold computation problem is formulated as an optimization problem and using LMI tools, algorithms are derived for the computation of these thresholds. Illustrative examples are given to elaborate the proposed methods. A comparative analysis of the proposed thresholds are also provided with the help of simulation examples. The adaptive thresholds are proposed based on the similar framework developed for constant thresholds. In this scheme, the norm of the instantaneous values of u is used instead of its bounds. This scheme considerably reduces the size of the constant threshold and as, a result, improves the fault detection capability. For dynamic threshold, an inequality on the upper bound on the modulus of the solution of the Lipschitz nonlinear systems is derived. This inequality has been proven to be an efficient tool for the computation of dynamic threshold. All of these thresholds are studied for both continuous- and discrete-time settings. Algorithms are proposed for the computation of these thresholds. The usefulness of the proposed methodology is shown by numerical examples given at the end of each Section. Finally a comparative analysis among different schemes is given.

In observer-based FD, the residual signal is obtained by comparing the process outputs with their estimates. In ideal situations, the residual signal should be affected by faults only; that is, it should go to zero if there is no fault and should deviate otherwise. However due to model uncertainties, process disturbances, and measurement noises; the residual signal is non-zero even if there is no fault in the system. This can be observed in the simulation results presented in Chapters 4 and 5. To this end, considering Figure 5.1, it is evident that before appearing the fault in the process, the residual is non-zero a value due to the effect of unknown inputs. In order to achieve successful fault detection, it is required to devise a strategy so that faults can be distinguished from unknown inputs. The process of residual evaluation and threshold settings serve this purpose. Figure 6.1 shows the schematic depiction of residual generation and evaluation scheme. In residual evaluation,

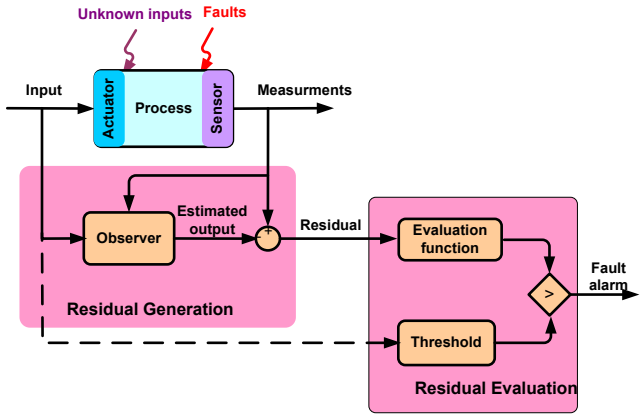

Figure 6.1: Schematic depiction of a complete FD scheme

an evaluated residual is compared with a bound, the so-called threshold, regarding the unknown inputs and model uncertainties. The presence of a fault is inferred if the former exceeds the later. Selection of suitable thresholds is very critical task in FD. Setting a threshold too high may result into a missed-detection, which means that a set of faults may remain undetected. Similarly, selecting a threshold too low may lead to false alarms. In which case, the FD system indicates a fault; however in reality, there is no fault in the system. Threshold is usually viewed as a tolerant limit for unknown inputs and model uncertainties. Due to this reason, the way of evaluating the unknown inputs plays an important role in the residual evaluation and determination of thresholds.

Different techniques have been reported in literature for designing thresholds for fault detection in linear systems (see [1, 11, 67–73] and the references therein). These thresholds can broadly be classified as i) constant thresholds and ii) variable thresholds. The constant thresholds are designed by considering the upper bound of the unknown inputs and admissible uncertainties. An extensive study on the computation of constant thresholds in linear systems can be found in [1], where different kinds of thresholds both under deterministic settings using signal norms of the unknown inputs and stochastic settings using statistical properties of unknown inputs, are proposed.

Different from constant thresholds, the variable thresholds vary with the instantaneous values of the process input and some system parameters. These include dynamic threshold and adaptive threshold. The work in [1] proposed adaptive thresholds for LTI systems which can be computed based on signal norms. These thresholds can be easily implemented on-line. In addition, a detailed study for the design of dynamic threshold for fault detection in LTI systems has been carried out in [71]. The proposed threshold is derived based on analytical solution of linear continuous-time systems with parametric uncertainty. The designed threshold generator is a dynamic system which is capable of detecting faults without generating false alarms.

Figure 6.2 shows an intuitive comparison between constant and variable thresholds. It is evident from this figure that the variable threshold varies according to the variation of the residual signal. Since the variable threshold is usually a function of the instantaneous values of the control input u instead of the norm values, its magnitude is smaller than

the constant threshold. In addition, the chances of false alarms and missed detection are likely to be more in constant threshold as compared to variable threshold. Furthermore, the fault detection time is smaller in a variable threshold as compared to the one in case of the constant threshold. Note that a fault detection time can be defined as the time between the appearance of the fault and the moment the residual exceeds a particular threshold due to that fault. A very close terminology, that is, FDR (fault detection rate) and FAR (false alarm rate) has been extensively studied in [1].

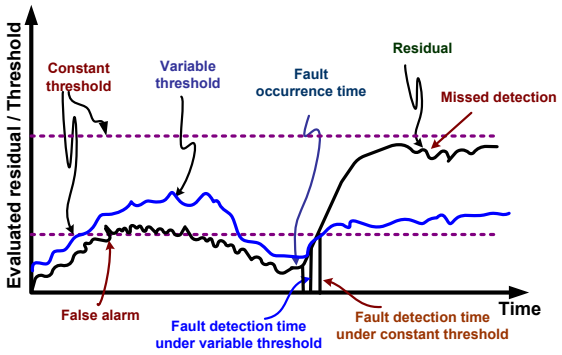

Figure 6.2: Comparison of constant and variable threshold

In contrast to LTI systems, very little attention has been devoted to the design of threshold for nonlinear systems [92, 132, 133]. The work in [132, 133] proposed the time-varying detection threshold for a class of nonlinear uncertain systems whose states are measurable. The central idea in these contributions is that the detection threshold depends on unstructured uncertainty which has a known bounding functional. This bounding functional is assumed to vary with the instantaneous values of states, control input and time. The dependence of the bounding functional on the states may lead the designed threshold to have reduced sensitivity because the states of the system are affected by the faults and hence the threshold. In spite of these results, a comprehensive study for threshold computation in nonlinear systems is still needed. The objective of this chapter is to develop a framework for the problems of residual evaluation and threshold computation in Lipschitz nonlinear uncertain systems in the presence of unknown inputs.

A solution is provided for designing constant threshold under the assumption of parametric uncertainty in the process model which is the most common type of structured uncertainty. For the purpose of residual evaluation and determination of constant thresholds, norm based framework is adopted. Besides requiring less on-line calculations, a norm based residual evaluation allows a systematic way of threshold computation. The peak and energy values of the residual are used for the purpose of evaluation. These evaluation functions are of very practical interest. Standard techniques from robust control theory; that is, $\mathscr{H}_\infty$ techniques, peak-to-peak gain minimization and generalized $\mathscr{H}_2-$ norm computation and LMI tools are employed in order to derive sufficient conditions for the computation of three kinds of constant thresholds. Section 6.1 introduces different evaluation functions which will be used in the remainder of this chapter. Section 6.2 presents an expound discussion for the computation of $J_{th,RMS,2}$ (6.2.2), $J_{th,Peak,Peak}$(6.2.3), and $J_{th,Peak,2}$(6.2.4) for discrete-time nonlinear systems. An illustrative example is provided in

subsection 6.2.5. Section 6.3 describes the computation of above mentioned thresholds for continuous-time settings. A simulation example is given in subsection 6.3.5 to elaborate the comparison of these thresholds.

One inherent feature of the constant thresholds is the use of bound on the norm of u and w. However, it is worth noting that u is generally available on-line during the process operation. If the bounds of u are substituted by the on-line values of u, the resultant threshold will be a function of the instantaneous values of u and will be no more constant. This strategy considerably reduces the size of the thresholds and enhances the fault detection capability. Note that the dependence of these thresholds on the instantaneous values of u shows that it is different under different operating conditions expressed in terms of u. Therefore, it is referred to as adaptive thresholds. Analogous to constant thresholds, different adaptive thresholds are proposed. Section 6.4 presents a brief description of these thresholds and elaborates the techniques how it can be designed.

For the computation of dynamic threshold, motivated by the results in [71], an inequality on the upper bound of the modulus of the residual signal using analytical solution of discrete-time nonlinear uncertain systems is derived. This inequality is then used for the design of dynamic threshold generator. The designed threshold generator acts as a dynamic systems taking the information of process input and some bounds on disturbances. Section 6.5 presents a comprehensive solution to the problem of computing a dynamic threshold for discrete-time Lipschitz nonlinear uncertain systems while Section 6.6 extends the same study to continuous-time settings. A brief comparison among the threshold computation schemes proposed in this Chapter has been presented in Section 6.7.

6.1 Evaluation functions

This chapter makes use of the norm-based framework for the residual evaluation. It is, therefore, indispensable to present the most commonly used evaluation functions from the FDI literature. For comprehensive study of these functions, the interested reader is referred to [1]. These functions will be used here to develop a residual evaluation and threshold computation scheme for nonlinear systems with Lipschitz nonlinearities.

The *Peak* value measure of the residual signal $r \in \mathfrak{R}^m$ is often used for evaluation. It can also be regarded as the peak norm of r.
For continuous-time $r(t)$, the peak norm is defined as

$$J_{Peak} = \|r(t)\|_{Peak} := \sup_{t\geq 0} \|r(t)\| := \sup_{t\geq 0} \sqrt{\sum_{i=1}^{m} r_i^2(t)}$$

For discrete-time $r(k)$, the peak norm is given as

$$J_{Peak} = \|r(k)\|_{Peak} := \sup_{k\geq 0} \|r(k)\| := \sup_{k\geq 0} \sqrt{\sum_{i=1}^{m} r_i^2(k)}$$

the corresponding decision logic is given as follows

$$\begin{aligned} J_{Peak} &> J_{th,Peak} \rightarrow \text{alarm (fault)} \\ J_{Peak} &\leq J_{th,Peak} \rightarrow \text{no alarm (fault-free)} \end{aligned}$$

where $J_{th,Peak}$ is the threshold and is defined as

$$J_{th,Peak} = \sup_{f=0} ||r(t)||_{Peak} \quad \text{or} \quad J_{th,Peak} = \sup_{f=0} ||r(k)||_{Peak}$$

The *Root Mean Square (RMS)* measures the average energy of a signal over a time interval $(t, t+T)$ (continuous-time case) and $(k, k+N)$ (discrete-time). For the purpose of evaluation, it is widely used in practice.
The RMS value of the residual signal for continuous-time is

$$J_{RMS} = ||r(t)||_{RMS} = \sqrt{\frac{1}{T}\int_{t}^{t+T} r^T(\tau)r(\tau)d\tau} \tag{6.1}$$

For discrete-time, the RMS of the residual signal $r(k)$ is defined as

$$J_{RMS} = ||r(k)||_{RMS} = \sqrt{\frac{1}{N}\sum_{i=1}^{N} ||r(k+i)||^2}$$

Let the threshold $J_{th,RMS}$ be defined as

$$J_{th,RMS} = \sup_{f=0} ||r(t)||_{RMS} \quad \text{or} \quad J_{th,RMS} = \sup_{f=0} ||r(k)||_{RMS} \tag{6.2}$$

then the decision logic for RMS of the residual signal can be formulated as follows

$$\begin{aligned} J_{RMS} &> J_{th,RMS} \rightarrow \text{alarm (fault)} \\ J_{RMS} &\leq J_{th,RMS} \rightarrow \text{no alarm (fault-free)} \end{aligned}$$

Another class of evaluation functions, which is often used, is based on the so-called weighted norm. For continuous-time, the weighted norm of the residual is defined as

$$J_\nu = ||r(t)||_\nu = \int_0^t \nu(t-\tau)|r(\tau)|d\tau$$

and for discrete-time

$$J_\nu = ||r(k)||_\nu = \sum_{h=0}^{k} \nu(k-h)|r(h)|$$

where ν is weighting function. It can be a rectangle window function as mentioned in [153] or exponential function as chosen by [71]. The purpose of using ν is to increase the influence of the recent data. Let J_{th} be the threshold defined as

$$J_{th} = \sup_{f=0,t\geq 0} ||r(t)||_\nu \quad \text{or} \quad J_{th} = \sup_{f=0,k\geq 0} ||r(k)||_\nu$$

The decision logic can then be given as

$$\begin{aligned} J_\nu &> J_{th} \rightarrow \text{alarm (fault)} \\ J_\nu &\leq J_{th} \rightarrow \text{no alarm (fault-free)} \end{aligned}$$

6.2 Constant threshold for discrete-time case

6.2.1 Problem formulation

Consider the following class of discrete-time nonlinear uncertain system

$$\mathscr{P}: \begin{cases} x_{k+1} &= Ax_k + Bu_k + \phi(x_k, u_k) + \eta(x_k, u_k, k) + E_w w_k + E_f f_k \\ y_k &= Cx_k + F_w w_k + F_f f_k \end{cases} \tag{6.3}$$

where the signals x, u, w, f, y and the matrices $A, B, C, D, E_w, F_w, E_f, F_f$ serve the same purpose as introduced in Section 5.1.1. Moreover, the term η represents the model uncertainty. Considering the FDF (5.2) and defining $e_k = x_k - \hat{x}_k$, the observer error dynamics can then be given as

$$\mathscr{E}: \begin{cases} e_{k+1} &= \bar{A}e_k + \phi(x_k, e_k, u_k) + \eta(x_k, u_k, k) + \bar{E}_w w_k + \bar{E}_f f_k \\ r_k &= W(Ce_k + F_w w_k + F_f f_k) \end{cases} \tag{6.4}$$

where $\bar{A} = A - LC$, $\bar{E}_w = E_w - LF_w$, $\bar{E}_f = E_f - LF_f$ and $\phi(x_k, e_k, u_k) = \phi(x_k, u_k) - \phi(x_k - e_k, u_k)$. Combining the nonlinear process (6.3) and observer error dynamics (6.4), the augmented form of the residual generator is represented as follows

$$\mathscr{R}: \begin{cases} x_{0,k+1} &= A_0 x_{0,k} + \Psi_0(x_{0,k}, w_{0,k}) + \eta_0(x_{0,k}, w_{0,k}, k) + E_0 w_{0,k} + E_{0,f} f_k \\ r_{0,k} &= C_0 x_{0,k} + F_0 w_{0,k} + F_{0,f} f_k \end{cases} \tag{6.5}$$

where $x_{0,k} = \begin{bmatrix} x_k^T & e_k^T \end{bmatrix}^T$, $w_{0,k} = \begin{bmatrix} u_k^T & w_k^T \end{bmatrix}^T$, $A_0 = diag(A, \bar{A})$, $E_{0,f} = \begin{bmatrix} E_f^T & \bar{E}_f^T \end{bmatrix}^T$, $C_0 = \begin{bmatrix} 0 & WC \end{bmatrix}$, $F_0 = \begin{bmatrix} 0 & WF_d \end{bmatrix}$, $F_{0,f} = WF_f$, $E_0 = \begin{bmatrix} B & E_d \\ 0 & \bar{E}_d \end{bmatrix}$.

$$\Psi_0(x_{0,k}, w_{0,k}) = \begin{bmatrix} \phi(x_k, u_k) \\ \phi(x_k, e_k, u_k) \end{bmatrix}, \quad \eta_0(x_{0,k}, w_{0,k}, k) = \begin{bmatrix} \eta(x_k, u_k, k) \\ \eta(x_k, u_k, k) \end{bmatrix}$$

It is worth noting that the residual generator (6.5) is not only influenced by f but also by w_0 and model uncertainty η.

Remark 6.2.1. *In order to analyze the effect of disturbances on the residual signal for the purpose of residual evaluation and determination of thresholds, a fault-free residual generator with the following dynamics is used*

$$\mathscr{R}_{\mathscr{D}}: \begin{cases} x_{0,k+1} &= A_0 x_{0,k} + \Psi_0(x_{0,k}, w_{0,k}) + \eta_0(x_{0,k}, w_{0,k}, k) + E_0 w_{0,k} \\ r_{0,k,w} &= C_0 x_{0,k} + F_0 w_{0,k} \end{cases} \tag{6.6}$$

where A_0, E_0 , C_0 , F_0, $\Psi_0(x_{0,k}, w_{0,k})$ and $\eta_0(x_{0,k}, w_{0,k}, k)$ are given in (6.5).

Remark 6.2.2. *The uncertainty η in the process model* (6.3) *may be regarded as structured or unstructured. In this study, the following form of parameterizable structured uncertainty is used*

$$\begin{aligned} \eta(x_k, u_k, k) &= \Delta(A)x_k + \Delta(B)u_k \\ &= E\Delta(k)\left(Gx_k + Hu_k\right) \end{aligned} \tag{6.7}$$

then the residual generator (5.6) *can be given as*

$$\mathscr{R}: \begin{cases} x_{0,k+1} & = (A_0 + \Delta A_0)\, x_{0,k} + \Psi_0(x_{0,k}, w_{0,k}) + (E_0 + \Delta E_0)\, w_{0,k} \\ & = \bar{A}_0 x_{0,k} + \Psi_0(x_{0,k}, w_{0,k}) + \bar{E}_0 w_{0,k} \\ r_{0,k,w} & = C_0 x_{0,k} + F_0 w_{0,k} \end{cases} \tag{6.8}$$

where

$$\Delta A_0 = \begin{bmatrix} \Delta A & 0 \\ \Delta A & 0 \end{bmatrix}, \quad \Delta E_0 = \begin{bmatrix} \Delta B & 0 \\ \Delta B & 0 \end{bmatrix}$$

and using (6.7)*, we have*

$$\begin{aligned} &[\Delta A_0 \quad \Delta E_0] = \bar{E}\Delta(k)\begin{bmatrix}\bar{G} & \bar{H}\end{bmatrix}, \\ &\bar{E} = \begin{bmatrix}E^T & E^T\end{bmatrix}^T, \quad \bar{G} = [G \quad 0], \quad \bar{H} = [H \quad 0], \quad |\Delta(k)| \le 1 \end{aligned}$$

Since the major focus of this chapter is on the computation of threshold, the following assumptions should hold for the subsequent study:

A1. The initial conditions are set equal to zero, that is, $x_0(0) = 0$,

A2. The fault-free residual generator dynamics (6.8) is a finite-gain $\mathscr{L}$ stable [98]; that is, for $\mathscr{L}_2$−norm

$$\|r_{0,k,w}\|_2 \le \rho_1 \|w_{0,k}\|_2 \tag{6.9}$$

and, for $\mathscr{L}_\infty$−norm

$$\|r_{0,k,w}\|_\infty \le \rho_2 \|w_{0,k}\|_\infty \tag{6.10}$$

where $\rho_1 > 0$, $\rho_2 > 0$.

Remark 6.2.3. *It is worth noting that the assumption $x_0(0) = 0$ does not lead to the loss of generality. In case $x_0(0) \neq 0$, it can be considered as an additional unknown input.*

Next, the design of different types of constant thresholds is presented. Note that determining a threshold means to find out the maximum effect of unknown inputs and model uncertainties on the residual signal under fault-free operation. To this end, the size of the unknown inputs and model uncertainties, size of the residual signal and finally their relation is very important. In this context, three different situations are introduced in which case the effect of the RMS and/or Peak values of the unknown inputs on the RMS or Peak values of the residual signal can be studied. These situations are interpreted in terms of thresholds $J_{th,RMS,2}$, $J_{th,Peak,Peak}$ and $J_{th,Peak,2}$. Sufficient conditions for the computation of these thresholds are derived in the subsequent subsections.

6.2.2 Computation of $J_{th,RMS,2}$

The RMS value of the residual signal is widely used for the purpose of evaluation. The threshold $J_{th,RMS,2}$ measures the change in the RMS value of the residual signal caused by the bounded changes in the energy of unknown inputs $w_{0,k}$ in the presence of admissible model uncertainties.

Definition 6.2.1. *Given the RMS value of the residual signal as*

$$J_{RMS} = \sup_{k\geq 0} \|r_{0,k,w}\|_{RMS}$$

then $J_{th,RMS,2}$ is defined as

$$J_{th,RMS,2} = \sup\left\{ J_{RMS} : \|r_{0,k,w}\|_{RMS} \leq \alpha \frac{\|w_{0,k}\|_2}{\sqrt{N}},\ \textit{for } x_0 = 0, f = 0,\ \forall\ |\Delta(k)| \leq 1 \right\}$$

where α is the $\mathcal{L}_2-$gain. It is to be noted that the RMS value of a signal is related to its $\mathcal{L}_2-$ norm as

$$\|r_{0,k,w}\|^2_{RMS} \leq \frac{1}{N}\|r_{0,k,w}\|^2_2$$

where N is the length of the evaluation window or observation time.

The following theorem presents the main result for the computation of $J_{th,RMS,2}$.

Theorem 6.2.1. *Suppose the residual generator* (6.8) *satisfies Assumptions A1-A2 and the model uncertainty is structured of the form* (6.7) *with $\Delta(k)^T\Delta(k) \leq I$, then for a given scalar $\alpha > 0$, the $\mathcal{L}_2$-gain residual generator* (6.8) *is less than or equal to α; that is,*

$$\|r_{0,k,w}\|_2 \leq \alpha \|w_{0,k}\|_2 \tag{6.11}$$

if there exist a symmetric positive definite matrix P and scalars $\xi_i|_{i=1,\cdots,5} > 0, \eta_1 > 0$, such that the following set of LMIs has a solution.

$$\mathscr{L}_1 := \begin{bmatrix} \eta_1 I & P \\ * & \eta_1 I \end{bmatrix} > 0 \tag{6.12}$$

$$\mathscr{L}_2 := \begin{bmatrix} -P & 0 & PA_0 & 0 & 0 & PE_0 & 0 & 0 & P\bar{E} \\ * & -I & C_0 & 0 & 0 & F_0 & 0 & 0 & 0 \\ * & * & \Omega_1 & A_0^T P & 0 & \xi_1 \bar{G}^T \bar{H} & 0 & 0 & 0 \\ * & * & * & -\xi_2 P & P\bar{E} & 0 & 0 & 0 & 0 \\ * & * & * & * & -\xi_4 I & 0 & 0 & 0 & 0 \\ * & * & * & * & * & \Omega_2 & E_0^T P & 0 & 0 \\ * & * & * & * & * & * & -\xi_3 P & P\bar{E} & 0 \\ * & * & * & * & * & * & * & -\xi_5 I & 0 \\ * & * & * & * & * & * & * & * & -\xi_1 I \end{bmatrix} < 0 \tag{6.13}$$

with $\Omega_1 = -P + \rho_1\gamma^2\eta_1 I + \rho_2 \bar{G}^T\bar{G}$, $\Omega_2 = -\alpha^2 I + \rho_3 \bar{H}^T\bar{H}$, $\rho_1 = (1 + \xi_2 + \xi_3)$, $\rho_2 = (\xi_1 + \xi_4)$, $\rho_3 = (\xi_1 + \xi_5)$, $\xi_i = \frac{1}{\epsilon_i}|_{i=1,\cdots,5}$ and $\epsilon_i > 0$.

Proof. Consider a quadratic Lyapunov function, that is, $V_k = x_{0,k}^T P x_{0,k}; P = P^T > 0$ and taking the difference along the trajectories of the residual generator (6.8)

$$\Delta V_k = V_{k+1} - V_k = x_{0,k+1}^T P x_{0,k+1} - x_{0,k}^T P x_{0,k}$$

or

$$\begin{aligned}\Delta V_k = &(\bar{A}_0 x_{0,k} + \bar{E}_0 w_{0,k})^T P (\bar{A}_0 x_{0,k} + \bar{E}_0 w_{0,k}) \\ &- x_{0,k}^T P x_{0,k} + x_{0,k}^T \bar{A}_0^T P \Psi_{0,k} + \Psi_{0,k}^T P^T \bar{A}_0 x_{0,k} \\ &+ w_{0,k}^T \bar{E}_0^T P \Psi_{0,k} + \Psi_{0,k}^T P^T \bar{E}_0 w_{0,k} + \Psi_{0,k}^T P \Psi_{0,k}\end{aligned} \tag{6.14}$$

In order to simplify the notation, use $\Psi_{0,k} \coloneqq \Psi_0(x_{0,k}, w_{0,k})$. Using Cashy-Schwarz inequality and Lemma A.3.1, then

$$\begin{aligned}\Delta V_k \leq &(\bar{A}_0 x_{0,k} + \bar{E}_0 w_{0,k})^T P (\bar{A}_0 x_{0,k} + \bar{E}_0 w_{0,k}) - x_{0,k}^T P x_{0,k} \\ &+ \epsilon_2 x_{0,k}^T \bar{A}_0{}^T P \bar{A}_0 x_{0,k} + \epsilon_3 w_{0,k}^T \bar{E}_0{}^T P \bar{E}_0 w_{0,k} + \rho_1 \gamma^2 \|P\| x_{0,k}^T x_{0,k}\end{aligned} \tag{6.15}$$

where $\rho_1 = (1 + \frac{1}{\epsilon_2} + \frac{1}{\epsilon_3})$. Let $\bar{\sigma}(P)$ be the largest singular value of P and further, assume there exists a positive scalar η_1, such that $\bar{\sigma}(P) < \eta_1 \Rightarrow 0 < \eta_1 I - \eta_1^{-1} P P$, which can be converted to LMI $\mathscr{L}_1$ in Theorem 6.2.1 by the use of Schur complements. Now (6.15) implies that

$$\begin{aligned}\Delta V_k \quad \leq \quad &(\bar{A}_0 x_{0,k} + \bar{E}_0 w_{0,k})^T P (\bar{A}_0 x_{0,k} + \bar{E}_0 w_{0,k}) - x_{0,k}^T P x_{0,k} \\ &+ \epsilon_2 x_{0,k}^T \bar{A}_0{}^T P \bar{A}_0 x_{0,k} + \epsilon_3 w_{0,k}^T \bar{E}_0{}^T P \bar{E}_0 w_{0,k} + \rho_1 \gamma^2 \eta_1 I x_{0,k}^T x_{0,k}\end{aligned} \tag{6.16}$$

Defining

$$\mathscr{J} = \sum_{k=0}^{\infty} r_{0,k}^T r_{0,k} - \alpha^2 w_{0,k}^T w_{0,k} \tag{6.17}$$

Under zero initial condition, it implies

$$\mathscr{J} < \sum_{k=0}^{\infty} r_{0,k,w}^T r_{0,k,w} - \alpha^2 w_{0,k}^T w_{0,k} + \Delta V_k \tag{6.18}$$

A sufficient condition for $\mathscr{J} \leq 0$ can thus be given as

$$r_{0,k,w}^T r_{0,k,w} - \alpha^2 w_{0,k}^T w_{0,k} + \Delta V_k \leq 0 \qquad \forall k \in [0, \infty) \tag{6.19}$$

It turns out

$$\begin{aligned}r_{0,k,w}^T r_{0,k,w} - \alpha^2 w_{0,k}^T w_{0,k} + \Delta V_k \leq &(\bar{C}_0 x_{0,k} + \bar{F}_0 w_{0,k})^T (\bar{C} x_{0,k} + \bar{F}_0 w_{0,k}) - \alpha^2 w_{0,k}^T w_{0,k} \\ &+ (\bar{A}_0 x_{0,k} + \bar{E}_0 w_{0,k})^T P (\bar{A}_0 x_{0,k} + \bar{E}_0 w_{0,k}) - x_{0,k}^T P x_{0,k} \\ &+ \epsilon_2 x_{0,k}^T \bar{A}_0^T P \bar{A}_0 x_{0,k} + \epsilon_3 w_{0,k}^T \bar{E}_0^T P \bar{E}_0 w_{0,k} + \rho_1 \gamma^2 \eta_1 I x_{0,k}^T x_{0,k}\end{aligned} \tag{6.20}$$

for sufficiency of $\mathscr{J} \leq 0$, the right hand side (RHS) of the above inequality needs to be negative. Hence representing the RHS of (6.20) as follows

$$\begin{bmatrix} x_{0,k}^T \\ w_{0,k}^T \end{bmatrix}^T \mathscr{M} \begin{bmatrix} x_{0,k} \\ w_{0,k} \end{bmatrix} < 0 \tag{6.21}$$

where

$$\mathscr{M} = \begin{bmatrix} \bar{A}_0^T & \bar{C}_0^T \\ \bar{E}_0^T & \bar{F}_0^T \end{bmatrix} \begin{bmatrix} P & 0 \\ 0 & I \end{bmatrix} \begin{bmatrix} \bar{A}_0 & \bar{E}_0 \\ \bar{C}_0 & \bar{F}_0 \end{bmatrix} + \begin{bmatrix} \Gamma_1 & 0 \\ 0 & \Gamma_2 \end{bmatrix}$$

and $\Gamma_1 = \epsilon_2 \bar{A}_0^T P \bar{A}_0 - P + \rho_1 \gamma^2 \eta_1$, $\Gamma_2 = \epsilon_3 \bar{E}_0^T P \bar{E}_0 - \alpha^2 I$. Using lemma A.3.2 and A.3.3 together with Schur complements, after some mathematical manipulations, the LMI $\mathscr{L}_2$ can be obtained.
This completes the proof. □

Algorithm 6.2.1. *Computation of $J_{th,RMS,2}$ for Lipschitz nonlinear uncertain system with norm bounded uncertainty*

Step I. Solve the optimization problem

$$\min \alpha$$

subject to (6.12) *and* (6.13) *for* $P > 0$, $\xi_* > 0$ *and finally set* $\alpha^* = \min \alpha$

Step II. Compute

$$J_{th,RMS,2} = \alpha^* \frac{\delta_{u,2} + \delta_{w,2}}{\sqrt{N}} \tag{6.22}$$

where $\alpha^* = \min(\alpha)$, N *is evaluation window and* $\|w_{0,k}\|_2 \leq (\delta_{u,2} + \delta_{w,2})$

6.2.3 Computation of $J_{th,Peak,Peak}$

The choice of peak value of the residual signal is fairly natural for the purpose of evaluation. Suppose the unknown input signal is bounded in amplitude, then in order to bound the peak amplitude of the residual signal, the peak-to-peak gain minimization is used. The problem of peak-to-peak gain minimization for LTI systems has been studied in [154–158] to list a few. This subsection uses this concept in order to compute the threshold $J_{th,Peak,Peak}$ which measures the maximum (instantaneous) changes in the residual signal due to the maximum bounded changes in the unknown inputs under admissible model uncertainties.

Definition 6.2.2. *Given the peak value of a residual signal $r_{0,k,w}$ as*

$$J_{Peak} = \sup_{k\geq 0} \|r_{0,k,w}\| \tag{6.23}$$

then $J_{th,Peak,Peak}$ is defined as

$$J_{th,Peak,Peak} = \sup\{J_{Peak} : \|r_{0,k,w}\|_{Peak} \leq \alpha, \text{ for } x_0 = 0, f = 0, \ \forall \ \|w_{0,k}\| \leq 1, |\Delta(k)| \leq 1\}$$

where α is the peak-to-peak gain of the residual generator (4.4).

Theorem 6.2.2. *Suppose the residual generator* (6.8) *satisfies Assumptions A1-A2 and the model uncertainty is structured of the form* (6.7) *with $\Delta(k)^T\Delta(k) \leq I$, then for a given scalar $\alpha > 0$ and $w_{0,k}^T w_{0,k} \leq 1$, the peak-to-peak gain of the residual generator is less than α, that is,*

$$\|r_{0,k,w}\|_{Peak} < \alpha \tag{6.24}$$

if there exist a symmetric positive definite matrix P and scalars $\xi_i|_{i=1,\cdots,6} > 0$, $\eta_1 > 0$, $0 < \lambda < 1$, $\mu > 0$, so that the following set of LMIs has a solution.

$$\mathscr{L}_1 := \begin{bmatrix} \eta_1 I & P \\ * & \eta_1 I \end{bmatrix} > 0 \tag{6.25}$$

$$\mathscr{L}_2 := \begin{bmatrix} -P & PA_0 & 0 & 0 & PE_0 & 0 & 0 & P\bar{E} \\ * & \Omega_1 & A_0^T P & 0 & 0 & 0 & 0 & 0 \\ * & * & -\xi_2 P & P\bar{E} & 0 & 0 & 0 & 0 \\ * & * & * & -\xi_4 I & 0 & 0 & 0 & 0 \\ * & * & * & * & \Omega_2 & E_0^T P & 0 & 0 \\ * & * & * & * & * & -\xi_3 P & P\bar{E} & 0 \\ * & * & * & * & * & * & -\xi_5 I & 0 \\ * & * & * & * & * & * & * & -\xi_1 I \end{bmatrix} < 0 \tag{6.26}$$

$$\mathscr{L}_3 := \begin{bmatrix} \alpha I & C_0 & F_0 \\ * & \lambda P & 0 \\ * & * & (\alpha - \mu) I \end{bmatrix} > 0 \tag{6.27}$$

where $\Omega_1 = -(1-\lambda)P + \rho_1\gamma^2\eta_1 I + \rho_2\bar{G}^T\bar{G}$, $\Omega_2 = \mu I + \rho_3\bar{H}^T\bar{H}$, $\rho_1 = (1+\xi_2+\xi_3)$, $\rho_2 = (\xi_1+\xi_4)$, $\rho_3 = (\xi_1+\xi_5)$ and $\xi_i = \frac{1}{\epsilon_i}|_{i=1,\cdots,5}$,

Proof. Consider a quadratic Lyapunov function of the form similar to the one used in the proof of Theorem 6.2.1, that is,

$$\begin{aligned} V_k &= x_{0,k}^T P x_{0,k} \qquad \forall P = P^T > 0 \\ \Delta V_k &= V_{k+1} - V_k = x_{0,k+1}^T P x_{0,k+1} - x_{0,k}^T P x_{0,k} < 0 \end{aligned}$$

Also assume

$$V_k < \frac{\mu}{\lambda} \qquad \exists \ \mu > 0, \quad 0 < \lambda < 1 \tag{6.28}$$

Considering

$$V_{k+1} + (\lambda - 1)V_k < \mu \tag{6.29}$$

for sufficiency of equation (6.28). Note that $\forall w_{0,k}^T w_{0,k}$, (6.29) ensures

$$V_{k+1} + (\lambda - 1)V_k < \mu w_{0,k}^T w_{0,k} \tag{6.30}$$

It can be noted that (6.28) holds if (6.30) is satisfied. Analysing the nonlinear terms in V_{k+1} in similar lines as in the proof of Theorem 6.2.1, the inequality (6.30) can then be represented as

$$\begin{aligned}&\begin{bmatrix} \bar{A_0}^T \\ \bar{E_0}^T \end{bmatrix} P \begin{bmatrix} \bar{A}_0 & \bar{E}_0 \end{bmatrix} + \begin{bmatrix} (\lambda-1)P & 0 \\ 0 & -\mu \end{bmatrix} \\ &+ \begin{bmatrix} \epsilon_2 \bar{A_0}^T P \bar{A}_0 + \rho_1 \gamma^2 \eta_1 & 0 \\ 0 & \epsilon_3 \bar{E_0}^T P \bar{E}_0 \end{bmatrix} < 0 \end{aligned} \tag{6.31}$$

or

$$\begin{bmatrix} \bar{A_0}^T \\ \bar{E_0}^T \end{bmatrix} P \begin{bmatrix} \bar{A}_0 & \bar{E}_0 \end{bmatrix} + \begin{bmatrix} -(1-\lambda)P + \epsilon_2 \bar{A_0}^T P \bar{A}_0 + \rho_1 \gamma^2 \eta_1 & 0 \\ 0 & -\mu I + \epsilon_3 \bar{E_0}^T P \bar{E}_0 \end{bmatrix} < 0$$

using Lemma A.3.3, a sufficient condition for (6.31) is

$$\begin{bmatrix} A_0^T \\ E_0^T \end{bmatrix} \left(P^{-1} - \epsilon_1 \bar{E}\bar{E}^T\right)^{-1} \begin{bmatrix} A_0 & E_0 \end{bmatrix} + \frac{1}{\epsilon_1} \begin{bmatrix} \bar{G} & \bar{H} \end{bmatrix}^T \begin{bmatrix} \bar{G} & \bar{H} \end{bmatrix} + \begin{bmatrix} \Gamma_1 & 0 \\ 0 & \Gamma_2 \end{bmatrix} < 0 \tag{6.32}$$

or

$$\begin{bmatrix} A_0^T \\ E_0^T \end{bmatrix} \left(P^{-1} - \epsilon_1 \bar{E}\bar{E}^T\right)^{-1} \begin{bmatrix} A_0 & E_0 \end{bmatrix} + \begin{bmatrix} \Gamma_1 + \frac{1}{\epsilon_1}\bar{G}^T\bar{G} & \frac{1}{\epsilon_1}\bar{G}^T\bar{H} \\ \frac{1}{\epsilon_1}\bar{H}^T\bar{G} & \Gamma_2 + \frac{1}{\epsilon_1}\bar{H}^T\bar{H} \end{bmatrix} < 0 \tag{6.33}$$

where

$$\begin{aligned}\Gamma_1 &= -(1-\lambda)P + A_0^T \left((\epsilon_2 P)^{-1} - \epsilon_4 \bar{E}\bar{E}^T\right)^{-1} A_0 + \frac{1}{\epsilon_4}\bar{G}^T\bar{G} + \rho_1\gamma^2\eta_1, \\ \Gamma_2 &= -\mu I + \frac{1}{\epsilon_4}\bar{H}^T\bar{H} + \bar{E_0}^T \left((\epsilon_3 P)^{-1} - \epsilon_5 \bar{E}\bar{E}^T\right)^{-1} E_0\end{aligned}$$

After applying Schur complements, the inequality (6.33) can be written as

$$\begin{bmatrix} -P & PA_0 & PE_0 & P\bar{E} \\ * & \Gamma_1 + \frac{1}{\epsilon_1}\bar{G}^T\bar{G} & \frac{1}{\epsilon_1}\bar{G}^T\bar{H} & 0 \\ * & * & \Gamma_2 + \frac{1}{\epsilon_1}\bar{H}^T\bar{H} & 0 \\ * & * & * & -\frac{1}{\epsilon_1}I \end{bmatrix} < 0 \tag{6.34}$$

using Lemma A.3.2 and some mathematical manipulations lead us to LMI $\mathscr{L}_2$ in (6.26). The LMI $\mathscr{L}_3$ in (6.27) can be obtained along the similar lines in [1, Chap 9].
This completes the proof. □

Algorithm 6.2.2. *Computation of $J_{th,Peak,Peak}$ for discrete-time Lipschitz nonlinear uncertain systems with norm bounded uncertainty*

Step I. Solve the optimization problem

$$\min \alpha$$

subject to (6.24) *and* (6.25)*, for some* $\xi_i|_{i=1,\cdots,6} > 0$*,* $\eta_1 > 0$*,* $0 < \lambda < 1$*,* $\mu > 0$*,* $P > 0$ *and finally set* $\alpha^* = \min \alpha$

Step II. Compute

$$J_{th,Peak,Peak} = \alpha^* \left(\delta_{u,\infty} + \delta_{w,\infty}\right) \tag{6.35}$$

where $\alpha^* = \min(\alpha)$ *and* $\|w_{0,k}\|_{Peak} \leq \left(\delta_{u,\infty} + \delta_{w,\infty}\right)$.

6.2.4 Computation of $J_{th,Peak,2}$

In Theorems 6.2.1 and 6.2.2, two important scenarios have been discussed. These are: i) using $\mathscr{H}_\infty$ techniques, an algorithm for the computation of $J_{th,RMS,2}$ is proposed which measures the bounded changes in the energy of the residual signal due to bounded changes in the energy of the unknown disturbances in the presence of uncertainties and ii) using the concept of peak-to-peak gain minimization, the design of $J_{th,Peak,Peak}$ has been studied which measures the maximum instantaneous changes in the residual signal due to the maximum bounded instantaneous changes in the unknown disturbances. In this subsection, the maximum changes in the residual signal due to the bounded changes in the energy of the unknown disturbances will be studied. The so-called $J_{th,Peak,2}$ serves this objective. For this purpose, the well established results from the generalized $\mathscr{H}_2$ performance for LTI systems ([159–164]) are extended to discrete-time nonlinear uncertain systems in order to compute $J_{th,Peak,2}$. This threshold measures the maximum (instantaneous) change in residual signal due to the bounded changes in the energy of the unknown inputs. It serves the same purpose as $J_{th,Peak,Peak}$ but with respect to energy of the unknown inputs.

Definition 6.2.3. *Given the residual generator* (6.8) *with model uncertainty of the form* (6.7)*. Assume that* $F_0 = 0$*, then for all* $w_{0,k} \in \ell_2[0, \infty)$*, the energy-to-peak gain can be given as*

$$\|r_{0,k,w}\|_{Peak} < \alpha_1 \|w_{0,k}\|_2 \quad \forall \ \ |\Delta(k)| \leq 1$$

Let the peak value of the residual signal is denoted by $J_{Peak} = \sup_{k\geq 0} \|r_{0,k,w}\|$*. Further, assume that* $w_{0,k}$ *is bounded in the sense i.e.* $\|w_{0,k}\|_2 \leq \delta_{w_0,2}$*, then* $J_{th,Peak,2}$ *is defined as*

$$J_{th,Peak,2} = \alpha_1 \delta_{w_0,2}$$

Remark 6.2.4. *If $F_0 \neq 0$, then the residual generator* (6.8) *can be decomposed into the following*

$$r_{0,k,w} = r_{10,k,w} + r_{20,k,w} \tag{6.36}$$

where $r_{10,k,w} = C_0 x_{0,k}$ shows the dynamical part of the residual generator (6.8) *and $r_{20,k,w} = F_0 w_{0,k}$, then considering*

$$\begin{aligned} ||r_{0,k,w}||_{Peak} &\leq ||r_{10,k,w}||_{Peak} + ||r_{20,k,w}||_{Peak} \\ &\leq ||r_{10,k,w}||_{Peak} + \bar{\sigma}(F_0)||w_{0,k}||_{Peak} \end{aligned} \tag{6.37}$$

where $\bar{\sigma}(F_0)$ is the maximum singular value of F_0. The threshold $J_{th,Peak,2}$ can then be defined as

$$J_{th,Peak,2} = \alpha_1 ||w_{0,k}||_2 + \bar{\sigma}(F_0)||w_{0,k}||_{Peak} \tag{6.38}$$

the term $\bar{\sigma}(F_0)||w_{0,k}||_{Peak}$ represents the peak value of $r_{20,k,w}$. Let there exists a scalar $\rho_2 > 0$, such that

$$\bar{\sigma}(F_0) \leq \alpha_2 \Rightarrow F_0^T F_0 \leq \alpha_2^2$$

or

$$F_0^T F_0 - \alpha_2^2 I \leq 0 \tag{6.39}$$

which shows that the Peak value of residual signal $r_{20,k,w}$ is less than or equal to $\rho_2 ||w_{0,k}||_{Peak}$.

Considering the remaining part, that is, $r_{10,k,w} = C_0 x_{0,k}$, the following theorem gives the main result for the computation of $J_{th,Peak,2}$.

Theorem 6.2.3. *Suppose the residual generator* (6.8) *satisfies Assumptions A1-A2 and the model uncertainty is structured of the form* (6.7) *with $\Delta(k)^T \Delta(k) \leq I$, then for given scalar $\rho_1 > 0$,*

$$||r_{10,k,w}||_{Peak} \leq \alpha_1 ||w_{0,k}||_2 \tag{6.40}$$

if there exist a symmetric positive definite matrix P and scalars $\xi_i|_{i=1,\cdots,5} > 0, \beta > 0$ so that the following set of LMIs has a solution.

$$\mathscr{L}_1 := \begin{bmatrix} \eta_1 I & P \\ * & \eta_1 I \end{bmatrix} > 0 \tag{6.41}$$

$$\mathscr{L}_2 := \begin{bmatrix} -P & PA_0 & 0 & 0 & PE_0 & 0 & 0 & P\bar{E} \\ * & \Omega_1 & A_0^T P & 0 & 0 & 0 & 0 & 0 \\ * & * & -\xi_2 P & P\bar{E} & 0 & 0 & 0 & 0 \\ * & * & * & -\xi_4 I & 0 & 0 & 0 & 0 \\ * & * & * & * & \Omega_2 & E_0^T P & 0 & 0 \\ * & * & * & * & * & -\xi_3 P & P\bar{E} & 0 \\ * & * & * & * & * & * & -\xi_5 I & 0 \\ * & * & * & * & * & * & * & -\xi_1 I \end{bmatrix} < 0 \tag{6.42}$$

$$\mathscr{L}_3 := C_0^T C_0 - P < 0 \tag{6.43}$$

where $\Omega_1 = -P + \rho_1\gamma^2\beta I + \rho_2\bar{G}^T\bar{G}$, $\Omega_2 = -\alpha_1^2 I + \rho_3\bar{H}^T\bar{H}$, $\rho_1 = (1 + \xi_2 + \xi_3)$, $\rho_2 = (\xi_1 + \xi_4)$, $\rho_3 = (\xi_1 + \xi_5)$, $\xi_* = \frac{1}{\epsilon_*}$ *and* $\epsilon_* > 0$

Proof. Assume the quadratic Lyapunov function of the form similar to the one as before i.e. $V_k = x_{0,k}^T P x_{0,k}$, $P = P^T > 0$ and considering that

$$\mathscr{J} \triangleq V_k - \alpha_1^2 \sum_{j=0}^{k-1} \|w_{0,j}\|^2 \qquad \forall w_{0,k} \in \ell_2[0,\infty) \tag{6.44}$$

for $k > 0$

$$\mathscr{J} \triangleq V_k - V_{k=0} - \alpha_1^2 \sum_{j=0}^{k-1} \|w_{0,j}\|^2 \triangleq \sum_{j=0}^{k-1} \Delta(V_j) - \alpha_1^2 w_{0,j}^T w_{0,j}$$

Considering $\mathscr{J} \leq 0$, the LMI $\mathscr{L}_2$ in (6.42) can be obtained along the same lines of the proof of Theorem 6.2.2. Also $\mathscr{J} \leq 0$ yields

$$V_k < \alpha_1^2 \sum_{j=0}^{k-1} \|w_{0,j}\|^2 \tag{6.45}$$

and

$$r_{10,k,d} < \alpha_1^2 \sum_{j=0}^{k-1} \|w_{0,j}\|^2 \tag{6.46}$$

provided that

$$C_0^T C_0 \leq P \tag{6.47}$$

which is the LMI $\mathscr{L}_3$ in (6.43).
This ends the proof. □

Algorithm 6.2.3. *Computation of* $J_{th,Peak,2}$ *for discrete-time Lipschitz nonlinear uncertain systems with norm bounded uncertainty*

Step I. Solve the optimization problem

$$\min \alpha_1$$

subject to (6.41), (6.42) *and* (6.43), *for some* $\xi_i|_{i=1,\cdots,6} > 0$, $\eta_1 > 0$, $0 < \lambda < 1$, $\mu > 0$, $P > 0$, *and*

$$\min \alpha_2$$

subject to (6.39), *and set* $\alpha_1^* = \min \alpha_1$, $\alpha_2^* = \min \alpha_2$

Step II. Compute

$$J_{th,Peak,2} = \alpha_1^* (\delta_{u,2} + \delta_{w,2}) + \alpha_2^* (\delta_{u,\infty} + \delta_{w,\infty})$$

where $\alpha_1^* = \min(\alpha_1)$, $\alpha_2^* = \min(\alpha_2)$, $\|w_{0,k}\|_2 \leq (\delta_{u,2} + \delta_{w,2})$ *and* $\|w_{0,k}\|_{Peak} \leq (\delta_{u,\infty} + \delta_{w,\infty})$.

It is worth noting that the results in the above theorems have been derived on the assumptions that $|\Delta(k)| \leq 1$, which do not lead to the loss of generality. If it does not hold, then the following remark is useful,

Remark 6.2.5. *If $|\Delta(k)| \leq \delta_\Delta I$ and $\delta_\Delta \neq 1$, then it can be defined as*

$$\bar{\Delta}(k) = \frac{\Delta(k)}{\sqrt{\delta_\Delta}} \quad \textit{and} \quad \begin{bmatrix} \tilde{G} & \tilde{H} \end{bmatrix} = \sqrt{\delta_\Delta}\,[G \;\; H]$$

Theorems 6.2.1, 6.2.2, and 6.2.3 provide all the needed informations for the design of constant thresholds using norm-based framework. The advantage of norm-based framework is that it provides an upper bound for the influence of the disturbances on the residual signal and that the computed thresholds are robust. These thresholds give a fair evaluation of the residual signal. For the purpose of early fault detection on one hand and low false alarm rate on the other hand, $J_{th,Peak,Peak}$ is used to activate the computation of $J_{th,Peak,2}$. Due to the assumption on energy of the unknown inputs $J_{th,Peak,2}$ is set higher than $J_{th,Peak,Peak}$. Note that the possibility of false alarms are precluded in both cases, however, residual evaluation using $J_{th,Peak,2}$ produces more conservativeness than $J_{th,Peak,Peak}$. Similarly, $J_{th,RMS,2}$ also eliminates the chances of false alarms. Further, residual evaluation using RMS values for a time window of length N produces smoothness in the residual signal and hence the influence of the unknown inputs is minimized. Since it requires observation over a long time window, the fault detection time become large.

6.2.5 A design example

This example illustrates the use of the algorithms proposed for the computation of constant thresholds. The coefficient matrices of the plant governed by (6.3), are given as

$$A = \begin{bmatrix} 0 & 0.456 \\ -0.762 & 0.19 \end{bmatrix}; \quad B = E_w = \begin{bmatrix} 0 \\ 1 \end{bmatrix}; \quad C = [1 \;\; 0]; D = F_w = 0; \quad E = \begin{bmatrix} 0 \\ 1 \end{bmatrix};$$

$$G = \begin{bmatrix} 0 & 0.01 \end{bmatrix}; H = J = 0.01; \quad F = 0; \quad E_f = \begin{bmatrix} 0 & 0 \\ 1 & 0 \end{bmatrix}; \quad F_f = [0 \;\; 1];$$

$$\phi(x_k) = 0.12 sin(x_{2,k}); \quad \text{with} \;\; \gamma = 0.12$$

The uncertainty is bounded $\Delta^T(k)\Delta(k) \leq 1$. The control input is assumed to be bounded by $\delta_{u,2} = 0.4472, \delta_{u,\infty} = 0.1000$. The process disturbance w_k is uniformly distributed over the interval $[-0.15, 0.15]$. The energy and peak values of w_k are bounded by $\delta_{w,2} = 0.4821, \delta_{w,\infty} = 0.1500$. Considering the FDF parameters $L = \begin{bmatrix} -0.3100 & -0.7596 \end{bmatrix}^T$ and $W = I$ and the evaluation window $N = 20[s]$ and using Theorem (6.2.1, 6.2.2, 6.2.3), the following parameters are computed

- $J_{th,RMS,2}$

$$\epsilon_2 = 0.3010 \quad \epsilon_3 = 0.4110$$

$$P = \begin{bmatrix} 0.6460 & -0.0684 & -0.0006 & 0.0020 \\ -0.0684 & 0.3246 & 0.0001 & -0.0002 \\ -0.0006 & 0.0001 & 1.2460 & -0.2005 \\ 0.0020 & -0.0002 & -0.2005 & 0.4649 \end{bmatrix};$$

$$\alpha = 1.2056; \quad J_{th,RMS,2} = 0.2505$$

- $J_{th,Peak,Peak}$

$$\epsilon_2 = 0.3010; \quad \epsilon_3 = 0.8010; \quad \lambda = 0.2010; \quad \mu = 11.2074;$$

$$P = \begin{bmatrix} 2.8938 & -0.2718 & -0.5083 & -0.1007 \\ -0.2718 & 1.5659 & -0.1282 & -0.2725 \\ -0.5083 & -0.1282 & 5.1007 & -0.1541 \\ -0.1007 & -0.2725 & -0.1541 & 2.6278 \end{bmatrix}$$

$$\alpha = 3.3477; \quad J_{th,Peak,Peak} = 0.8333$$

- $J_{th,Peak,2}$

$$\epsilon_2 = 0.4010; \quad \epsilon_3 = 0.7010;$$

$$P = \begin{bmatrix} 0.3649 & -0.0303 & -0.1363 & 0.0013 \\ -0.0303 & 0.1958 & -0.0427 & -0.0591 \\ -0.1363 & -0.0427 & 1.0542 & -0.0380 \\ 0.0013 & -0.0591 & -0.0380 & 0.4274 \end{bmatrix}$$

$$\alpha_1 = 1.0954; \quad \alpha_2 = 1.4827 \times 10^{-9}; \quad J_{th,peak,2} = 1.0179;$$

The simulation is carried out for $100[s]$. A sensor fault is generated using unit step function at $20[s]$. Figure 6.3 shows the RMS of the residual and threshold ($J_{th,RMS,2}$) while Figure 6.4 shows the peak value of the residual and the thresholds ($J_{th,Peak,Peak}$ and $J_{th,Peak,2}$). Note that the residual signal is affected by the unknown external disturbances w_k and control input through model uncertainty. Due to this reason, the residual signal is non-zero before the occurrence of the fault. The proposed thresholds ensure no false alarm. When fault appeared in the system, the residual exceeds the threshold ($J_{th,RMS,2}$ in Figure 6.3 and $J_{th,Peak,Peak}$, $J_{th,Peak,2}$ in Figure 6.4) and hence fault alarm is generated.

It is also evident from Figure 6.4 that $J_{th,Peak,2}$ is set higher than $J_{th,Peak,Peak}$. It is usually the case in practice that with the aim of early fault detection together with low false alarm rate $J_{th,Peak,Peak}$ is used to activate the computation of $J_{th,Peak,2}$.

Note that the effect of unknown inputs is reduced while evaluating the RMS value of the residual signal (Figure 6.3) as compared to the peak value of the residual signal (Figure 6.4). It is due to the averaging of the instantaneous values of the residual signal over time window N. Similarly considering evaluation of peak value of the residual signal (Figure 6.4), $J_{th,Peak,2}$ is higher than $J_{th,Peak,Peak}$ due to the assumption of the energy of the unknown inputs. It is helpful to eliminate the chances of false alarms on one hand while introducing conservativeness on the other hand which may sometimes lead to missed-detection.

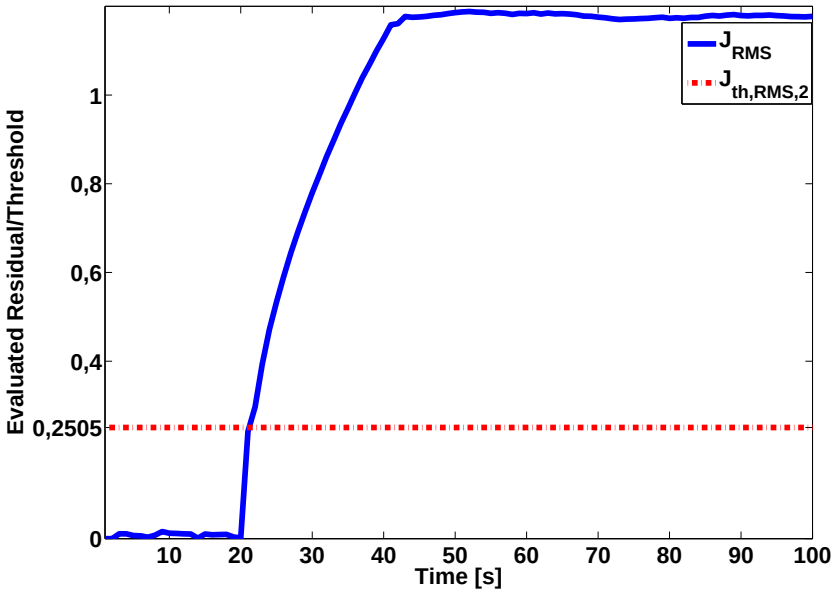

Figure 6.3: Detection of sensor fault under the evaluation of RMS value of residual signal. The solid line represents the evaluated residual signal J_{RMS}, dotted lines denotes the threshold $J_{th,RMS,2}$

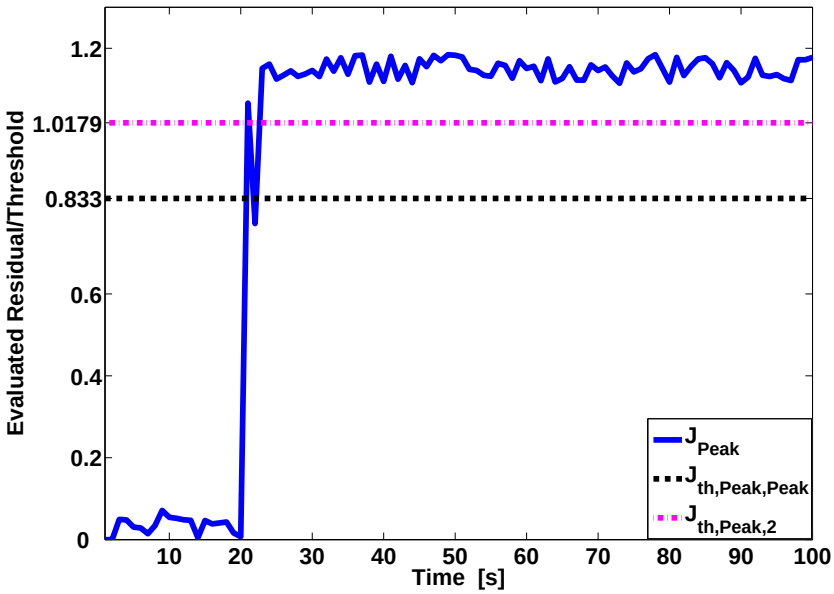

Figure 6.4: Detection of sensor fault under the evaluation of Peak value of residual signal. The solid line represents the evaluated residual signal J_{Peak}, dotted lines and dash-dotted lines denote the thresholds $J_{th,Peak,Peak}$ $J_{th,Peak,2}$ respectively

6.3 Constant threshold for continuous-time case

In this section, the design schemes of the above three kinds of thresholds for continuous-time Lipschitz nonlinear uncertain systems are studied. In addition, the uncertainty is also introduced in the output channel. Further, the assumption on the uncertainty remains the same; that is, norm bounded.

6.3.1 Problem formulation

Consider the following type of a continuous-time Lipschitz nonlinear uncertain systems

$$\Sigma : \begin{cases} \dot{x} = \bar{A}x + \bar{B}u + \bar{E}_w w + \phi(x,u) + E_f f \\ y = \bar{C}x + \bar{D}u + \bar{F}_w w + F_f f \end{cases} \tag{6.48}$$

where $\bar{X} = X + \Delta X$ represents the modeling errors and uncertainties. Considering the FDF (5.35) and defining estimation error as $e = x - \hat{x}$, then the error dynamics can be given as follows

$$\Sigma_\xi : \begin{cases} \dot{e} = (A - LC)e + (\Delta A - L\Delta C)x + (\Delta B - L\Delta D)u \\ \quad +(\bar{E}_w - L\bar{F}_w)w + \phi(x,u) - \phi(\hat{x},u) + (E_f - LF_f)f \\ r = W(Ce + \Delta Cx + \Delta Du + \bar{F}_w w + F_f f) \end{cases} \tag{6.49}$$

the residual generator dynamics for uncertain system (6.48) can finally be represented as follows

$$\Sigma_{aug} : \begin{cases} \dot{x}_0 = \bar{A}_0 x_0 + \bar{E}_0 w_0 + E_{0,f} f + \Psi_0(x,\hat{x},u) \\ r_0 = \bar{C}_0 x_0 + \bar{F}_0 w_0 + F_{0,f} f \end{cases} \tag{6.50}$$

where

$$x_0 = \begin{bmatrix} x \\ e \end{bmatrix}; \quad w_{0,} = \begin{bmatrix} u \\ w \end{bmatrix}; \quad A_0 = \begin{bmatrix} A & 0 \\ 0 & A - LC \end{bmatrix};$$
$$E_0 = \begin{bmatrix} B & E_w \\ 0 & E_w - LF_w \end{bmatrix}; \quad E_{0,f} = \begin{bmatrix} E_f \\ E_f - LF_f \end{bmatrix};$$
$$\Psi_0(x,\hat{x},u) = \begin{bmatrix} \phi(x,u) \\ \phi(x,u) - \phi(\hat{x},u) \end{bmatrix}; \quad C_0 = \begin{bmatrix} 0 & WC \end{bmatrix};$$
$$F_0 = \begin{bmatrix} 0 & WF_w \end{bmatrix}; \quad F_f = \begin{bmatrix} 0 & WF_f \end{bmatrix};$$

$$\Delta A_0 = \begin{bmatrix} \Delta A & 0 \\ \Delta A - L\Delta C & 0 \end{bmatrix}; \quad \Delta C_0 = \begin{bmatrix} V\Delta C & 0 \end{bmatrix};$$
$$\Delta E_0 = \begin{bmatrix} \Delta B & \Delta E_w \\ \Delta B - L\Delta D & \Delta E_w - L\Delta F_w \end{bmatrix};$$
$$\Delta F_0 = \begin{bmatrix} V\Delta D & V\Delta F_w \end{bmatrix}$$

$$\begin{aligned}\begin{bmatrix} \Delta A_0 & \Delta E_0 \\ \Delta C_0 & \Delta F_0 \end{bmatrix} &= \begin{bmatrix} \bar{E} \\ \bar{F} \end{bmatrix} \Delta(t) \begin{bmatrix} \bar{G} & \bar{H} \end{bmatrix}; \\ \Delta(t)^T \Delta(t) &\leq \delta_\Delta I, \delta_\Delta > 0 \end{aligned} \tag{6.51}$$

with

$$\begin{aligned}\bar{G} &= \begin{bmatrix} G & 0 \end{bmatrix}; \ \bar{H} = \begin{bmatrix} H & J \end{bmatrix}; \ \bar{F} = F \\ \bar{E} &= \begin{bmatrix} E^T & (E - LF)^T \end{bmatrix}^T \end{aligned}$$

Remark 6.3.1. *Analogous to the Remark 6.2.1, the fault-free residual generator will be used in order to study and analyze the effect of the unknown inputs. To this end, the following form of residual generator* (6.50) *will be used in the remainder of this chapter:*

$$\Sigma_{\mathscr{R}} : \begin{cases} \dot{x}_0 = \bar{A}_0 x_0 + \bar{E}_0 w_0 + \Psi_0(x, \hat{x}) \\ r_{0,w} = \bar{C}_0 x_0 + \bar{F}_0 w_0 \end{cases} \tag{6.52}$$

Similar to the discrete-time case, the above residual generator also holds the assumptions A1-A2 but in continuous-time settings. The following subsections presents sufficient conditions for $J_{th,RMS,2}$, $J_{th,Peak,Peak}$, and $J_{th,Peak,2}$ in the form of three Theorems respectively. Algorithms are presented at the end of each subsections in order to ease the design of a respective threshold.

6.3.2 Computation of $J_{th,RMS,2}$

Theorem 6.3.1. *Suppose the residual generator* (6.52) *holds Assumptions A1-A2 and the model uncertainty is structured of the form* (6.51) *with* $\Delta(t)^T \Delta(t) \leq I$*, then for a given scalar* $\alpha > 0$*, the residual generator* (6.52) *has* $\mathscr{L}_2$*−gain is less than or equal to* α*; that is,*

$$\|r_{0,w}\|_2 \leq \alpha \|w_0\|_2 \tag{6.53}$$

if there exists a symmetric positive (semi-) definite matrix P *and nonnegative scalars* $\epsilon_i|_{i=1,2}$ *such that the following LMI has a solution*

$$\mathscr{L} := \begin{bmatrix} \Omega_1 & \Omega_2 & C_0^T & P\bar{E} & \epsilon_1 P & \frac{1}{\epsilon_1}\gamma I \\ * & \Omega_3 & F_0^T & 0 & 0 & 0 \\ * & * & -I & F & 0 & 0 \\ * & * & * & -\epsilon_2 I & 0 & 0 \\ * & * & * & * & -I & 0 \\ * & * & * & * & * & -I \end{bmatrix} < 0 \tag{6.54}$$

where $P = P^T = diag(P_1, P_2)$*,* $\Omega_1 = PA_0 + A_0^T P + \epsilon_2 \bar{G}^T \bar{G}$*,* $\Omega_2 = PE_0 + \epsilon_2 \bar{G}^T \bar{H}$*,* $\Omega_3 = -\alpha^2 I + \epsilon_2 \bar{H}^T \bar{H}$ *and* $\epsilon_i|_{i=1,2} > 0$*.*

Proof. see Appendix B.1 for proof. □

Algorithm 6.3.1. *Computation of $J_{th,RMS,2}$ for continuous-time Lipschitz nonlinear systems with norm bounded uncertainty*

Step I. Solve the optimization problem

$$\min \alpha$$

subject to (6.54) *for* $P > 0, \epsilon_* > 0$ *and finally set* $\alpha^* = \min \alpha$

Step II. Compute

$$J_{th,RMS,2} = \alpha^* \frac{\delta_{u,2} + \delta_{w,2}}{\sqrt{T}}$$

where T is the observation window to be selected and $||w_0||_{2,T} \leq (\delta_{u,2} + \delta_{w,2})$

6.3.3 Computation of $J_{th,Peak,Peak}$

Theorem 6.3.2. *Suppose the residual generator* (6.52) *holds Assumptions A1-A2 and the model uncertainty is structured of the form* (6.51) *with* $\Delta(t)^T \Delta(t) \leq I$*, the for a given scalar* $\alpha > 0$ *and* $\forall ||w_0||_{Peak} \leq 1$*, the the Peak norm of the residual generator* (6.52) *is less than or equal to* α*; that is,*

$$||r_{0,w}||_{Peak} \leq \alpha \tag{6.55}$$

if there exists a symmetric positive (semi-) definite matrix P, nonnegative scalars $\epsilon_i|_{i=1,.,3}$, positive scalars λ and μ such that the following set of LMIs has a solution.

$$\mathscr{L}_1 := \begin{bmatrix} \Omega_1 & \Omega_2 & P\bar{E} & \epsilon_1 P & \frac{1}{\epsilon_1}\gamma \\ * & \Omega_3 & 0 & 0 & 0 \\ * & * & -\epsilon_2 I & 0 & 0 \\ * & * & * & -I & 0 \\ * & * & * & * & -I \end{bmatrix} < 0 \tag{6.56}$$

$$\mathscr{L}_2 := \begin{bmatrix} I & C_0 & F_0 & \bar{F} \\ * & \Omega_4 & -\epsilon_3 \bar{G}^T \bar{H} & 0 \\ * & * & \Omega_5 & 0 \\ * & * & * & \epsilon_3 I \end{bmatrix} > 0 \tag{6.57}$$

where $P = P^T$,. $\Omega_1 = PA_0 + A_0^T P + \epsilon_2 \bar{G}^T \bar{G} + \lambda P$, $\Omega_2 = PE_0 + \epsilon_2 \bar{G}^T \bar{H}$, $\Omega_3 = -\mu I + \epsilon_2 \bar{H}^T \bar{H}$,$\Omega_4 = \lambda P - \epsilon_3 \bar{G}^T \bar{G}$, $\Omega_5 = (\alpha^2 - \mu) I - \epsilon_3 \bar{H}^T \bar{H}$.

Proof. see Appendix B.2 for proof. □

Algorithm 6.3.2. *Computation of $J_{th,Peak,Peak}$ for continuous-time Lipschitz nonlinear uncertain systems with norm bounded uncertainty*

Step I. Solve the optimization problem

$$\min \alpha$$

subject to (6.56) *and* (6.57) *for* $P > 0, \epsilon_* > 0, \mu > 0, 0 < \lambda < 1$ *and finally set* $\alpha^* = \min \alpha$

Step II. Compute

$$J_{th,Peak,Peak} = \alpha^* \left(\delta_{u,\infty} + \delta_{w,\infty}\right)$$

where $||w_0||_{Peak} \leq \left(\delta_{u,\infty} + \delta_{w,\infty}\right)$

6.3.4 Computation of $J_{th,Peak,2}$

Theorem 6.3.3. *Suppose the residual generator* (6.52) *holds Assumptions A1-A2 and the model uncertainty is structured of the form* (6.51) *with* $\Delta(t)^T \Delta(t) \leq I$*, then for a given scalars* $\alpha_1 > 0$ *and* $\alpha_2 > 0$*, the Peak-to-2 gain of the residual generator* (6.52) *is given by the following relation*

$$||r_{0,w}||_{Peak} = \alpha_1 ||w_0||_2 + \alpha_2 ||w_0||_{Peak} \tag{6.58}$$

if there exists a symmetric positive definite matrix P*, nonnegative scalars* ϵ_* *such that the following set of LMIs has a solution.*

$$\mathscr{L}_1 := \begin{bmatrix} \Omega_1 & \Omega_2 & P\bar{E} & \epsilon_1 P & \frac{1}{\epsilon_1}\gamma \\ * & \Omega_3 & 0 & 0 & 0 \\ * & * & -\epsilon_2 I & 0 & 0 \\ * & * & * & -I & 0 \\ * & * & * & * & -I \end{bmatrix} < 0 \tag{6.59}$$

$$\mathscr{L}_2 := \begin{bmatrix} -I & C_0 & F \\ * & -P + \epsilon_3 \bar{G}^T \bar{G} & 0 \\ * & * & -\epsilon_3 I \end{bmatrix} < 0 \tag{6.60}$$

$$\mathscr{L}_3 := \begin{bmatrix} I & F_0 & F \\ * & \alpha_2^2 I - \epsilon_4 \bar{H}^T \bar{H} & 0 \\ * & * & \epsilon_4 I \end{bmatrix} \geq 0 \tag{6.61}$$

where $P = P^T = \begin{bmatrix} P_1 & 0 \\ 0 & P_2 \end{bmatrix}$, $\Omega_1 = PA_0 + A_0^T P + \epsilon_2 \bar{G}^T \bar{G}, \Omega_2 = PE_0 + \epsilon_2 \bar{G}^T \bar{H}, \Omega_3 = -\alpha_1^2 I + \epsilon_2 \bar{H}^T \bar{H}$ *and* $\epsilon_* > 0$

Proof. see Appendix B.3 for proof. □

Algorithm 6.3.3. *Computation of $J_{th,Peak,2}$ for continuous-time Lipschitz nonlinear systems with norm bounded uncertainty*

Step I. Solve the optimization problem

$$\min \alpha_1$$

subject to (6.59), (6.60) *and*

$$\min \alpha_2$$

subject to (6.61) *for* $P = P^T > 0, \epsilon_* > 0$ *and finally set* $\alpha_1^* = \min \alpha_1$ *and* $\alpha_2^* = \min \alpha_2$

Step II. Compute

$$J_{th,Peak,2} = \alpha_1^* \left(\delta_{u,2} + \delta_{w,2}\right) + \alpha_2^* \left(\delta_{u,\infty} + \delta_{w,\infty}\right)$$

6.3.5 A design example

Consider the Lipschitz nonlinear system governed by (6.48) with the following coefficient matrices

$$A = \begin{bmatrix} 0 & 1 \\ -0.6 & -1.5 \end{bmatrix}; \quad B = \begin{bmatrix} 1 \\ 1 \end{bmatrix}; \quad C = [1 \;\; 0]; \quad D = 0; \quad E_w = \begin{bmatrix} 1 \\ 1 \end{bmatrix}; \quad F_w = D;$$
$$E = \begin{bmatrix} 0.1 \\ 0.15 \end{bmatrix}; \quad G = \begin{bmatrix} 0.2 & 0.1 \end{bmatrix}; \quad H = J = 0.1; \quad F = 0; E_f = \begin{bmatrix} 1 & 0 \\ 1 & 0 \end{bmatrix}; \quad F_f = [0 \;\; 1];$$
$$\phi(x) = 0.21 sin(x_2); \quad \text{with} \quad \gamma = 0.21.$$

The disturbance is assumed to be uniformly randomly distributed over the interval $(-0.01, 0.1)$. The parameter for robust FDF are given as follows:

$$L = [5.6917 \quad 5.1084]^T; \qquad W = 1.5;$$

The disturbances and the input vector are bounded by

$$\delta_{u,2} = 0.3162 \qquad \delta_{w,2} = 0.0250 \qquad T = 10 \;\; sec$$
$$\delta_{u,\infty} = 0.1000; \qquad \delta_{w,\infty} = 0.01;$$

Similarly using algorithms (6.3.1,6.3.2,6.3.3), the following parameters are computed

- $J_{th,RMS,2}$

$$\epsilon_1 = 1.9201, \quad \epsilon_2 = 0.0019,$$
$$P = \begin{bmatrix} 0.0481 & 0.0538 & 0.0001 & -0.0135 \\ 0.0538 & 0.1250 & -0.0017 & -0.0559 \\ 0.0001 & -0.0017 & 0.6465 & 0.0265 \\ -0.0135 & -0.0559 & 0.0265 & 0.1115 \end{bmatrix}$$
$$\alpha = 0.6256; \quad J_{th,RMS,2} = 0.0955;$$

- $J_{th,Peak,Peak}$

$$\mu = 6.7470, \ \lambda = 0.2010, \ \epsilon_1 = 0.8001, \ \epsilon_2 = 0.0393, \ \epsilon_3 = 4.0849 \times 10^{-4}$$
$$P = \begin{bmatrix} 0.4366 & 0.6183 & 0.0042 & -0.1676 \\ 0.6183 & 1.4617 & 0.0114 & -0.5394 \\ 0.0042 & 0.0114 & 11.3009 & 0.4233 \\ -0.1676 & -0.5394 & 0.4233 & 1.9336 \end{bmatrix}$$
$$\alpha = 2.5975; \quad J_{th,Peak,Peak} = 0.2856;$$

- $J_{th,Peak,2}$

$$\epsilon_1 = 2.0010, \ \epsilon_2 = 0.2117, \ \epsilon_3 = 0.0123$$
$$P = \begin{bmatrix} 0.0731 & 0.1034 & -0.0013 & -0.0018 \\ 0.1034 & 0.2741 & 0.0006 & -0.0066 \\ -0.0013 & 0.0006 & 2.2503 & -0.0112 \\ -0.0018 & -0.0066 & -0.0112 & 0.5960 \end{bmatrix},$$
$$\alpha_1 = 1.0065; \ \alpha_2 = 5.0015 \times 10^{-6}; \quad J_{th,Peak,2} = 0.3434;$$

Figure 6.5 shows the RMS value of residual signal affected by actuator fault at time $t = 50[s]$ and threshold $J_{th,RMS,2}$. Similarly Figure 6.6 shows the peak value of the faulty residual (actuator fault at $t = 50[s]$) and the thresholds, that is, $J_{th,Peak,Peak}$ and $J_{th,Peak,2}$.

6.4 Adaptive threshold generation

In sections 6.2 and 6.3, constant thresholds are proposed by considering the bounds on unknown inputs and control inputs. Note that control input was also considered as unknown input while designing these thresholds. However, it is evident that control input u is usually available on-line during the process operation. If the on-line information of u; that is, the instantaneous values of u are used, then the size of the threshold is considerably reduced, which, in turn, increases the fault detection capability. This methodology makes the threshold sensitive to input u and leads us to the so-called adaptive threshold. In this threshold, the gain of the unknown inputs to the residual signal is derived in the manner similar to the one presented in Sections 6.2 and 6.3. Then, instead of using the

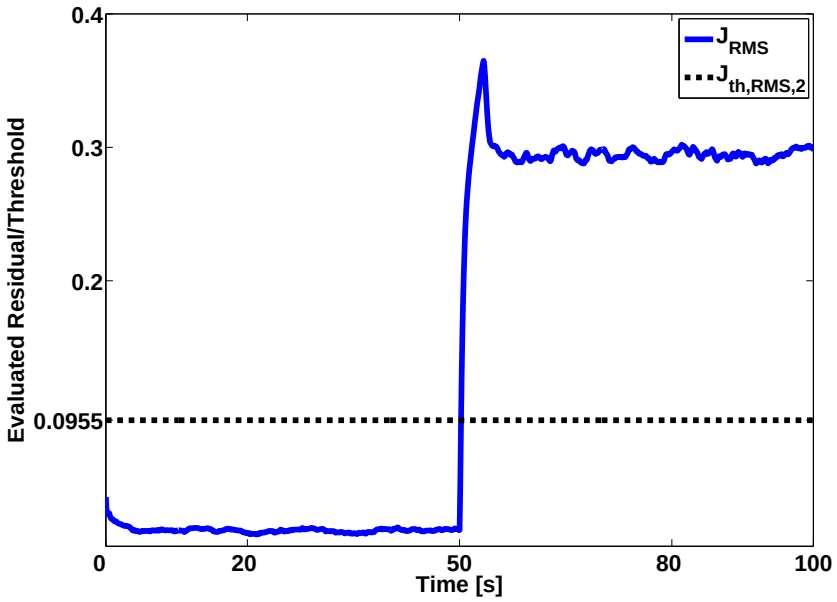

Figure 6.5: Response of the residual to the actuator fault: The solid line represents the evaluated residual signal J_{RMS}, dotted lines denotes the threshold $J_{th,RMS,2}$

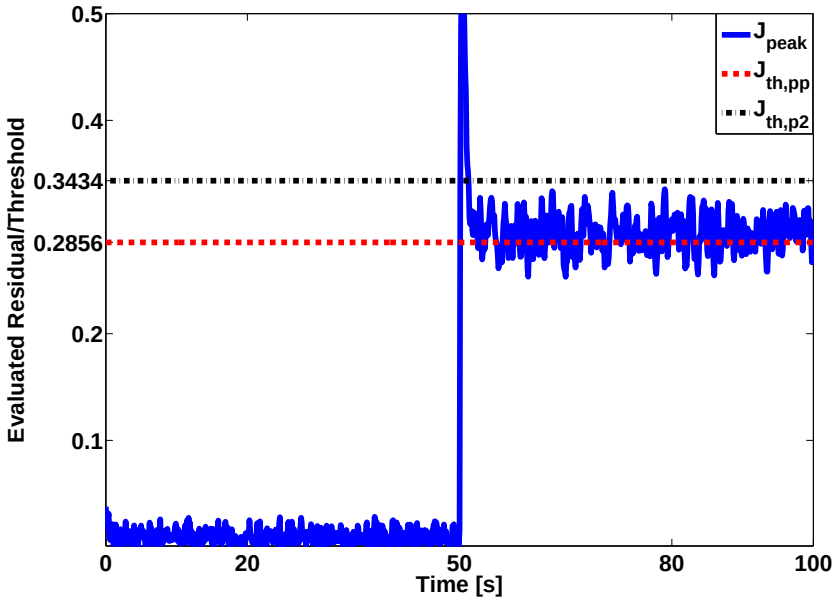

Figure 6.6: Response of the residual to the actuator fault: The solid line represents the evaluated residual signal J_{Peak}, dotted line and dash-dotted line denote the thresholds $J_{th,Peak,Peak}$ $J_{th,Peak,2}$ respectively

bound on u, the instantaneous values of u are used and, as a result, the threshold is a function of the instantaneous values of u. Motivated by the results presented in [1] for LTI systems, the study from Sections 6.2 and 6.3 can be extended to propose adaptive threshold for Lipschitz nonlinear uncertain systems (6.3) and (6.48). To this end, $\delta_{u,\infty}$ is replaced by

$$\|u(k)\| = \sqrt{u^T(k)u(k)}$$

for discrete-time, and

$$\|u(t)\| = \sqrt{u^T(t)u(t)}$$

for continuous-time settings. Furthermore, $\delta_{u,2}$ will be approximated by

$$\|u(k)\|_{2,N} = \sqrt{\sum_{j=0}^{N} \|u(k+j)\|^2}$$

for discrete-time, and

$$\|u(t)\|_{2,T} = \sqrt{\int_{t}^{t+T} \|u(\tau)\| d\tau}$$

for continuous-time settings. Finally, the threshold presented in Sections 6.2 and 6.3 are replaced by the following adaptive thresholds. The threshold $J_{th,RMS,2}$ is replaced by

$$J_{adap,RMS,2}(k) = \frac{\alpha_{RMS}}{\sqrt{N}} \left(\delta_{d,2} + \|u(k)\|_{2,N}\right) \quad \text{or}$$
$$J_{adap,RMS,2}(t) = \frac{\alpha_{RMS}}{\sqrt{T}} \left(\delta_{d,2} + \|u(t)\|_{2,T}\right)$$

Similarly, the threshold $J_{th,Peak,Peak}$ is replaced by

$$J_{adap,Peak,Peak}(k) = \alpha_{Peak,Peak} \left(\delta_{d,\infty} + \|u(k)\|_{Peak}\right) \quad \text{or}$$
$$J_{adap,Peak,Peak}(t) = \alpha_{Peak,Peak} \left(\delta_{d,\infty} + \|u(t)\|_{Peak}\right)$$

and the threshold $J_{th,Peak,2}$ is replaced by

$$J_{adap,Peak,2}(k) = \alpha_{Peak,21} \left(\delta_{d,\infty} + \|u(k)\|_{Peak}\right) + \alpha_{Peak,22} \left(\delta_{d,2} + \|u(k)\|_{2,N}\right) \quad \text{or}$$
$$J_{adap,Peak,2}(t) = \alpha_{Peak,21} \left(\delta_{d,\infty} + \|u(t)\|_{Peak}\right) + \alpha_{Peak,22} \left(\delta_{d,2} + \|u(t)\|_{2,N}\right)$$

It is worth noting that the above thresholds depend on the instantaneous values of the energy of u, which, in turn, shows that these thresholds will be different under different operating conditions, expressed in terms of u and, hence, are referred to as adaptive threshold. Note that the use of the instantaneous values of the energy of u considerably reduces the size of the corresponding threshold and hence enhances fault detection capability. A further advantage of these thresholds is the computational simplicity and its ability to be implemented on-line very easily. In addition, it does not require much on-line computations. The following example shows that these thresholds are less conservative to those presented in Sections 6.2 and 6.3.

6.4.1 A design example

The Example 6.2.5 is considered again in order to perform a comparative analysis. All the coefficient matrices and the distribution of the unknown input vector are kept the same. The filter gain and post filter are also kept the same. The input u is assumed as a sinusoidal signal with amplitude 0.1, that is, $u(k) = 0.1sin(k/2)$. The evaluation window is also kept the same, that is, $N = 20[s]$. The following thresholds are computed

$$J_{adap,RMS,2}(k) = 0.1347 + 0.2987 \times ||u(k)||_{2,N}$$
$$J_{adap,Peak,Peak}(k) = 0.5024 + 3.3814 \times ||u(k)||$$
$$J_{adap,Peak,2}(k) = 0.5063 + 1.4827 \times 10^{-9} \times ||u(k)|| + 1.1230 \times ||u(k)||_{2,N}$$

As shown in Figure 6.7, a fault is simulated as an incipient fault with a constant slope. Figure 6.8 shows the comparison of constant threshold and adaptive threshold computed under the framework of RMS settings. Figure 6.9 and 6.10 show the comparison between the thresholds computed under the framework of Peak norm. It is evident from this simulation study that the proposed adaptive thresholds are not only simple to implement but also less conservative as compared to the constant thresholds computed using the respective framework. For instance, consider the Figure 6.9, the fault started at $40[s]$ and detected at approx. 60 [s] due to adaptive threshold as compared to the corresponding constant one, in which case, it is detected at approx. 75[s]. This further shows that the fault detection time is also reduced in adaptive threshold.

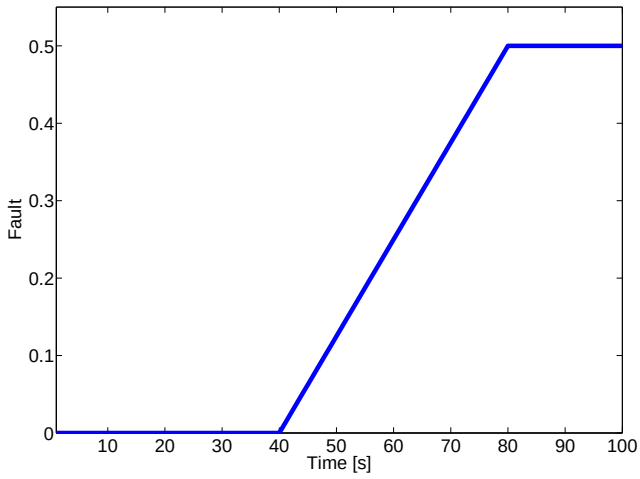

Figure 6.7: Generated sensor fault

6.5 Dynamic threshold generation for discrete-time case

In this section, the design of dynamic threshold for discrete-time Lipschitz nonlinear systems is addressed. As the name indicates, this threshold is generated using a dynamic

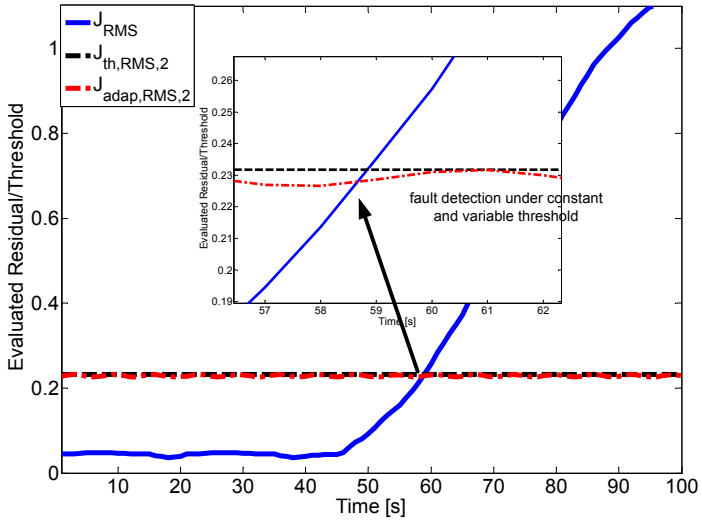

Figure 6.8: Adaptive threshold using RMS framework: J_{RMS}, $J_{th,RMS,2}$, and $J_{adap,RMS,2}$ represents RMS of the residual signal (solid line), constant threshold (straight solid line), adaptive threshold (dotted line) respectively

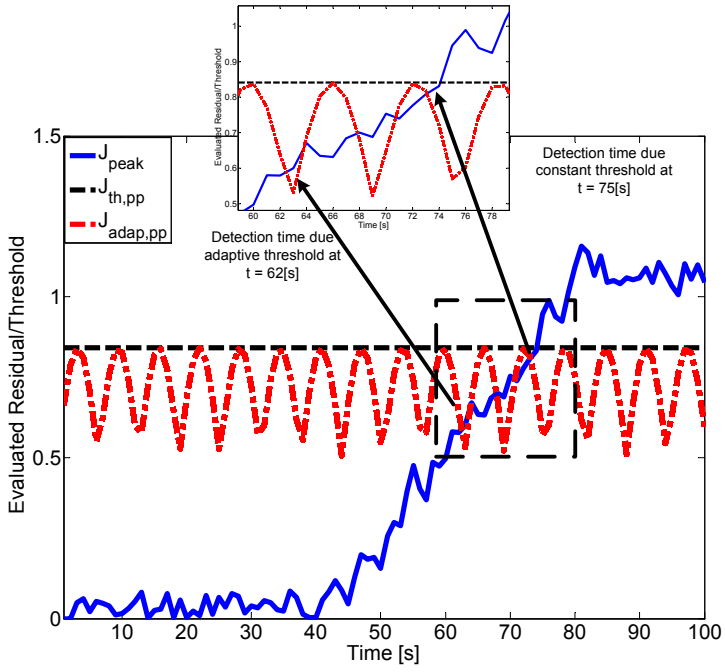

Figure 6.9: Adaptive threshold using Peak-to-Peak framework: J_{Peak}, $J_{th,PP}$, and $J_{adap,PP}$ represents Peak norm of the residual signal (solid line), constant threshold (dotted line), adaptive threshold (dash-dotted line) respectively

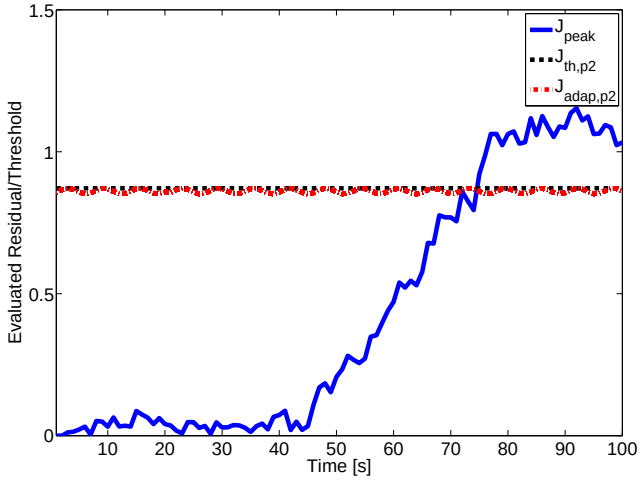

Figure 6.10: Adaptive threshold using Peak-to-2 framework:J_{Peak}, $J_{th,P2}$, and $J_{adap,P2}$ represents Peak norm of the residual signal (solid line), constant threshold (dotted line), adaptive threshold (dash-dotted line)

system, which takes the information of the process input in the presence of model uncertainties. The crux of this scheme is an inequality on the upper bound on the modulus of the solution of Lipschitz nonlinear uncertain systems. This inequality has been shown to be a useful tool for the computation dynamic threshold.

6.5.1 Notations and preliminaries

The following notations will be used in the remainder of this chapter. Note that most of these notations are based on [71].

The convolution between two functions F and G will be represented as $\mathbf{F}\mathrm{G}$, that is, $\mathbf{F}G \triangleq F * G$. Inequalities between matrices are interpreted element-wise; for example, with $X = [x_{ij}]_{m\times n}, Y = [y_{ij}]_{m\times n}$ then $X \leqq Y$ means that $x_{ij} \leq y_{ij}$ for all $i \in 1\cdots n$ and all $j \in 1\cdots m$. $|\cdot|$ will represent the matrix modulus function, that is, element-wise absolute value, thus $|X| = [|x_{ij}|]_{m\times n}$. For functions, $|\cdot|$ will be interpreted point-wise, so that $|F|(k) \triangleq |F(k)|$. Inequalities between functions are also intended pointwise, that is, $F \leqq G$ means $F(k) \leq G(k)$ for all $k \geq 0$.

In the sequel, a property and two lemmas are presented that will be used for the derivation of the results proposed in the remainder of this Chapter.

Property 6.5.1. *[71] Let c be an arbitrary scalar and let A, B and C be matrices of compatible dimensions. Then*

a. $|A + B| \leqq |A| + |B|$

b. $|AC| \leqq |A||C|$

c. $|cA| = |c||A|$

Lemma 6.5.1. *[71] Let $F \in \mathbb{L}_{pe}^{n\times m}$ and $G, H \in \mathbb{L}_{qe}^{m\times r}$, $1 \le p \le \infty$ and $1/p + 1/q = 1$. Furthermore, let $J \in \mathbb{L}_{\infty e}^{r\times s}$ and define*

$$\bar{J}(k) \triangleq \sup_{\kappa\in[0,k]} |J(\kappa)| \tag{6.62}$$

Then

a. If $F(k) \ge 0$ for all k and $H \ge G$ then $F * H \ge F * G$

b. $|F * G| \le |F| * |G|$

c. If $F(k) \ge 0$ for all k, then $F * |GJ| \le (F * |G|)\bar{J}$

and all the convolutions above are finite for all $k \ge 0$

Lemma 6.5.2. *[71] Let $G \in \mathbb{L}_{pe}^{n\times n}$, $1 \le p \le \infty$ and define the linear operator $\mathbf{G}$ by $\mathbf{G}F \triangleq G * F$. Let $\mathbf{M} \triangleq (I - \mathbf{G})^{-1} - I$ and define M as the function such that $\mathbf{M}F \triangleq M * F$. If $\|\mathbf{G}\|_p \le 1$ and $G(k) \ge 0$ for all $k \ge 0$ then $\|\mathbf{M}\|_p \le 1$ and $M(k) \ge 0$ for all $k \ge 0$.*

In the above lemmas, the space $\mathbb{L}_{pe}^{n\times m}$, for example, represents the set of functions from $\mathbb{R}_+$ to $\mathbb{R}^{n\times m}$ such that $\|\mathcal{P}_\kappa x\|_p < \infty$ for all $\kappa > 0$, where $\|\cdot\|$ is some matrix norm and the truncation operator $\mathcal{P}_\kappa$ is defined as

$$(\mathcal{P}_\kappa x)(k) = \begin{cases} x(k) & k \le \kappa \\ 0 & \text{otherwise} \end{cases}$$

6.5.2 Problem formulation

Consider the discrete-time nonlinear system with Lipschitz nonlinearity given in (6.3) and the associated residual generator (6.8). In order to facilitate the analysis for the computation of threshold, a fault-free operation is assumed. To this end, re-stating the residual generator (6.6) as below

$$x_{0,k+1} = A_0 x_{0,k} + B_0 u_k + \Psi_0(x_{0,k}, u_k) + \eta_0(x_{0,k}, u_k, k) + E_0 w_k \tag{6.63}$$
$$r_{0,k,w} = C_0 x_{0,k} + F_0 w_w \tag{6.64}$$

where $B_0 = [B^T \;\; 0]^T$, $E_0 = \left[E_w^T \;\; \bar{E}_w^T\right]^T$, and $\eta_0(x_{0,k}, u_k, k) = \Delta(A_0)x_{0,k} + \Delta(B_0)u_k$. The rest of the coefficient matrices in the above equations are defined in (6.8). The only difference is the bound on the uncertainty. In the sequel, the uncertainty is assumed to be bounded in the sense $|\Delta| \le \Pi$.

6.5.3 Computation of dynamic threshold

Theorem 6.5.1. *Consider the residual generator* (6.63)-(6.64). *Suppose that A_0 is assumed to be invertible and Schur stable; that is, the modulus of its eigenvalues is smaller than unity. Furthermore, the uncertain terms $\Delta(A_0)$ and $\Delta(B_0)$ has the form given in* (6.8) *with $|\Delta(k)| \le \Pi, \forall k \ge 0$. Let $\psi(k) = A_0^k$ and there exist a matrix M such that*

$M(k) \geq |\psi(k)|$. Further, $M(k)$ is so selected that $(I - \bar{\mathbf{M}}\mathscr{N}_1)^{-1}\bar{\mathbf{M}}$ is stable, then the modulus of the residual signal $r_{0,k,w}$ is

$$|r_{0,k,w}| \leq |C_0|(I - \bar{\boldsymbol{M}}\mathscr{N}_1)^{-1}\left(M|\zeta_0| + \bar{\boldsymbol{M}}(\mathscr{N}_2|u_k| + |E_0|\delta_{0,w})\right) + |F_0|\delta_{0,w} \tag{6.65}$$

where $\bar{M}(k) = |A_0^{-1}|\,(M * I - I)$, $\mathscr{N}_1 = (\gamma I + |E|\Pi|G|)$, $\mathscr{N}_2 = \left(|B_0| + |\bar{E}|\Pi|H|\right)$, and $|w_{0,k}| \leq \delta_{0,w}$.

Proof. Let us consider (6.63), as shown

$$x_{0,k+1} = A_0 x_{0,k} + B_0 u_k + \Psi_0(x_{0,k}, u_k) + \eta_0(x_k, u_k, k) + E_0 w_k$$

The solution can be expressed by

$$\begin{aligned} x_{0,k} &= A_0^k \zeta_0 + \sum_{h=0}^{k-1} A_0^{k-1-h}\Psi_0(x_{0,h}, u_h) + \sum_{h=0}^{k-1} A_0^{k-1-h}\left[B_0 u_h + \eta_0(x_{0,h}, u_0, h) + E_0 w_h\right] \\ &= A_0^k \zeta_0 + A_0^{-1}\left\{\sum_{h=0}^{k} A_0^{k-h}\Psi_0(x_{0,h}, u_h) + \sum_{h=0}^{k} A_0^{k-h}\left[B_0 u_h + \eta_0(x_{0,h}, u_h, h) + E_0 w_h\right]\right. \\ &\left. -\Psi_0(x_{0,k}, w_{0,k}) - B_0 u_k - \eta_0(x_{0,k}, u_k, k) - E_0 w_k \right\} \end{aligned}$$

where ζ_0 is the initial condition, A_0^k is the state transition matrix and can be denoted by $\psi(k)$ in sequel. Similarly for notational simplicity, use $\Psi_0(k) = \Psi_0(x_{0,k}, w_{0,k})$ and $\eta_0(k) = \eta_0(x_{0,k}, w_{0,k}, k)$, Then

$$\begin{aligned} x_{0,k} &= \psi(k)\zeta_0 + A_0^{-1}\left\{\sum_{h=0}^{k} \psi(k-h)\Psi_0(h) + \sum_{h=0}^{k} \psi(k-h)\left[B_0 u_h + \eta_0(h) + E_0 w_{0,h}\right]\right. \\ &\left. -\Psi_0(k) - B_0 u_k - \eta_0(k) - E_0 w_k \right\} \\ &= \psi(k)\zeta_0 + A_0^{-1}\left\{ \psi(k) * \Psi_0(k) + \psi(k) * \eta_0(k)\right. \\ &\left. +\psi(k) * B_0 u_k + \psi(k) * E_0 w_k - \Psi_0(k) - \eta_0(k) - B_0 u_k - E_0 w_k \right\} \end{aligned}$$

where $*$ represents the convolution operator. Taking modulus of both sides

$$\begin{aligned} |x_{0,k}| = |\,&\psi(k)\zeta_0 + A_0^{-1}\left\{ \psi(k) * \Psi_0(k) + \psi(k) * \eta_0(k)\right. \\ &\left. +\psi(k) * B_0 u_k + \psi(k) * E_0 w_k - \Psi_0(k) - \eta_0(k) - B_0 u_k - E_0 w_{0,k} \right\}| \end{aligned}$$

using Property 1, the upper bound on the modulus of $x_{0,k}$ is

$$
\begin{aligned}
|x_{0,k}| \leqq & |\psi(k)\zeta_0| + |A_0^{-1}| \Big\{ |\psi(k) * \Psi_0(k)| + |\psi(k) * \eta_0(k)| + |\psi(k) * B_0 u_k| + |\psi(k) * E_0 w_k| \\
& - |\Psi_0(k) + \eta_0(k) + B_0 u_k + E_0 w_k| \Big\} \\
\leqq & M|\zeta_0| + |A_0^{-1}| \Big\{ M * |\Psi_0(k)| + M * |\eta_0(k)| + M * |B_0 u_k| + M * |E_0 w_k| \\
& - |\Psi_0(k)| - |\eta_0(k)| - |B_0 u_k| - |E_0 w_k| \Big\} \\
\leqq & M|\zeta_0| + |A_0^{-1}| \Big\{ M * \gamma|x_{0,k}| + M * |\bar{E}\Delta(k)\bar{G}x_{0,k} + \bar{E}\Delta(k)Hu_k + B_0 u_k + E_0 w_k| \\
& - \gamma|x_{0,k}| - |\bar{E}\Delta(k)\bar{G}x_{0,k} + \bar{E}\Delta(k)Hu_k + B_0 u_k + E_0 w_k| \Big\} \\
\leqq & M|\zeta_0| + |A_0^{-1}| \left\{ (M * \mathscr{N}_1 - \mathscr{N}_1) |x_{0,k}| + (M * I - I) \left(\left| \left[\bar{E}\Delta(k)H + B_0 \right] u_k + E_w w_k \right| \right) \right\} \\
\leqq & M|\zeta_0| + |A_0^{-1}| \left\{ (M * I - I) \mathscr{N}_1 |x_{0,k}| \right\} + |A_0^{-1}| \left\{ (M * I - I) \left(\left| \left[\bar{E}\Delta(k)H + B_0 \right] u_k \right| \right) \right\} \\
& + |A_0^{-1}| \left\{ (M * I - I) |E_w w_k| \right\} \\
\leqq & M|\zeta_0| + \bar{M}\mathscr{N}_1 |x_{0,k}| + \bar{M} \left(\left| \left[\bar{E}\Delta(k)H + B_0 \right] u_k + E_0 w_k \right| \right) \\
\leqq & M|\zeta_0| + \bar{M}\mathscr{N}_1 |x_{0,k}| + \bar{M} \left(\left| \left[\bar{E}\Delta(k)H + B_0 \right] u_k \right| + |E_0 w_k| \right) \\
\leqq & M|\zeta_0| + \bar{M}\mathscr{N}_1 |x_{0,k}| + \bar{M} \left(\left[|\bar{E}|\Pi|H| + |B_0| \right] |u_k| + |E_0 w_k| \right) \\
\leqq & M|\zeta_0| + \bar{M}\mathscr{N}_1 |x_{0,k}| + \bar{M} \left(\mathscr{N}_2 |u_k| + |E_0 w_k| \right)
\end{aligned}
$$

where $M \geqq |\psi(k)|$, $|\Psi_0(x_{0,k}, w_{0,k})| \leq \gamma|x_{0,k}|$, $\mathscr{N}_1 = \gamma I + |E|\Pi|G|$, $\mathscr{N}_2 = \left[|\bar{E}|\Pi|H| + |B_0| \right] |$ $\bar{M} = |A_0^{-1}| (M * I - I)$. Using the notation for convolution of two functions and lemma (6.5.1) and (6.5.2), after some mathematical manipulations,

$$
|x_{0,k}| \leqq \left[I - \bar{\mathbf{M}}\mathscr{N}_1 \right]^{-1} \left(M|\zeta_0| + \bar{\mathbf{M}} \left(\mathscr{N}_2 |u_k| + |E_0|\delta_{0,w} \right) \right) \tag{6.66}
$$

Considering (6.64) and (6.66), the modulus of the residual signal is given as

$$
|r_{0,k,w}| \leqq |C_0| \left[I - \bar{\mathbf{M}}\mathscr{N}_1 \right]^{-1} \left(M|\zeta_0| + \bar{\mathbf{M}} (\mathscr{N}_2 |u_k| + |E_0|\delta_{0,w}) \right) + |F_0|\delta_{0,w} \tag{6.67}
$$

This completes the proof. □

Remark 6.5.1. *Theorem 6.5.1 assumes the uncertainty is structured. However, for unstructured uncertainty of the form $|\eta_0(x_{0,k}, u_k, k)| \leq \bar{\eta}_0(u_k, k)$, similar results can be derived by putting $\mathscr{N}_1 = \gamma I$ and substituting $\mathscr{N}_2|u_k| = |B_0 u_k| + \bar{\eta}_0(u_k, k)$. Similarly the uncertain term η_0 bounded in the sense, that is, $\eta_0(x_{0,k}, u_k, k) \leq \bar{\eta}_0(x_{0,k}, u_k, k)$ as the one considered in [132, 133] can also be chosen, but it requires the condition of full state measurement. The assumption of the full state measurement limits the use of threshold. Further, the threshold designed based on this assumption may have reduced sensitivity as the states of the system carries the information of faults. Another choice of bounding the uncertainty is $\eta_0(x_{0,k}, u_k, k) \leq \bar{\eta}_0(y_k, u_k, k)$ as given in [127, 130, 165]. This choice of bound may also present some difficulty to compute threshold insensitive to faults because this requires the information of process outputs, which carries the information of faults.*

To this point, a concrete background have been developed which gives us an elegant tool for the calculation of dynamic threshold in the form of Theorem 6.5.1. The only question remains unanswered is how to compute the matrix M. To this end, the following lemma is useful.

Lemma 6.5.3. *Let a matrix $U(k) = \mathcal{G}^k$, where $\mathcal{G}$ has complex eigenvalues whose magnitude is less than unity. Also assume that the matrix G is diagonalizable such that $\mathcal{G} = \mathcal{W}\Xi\mathcal{W}^{-1}$, where Ξ is a diagonal matrix containing the eigenvalues of $\mathcal{G}$ at the diagonal and $\mathcal{W}$ contains the eigenvector corresponding to the eigenvalues of $\mathcal{G}$. Further, suppose Ξ_{real} and Ξ_{imag} are diagonal matrices representing the real and imaginary part of Ξ, also $|\Xi| = \sqrt{|\Xi|^2_{real} + |\Xi|^2_{imag}}$, Then*

$$|U(k)| \leq M(k) = |\mathcal{W}||\Xi|^k|\mathcal{W}^{-1}|$$

Proof. The proof is divided in two parts.

Part 1: Let G be diagonalizable such that $\mathcal{G} = \mathcal{W}\Xi\mathcal{W}^{-1}$, then

$$\begin{aligned} U(k) = \mathcal{G}^k &= \left(\mathcal{W}\Xi\mathcal{W}^{-1}\right)^k \\ &= \left(\mathcal{W}\Xi\mathcal{W}^{-1}\right)\left(\mathcal{W}\Xi\mathcal{W}^{-1}\right)\cdots\left(\mathcal{W}\Xi\mathcal{W}^{-1}\right) \\ &= \mathcal{W}\Xi\left(\mathcal{W}^{-1}\mathcal{W}\right)\Xi\left(\mathcal{W}^{-1}\mathcal{W}\right)\cdots\left(\mathcal{W}^{-1}\mathcal{W}\right)\Xi\mathcal{W}^{-1} = \mathcal{W}\Xi^k\mathcal{W}^{-1} \end{aligned}$$

Now considering the modulus of $\mathcal{G}^k$, as

$$|\mathcal{G}^k| = |\mathcal{W}\Xi^k\mathcal{W}^{-1}| \leq |\mathcal{W}||\Xi^k||\mathcal{W}^{-1}|$$

Part 2: Let a complex number $a = b + ic$ be represented using polar coordinates as $a = |a|\left(\cos(\theta) + i\sin(\theta)\right)$. Where $|a| = \sqrt{b^2 + c^2}, \theta = \tan^{-1}(\frac{c}{b})$. Then using De Movier's formula for Integer powers, $a^n = |a|^n\left(\cos(n\theta) + i\sin(n\theta)\right)$ and hence $|a^n| = |a|^n$. Using these arguments, the absolute value of diagonal matrix $|\Xi^k|$ is $|\Xi^k| = |\Xi|^k$ and hence

$$|\mathcal{G}^k| \leq |\mathcal{W}||\Xi^k||\mathcal{W}^{-1}| = |\mathcal{W}||\Xi|^k|\mathcal{W}^{-1}| = M(k)$$

This completes the proof. □

Next, a theorem is presented which eases the computation of $M(k)$ when $\mathcal{G}$ has real eigenvalues.

Theorem 6.5.2. *Let a matrix $U(k) = \mathcal{G}^k$ with G has real eigenvalues and $|U(k)| \leq M(k)$ and if the matrix $\mathcal{G}$ is diagonalizable such that $\mathcal{G} = \mathcal{W}\Xi\mathcal{W}^{-1}$, then*

$$|\mathcal{G}^k| \leq M(k) = |\mathcal{W}||\Xi|^k|\mathcal{W}^{-1}|$$

where Ξ is a diagonal matrix containing the eigenvalues of $\mathcal{G}$ at the diagonal. $\mathcal{W}$ contains the eigenvector corresponding to the eigenvalues of $\mathcal{G}$.

Proof. The proof follows from lemma 6.5.3. □

Theorem 6.5.1 is useful in finding robust thresholds using an upper bound on the modulus of the residual signal. The corresponding dynamic threshold can then be defined as

$$\begin{aligned} J_{th} &= \sup_{f=0,k\geq 0} \|r_{0,k,w}\|_{\nu} \\ &= \sum_{h=0}^{k} \nu(k-h)|r_{0,h,w}| = \nu * |r_{0,k,w}| = \mathbf{v}|r_{0,k,w}| \\ &= \mathbf{v}\left[|C_0|\left[I - \bar{\mathbf{M}}\mathscr{N}_1\right]^{-1}\left(M|\zeta_0| + \bar{\mathbf{M}}[\mathscr{N}_2|u_k| + |E_0|\delta_{0,w}]\right) + |F_0|\delta_{0,w}\right] \end{aligned} \tag{6.68}$$

where ν is the weighting function which increases the influence of the most recent data. It can be a rectangle window function as mentioned in [153] or exponential function as chosen by [71]. Note that the above threshold is a dynamic system which takes the instantaneous values u_k as input.

Algorithm 6.5.1. *Computation of dynamic threshold*

Step I. *Diagonalize the matrix* $A_0 = \begin{bmatrix} A & 0 \\ 0 & A - LC \end{bmatrix}$ *and compute the matrices* $\mathcal{W}$ *and* Ξ.

Step II. *Find* M_k *according to Lemma 6.5.3.*

Step III. *Compute* $\mathscr{N}_1$ *and* $\mathscr{N}_2$.

Step IV. *Choose a weighting function* ν_k.

Step V. *Using the absolute value of residual signal* (6.65) *and the weighting function* ν_k, *compute the dynamic threshold using relation* (6.68)

6.5.4 A design example

This example elaborates the design procedure for dynamic threshold. Consider the same system with coefficient matrices as given in Example 6.2.5. The external disturbance vector w_k is assumed to have the same distribution as the one in Example 6.2.5, the process input is a sinusoidal signal with amplitude 3.5 and frequency 5 rad. The fault is assumed to be a unit step function and introduced in the sensor at $20[s]$. Considering similar FDF parameters as in Example 6.2.5, the eigenvalues of A are $\{0.0950 + 0.5818i, 0.0950 - 0.5818i\}$ and that of $A - LC$ are $\{0.3000, 0.2000\}$, which lie in unit circle. Diagonalizing A_0, the diagonal matrix Ξ containing the eigenvalues of A_0, and a matrix W whose columns are

the eigenvector corresponding to the eigenvalues of A_0 are given as follows,

$$\Xi = \begin{bmatrix} 0.0950 + 0.5818i & 0 & 0 & 0 \\ 0 & 0.0950 - 0.5818i & 0 & 0 \\ 0 & 0 & 0.3000 & 0 \\ 0 & 0 & 0 & 0.2000 \end{bmatrix}$$

$$\mathcal{W} = \begin{bmatrix} 0.0986 - 0.6039i & 0.0986 + 0.6039i & 0 & 0 \\ 0.7910 & 0.7910 & 0 & 0 \\ 0 & 0 & 0.9998 & -0.9721 \\ 0 & 0 & -0.0218 & 0.2346 \end{bmatrix}$$

Using Lemma 6.5.3, $M(k)$ is found as follows

$$M(k) = |\mathcal{W}||\Xi|^k|\mathcal{W}^{-1}| = \begin{bmatrix} M_{11}(k) & 0 \\ 0 & M_{22}(k) \end{bmatrix}$$

where

$$M_{11}(k) = \begin{bmatrix} 1.0133(0.5895)^k & 0.7838(0.5895)^k \\ 1.3099(0.5895)^k & 1.0133(0.5895)^k \end{bmatrix}$$

$$M_{22}(k) = \begin{bmatrix} 0.099(0.2)^k + 1.099(0.3)^k & 4.5550(0.2)^k + 4.5550(0.3)^k \\ 0.0240(0.2)^k + 0.0240(0.3)^k & 1.099(0.2)^k + 0.099(0.3)^k \end{bmatrix}$$

Let $\Pi \leq 1$, then $\mathscr{N} = diag(\mathscr{N}_{11}, \mathscr{N}_{22})$, where $\mathscr{N}_{11} = \mathscr{N}_{22} = diag(0.12, 0.13)$, choosing $\nu_k = 0.3(0.3)^k$, the threshold, defined in (6.68), for this example is then given as

$$\begin{aligned} J_{th} &= \nu * |r_{0,k,d}| \\ &= 0.3(0.3)^k * \\ &\quad \Big\{\big(0.1317(0.2)^k - 1.5277(0.287)^k + 1.07763(0.3)^k + 20.6272(0.7878)^k\big)\,|\zeta_0| \\ &\quad + \big[2.4949(0.2919)^k + 48.075(0.788)^k\big] * (|E|\Pi||Hu_k| + \delta_{w0})\Big\} \end{aligned}$$

which may be easily implemented using discrete-time filter. Figure 6.11 shows the simulation results for evaluated residual (solid line) with dynamic threshold (dotted line). Note that the threshold is varying with the control input in the presence of model uncertainty and disturbances. The simulation results show successful elimination of false alarms and efficient fault detection.

6.6 Dynamic threshold for continuous-time case

In this section, the discussion is extended to continuous-time systems. A theorem is provided which gives the needed information for the design of dynamic threshold for continuous-time settings.

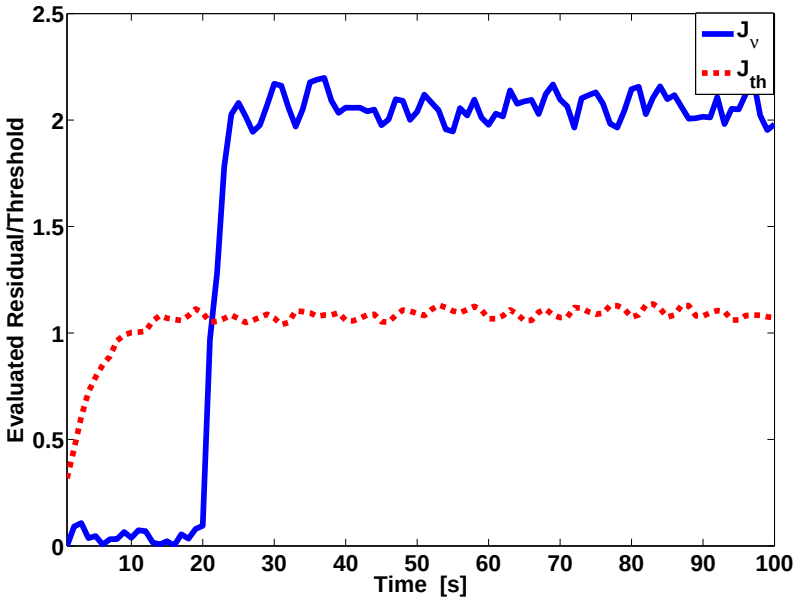

Figure 6.11: Detection of sensor fault using dynamic threshold framework: J_ν and J_{th} represent the evaluated residual and dynamic threshold respectively

Theorem 6.6.1. *Consider the residual generator given below*

$$\dot{x}_0 = A_0 x_0 + B_0 u + \Psi_0(x_0, u) + \eta_0(x_0, u, t) + E_0 w_0 \tag{6.69}$$

$$r_{0,w} = C_0 x_0 + F_0 w_0 \tag{6.70}$$

where A_0 is Hurwitz. The nonlinear function Ψ_0 is Lipschitz with Lipschitz constant γ. The uncertain term η_0 is given as $\eta_0(x_0, u, t) = \Delta(A_0)x_0 + \Delta(B_0)u$. Let $\psi(t) \triangleq \exp(A_0 t)$ and suppose there exists a time varying function $M(t)$ such that $M(t) \geq |\psi(t)|$. If $\|M(t)\|$ is so selected that $(1 - \boldsymbol{M}\mathscr{N}_1)^{-1}\boldsymbol{M}$ is stable, then

$$|r_{0,w}| \leqq |C_0|\left(I - \boldsymbol{M}(t)\mathscr{N}_1\right)^{-1}\left[M(t)|\zeta_0| + \boldsymbol{M}(t)\{\mathscr{N}_2|u(t)| + |E_0|\delta_{0,w}\}\right] + |F_0|\delta_{0,w} \tag{6.71}$$

where $|w_0| \leq \delta_{0,w}$, $\mathscr{N}_1 = \gamma I + |\bar{E}|\Pi|\bar{G}|$, $\mathscr{N}_2 = \left[|B_0| + |\bar{E}|\Pi|H|\right]$. If a solution for (6.71) is found, the threshold can then be computed as

$$\begin{aligned} J_{th} &= \sup_{f=0, t\geq 0} \|r_{0,w}\|_\nu \\ &= \int_0^t \nu(k-\tau)|r_{0,w}|d\tau = \nu * |r_{0,w}| = \boldsymbol{v}|r_{0,w}| \\ &= \boldsymbol{v}\left[|C_0|\left(I - \boldsymbol{M}(t)\mathscr{N}_1\right)^{-1}\left[M(t)|\zeta_0| + \boldsymbol{M}(t)\{\mathscr{N}_2|u(t)| + |E_0|\delta_{0,w}\}\right] + |F_0|\delta_{0,w}\right] \end{aligned} \tag{6.72}$$

Proof. The proof can be found in Appendix B.4 □

Note that the only issue in this Theorem is the computation of $M(t)$. To this end, Theorem A.3.1 is useful. In order to facilitate the design dynamic threshold for continuous-time nonlinear systems of the form (6.69)-(6.70), an algorithm is given as follows:

Algorithm 6.6.1. *Computation of dynamic threshold*

Step I. *Diagonalize the matrix* $A_0 = \begin{bmatrix} A & 0 \\ 0 & A - LC \end{bmatrix}$ *and substitute* $e^{A_0 t} = \mathcal{W} e^{\Xi t} \mathcal{W}^{-1}$. Ξ *is the diagonal matrix containing the eigenvalues of* A_0 *and* $\mathcal{W}$ *is the matrix of eigenvectors corresponding to the eigenvalues of* A_0.

Step II. *Find* $M(t)$ *according to Theorem A.3.1.*

Step III. *Compute* $\mathcal{N}_1$ *and* $\mathcal{N}_2$ *as defined in the above theorem.*

Step IV. *Choose a weighting function* $\nu(t)$

Step V. *Using the absolute value of residual signal* (6.71) *and the weighting function* $\nu(t)$*, compute the dynamic threshold using relation* (6.72)

6.7 A comparison

One common feature considered in the design of thresholds proposed in this chapter is the elimination of false alarms. Note that the simulation results presented in various sections show that the chances of false alarms are completely eliminated which, in turn, illustrate that this objective has been successfully achieved. It is also worth noting that size of different thresholds vary depending upon the framework under which it is used. Therefore, it is needed that the conservativeness of different thresholds is studied and compared. The following lines show the comparison of different thresholds with this perspective.

The constant thresholds are proposed for different situations. For instance, $J_{th,RMS,2}$ is useful when the RMS values of the residual are used for the purpose of evaluation. Similarly $J_{th,Peak,Peak}$ and $J_{th,Peak,2}$ are advantageous if one is interested to observe the effect of peak and energy values of the unknown inputs on the peak values of the residual signal. It is evident from the simulation results (e.g., Figure 6.4 and 6.6) that $J_{th,Peak,2}$ is more conservative than $J_{th,Peak,Peak}$ since it is computed on the basis of the energy of the unknown inputs. In practice, $J_{th,Peak,Peak}$ is set low for the purpose of early fault detection. It is also used to activate the computation of $J_{th,Peak,2}$. Similarly, the RMS-based evaluation scheme produces smoothness in the residual signal due to the computation of RMS values of the residual signal over a moving time window of certain length. This scheme is more useful in reduction of false alarms as compared to evaluation under the framework of peak-norm. Hence, the threshold $J_{th,RMS,2}$ is mainly used in order to reduce false alarms. Figure 6.3 and 6.5 show that the residual signal is sufficiently smooth under the RMS framework. Furthermore, the size of $J_{th,RMS,2}$ is such that any possibility of false alarms is eliminated together with ensuring detection of fault. The smoothness in the residual signal can be improved by increasing the time window. An associated problem with the increase in time window is that it may sometimes result into a delayed fault alarm. It means that the fault detection time increases due to taking the RMS over a large time

window. Consequently, the size of the evaluation window should be carefully chosen.

The adaptive threshold is less conservative than the respective constant threshold due to the use of the instantaneous values of u. These thresholds can also be compared in a similar fashion as above. In addition, as shown from the proposed scheme for $J_{th,Peak,Peak}$, it is evident that it requires more off-line computation (due to search for suitable λ and μ which can be performed iteratively) as compared to $J_{th,Peak,2}$ and $J_{th,RMS,2}$. On the other hand, $J_{th,RMS,2}$ and $J_{th,Peak,2}$ requires more on-line computation as compared to $J_{th,Peak,Peak}$ because of the iterative computation of the $\mathscr{L}_2-$norm of u for a moving time window of length N or T. However, the RMS framework is useful not only by increasing the smoothness in the residual signal but also reducing the size of the threshold $J_{th,RMS,2}$.

The dynamic threshold is computed using the upper bound on the modulus of the residual signal. It is referred to as a dynamic thresholds because this upper bound is generated using a dynamic system. Note, however, that this scheme requires much on-line computation as compared to the proposed adaptive thresholds. Furthermore, the on-line implementation of adaptive threshold is easier than the dynamic threshold. In addition, evaluation under the framework of RMS strategy is more useful than the other schemes because of the fact that the former scheme is less sensitive to the unknown inputs.

6.8 Summary

In this chapter, methods for the computation of thresholds for Lipschitz nonlinear uncertain systems subject to exogenous disturbances have been presented. Both structured and unstructured model uncertainties were addressed. Various kind of thresholds including constant threshold, adaptive threshold, and dynamic thresholds are presented. For constant threshold, a generalized framework was proposed followed by an algorithm which elaborated the design steps of the respective threshold. These thresholds gave a fair evaluation of the residual and covered all the practical scenarios which can be addressed under the domain of constant threshold. A comparative analysis was presented with the help of design examples. For designing adaptive threshold, the methodology proposed for constant threshold is adopted. The only difference is the use of the instantaneous values of u instead of its bound. This scheme reduced the conservativeness of the corresponding constant thresholds and enhanced fault detection capability which was illustrated with the help of simulation example given in that section. For designing dynamic threshold, an inequality on the upper bound of the solution of the nonlinear system was derived. Using this inequality, a framework for the computation of dynamic threshold has been proposed. The usefulness of the proposed methodology was elaborated by simulating a discrete-time nonlinear uncertain system in the presence of exogenous disturbances. All of these thresholds are studied for both discrete- and continuous-times settings. A comprehensive discussion was presented on all the proposed thresholds in the last part of this chapter.

Chapter 7

Application to benchmark problems

This chapter presents the results obtained by the application of the proposed algorithms to benchmark problems. The nonlinear fault detection algorithms developed in this thesis were applied to two different physical systems. The first one is a ***Three-tank system: DTS200*** *consisting of three circular tanks coupled via interconnecting pipes showing a typical characteristics of tanks, pipelines etc. often used in chemical industry. The nonlinear dynamics of three tank system make it a nice example for testing and validating the nonlinear FD algorithms. The second chosen benchmark is* ***The inverted pendulum control system: LIP100****. This application is also dynamically nonlinear and unstable. It shows a typical characteristics of electromechanical systems. Due to its highly nonlinear behavior and open loop instability in nature, it becomes an excellent candidate for illustrating the usefulness of the closed loop FD techniques for nonlinear systems.*

7.1 Three-tank system

The three-tank system consists of three circular tanks coupled via interconnecting pipes showing a typical characteristics of tanks, pipelines, and pumps used in chemical industry. The highly nonlinear dynamic behavior makes it a very good example to show the superiority and usefulness of nonlinear FDI techniques. Due to this reason, it has widely been used as a benchmark for implementation and realization of different control and FD algorithms in software and in real time; see, for instance, some references [166–172].

In this section, a complete FD scheme (residual generation and threshold computation) for discrete-time nonlinear nonlinear three-tank system is designed using the algorithms proposed in this thesis. The FD scheme, thus designed, is then implemented with the actual nonlinear model of the plant. The underlying philosophy is illustrated with the help of open loop FD schemes. Figure 7.1 shows the experimental setup for three-tank system available at our Institute (AKS). It consists of two major parts: the three-tank system DTS200 [173] as the controlled plant and a Wireless networked control system (*WiNC*) which is a real-time experimentation platform developed recently at AKS [174]. For studying the implementation of FDI algorithms in real-time, a DSP system [141] instead of *WiNC* [174] can also be employed.

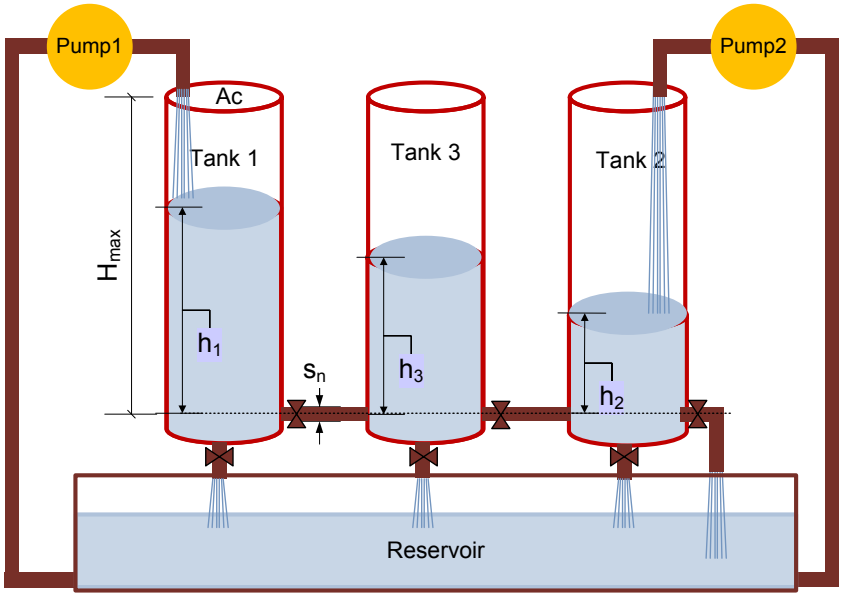

Figure 7.1: Three-tank system

Nonlinear model, description of faults and unknown inputs

The nonlinear model and the operation of DTS200 has been briefly described in Chapter 3. Here, it has been re-stated together with fault and unknown inputs as follows:

$$\begin{aligned} \dot{x} &= a(x) + Bu + E_f f \\ y &= Cx + F_w w + F_f f \end{aligned} \tag{7.1}$$

where a, B, and C serve the same purpose as f, G, h in (3.26) and

$$E_f = [0_{3\times2}\ B\ I_{3\times2}] \in \Re^{3\times6},\ F_f = [I_2\ 0_{2\times4}] \in \Re^{2\times6}; F_w = I_2;$$
$$f = [f_1\ f_2\ f_3\ f_4\ f_5\ f_6]^T, w = [w_1\ w_2]^T$$

In DTS200, different faults can be simulated and their effect can be studied. These include:

- **Sensor faults**: These faults may be due to offset or scaling in the sensor measurement or combination of both. In DTS200, sensor faults are realized by introducing offset in the sensor, scaling the sensor measurements, and their combination. The scaling is varied from 0% (which corresponds to the complete sensor failure) to 100% (which corresponds to healthy sensor measurement). The offset value is in between 0 and $H_{\max}$ – set-point. Any magnitude of fault more than this value will cause the corresponding pump to switch-off. These faults are represented mathematically as follows:

  $$\text{sensor fault} = \text{sensor offset} + \text{scaling} \times \text{measurement of the corresponding sensor}$$

  These faults are denoted by f_1, f_2 for sensors 1 and 2 measuring the water levels in Tanks 1 and 2 respectively.

- **Actuator faults**: Since there are two pumps in DTS200, at most two actuator faults can be observed. These faults can also be realized by scaling the actuators from 0% (which corresponds to zero flow rate, that is, no water flows) to 100% (which corresponds to the 100 % flow rate showing fault free operation). The mathematical expression for these faults is given as follows

  $$\text{actuator fault} = \text{scaling} \times \text{flow rate in pump}$$

  These faults are represented by f_3 and f_4 for pump 1 and 2 respectively.

- **Component faults**: There may be leakage in tanks. For the purpose of implementing leaks, each tank in DTS200 has a circular opening with cross section s_l and a manually adjustable ball valve in series which is shown in Figure 7.1 with the label "Outflow valve". In addition, the interconnecting valves are also used to implement plugging between the two neighboring tanks. In the present study, leaks from different tanks to the reservoir are implemented. It is assumed, for simplicity, that leaks occurred at the bottom of the tanks. These faults are represented by f_5 and f_6.

The source of disturbances in DTS200 is the water bubbles due to the fall of water from each pump and measurement noises in sensors measuring the water level in different tanks. These disturbances are modeled as output disturbances with the distribution matrix F_w given in (7.1).

7.1.1 Fault detection for three-tank system

In this subsection, the algorithms proposed for residual generation and threshold computation in this thesis are used to study FD problem for three-tank system. Since these algorithms are mainly developed for Lipschitz nonlinear systems, it is necessary to obtain the Lipschitz equivalent model of the plant. It is worth noting that the Lipschitz equivalent model is only needed for the design of the parameters of the residual generator L, V and thresholds $J_{th,RMS,2}$, $J_{th,Peak,Peak}$, and $J_{th,Peak,2}$. For the implementation purposes, we shall use the actual nonlinear model and the corresponding residual generator with the parameters computed by the proposed techniques.

A Lipschitz equivalent model

In Chapter 3, it was shown that a nonlinear system of the form $\dot{x} = a(x)$ can be transformed into $\dot{x} = Ax + \phi(x)$, with $\phi(x) = a(x) - Ax$ for a bounded range of system operation. In addition, the nonlinear function $\phi(x)$ under certain conditions admits the properties of a Lipschitz nonlinearity for the bounded range of system operation. Since the operation of the DTS200 is bounded by $45cm < x_1 \leq 60cm$, $0 < x_2 \leq 30cm$ and $30cm < x_3 \leq 45cm$, it is useful to transform the nonlinear model into its Lipschitz equivalent model and use the algorithms proposed to study fault detection for actual nonlinear system; that is, $\dot{x} = a(x)$. Recall that the coefficient matrix A is obtained by linearizing the model $a(x)$ at operating

point. To this end, the Lipschitz equivalent model is expressed as

$$\begin{aligned}\dot{x} &= Ax + [a(x) - Ax] + Bu + E_f f \\ &= Ax + \phi(x) + Bu + E_f f \\ y &= Cx + F_w w + F_f f \end{aligned} \tag{7.2}$$

where

$$A = \begin{bmatrix} -0.0085 & 0 & 0.0085 \\ 0 & -0.0195 & 0.0084 \\ 0.0085 & 0.0084 & -0.0169 \end{bmatrix}, \quad B = \begin{bmatrix} 0.0065 & 0 \\ 0 & 0.0065 \\ 0 & 0 \end{bmatrix}$$

$$E_f = \begin{pmatrix} 0 & 0 & 0 & 0.0065 & 0 & 1 & 0 & 0 \\ 0 & 0 & 0 & 0 & 0.0065 & 0 & 1 & 0 \\ 0 & 0 & 0 & 0 & 0 & 0 & 0 & 0 \end{pmatrix}; C = I_{2\times 3} \quad F_w = I_2, \quad F_f = [I_2 \ 0_{2\times 6}]$$

$$\phi(x) = [a(x) - Ax] = \begin{bmatrix} \phi_1(x) \\ \phi_2(x) \\ \phi_3(x) \end{bmatrix}$$

$$\begin{bmatrix} -\frac{1}{A_c} a_1 s_{13} \text{sgn}(x_1 - x_3)\sqrt{2g|x_1 - x_3|} + 0.0085x_1 - 0.0085x_3 \\ \frac{1}{A_c}\left(a_3 s_{23} \text{sgn}(x_3 - x_2)\sqrt{2g|x_3 - x_2|} - a_2 s_0 \sqrt{2g x_2}\right) + 0.0195x_2 - 0.0084x_3 \\ \frac{1}{A_c}\left(a_1 s_{13} \text{sgn}(x_1 - x_3)\sqrt{2g|x_1 - x_3|} - a_3 s_{23} \text{sgn}(x_3 - x_2)\sqrt{2g|x_3 - x_2|}\right) \\ -0.0085x_1 - 0.0084x_2 + 0.0169x_3 \end{bmatrix}$$

The nonlinear function $\phi(x)$ is considered to be Lipschitz with Lipschitz constant γ. The upper bound on γ is found to be 0.00267, which is estimated by computing $\|\frac{\partial \phi(x)}{\partial x}\|$ over the operating range $45cm < x_1 \leq 60cm$, $0 < x_2 \leq 30cm$ and $30cm < x_3 \leq 45cm$, that is, $\|\frac{\partial \phi(x)}{\partial x}\| \leq \gamma$

Discretization of the process

The nonlinear model (7.2) is discretized using Euler discretization with sampling time $T_s = 50 \times 10^{-3}[s]$, in order to design discrete-time FD scheme which is useful for the real-time implementation. The following discrete-time model is obtained:

$$\begin{aligned} x_{k+1} &= A_D x_k + B_D u_k + \phi_D(x_k, u_k) + E_{f,D} f \\ y_k &= C_D x_k + F_{w,D} w_k + F_{f,D} f_k \end{aligned} \tag{7.3}$$

where

$$A_D = (I + T_s A) = \begin{bmatrix} 0.9996 & 0 & 0.0004 \\ 0 & 0.9999 & 0.0004 \\ 0.0004 & 0.0004 & 0.9992 \end{bmatrix}; \qquad B_D = T_s B = 10^{-3} \times \begin{bmatrix} 0.3250 & 0 \\ 0 & 0.3250 \\ 0 & 0 \end{bmatrix}$$

$$E_{f,D} = T_s E_f = 10^{-3} \times \begin{bmatrix} 0 & 0 & 0 & 0.3250 & 0 & 50 & 0 & 0 \\ 0 & 0 & 0 & 0 & 0.3250 & 0 & 50 & 0 \\ 0 & 0 & 0 & 0 & 0 & 0 & 0 & 0 \end{bmatrix}$$

$$\phi_D(x) = T_s \phi(x), \gamma_D = Ts \times \gamma = 0.05 \times 0.00267 = 0.00013$$

$$C_D = C, F_{w,D} = F_w, F_{f,D} = F_f$$

Residual generation

For the purpose of the residual generation for the system (7.3), the following FDF with filter gain L and post-filter V is used,

$$\begin{aligned} \hat{x}_{k+1} &= A_D\hat{x}_k + \phi_D(\hat{x}_k) + B_D u_k + L\left(y_k - \hat{y}_k\right) \\ \hat{y}_k &= C_D\hat{x}_k, \qquad r_k = V\left(y_k - \hat{y}_k\right) \end{aligned} \tag{7.4}$$

Defining $x_{0,k} = x_k - \hat{x}_k$, the residual generator for DTS200 is given as

$$\begin{aligned} x_{0,k+1} &= A_0 x_{0,k} + \Psi_0 + E_{0,f} f_k + E_{0,f} w_k \\ r_k &= C_0 x_{0,k} + F_{0,f} f_k + F_0 w_k \end{aligned} \tag{7.5}$$

where $A_0 = (A_D - LC_D)$, $\Psi_0 = \phi_D(x_k) - \phi_D(\hat{x}_k)$, $E_{0,f} = (E_{f,D} - LF_{f,D})$, $E_0 = -LF_{w,D}$, $C_0 = VC$, $F_{0,f} = VF_{f,D}$, and $F_0 = VF_0$. The FDF parameters L and V are so computed that the effect of the disturbances are reduced by a desired attenuation level (α). These parameters are computed using LMIs (5.9) and (5.10) in Theorem 5.1.1 and are given below

$$L = \begin{bmatrix} 1.1740 & 0.3893 \\ 0.3898 & 1.1646 \\ 722.6210 & 713.2594 \end{bmatrix}, V = I_2, \alpha = 3.1576 \tag{7.6}$$

Threshold computation

The common feature of the algorithms for threshold computation proposed in Chapter 6 is the requirement of the knowledge about the disturbances. To this end, the disturbance is assumed to be random and uniformly distributed over the interval $\{-0.001, 0.001\}$. The evaluation window was selected as $N = 20[s]$ in order to study the behavior of the evaluated residual under RMS framework. The peak and $\mathscr{L}_{2,N}$-norm of the disturbances are bounded by $\delta_{w,peak} = 0.001$ and $\delta_{w,2} = 0.0032$. Using the above bounds on the process disturbances, the following thresholds are computed:

- $J_{th,RMS,2}$: The following threshold value for $J_{th,RMS,2}$ is computed by solving the optimization problem proposed in Algorithm 6.2.1 for the given FDF parameters (7.6)

$$\alpha_{RMS} = 3.1576, \qquad J_{th,RMS,2} = \alpha_{RMS}\frac{\delta_{w,2}}{\sqrt{(20)}} = 0.0023$$

- $J_{th,Peak,Peak}$: The following threshold value for $J_{th,Peak,Peak}$ is computed by solving the optimization problem proposed in Algorithm 6.2.2 for the given FDF parameters (7.6)

$$\alpha_{Peak,Peak} = 3.3522, \qquad J_{Peak,Peak} = \alpha_{Peak,Peak}\delta_{w,Peak} = 0.0035$$

- $J_{th,Peak,2}$: The following threshold value for $J_{th,Peak,2}$ is computed by solving the optimization problem proposed in Algorithm 6.2.3 for the given FDF parameters (7.6)

$$\alpha_{1,Peak,2} = 1.000, \qquad \alpha_{2,Peak,2} = 1.5954,$$
$$J_{Peak,2} = \alpha_{1,Peak,2}\delta_{w,peak} + \alpha_{2,Peak,2}\delta_{w,2} = 0.0061$$

7.1.2 Simulation results and discussion

To validate the results, the discrete-time nonlinear model of the three-tank system (7.1) is considered. Using the filter gain L and post filter gain V computed in the above subsection, the following fault detection filter is used for the purpose of implementation

$$\begin{aligned} \hat{x}_{k+1} &= a_D(\hat{x}_k) + B_D u_k + L\left(y_k - C_D\hat{x}_k\right) \\ r_k &= V\left(y_k - C_D\hat{x}_k\right) \end{aligned} \tag{7.7}$$

It is worth noting that the above FDF is the modified form of (7.4). The FDF (7.4) is used only for the design purposes while the later is used for implementation purposes. Note also that the FDF (7.4) can be reduced to FDF (7.7). The discrete-time model of nonlinear three-tank system (3.27) together with fault detection filter (7.7) are implemented in Simulink®. The conceptual depiction of the experimental setup of the process together with FD and controller loop is shown in Figure 7.2. It is evident that the input to the FD system are the controlled inputs u_1, u_2 and the process outputs y_1, y_2 which is a typical layout of open loop FD. The following points are considered in the implementation process

- Setpoints/reference signals in both cases are kept the same and constant. For the present case, these have been chosen as $\nu_1(k) = 30cm$, $\nu_2(k) = 20cm$.
- The FDF parameters and thresholds are computed off-line.
- The Peak and RMS values of the residual signal are obtained on-line.
- The fault decision is made on-line by comparing the evaluated residual signals with the corresponding thresholds.
- Leakages, sensor, and actuator faults are realized with the assumption that one fault occurs at a time so that the detectability of each fault is studied.

The following lines describes the detection of different faults under open loop FD strategy.

Sensor fault detection (SFD): Figure 7.3 to 7.4 show the simulation results, when one of the sensor is faulty. The nature of the fault is a scaling fault and its magnitude is kept the same for all sensors during the whole experiment, that is, 10%. It means that the faulty sensor is measuring 90% of the actual value or in other words the sensor reading is dropped by 10%. Both Peak and RMS values of the residual signal are obtianed and compared with the corresponding thresholds. It can be observed from figures 7.3 to 7.4 that the evaluated residual signal shows significant response to any of the sensor fault. It can also be noted that before appearing the fault in the sensor, the residual signal

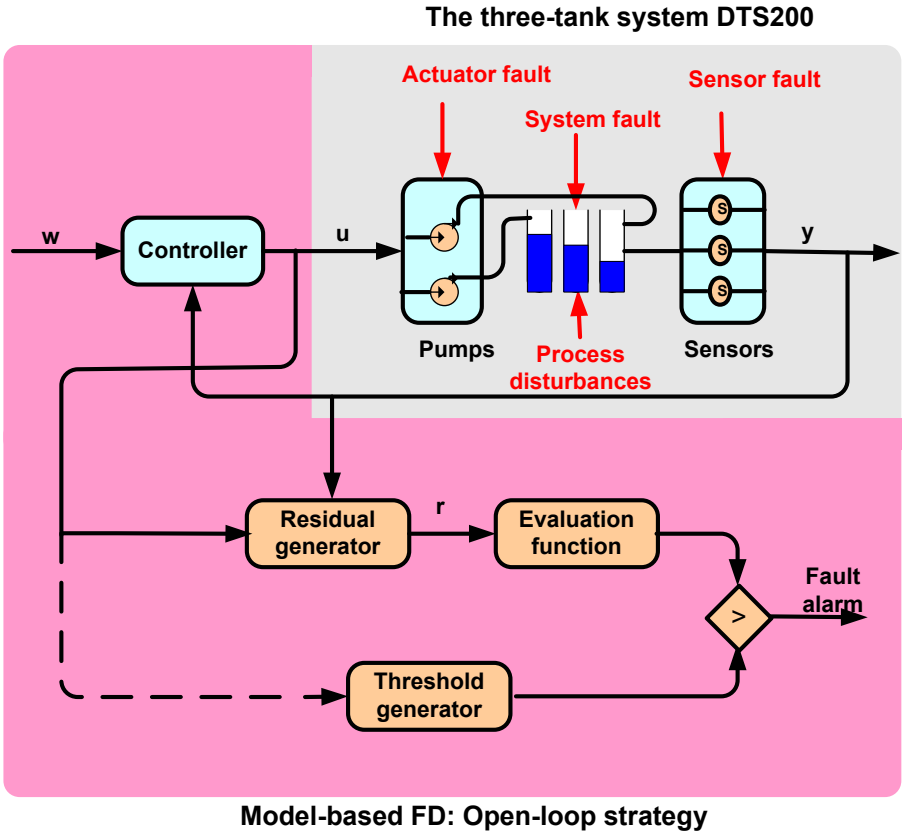

Figure 7.2: Open Loop FD System

is nonzero due to disturbances in the process. However, due of the threshold settings, the residual is below the thresholds and hence there is no chance of false alarms. It is also worth noting that the residual signal is more smooth in RMS framework than evaluating in Peak norm framework. It is due to the computation of RMS values of the residual over observation window N. If the observation window is chosen to be sufficiently large, the smoothness in the residual will further increase. However, due to evaluation for a large time window, the fault detection time becomes large which will reduce the efficiency of FD system in the context of fault detection time. Further, note that in the framework of Peak-norm based residual evaluation, the threshold $J_{th,Peak,2}$ provides more conservativeness as compared to $J_{th,Peak,Peak}$. This is due to the assumption on energy of the disturbances. This conservativess, indeed, precludes the possiblity of false alarms on one hand but increases the chance of missed detection on the other hand. [1]

Actuator fault detection (AFD): Figure 7.5a to 7.6b show the behavior of the evaluated residual signal in the presence of actuator fault. The fault is realized by scaling the original measurement, that is, flow rate in Pump. The size of the fault is 60 % of the actual actuator value and the nature of the fault is abrupt (step - down fault). It means

[1] The explanatory sentence for J_{Peak}, $J_{th,PP}$, $J_{th,P2}$, J_{RMS}, and $J_{th,RMS,2}$, given in the caption of Figure 7.3, serve for all the subsequent figures in this chapter. It is, therefore, dropped in the captions in order to avoid any redundancy.

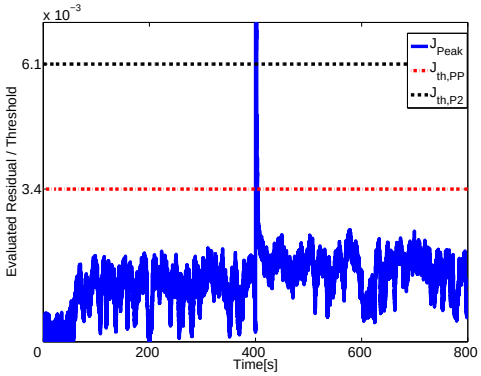

(a) Evaluated residual and thresholds: Peak norm framework. J_{Peak}, $J_{th,pp}$ and $J_{th,p2}$ represent the peak value of the evaluated residual signal, peak-to-peak threshold and peak-to-2 threshold.

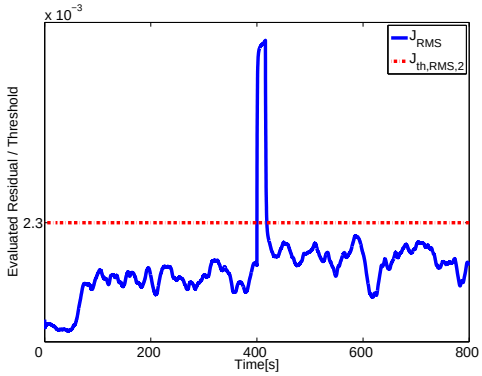

(b) Evaluated residual and threshold: RMS framework. J_{RMS} and $J_{th,RMS,2}$ represent the RMS value of the evaluated residual signal, RMS-to-2 threshold.

Figure 7.3: Detection of fault of magnitude 10% scaling in sensor measuring the level in Tank 1 under open loop FD

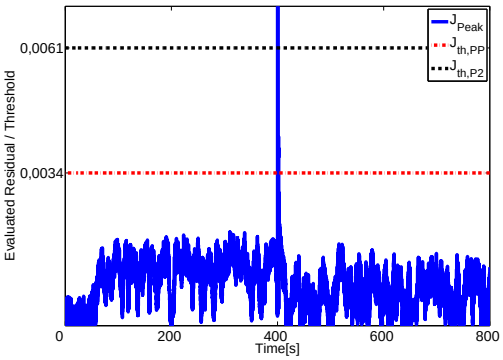

(a) Evaluated residual and thresholds: Peak norm framework

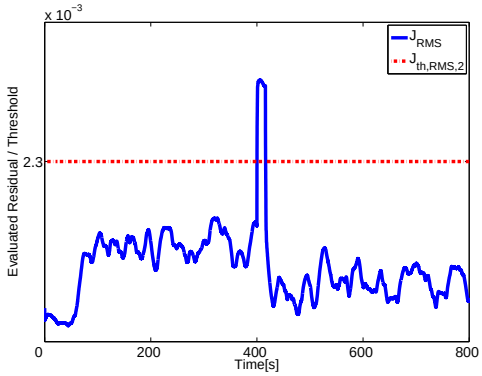

(b) Evaluated residual and threshold: RMS framework

Figure 7.4: Detection of fault of magnitude 10% scaling in sensor measuring the level in Tank 2 under open loop FD

that the flow rate in a paricular pump is reduced by 60 % under faulty conditions. The magnitude is kept the same for both faults in the whole experiment. The results show that the evaluated residual (Peak and RMS) reacts promptly to the fault in any of the pump (actuator fault). In addition, different from sensor faults, the effect of actuator fault on the residual signal endures for the whole operation time. It is also worth noting that the proposed FD scheme and thresholds settings have successfully classified the disturbances and faults in the process. Further, the residual signal is nonzero even before the fault to appear. But the thresholds are so designed that it does not exceed the threshold value in any case, which implies that the chances of false alrms are completely precluded. In addition, note that the generated residual signal quickly responds to the faults which shows the effectiveness of the proposed FD scheme. The efficiency of different thresholds can be seen in these results. For instance, refere to Figure 7.5a, the fault appeared in the actuator 1 (Pump 1) at $t = 400[s]$. The fault alarm is set due to $J_{th,Peak,Peak}$ at approx. $450[s]$. However, due to the high value of $J_{th,Peak,2}$, the faulty residual does not cross this threshold resulting into a missed detection. The setting of $J_{th,Peak,2}$ to a high value is because of the inherent assumption on the energy of the disturbances during its design.

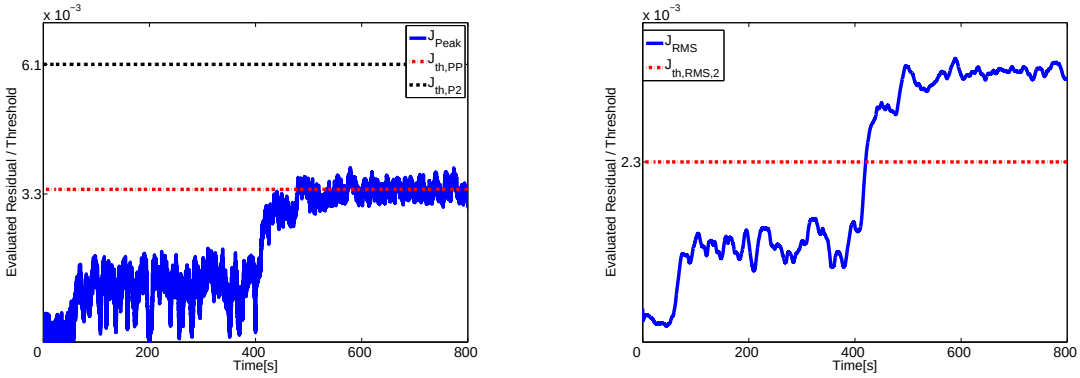

(a) Evaluated residual and thresholds: Peak norm framework

(b) Evaluated residual and threshold: RMS framework

Figure 7.5: Detection of fault of magnitude 60% scaling in Pump 1 under open loop FD

Leakages detection (LD) in different Tanks: Leakages are realized by opening the valve situated at the bottom of the each tank. These valves are labeled as "Outflow valves" in Figure 7.1. It is worth noting that leakages from tanks may be of different nature, for instance, slowly developing, and constant etc. In this study, constant leakage is assumed. It is obtained by opening the outflow valves one at a time and kept it unaltered during the whole simulation. The efficiency of the proposed algorithms for open loop FD under the evaluation of peak and RMS values of the residual signal is observed. It is evident from Figures 7.7-7.8 that all the leaks are successfully detected by the designed FD system.

7.2 Inverted pendulum control system

Inverted pendulum model is a classical laboratory system that is widely used as a benchmark problem for implementing control and observer algorithms. It is highly nonlinear and

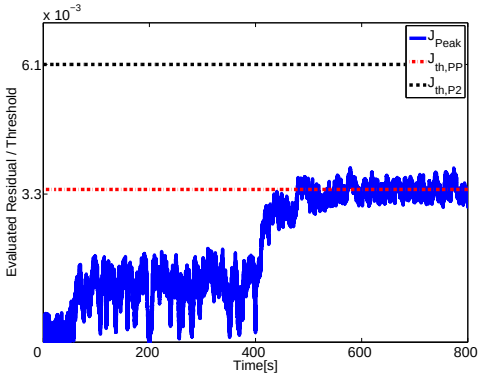

(a) Evaluated residual and thresholds: Peak norm framework

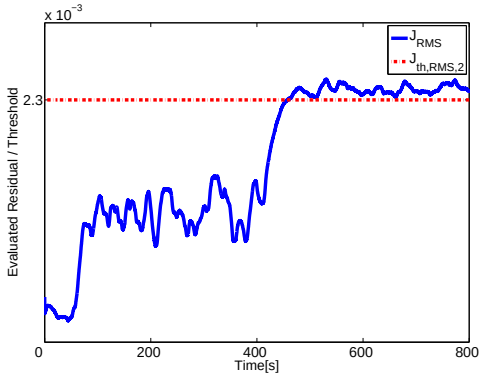

(b) Evaluated residual and threshold: RMS framework

Figure 7.6: Detection of fault of magnitude 80% scaling in Pump 2 under open loop FD

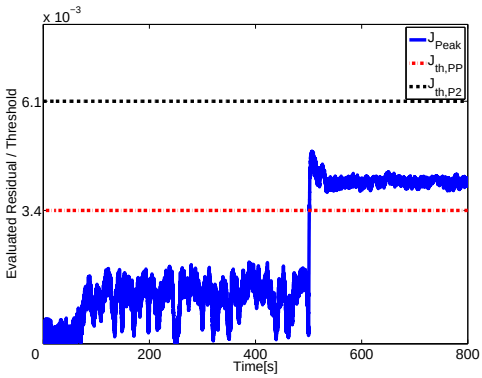

(a) Evaluated residual and thresholds: Peak norm framework

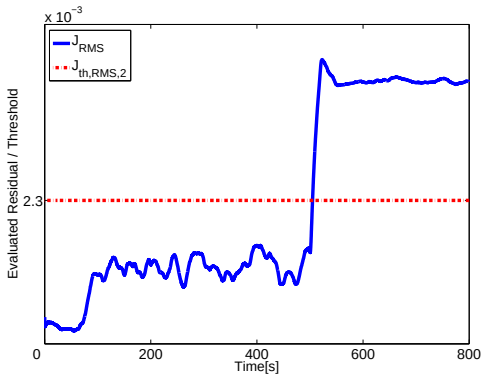

(b) Evaluated residual and threshold: RMS framework

Figure 7.7: Detection of leakage of amount $28cm^3/s$ in Tank 1 under open loop FD.

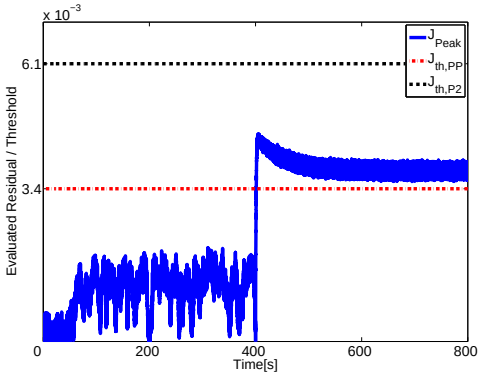

(a) Evaluated residual and thresholds: Peak norm framework

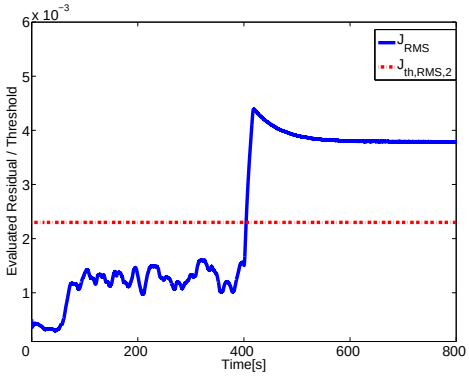

(b) Evaluated residual and thresholds: RMS framework

Figure 7.8: Detection of leakage of amount $19.68cm^3/s$ in Tank 2 under open loop FD.

unstable in open-loop. Besides the nonlinear dynamics, other nonlinearities, that is, static friction and dry friction (Coulomb friction) are also present in the system. These features make it more complex and challenging to work with. Since it is open-loop unstable, it is always desired to make it stable using some control strategy. Due to these reasons, it is an excellent example to study the closed-loop fault detection techniques. The inverted pendulum is related to rocket or missile guidance, where thrust is actuated at the bottom of a tall vehicle.

Figure 7.9 shows the inverted pendulum experimental setup (LIP100). It consists of a cart that moves along a metal guiding bar. An aluminum rod with a cylindrical weight (also called pendulum) is connected to the cart at a pivoting point. The pendulum can rotate freely around its pivot point. The cart is connected to a drive wheel through a transmission belt. The wheel is driven by a current controlled DC motor which produces a torque proportional to the acting voltage such that the cart is accelerated.

Three sensors are mounted on the system to measure different states of the LIP100; for instance, the angular position of the pendulum is measured by a layer potentiometer which is fixed at the pivoting point, the linear position of the cart is measured by a circular-coil potentiometer that is fixed at the driving shaft of the motor, and the velocity of the cart is by a tachogenerator which is fixed to the motor.

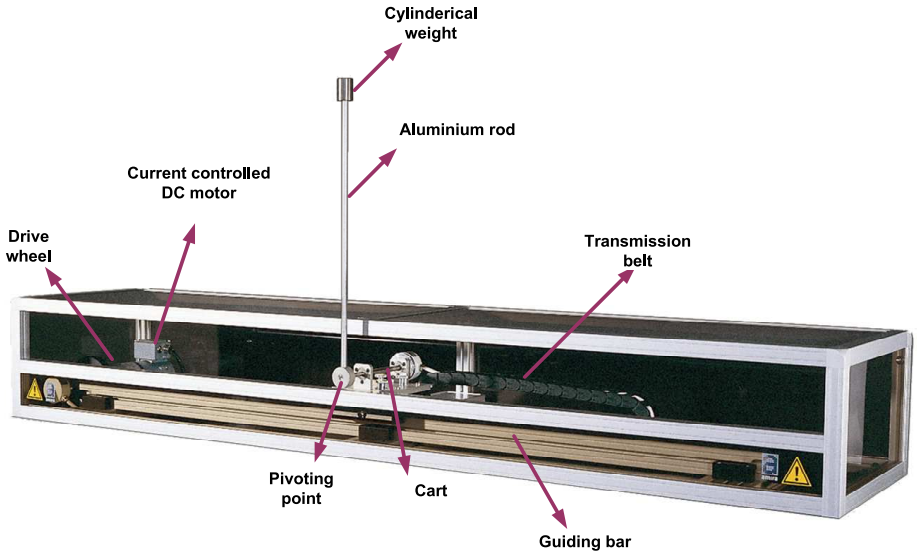

Figure 7.9: The inverted pendulum: LIP100

7.2.1 Nonlinear model

In order to describe the dynamic behavior of the inverted pendulum, the following nonlinear model is adopted [1]:

$$\begin{aligned}
\dot{x_1} &= x_3 \\
\dot{x_2} &= x_4 \\
\dot{x_3} &= \beta(x_2)\left(a_{32}\sin x_2\cos x_2 + a_{33}x_3 + a_{34}x_4\cos x_2 + a_{35}x_4^2\sin x_2 + b_3u\right) \\
\dot{x_4} &= \beta(x_2)\left(a_{42}\sin x_2 + a_{43}x_3\cos x_2 + a_{44}x_4x_4 + a_{45}x_4^2\cos x_2\sin x_2 + b_4u\cos x_2\right)
\end{aligned} \tag{7.8}$$

The more compact representation of the above model is given as follows

$$\dot{x} = a(x) + B(x)u, \quad y = c(x) \tag{7.9}$$

with

$$a(x) = \begin{bmatrix} x_3 \\ x_4 \\ \beta(x_2)\left(a_{32}\sin x_2\cos x_2 + a_{33}x_3 + a_{34}x_4\cos x_2 + a_{35}x_4^2\sin x_2\right) \\ \beta(x_2)\left(a_{42}\sin x_2 + a_{43}x_3\cos x_2 + a_{44}x_4 - a_{45}x_4^2\cos x_2\sin x_2\right) \end{bmatrix}$$

$$B(x) = \beta(x_2)\begin{bmatrix} 0 \\ 0 \\ b_3 \\ b_4\cos x_2 \end{bmatrix}, \quad c(x) = \begin{bmatrix} x_1 \\ x_2 \\ x_3 \end{bmatrix}$$

where

$$\begin{aligned}
\beta(x_2) &= \frac{1}{MJ - N^2\cos^2 x_2} = \left(1 + \frac{N^2}{N_{01}^2}\sin x_2\right)^{-1}, \quad N = m_2l_c, \quad N_{01}^2 = MJ - N^2; \\
a_{32} &= -\frac{N^2}{N_{01}^2}g, \quad a_{33} = -\frac{J}{N_{01}^2}K_r, \quad a_{34} = \frac{NC}{N_{01}^2}, \quad a_{35} = \frac{NJ}{N_{01}^2}g, \quad b_3 = \frac{J}{N_{01}^2}, \\
a_{42} &= \frac{MN}{N_{01}^2}g, \quad a_{43} = \frac{K_rN}{N_{01}^2}, \quad a_{44} = -\frac{MC}{N_{01}^2}, \quad a_{45} = -\frac{N^2}{N_{01}^2}, \quad b_4 = -\frac{N}{N_{01}^2}
\end{aligned}$$

where N, M, N_{01}, J, m_2, l_c, K_r, C are the system parameters and their numerical values are given in Table C.2.

Lipschitz equivalent model

The Lipschitz equivalent model for the nonlinear inverted pendulum (7.9) is obtained as follows

$$\Sigma : \begin{cases} \dot{x} &= \mathscr{A}x + \mathscr{B}u + \left[a(x) + B(x)u - \mathscr{A}x - \mathscr{B}u\right] \\ &= \mathscr{A}x + \mathscr{B}u + \phi(x,u) \\ y &= \mathscr{C}x \end{cases} \tag{7.10}$$

where the coefficient matrices $\mathscr{A}$, $\mathscr{B}$, and $\mathscr{C}$ are obtained from the linearization of the process (7.9) around the operating point $x^* = (0.2, 0, 0, 0), u^* = 0$. These matrices are given as follows

$$\mathscr{A} = \begin{bmatrix} 0 & 0 & 1 & 0 \\ 0 & 0 & 0 & 1 \\ 0 & -0.8809 & -1.9148 & 0.0056 \\ 0 & 21.4745 & 3.8498 & -0.1362 \end{bmatrix}, \quad \mathscr{B} = \begin{bmatrix} 0 \\ 0 \\ 0.3088 \\ 0.6209 \end{bmatrix},$$
$$\mathscr{C} = \begin{bmatrix} 1 & 0 & 0 & 0 \\ 0 & 1 & 0 & 0 \\ 0 & 0 & 1 & 0 \end{bmatrix}$$

It is worth noting that the process model (7.10) is exact replica of the nonlinear model (7.9). Now considering the disturbances and faults in the system, the dynamics can then be written as

$$\Sigma_{\mathscr{P}} : \begin{cases} \dot{x} &= \mathscr{A}x + \mathscr{B}u + \phi(x,u) + \mathscr{E}_w w + \mathscr{E}_f f \\ y &= \mathscr{C}x + \mathscr{F}_w w + \mathscr{F}_f f \end{cases} \tag{7.11}$$

Note that the inverted pendulum is equipped with three sensors and one actuator and these signals are measured in terms of electrical voltages. In order to make the interpretation easy, the nonlinear model (7.11) is normalized using the following transformation,

$$x_n = Nx, \qquad u = K_f u_s, \qquad N = diag(n_{11}, n_{22}, n_{33}, n_{44}) \tag{7.12}$$

Therefore

$$\begin{aligned} \dot{x}_n &= N\mathscr{A}N^{-1}x_n + N\mathscr{B}K_f u_s + N\phi(N^{-1}x_n, K_f u_s) \\ &= A_n x_n + B_n u_s + \phi_n(x_n, u_s) \end{aligned} \tag{7.13}$$

The normalized plant model can thus be expressed as follows

$$\dot{x}_n = A_n x_n + B_n u_s + \phi_n(x_n, u_s) + E_{n,w} w + E_{n,f} f \tag{7.14}$$
$$y_n = C x_n + F_w w + F_f f \tag{7.15}$$

with coefficient matrices are

$$A_n = \begin{bmatrix} 0 & 0 & -1.95 & 0 \\ 0 & 0 & 0 & 1.0 \\ 0 & -0.12864 & -1.9148 & -0.0082 \\ 0 & 21.4745 & 26.31 & -0.1362 \end{bmatrix}, \quad B_n = \begin{bmatrix} 0 \\ 0 \\ -6.1343 \\ 84.303 \end{bmatrix}, \quad \phi_n = \begin{bmatrix} \phi_{1,n} \\ \phi_{2,n} \\ \phi_{3,n} \\ \phi_{4,n} \end{bmatrix}$$

$$\phi_{1,n} = \phi_{2,n} = 0,$$
$$\begin{aligned} \phi_{3,n} = {} & n_{33}\beta(x_{2,n}) \left[a_{32} \sin x_{2,n} \cos x_{2,n} + a_{33} x_{3,n} + a_{34} x_{4,n} \cos x_{2,n} + a_{35} x_{4,n}^2 \sin x_{2,n} + b_3 K_f u_s \right] \\ & + 0.12864 x_{2,n} + 1.9148 x_{3,n} + 0.0082 x_{4,n} + 6.1343 u_s, \end{aligned}$$
$$\begin{aligned} \phi_{4,n} = {} & n_{44}\beta(x_{2,n}) \left[a_{42} \sin x_{2,n} + a_{43} x_{3,n} \cos x_{2,n} + a_{44} x_{4,n} x_4 + a_{45} x_{4,n}^2 \cos x_{2,n} \sin x_{2,n} \right. \\ & \left. + b_4 K_f u_s \cos x_{2,n} \right] - 21.4745 x_{2,n} - 26.31 x_{3,n} + 0.1362 x_{4,n} - 84.303 u_s, \end{aligned}$$
$$E_{n,w} = B_n, \quad F_w = [0.1\ 0.1\ 0.1]^T, \quad E_{n,f} = [B_n \quad 0_3], \quad F_f = [0_{3\times 1} \quad I_3]$$

Note that the nonlinear function ϕ is considered as Lipschitz for the operating range $|u_s| \leq 10V, |r| \leq 0.5, |\theta| \leq 40^\circ$ with the Lipschitz constant 0.1974. Therefore, the nonlinear model of the inverted pendulum given in (7.14) is regarded as a locally Lipschitz nonlinear system. Further, note that for the coefficient matrices A_n, B_n, and C_n; the pair (A_n, B_n) is controllable and (A_n, C_n) is observable which means that a state feedback controller and an observer based residual generator can be designed.

Controller design

It is evident from the open loop linear model of the inverted pendulum that it has one unstable pole that makes the the equilibrium point $(0.2, 0, 0, 0)$ unstable. For the purpose of FD, it is needed that the system should be stable. To this end, a control law of the form $u = -K_1(x) + K_2\nu$ is proposed which not only ensures the stability but also tracking the reference input ν. The gain matrix K_1 consists of the parameters of the state feedback controller and K_2 is pre-filter gain. The closed loop model can thus be given as

$$\begin{aligned} \dot{x} &= Ax + B\nu + \phi(x, \nu) + E_w w + E_f f \\ y &= Cx + F_w w + F_f f \end{aligned} \tag{7.16}$$

where $A = (A_n - B_n K_1)$, $B = B_n K_2$, $\phi(x, \nu) = \phi_n(x, -K_1(x) + K_2\nu)$, $E_w = E_{n,w}$ and $E_f = E_{n,f}$. The following controller parameters are computed using the methods proposed in [175, 176]:

$$K_1 = \begin{bmatrix} -1.6228 & 1.9357 & 3.2231 & 0.4207 \end{bmatrix} \qquad K_2 = -1.6228; \tag{7.17}$$

Residual generation

For the purpose of residual generation for the closed loop model of LIP100 (7.16), the following FDF with the filter gain L and post filter V is used:

$$\begin{aligned} \dot{\hat{x}} &= A\hat{x} + B\nu + \phi(\hat{x}, \nu) + L(y - \hat{y}) \\ \hat{y} &= C\hat{x}, \qquad r = V(y - \hat{y}) \end{aligned} \tag{7.18}$$

Defining the observation error $x_0 = x - \hat{x}$, the residual generator is given as follows

$$\dot{x}_0 = A_0 x_0 + E_0 w_0 + \Psi_0 + E_{0,f} f \tag{7.19}$$

$$r = C_0 x_0 + F_0 w_0 + F_{0,f} f_0 \tag{7.20}$$

where A_0, E_0, $E_{0,f}$, C_0, F_0, $F_{0,f}$, Ψ_0, and x_0 are defined in a similar fashion as in (5.37). Using LMI (5.42) in Chapter 5, the following parameters for the residual generator are computed which renders the attenuation level of the residual signal below certain level α; that is, $\|r\|_2 \leq \alpha \|w_0\|_2$

$$L = \begin{bmatrix} 23.2299 & 0.0584 & -1.9940 \\ -0.5703 & 22.2502 & -4.1160 \\ -11.6129 & 7.2646 & 31.2699 \\ 144.1065 & -121.6486 & -198.0070 \end{bmatrix}, \qquad V = I_3, \qquad \alpha = 0.6939 \tag{7.21}$$

Threshold computation

For the computation of different kinds of thresholds, the residual generator (7.19) with FDF parameters computed is considered. The following thresholds are computed:

- $J_{th,RMS,2}$: Using Algorithm 6.3.1 and the FDF parameters (7.21), the following threshold value for $J_{th,RMS,2}$ is obtained

$$\alpha_{RMS} = 0.6939, \qquad J_{th,RMS,2} = 0.0717$$

- $J_{th,Peak,Peak}$: Using Algorithm 6.3.2 and the FDF parameters (7.21), the following threshold value for $J_{th,Peak,Peak}$ is obtained

$$\alpha_{Peak} = 1.0683, \qquad J_{th,Peak,Peak} = 0.1068$$

- $J_{th,Peak,2}$: Using Algorithm 6.3.3 and the FDF parameters (7.21), the following threshold value for $J_{th,Peak,2}$ is obtained

$$\alpha_{1,p2} = 0.9013; \qquad \alpha_{2,p2} = 0.1732; \qquad J_{th,Peak,2} = 0.1467$$

7.2.2 Simulation results and discussion

In this subsection, the usefulness of the algorithms proposed for continuous-time nonlinear systems are illustrated. The simulations are performed for closed loop model of LIP100 as shown in Figure 7.10. In a typical closed-loop FD, the FD block takes the information of the reference signals and outputs of the process. Figure 7.10 illustrates this strategy for LIP100.

The following points are considered for the simulation of the proposed FD techniques.

- The length of the evaluation window is $N = 10[s]$
- The disturbance is assumed to be a random number distributed uniformly over the interval $[-0.1, 0.1]$.
- The $\mathscr{L}_{2,N}$ and Peak norm of the disturbance are bounded by

$$\delta_{w,2} = 0.3268; \qquad \delta_{w,\infty} = 0.1000;$$

- The reference signal is kept constant at $\nu = 0.1$
- All the faults are modeled as step signal and are realized by introducing offsets in the respective readings
  - the offset in actuator is introduced at $t = 250[s]$ with magnitude equal to $5V$
  - offset in the position sensor of the cart occurs at $t = 250[s]$ with magnitude equal to $0.35m$
  - offset in the angular position sensor of the pendulum occurs at $t = 250[s]$ with magnitude equal to $0.60rad = 34.3775°$

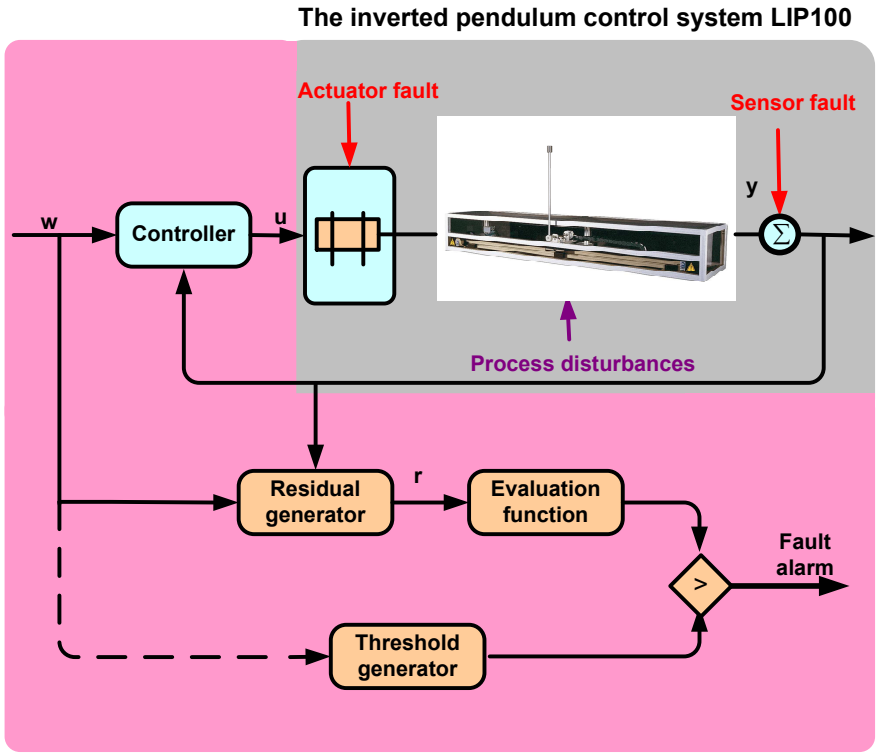

Figure 7.10: Closed loop FD for LIP100

– offset in the velocity sensor of the cart occurs at $t = 250[s]$ with magnitude equal to $0.35m/s$

- The controller parameters and pre-filter gain are computed off-line.
- The parameters for robust FDF and the values for different thresholds are computed off-line.
- The fault decision is made on-line by comparing the evaluated residual signal (RMS or Peak value) with the respective thresholds ($J_{th,RMS,2}$ in case of RMS value evaluation, and $J_{th,Peak,Peak}$ and $J_{th,Peak,2}$ in case of evaluation based on peak-norm)

Actuator fault detection (AFD)

Figure 7.11a and 7.11b show the dynamic behavior of the peak and RMS value of the evaluated residual signal in the presence of actuator fault. The fault is realized by introducing an offset of $5V$ in the actuator signal. The threshold settings ensured successful elimination of false alarms and detection of faults.

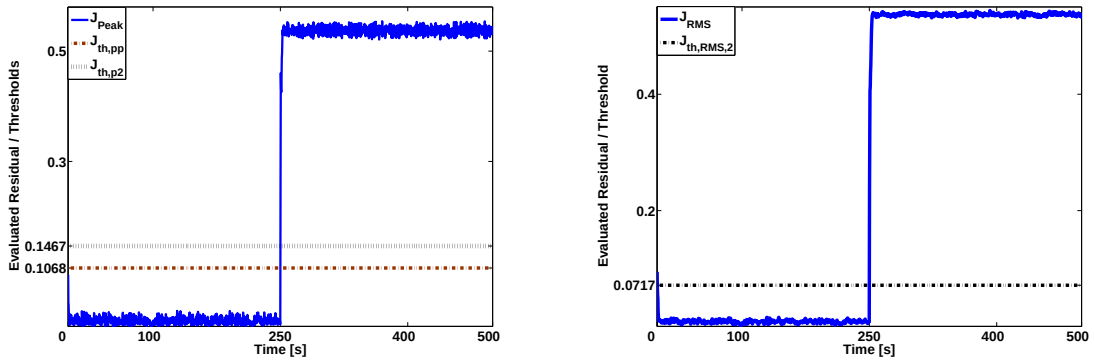

(a) Evaluated residual and thresholds: Peak norm framework

(b) Evaluated residual and threshold: RMS framework

Figure 7.11: Detection of offset of magnitude 5 V in actuator

Sensor fault detection (SFD)

Figure 7.12a and 7.12b show the behavior of the evaluated residual signal to the occurrence of fault in the sensor measuring the position of the cart. An offset of $0.35m$ is introduced in the sensor. Notice that the residual shows an impulsive response to this fault at the time of its occurrence and then attain the original position. It is due to the tracking controller. Since the position of the cart is tracked in LIP100, any change in this sensor is compensated. Figure 7.13a and 7.13b show the response of the residual signal to the fault in the sensor measuring the angular position of the pendulum. A relatively large offset is introduced in order to observe the stability of the controller and fault detection filter. The offset amounts $0.60rad \approx 34.5°$ which means $31.36V$. Following the similar arguments, any offset in this sensor affects the position of the cart which then activates the controller to react. Due to this reason the residual tries to recover its dynamic behavior after the occurrence of the fault. The behavior of the residual under fault in velocity sensor is shown in Figure 7.14a and 7.14b. An offset of $0.35rad/s$ is introduced. The proper threshold setting eliminated any possibility of false alarms together with successful detection of faults.

7.3 Summary

In this chapter, the use of proposed algorithms of this thesis have been demonstrated with the help of two benchmark problems, that is, three-tank system and the inverted pendulum control system. A robust residual generator was designed which rendered the disturbance attenuation level below a prescribed level. In addition, three different kinds of thresholds were designed for both applications. For three-tank systems, the FD scheme was designed using the algorithms proposed for discrete-time nonlinear systems. The complete FD system together with the process was implemented in MATLAB/SIMULINK® in order to illustrate the open loop FD strategy. The efficiency of the proposed FD scheme was shown by the detection of leakages, sensors, and actuators faults. For inverted pendulum

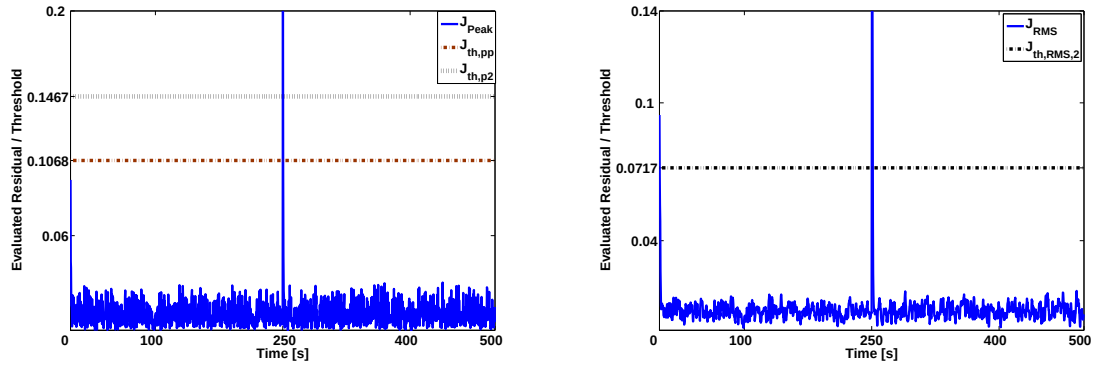

(a) Evaluated residual and thresholds: Peak norm framework

(b) Evaluated residual and threshold: RMS framework

Figure 7.12: Detection of offset of magnitude $0.35m$ in sensor measuring the linear position of the cart

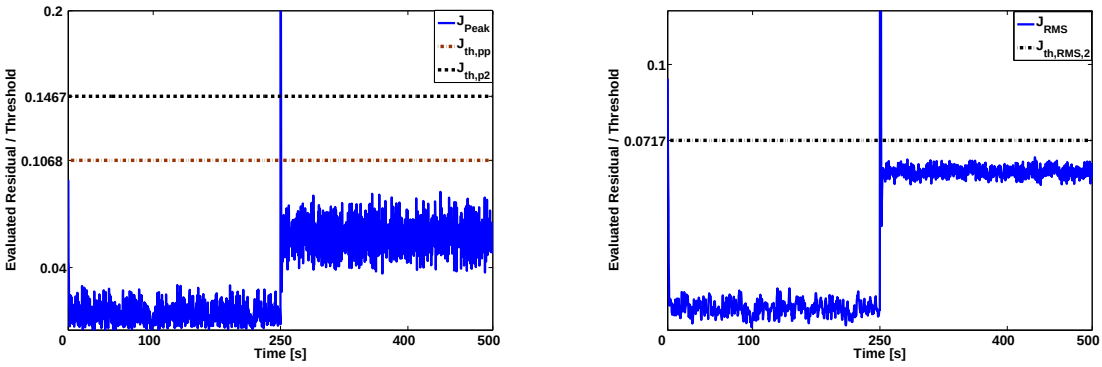

(a) Evaluated residual and thresholds: Peak norm framework

(b) Evaluated residual and threshold: RMS framework

Figure 7.13: Detection of offset of magnitude 0.6rad in sensor measuring the angular position of the pendulum

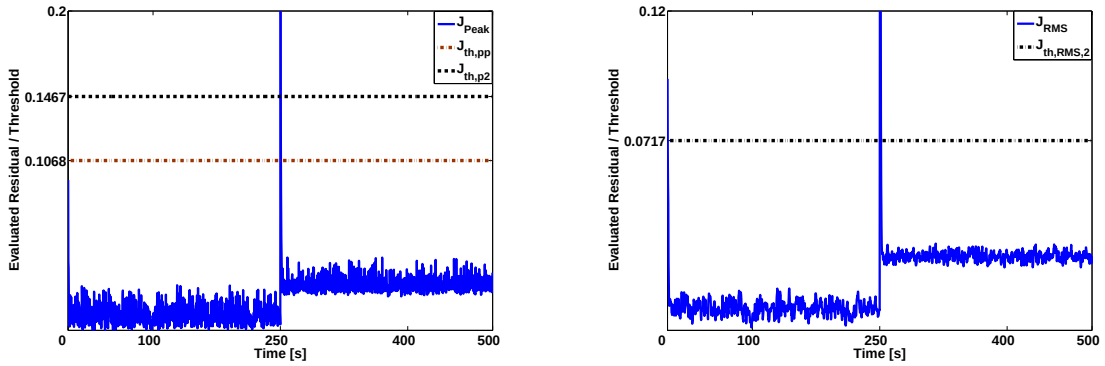

(a) Evaluated residual and thresholds: Peak norm framework

(b) Evaluated residual and threshold: RMS framework

Figure 7.14: Detection of an offset of magnitude 0.35m/[s] in sensor measuring the velocity of the cart

control system, the FD system was designed using the algorithms proposed for continuous-time nonlinear system. The nonlinear process and the associated FD system was realized in MATLAB/SIMULINK®. Since the inverted pendulum is unstable in open loop, the closed loop FD strategy was implemented. Sensors and actuator faults were shown to have been successfully detected by the proposed FD system.

Chapter 8

Conclusions and recommendations

This chapter summarizes the results obtained in this dissertation, and presents some concluding remarks based on these results. It also highlights some future directions for further developments of the proposed approaches.

8.1 Conclusions

In practice most of the fault diagnosis problems, we face, are nonlinear and uncertain. This uncertainty is due to process disturbances, parameter variations, and measurement noises. In this thesis, observer-based fault detection in nonlinear systems in the presence of model uncertainties, process disturbances, and measurement noises has been investigated. The main concern of this thesis is the development of observer-based fault detection methods and proposing algorithms for nonlinear uncertain systems which are computationally tractable and user oriented.

The prime objectives of this thesis was precisely defined in Chapter 1. The first one was designing an optimal residual generator which simultaneously produces robustness against unknown inputs and sensitivity to faults. In order to achieve this objective, a game-theoretic approach together with dissipation inequality was employed to propose three different fault detection filters (FDFs) for input-affine nonlinear systems. These FDFs were designed using $\mathscr{H}_-$–, $\mathscr{H}_\infty$–, and the mixed $\mathscr{H}_-/\mathscr{H}_\infty$– optimization. These optimization indices has been widely utilized to analyze the FD problems for LTI systems in frequency domain, however, it is very difficult to use them to study the FD of nonlinear systems in frequency domain. In order to facilitate the analysis, the time domain definition of $\mathscr{H}_-$– index was proposed. Similarly, the definition of $\mathscr{H}_\infty$–norm is adopted from the well-established robust control theory. The problem of optimal residual generation has been studied in both the finite-horizon and the infinite-horizon. It was shown that the generalized results obtained can also be used to study the problem of fault detection for linear discrete-time systems. As mentioned in Chapter 3, any nonlinear system depending on the type of nonlinearity can be considered as Lipschitz, locally or globally. Owing to the salient features of LMIs and wide use of Lipschitz nonlinear systems, the problem of optimal residual generation, that is, mixed $\mathscr{H}_-/\mathscr{H}_\infty$–FDF for Lipschitz nonlinear systems was formulated as convex optimization problem and sufficient conditions was presented in the form of LMIs for both continuous-time and discrete-time Lipschitz nonlinear systems. Design examples were provided to illustrate the proposed methodologies. From the discussion presented in these chapters, the following conclusions can be drawn:

1. It is not possible to study the $\mathscr{H}_\infty$–norm and $\mathscr{H}_-$– index for nonlinear systems in frequency domain. Consequently, these indices were defined in time domain to facilitate the analysis for nonlinear systems.

2. It is often misled that similar to $\mathscr{H}_\infty$– nonlinear filtering, the $\mathscr{H}_\infty$–FDF for nonlinear systems has also been extensively studied, but it is not the case in reality. The problem of $\mathscr{H}_\infty$–FDF for nonlinear systems, in discrete-time settings in particular, has not been studied. However for continuous-time setting, a few studies can be found in literature.

3. Similarly, the problem of designing $\mathscr{H}_-$–FDF has not been studied for nonlinear systems.

4. $\mathscr{H}_-$–FDF enhances the sensitivity to faults to certain desired level, but it does not give any indication of the robustness against the unknown inputs. It is possible that this filter may also increase the sensitivity of the residual signal against unknown inputs.

5. A similar argument can be established for $\mathscr{H}_\infty$–FDF; where providing robustness against unknown inputs may result in reducing the effects of faults on the residual signal.

6. $\mathscr{H}_-/\mathscr{H}_\infty$–FDF is a mixed problem which simultaneously makes the residual sensitive to faults and robust against unknown inputs. It may possible that the sensitivity level of the residual to faults in case of $\mathscr{H}_-/\mathscr{H}_\infty$–FDF is less than the residual generated by $\mathscr{H}_-$–FDF. Similarly, the residual generated by $\mathscr{H}_-/\mathscr{H}_\infty$–FDF may have less robustness against unknown inputs than the one generated with $\mathscr{H}_\infty$–FDF. However, in the mixed $\mathscr{H}_-/\mathscr{H}_\infty$–FDF problem, the objective is always to maximize the ratio of fault sensitivity to disturbance attenuation.

After residual generation, the next task for a successful fault detection is residual evaluation, thereby the presence of fault can be inferred. In residual evaluation, some function of the residual signal (evaluation function) is compared with a threshold, and if the former exceeds the latter, an alarm is released indicating the presence of a fault in the system. The role of a threshold is, therefore, indispensable in successful detection of faults. If the threshold is selected too high, a set of faults might be unable to cause the evaluated residual signal to exceed the threshold, and causes a missed detection. Conversely, if selected too low, some of the unknown inputs may cause the evaluated residual to cross the threshold, and result into a false alarm. Consequently, the proper selection of threshold is always demanded, and therefore designing a suitable framework for the computation of a threshold was the second objective of this dissertation. In order to achieve this goal, various threshold settings have been proposed in this thesis. For constant thresholds, different kinds of thresholds based on signal norms, that is, Peak and RMS, were proposed. These thresholds included, $J_{th,RMS,2}$, $J_{th,Peak,Peak}$, and $J_{th,Peak,2}$. Since these thresholds were computed using Peak and RMS values of the unknown inputs, the degree of conservativeness is also varied from one threshold to another. To avoid this conservativeness, a variable threshold, which varies with the instantaneous values of the control inputs in

the presence of model uncertainties, can be designed. The design of a variable threshold was also focused in this dissertation. Two kind of variable thresholds; that is, adaptive threshold and dynamic threshold ware proposed. The framework proposed for adaptive threshold was similar to the one suggested for constant threshold. The gain from the unknown inputs to the residual was computed in the similar way. Then, the instantaneous values of the energies of u were used instead of its bound in order to compute this threshold. The dynamic threshold, as the name indicates, is a dynamic system which gives the upper bound on the modulus of the residual signal. The crux of the design was that an inequality on the upper bound on the solution of the Lipschitz nonlinear systems in the presence of model uncertainties and exogenous disturbances, was derived. Design examples were provided to show the usefulness of the proposed methodology. The following conclusions can be drawn from the discussion carried out therein:

7. Threshold $J_{th,Peak,2}$ is set higher than $J_{th,Peak,Peak}$ due to the assumption on the energy of the unknown inputs. As a result, it is more conservative. Though false alarms can be completely eliminated, the possibility of missed detection will also increase.

8. $J_{th,Peak,Peak}$ is computed on the peak norm of the unknown inputs. It is used to activate $J_{th,Peak,2}$ which means that it is less conservative. Apparently, this threshold might be a good choice due to low conservativeness but it may also sometimes release false alarms.

9. $J_{th,RMS,2}$ is designed based on the RMS values for a particular time window (observation window) N or T. Evaluating the residual in the framework of RMS values results into increased smoothness, thereby reducing the possibility of false alarms. The size of the observation window plays an important role in determination of this threshold.

10. In order to improve the performance of FD system, a variable threshold may be introduced instead of constant threshold. The variable threshold should vary as close to the residual signal as possible.

11. The adaptive threshold is proposed which is sensitive to the instantaneous energies of the control input u and hence varies more closely with the control input. This scheme is less conservative to the corresponding constant thresholds. Furthermore, it requires less on-line computation and can be easily implemented.

12. The dynamic threshold generator proposed in this thesis is different from the adaptive threshold which is designed using norm-based approach. In the later approach, the adaptive threshold is generated using some norm of the instantaneous values of the control input times the gain of the residual to the unknown inputs computed in case of respective constant thresholds. The dynamic threshold generator designed in this work is a dynamic system which takes the modulus of the instantaneous values of the control input in the presence of a bound on the modulus of the unknown inputs and model uncertainty and generates an upper bound on the modulus of the residual signal. This upper bound acts as dynamic threshold. Since the upper bound on the

residual is generated by a dynamic system, it is referred to as a dynamic threshold. This scheme also eliminates the chances of false alarms and ensures fault detection.

8.2 Future directions

The preceding section summarized the results obtained in this dissertation. The proposed techniques and their application to improve fault detection of nonlinear systems were briefly described. Based on the analysis presented therein, some conclusions were also drawn. From the goal point of view, this dissertation provides with the methods, tools, and algorithms, which are user friendly, computationally tractable, and best suited to study a wide class of nonlinear systems. However, besides these esteemed features, there is a room for further improvements. In the following, some possible research directions for further extension of this work are outlined.

- Chapter 4 proposed three kinds of fault detection filters for optimal residual generation in the framework of dissipation inequality and two-player zero-sum differential game theory. As mentioned in Remark 4.2.1, the filter gain, obtained using the proposed methodology, depends on the systems states. Since the system states are, in general, not available, it makes the filter impractical. One solution was suggested in Remark 4.2.2 to search for a suboptimal solution instead of optimal one. Another possibility of getting a filter gain independent of the system states is to modify the structure of the filter. The filter structure recently proposed in [109], seems a suitable candidate for studying this problem and can be a very good extension of the work proposed in this dissertation.

- Notice that in Chapter 4, the control input u was considered as unknown input and included with the disturbances; that is, $w_0 = \begin{bmatrix} u \\ w \end{bmatrix}$. Using this convention, the problem of attenuating the unknown inputs, that is, $\frac{\|r_{0,w_0}\|_2}{\|w_0\|} \leq \alpha$ is achieved. This strategy results into a conservative solution. Since the control input is on-line available, it could be utilized to reduce the conservativeness of the design.

  An associated problem is the stability analysis. It is well known that the residual generator should be stable and the residual should approach to zero as the time tends to infinity, in the presence of all admissible control inputs, provided the disturbances and faults are set equal to zero. In the proposed framework, as mentioned in the proof of Lemma 4.2.2, the $\mathscr{L}_2$ stability of the residual generator has been studied. In this framework, the stability of $x_0 = 0$ can be achieved when w_0 is put equal to zero which means that the control input u is also equal to zero. This is, however, not a realistic strategy, especially for the filter error dynamics. A possible future direction is to study the optimal residual generation problem and to show the convergence of the estimates to the true states in the presence of admissible control input u.

- Chapter 5 solves the optimal residual generation problem for Lipschitz nonlinear systems using linear matrix inequalities (LMIs) tools. As proposed in Remark 5.1.1, the proposed LMIs can be solved by putting $P = Q$. This approach has eased the

problem of solving the LMIs and computing the filter gain L and post filter gain V. However, this assumption leads to an over conservative design and may also sometimes make the proposed problem infeasible. A possible extension of this work is to use iterative LMI approach similar to the one mentioned in [66] for LTI systems.

- Chapter 6 proposed tools for the computation of different thresholds. The inherent philosophy in the design of these methods is the elimination of false alarms. However, the fault detection capability has not been addressed in the design. Though, it was considered while evaluating the performance of different thresholds with the help of simulation examples presented therein and benchmark problems presented in Chapter 7. A possible future extension of this work is to use a threshold which should not only be designed with the objective of eliminating false alarms but also aiming to ensure quick detectability of faults. To this end, the approach adopted in [72] for LTI system can be extended to nonlinear systems.

Appendix A

Important mathematical tools

A.1 Implicit function theorem

Theorem A.1.1. *[98] Assume that $f : \Re^n \times \Re^m \to \Re^n$ is a continuously differentiable function at each point (x, y) of an open set $S \subset \Re^n \times \Re^m$. Let (x_0, y_0) be a point in S for which $f(x_0, y_0) = 0$ and for which the Jacobian matrix $[\partial f/\partial x](x_0, y_0)$ is nonsingular. Then there exist neighborhoods $U \subset \Re^n$ of x_0 and $V \subset \Re^m$ of y_0 such that for each $y \in V$ the equation $f(x, y) = 0$ has a unique solution $x \in U$. Moreover, this solution can be given as $x = g(y)$, where g is continuously differentiable at $y = y_0$.*

A.2 Two-player, zero-sum differential game

In game theory, the two-player zero-sum game describes a situation where one player's gain or loss is exactly balanced by the gain or loss of the other player. One player is known as maximizing player and the other is minimizing. The sum of the costs of both players is zero [145, 146]. Consider a two-player, zero-sum differential game described by the following equation

$$x_{k+1} = f(x_k, L_k, w_k) \tag{A.1}$$

with finite horizon cost functional

$$\mathcal{J}(L_k, w_k) = \sum_{k=0}^{K} \left(\|r_{L_k, w_k}\|_2^2 - \alpha^2 \sum_{k=0}^{K} \|w_k\|_2^2 \right) \tag{A.2}$$

which is to be minimized by L_k (minimizing player) and maximized by w_k (maximizing player). An equilibrium point solution $\mathcal{J}(L_k^*, w_k^*)$ is said to exist if and only if there exists a function $V(\cdot) : [0, N] \times \Re^n \to \Re$ satisfying the following discrete-time Hamilton-Jacobi-Isaac equation (HJIE)

$$V(x_k, k) = \inf_{L_k \in \Re^{n \times m}} \sup_{w_k \in \Re^r} \left\{ \frac{1}{2} \|r_{L_k, w_k}\|^2 - \frac{1}{2} \alpha^2 \|w_k\|_2^2 + V(x_{k+1}, k+1) \right\} \tag{A.3}$$

A.3 Some useful Lemmas

Lemma A.3.1. *for any given constant $\rho > 0$, and defining*

$$\mathcal{S} = \left(\rho^{\frac{1}{2}} x^T(k) A^T P^{\frac{1}{2}} - \rho^{-\frac{1}{2}} \phi^T(k) P^{\frac{1}{2}}\right)$$

the inequality

$$\mathcal{S}\mathcal{S}^T \geq 0 \Rightarrow$$

$$x^T(k)A^T P\phi(k) + \phi^T(k)PAx(k) \leq$$
$$\rho x^T(k)A^T PAx(k) + \rho^{-1}\phi^T(k)P\phi(k)$$

Proof. By the direct multiplication. □

Lemma A.3.2. *[177] For any $Q > 0$, then*

$$\begin{bmatrix} M_{11} & M_{12} \\ M_{12}^T & -P + E^T Q E \end{bmatrix} < 0$$

iff

$$\begin{bmatrix} M_{11} & M_{12} & 0 \\ M_{12}^T & -P & E^T \\ 0 & E & -Q^{-1} \end{bmatrix} < 0$$

and

$$\begin{bmatrix} M_{11} & M_{12} & M_{13} \\ M_{12}^T & -P + E^T Q E & M_{23} \\ M_{13}^T & M_{23}^T & M_{33} \end{bmatrix} < 0$$

iff

$$\begin{bmatrix} M_{11} & M_{12} & 0 & M_{13} \\ M_{12}^T & -P & E^T & M_{23} \\ 0 & E & -Q^{-1} & 0 \\ M_{13}^T & M_{23}^T & 0 & M_{33} \end{bmatrix} < 0$$

Lemma A.3.3. *[178] Let $G, L, E, F(k)$ be real matrices of appropriate dimensions with $F(k)$ being a matrix function and $F(k)^T F(k) \leq I$, then for any $\epsilon > 0, P > 0$ satisfying $P^{-1} - \epsilon E^T E > 0$,*

$$(G + LF(k)E)P((G + LF(k)E))^T \leq G(P^{-1} - \epsilon E^T E)^{-1} G^T + \frac{1}{\epsilon} LL^T$$

Theorem A.3.1. *[179] Let $T(t) = Ce^{A_0 t}B$ where A_0 is diagonalizable as $A_0 = W\Xi W^{-1}$ where Ξ is a diagonal matrix with the eigenvalues of A_0 on the diagonal and the columns of W consists of n linearly independent eigenvectors of A_0. Furthermore, let Ξ_{real} and Ξ_{imag} be, respectively the diagonal matrices with the real and complex part of the eigenvalues of A_0 on the diagonal. Then*

$$|T(t)| \leq U(t) = |CW|e^{\Xi_{real}}|BW^{-1}| \tag{A.4}$$

Appendix B

Proofs

B.1 Proof of Theorem 6.3.1

Consider a quadratic Lyapunov function

$$V_x = x_0^T P x_0 \qquad P = P^T > 0$$

Differentiating along the trajectories of the residual generator (6.52) as

$$\dot{V}(x) = \dot{x}_0^T P x_0 - x_0^T P \dot{x}_0$$

$$\Rightarrow \dot{V}(x) = (\bar{A}_0 x_0 + \bar{E}_0 w_0)^T P x_0 + x_0^T P(\bar{A}_0 x_0 + \bar{E}_0 w_0) + \underbrace{x_0^T P \Psi_0 + \Psi_0^T P^T x_0} \tag{B.1}$$

Notice that the terms indicated under braced contain the nonlinear function. Now using Lemma A.3.1, for any $\epsilon_1 > 0$,

$$x_0^T P \Psi_0 + \Psi_0^T P^T x_0 \leq x_0^T \epsilon_1^2 P P x_0 + \frac{1}{\epsilon_1^2} \Psi_0^T \Psi_0 \tag{B.2}$$

and similarly using Cauchy-Schwarz inequality

$$\Psi_0^T \Psi_0 \leq \|\Psi_0^T\| . \|\Psi_0\| \leq \gamma^2 x_0^T x_0 \tag{B.3}$$

Now using (B.2) and (B.3), (B.1) can be expressed as

$$\dot{V} \leq (\bar{A}_0 x_0 + \bar{E}_0 w_0)^T P x_0 + x_0^T P(\bar{A}_0 x_0 + \bar{E}_0 w_0) + x_0^T \epsilon_1^2 P P x_0 + \frac{1}{\epsilon_1^2} \gamma^2 x_0^T x_0 \tag{B.4}$$

Defining an index similar to the one in the proof of Theorem 6.2.2 as

$$\mathscr{J} = \|r_{0,w}\|_2 - \alpha \|w_0\|_2 \Rightarrow \tag{B.5}$$

$$= \int_0^\infty \left\{ r_{0,w}^T(t) r_{0,w}(t) - \alpha^2 w_0^T(t) w_0(t) \right\} dt \tag{B.6}$$

under zero initial conditions, we can write

$$\mathscr{J} < \int_0^\infty \left\{ r_{0,w}^T(t) r_{0,w}(t) - \alpha^2 w_0^T(t) w_0(t) + \dot{V} \right\} dt \tag{B.7}$$

Now

$$r_{0,w}^T r_{0,w} - \alpha^2 w_0^T w_0 + \dot{V} < 0 \quad \forall t \in [0, \infty) \tag{B.8}$$

suffices the index $\mathscr{J}$ to be less than or equal to zero, that is, $\mathscr{J} \leq 0$. It comes out from equation (B.8) that

$$\begin{aligned} r_{0,w}^T r_{0,w} - \alpha^2 w_0^T w_0 + \dot{V} \leq \quad & (\bar{C}_0 x_0 + \bar{F}_0 w_0)^T (\bar{C} x_0 + \bar{F}_0 w_0) - \alpha^2 w_0^T w_0 \\ & + (\bar{A}_0 x_0 + \bar{E}_0 w_0)^T P x_0 + x_0^T P (\bar{A}_0 x_0 + \bar{E}_0 w_0) \\ & + x_0^T \epsilon_1^2 P P x_0 + \frac{1}{\epsilon_1^2} \gamma^2 x_0^T x_0 \Rightarrow \end{aligned} \tag{B.9}$$

$$\begin{bmatrix} x_0^T \\ w_0^T \end{bmatrix}^T \chi \begin{bmatrix} x_0 \\ w_0 \end{bmatrix} < 0 \tag{B.10}$$

where

$$\chi = \begin{bmatrix} \bar{C_0}^T \\ \bar{F_0}^T \end{bmatrix} \begin{bmatrix} \bar{C_0} & \bar{F_0} \end{bmatrix} + \begin{bmatrix} \Omega_1 & P\bar{E}_0 \\ \bar{E_0}^T P & -\alpha^2 I \end{bmatrix} < 0$$

and $\Omega_1 = \bar{A_0}^T P + P\bar{A_0} + \epsilon_1^2 PP + \frac{1}{\epsilon_1^2}\gamma^2 I$ applying schur complement together with Lemma A.3.3, a sufficient condition for (B.10) is

$$\begin{bmatrix} \Omega_1 & P\bar{E}_0 & \bar{C_0}^T \\ \bar{E_0}^T P & -\alpha^2 I & \bar{F_0}^T \\ \bar{C_0} & \bar{F_0} & -I \end{bmatrix} < 0 \tag{B.11}$$

$$\begin{aligned} & \begin{bmatrix} A_0^T P + P A_0 + \epsilon_1^2 PP + \frac{1}{\epsilon_1^2}\gamma^2 I & PE_0 & C_0^T \\ E_0^T P & -\alpha^2 I & F_0^T \\ C_0 & F_0 & -I \end{bmatrix} \\ & + \begin{bmatrix} \Delta A_0^T P + P \Delta A_0 & P\Delta E_0 & \Delta C_0^T \\ \Delta E_0^T P & 0 & \Delta F_0^T \\ \Delta C_0 & \Delta F_0 & 0 \end{bmatrix} < 0 \end{aligned} \tag{B.12}$$

$$\begin{aligned} & \begin{bmatrix} \Delta A_0^T P + P \Delta A_0 & P\Delta E_0 & \Delta C_0^T \\ \Delta E_0^T P & 0 & \Delta F_0^T \\ \Delta C_0 & \Delta F_0 & 0 \end{bmatrix} = \\ & \begin{bmatrix} \bar{E}_0 \\ 0 \\ F \end{bmatrix} \Delta(t) \begin{bmatrix} \bar{G} & 0 & \bar{H} \end{bmatrix} + \left(\begin{bmatrix} \bar{E}_0 \\ 0 \\ F \end{bmatrix} \Delta(t) \begin{bmatrix} \bar{G} & 0 & \bar{H} \end{bmatrix} \right)^T \end{aligned}$$

using lemma A.3.1, we can end up with the following result

$$\begin{bmatrix} \Omega_1 & PE_0 & C_0^T \\ E_0^T P & -\alpha^2 I & F_0^T \\ C_0 & F_0 & -I \end{bmatrix} + \frac{1}{\epsilon_1} \begin{bmatrix} \bar{E}_0 \\ 0 \\ F \end{bmatrix} \begin{bmatrix} \bar{E}_0 \\ 0 \\ F \end{bmatrix}^T + \epsilon_1 \begin{bmatrix} \bar{G} & \bar{H} & 0 \end{bmatrix} \begin{bmatrix} \bar{G} & \bar{H} & 0 \end{bmatrix}^T < 0 \tag{B.13}$$

where Ω_1 is already defined. Finally applying the Schur complement again, the LMI (6.54) in Theorem 6.3.1 can be obtained.

B.2 Proof of Theorem 6.3.2

The proof begins by considering quadratic Lyapunov function of the similar similar to one used in B.1

$$V = x_0^T P x_0 \quad P = P^T > 0$$

Also assume $\exists\, \mu > 0$, and $0 < \lambda < 1$

$$V < \frac{\mu}{\lambda} \tag{B.14}$$

Considering

$$\dot{V} + \lambda V - \mu I < 0 \tag{B.15}$$

for sufficiency of equation (B.15).

$$\dot{V} + \lambda V - \mu I w_0^T w_0 < 0 \qquad \forall w_0^T w_0 \leq 1 \tag{B.16}$$

It can be noted that (B.16) ensures (B.15) and hence (B.14). Now based on (B.16), it can expressed as

$$\begin{aligned}(\bar{A}_0 x_0 + \bar{E}_0 w_0)^T P x_0 + x_0^T P(\bar{A}_0 x_0 + \bar{E}_0 w_0) + x_0^T \epsilon_1^2 P P x_0 \\ + \frac{1}{\epsilon_1^2}\Psi^T(x_0)\Psi(x_0) + x_0^T \lambda P x_0 - \mu w_0^T w_0 < 0\end{aligned}$$

using the similar treatment as done in the proof of Theorem 6.2.1 yields LMI $\mathscr{L}_1$ in equation (6.56).

Now consider the equation

$$r_{0,w}^T r_{0,w} < \alpha^2 w_0^T w_0 + \lambda V - \mu w_0^T w_0 \Rightarrow r_{0,w}^T r_{0,w} < \alpha^2 \quad \forall w_0^T w_0 \leq 1 \tag{B.17}$$

using equation (B.17)

$$\begin{bmatrix} C_0^T \\ F_0^T \end{bmatrix} \left(I - \epsilon_3 (\bar{F})(\bar{F})^T\right)^{-1} \begin{bmatrix} C_0 & F_0 \end{bmatrix} + \frac{1}{\epsilon_3}\tilde{G}^T\tilde{G} < \begin{bmatrix} \lambda P & 0 \\ 0 & (\alpha^2 - \mu) I \end{bmatrix} \tag{B.18}$$

where $\tilde{G} = \begin{bmatrix} \bar{G} & \bar{H} \end{bmatrix}$. Using schur complement lemma again, the LMI $\mathscr{L}_2$ in equation (6.57) is obtained.

B.3 Proof of Theorem 6.3.3

As it is evident from the equation(6.52) that the residual signal $r_{0,w}$ is affected by disturbance w_0 via matrices F_0 directly and via matrix E_0 through x. It is also evident that the maximum change in $r_{0,w}(t)$ caused by w_0 via F_0 is given by $\alpha_2^*(\delta_{u,\infty} + \delta_{d,\infty})$ with

$$\sup_{\bar{\sigma}(\Delta(t)) \leq \delta_\Delta} (F_0 + \bar{F}\Delta(t)\bar{H})^T (F_0 + \bar{F}\Delta(t)\bar{H}) \leq \alpha_2^2 I,$$

using lemma A.3.1, then

$$F_0^T(I - \xi_4(\bar{F})(\bar{F})^T)^{-1}F_0 + \frac{1}{\xi_4}\bar{H}^T\bar{H} \leq \alpha_1^2 I,$$

using Schur complement lemma, and replacing ξ_4 by $\frac{1}{\epsilon_4}$, It can be transformed in to LMI $\mathscr{L}_3$. Similarly considering the remaining part of the systems by taking $r_{20,w} = C_0 x_0$. Assume the same quadratic Lyapunov function as before and considering that

$$\dot{V} < \alpha_2^2 ||w_0||^2 \Longrightarrow \dot{V} - \alpha^2 w_0^T w_0 < 0 \tag{B.19}$$

dealing with (B.19) in the manner similar to one before, we end up with LMI $\mathscr{L}_2$ of (6.59). Also consider that (B.19) yields after integration

$$V(x(T)) < \alpha_1^2 \int_0^T w_0^T(t) w_0(t) dt \tag{B.20}$$

also we have

$$\begin{aligned} \int_0^T r_{20,w}^T(t) r_{20,w}(t) dt &< \alpha_1^2 \int_0^T w_0^T(t) w_0(t) dt \\ \Longrightarrow r_{20,w}^T(T) r_{20,w}(T) &< \alpha_1^2 \int_0^T w_0^T(t) w_0(t) dt \end{aligned} \tag{B.21}$$

A sufficient condition for (B.21) is

$$r_{20,w}^T(T) r(T)_{20,w} < V(x(T)) \Longrightarrow \bar{C}_0^T \bar{C}_0 \leq P \tag{B.22}$$

with the help on Lemma A.3.1, we can write

$$C_0^T(I - \xi_3(\bar{F})(\bar{F})^T)^{-1}C_0 + \frac{1}{\xi_3}\bar{G}^T\bar{G} \leq P \tag{B.23}$$

the use Schur complement Lemma, and replacing ξ_3 by $\frac{1}{\epsilon_3}$, leads us to the LMI $\mathscr{L}_2$ in equation (6.60).

B.4 Proof of Theorem 6.6.1

Consider the equation

$$\dot{x}_0 = A_0 x_0(t) + B_0 u(t) \Psi_0(x_0(t), u(t)) + \eta_0(x_0(t), u(t), t) + E_0 w(t) \tag{B.24}$$

the solution is expressed as

$$
\begin{aligned}
x_0 &= \exp(A_0 t)\zeta_0 + \int_0^t \exp(A_0(t-\tau))\{B_0 u(\tau) + \Psi_0(x_0(\tau), u(\tau)) + \eta_0(x_0(\tau), u(\tau), \tau)\}d\tau \\
&\quad + \int_0^t \exp(A_0(t-\tau))E_0 w(\tau)d\tau \\
&= \exp(A_0 t)\zeta_0 + \int_0^t \exp(A_0(t-\tau))\{\Psi_0(x_0(\tau), u(\tau)) + \Delta(A_0)x_0(\tau)\}d\tau \\
&\quad + \int_0^t \exp(A_0(t-\tau))\{[B_0 + \Delta(B_0)]\, u(\tau) + E_0 w(\tau)\}d\tau \\
&= \exp(A_0 t)\zeta_0 + \int_0^t \exp(A_0(t-\tau))\{\Psi_0(x_0(\tau), u(\tau)) + \bar{E}\Delta(\tau)\bar{G}x_0(\tau)\}d\tau \\
&\quad + \int_0^t \exp(A_0(t-\tau))\{\left[B_0 + \bar{E}\Delta(\tau)H\right] u(\tau) + E_0 w(\tau)\}d\tau \\
&= \exp(A_0 t)\zeta_0 + \exp(A_0 t) * \{\Psi_0(x_0(t), u(t) + \bar{E}\Delta(t)\bar{G}x_0(t)\} \\
&\quad + \exp(A_0 t) * \{\left[B_0 + \bar{E}\Delta(t)H\right] u(t) + E_0 w(t)\}
\end{aligned}
$$

Taking the modulus and using the Property 1

$$
\begin{aligned}
|x_0| &\leqq |\exp(A_0 t)\zeta_0 + \exp(A_0 t) * \{\Psi_0(x_0(t), u(t) + \bar{E}\Delta(t)\bar{G}x_0(t)\}| \\
&\quad + |\exp(A_0 t) * \{\left[B_0 + \bar{E}\Delta(t)H\right] u(t) + E_0 w(t)\}| \\
&\leqq |\exp(A_0 t)||\zeta_0| + |\exp(A_0 t)| * \{|\Psi_0(x_0(t), u(t)| + |\bar{E}\Delta(t)\bar{G}||x_0(t)|\}| \\
&\quad + |\exp(A_0 t)| * \{|\left[B_0\right| + |\bar{E}||\Delta(t)||H|\right]|u(t)| + |E_0 w(t)|\} \\
&\leqq M(t)|\zeta_0| + M(t) * \{\gamma|x_0(t)| + |\bar{E}|\Pi|\bar{G}||x_0(t)| \\
&\quad + M(t) * \{|\left[B_0\right| + |\bar{E}|\Pi|H|\right]|u(t)| + |E_0 w(t)|\} \\
&\leqq M(t)|\zeta_0| + M(t) * \mathscr{N}_1|x_0(t)| + M(t) * \{\mathscr{N}_2|u(t)| + |E_0 w(t)|\} \\
&\leqq M(t)|\zeta_0| + \mathbf{M}(t)\mathscr{N}_1|x_0(t)| + \mathbf{M}(t)\{\mathscr{N}_2|u(t)| + |E_0 w(t)|\}
\end{aligned}
$$

where $\mathscr{N}_1 = \gamma I + |\bar{E}|\Pi|\bar{G}|$, $\mathscr{N}_2 = \left[|B_0| + |\bar{E}|\Pi|H|\right]$. The upper bound on the modulus of the state x_0 is

$$
\begin{aligned}
(I - \mathbf{M}(t)\mathscr{N}_1)\,|x_0(t)| &\leqq M(t)|\zeta_0| + \mathbf{M}(t)\{\mathscr{N}_2|u(t)| + |E_0 w(t)|\} \\
|x_0(t)| &\leqq (I - \mathbf{M}(t)\mathscr{N}_1)^{-1}\left[M(t)|\zeta_0| + \mathbf{M}(t)\{\mathscr{N}_2|u(t)| + |E_0 w(t)|\}\right] \quad \text{(B.25)}
\end{aligned}
$$

Considering (6.70) and (B.25), the modulus of the residual signal is

$$
|r_{0,w}| \leqq |C_0|\,(I - \mathbf{M}(t)\mathscr{N}_1)^{-1}\left[M(t)|\zeta_0| + \mathbf{M}(t)\{\mathscr{N}_2|u(t)| + |E_0|\delta_{0,w}\}\right] + |F_0|\delta_{0,w} \quad \text{(B.26)}
$$

Appendix C

Technical data for benchmark systems

C.1 Parameters of the three-tank system (DTS200)

Table C.1: Numerical values of the parameters of DTS200 [141]

Parameters	Symbol	Value	Unit
cross section area of tanks	A_c	154	cm^2
cross section area of pipes	s_n	0.5	cm^2
max. height of tanks	H_{max}	62	cm
max. flow rate of pump 1	$Q_{1_{max}}$	100	cm^3/sec
max. flow rate of pump 2	$Q_{2_{max}}$	100	cm^3/sec
coefficient of flow for pipe 1	a_1	0.46	
coefficient of flow for pipe 2	a_2	0.60	
coefficient of flow for pipe 3	a_3	0.45	

C.2 Parameters of the inverted pendulum control system (LIP100)

Table C.2: Numerical values of the parameters of LIP100 [1]

Constant	Numerical value	Unit	Constant	Numerical value	Unit
K_r	2.6	N/V	n_{11}	14.9	V/m
n_{22}	-52.27	V/rad	n_{33}	-7.64	Vs/m
n_{44}	-52.27	Vs/rad	M_0	3.2	kg
M_1	0.329	kg	M	3.529	kg
l_s	0.44	m	J_L	0.072	kgm^2
N	0.1446	kgm	N_{01}^2	0.23315	kg^2m^2
C	0.009	kgm^2/s	F_r	6.2	kg/s

Bibliography

[1] S. X. Ding, *Model-based Fault Diagnosis Techniques, Design Schemes, Algorithms, and Tools*. Springer, 2008.

[2] I. Izadi, S. L. Shah, D. S. Shook, and T. Chen, "An introduction to alarm analysis and design," in *Proc. of IFAC SafeProcess'09*, (Barcelona, Spain), June 30- July 3, 2009.

[3] "Abnormal situation management consortium." `http://www.asmconsortium.com/`.

[4] H. Vedam and V. Venkatasubramanian, "Pca-sdg based process monitoring and fault diagnosis," *Control Engg. Practice*, vol. 7, pp. 903–917, 1999.

[5] K. Hideo and T. Hiroyuki, "Crash of japan airlines b-747 at mt. osutaka," *Failure knowledge database / 100 selected cases*. `http://shippai.jst.go.jp/en/`.

[6] "Chernobyl accident." `http://www.world-nuclear.org/info/chernobyl/`.

[7] "Piper alpha." `http://home.versatel.nl/the_sims/rig/pipera.htm`.

[8] J. Chen and R. J. Patton, *Robust Model-Based Fault Diagnosis for Dynamic Systems*. Kluwer Acedemic Publisher, Bosten, 1999.

[9] M. Mahmoud, J. Jiang, and Y. Zhang, *Active fault tolerant control systems*. Lecture notes in control and Information Science (LNCIS), Springer, 2003.

[10] K. Pattan, *Artificial Neural Networks for the Modelling and Fault Diagnosis of Technical Processes*. Springer, 2008.

[11] J. J. Gertler, *Fault Detection and Diagnosis in Engineering Systems*. Marcel Dekker, 1998.

[12] R. Isermann, *Fault-Diagnosis Systems*. Springer, 2006.

[13] M. Blanke, M. Kinnaert, J. Lunze, and M. Staroswiecki, *Diagnosis and Fault Tolerant Control*. Springer, 2nd ed., 2006.

[14] **A. Q. Khan**, M. Abid, W. Chen, and S. X. Ding, "On optimal fault detection of nonlinear systems," in *Proc. 48th IEEE Conf. Decis. Contr.(CDC)*, (Shanghai, China), pp. 1032–1037, December 16-18, 2009.

[15] **A. Q. Khan**, M. Abid, W. Chen, and S. X. Ding, "Mixed $\mathscr{H}_-/\mathscr{H}_\infty-$ fault detection filter design for discrete-time nonlinear systems," *Submitted to Int. J. Contr.*, 2010.

[16] **A. Q. Khan** and S. X. Ding, "Threshold computation for robust fault detection in a class of continuous time nonlinear systems," in *Proc. Europ. Contr. Conf.*, (Budapest, Hungary), pp. 3088–3093, August 23-26, 2009.

[17] **A. Q. Khan** and S. X. Ding, "Threshold computation for fault detection in a class of discrete time nonlinear systems," *Int. J. Adapt. Control Signal Process (DOI: 10.1002/acs).*, 2010.

[18] **A. Q. Khan**, S. X. Ding, and M. Abid, "Residual generation and evaluation scheme for detection of faults in nonlinear systems using convex optimization," in *Proc. of 6th Workshop on Advanced Control and Diagnosis*, (Coventry University UK), pp. 84–89, November 27-29, 2008.

[19] **A. Q. Khan**, S. X. Ding, C. I. Chihaia, M. Abid, and W. Chen, "Robust fault detection of nonlinear systems: A three-tank benchmark application," in *To appear in 2010 Conf. on Control & Fault-tolerant systems (SysTol'10)*, (Niece, France), October 6-8, 2010.

[20] R. Isermann and P. Balle, "Trends in the application of model-based fault detection and diagnosis of technical processes," *Control Engg. Practice*, vol. 5, pp. 709–719, 1997.

[21] P. M. Frank, "Analytical and qualitative model-based fault diagnosis-a survey," *Europ. J. Control*, vol. 2, pp. 6–28, 1996.

[22] P. M. Frank, "On-line fault detection in uncertain nonlinear systems using diagnostic observers: a survey," *Int. J. Systems Sci.*, vol. 25/12, pp. 2129–2154, 1994.

[23] D. Sauter, N. Mary, F. Sirou, and A. Thieltgen, "Fault diagnosis in systems using fuzzy logic," in *Proc. 3rd IEEE Conf. Contr. Appl.*, (Glasgow, UK), pp. 883–888, August 1994.

[24] V. Venkatasubramanian, R. Rengaswamy, K.Yin, and S. N. Kavuri, "A review of process fault detection and diagnosis part ii: quantitative model based methods," *Computers and Chemical Engineering*, vol. 27, pp. 313–326, 2003.

[25] L. H. Chiang, E. L. Russel, and R. D. Bratz, *Fault Detection and Diagnosis in Industrial Systems*. Springer, 2001.

[26] E. Y. Chow and A. S. Willsky, "Analytical redundancy and the design of robust failure detection systems," *IEEE Trans. Automat. Contr.*, vol. 29, pp. 603–614, 1984.

[27] J. Gertler and D. Singer, "A new structural framework for parity equation based failure detection and isolation," *Automatica*, vol. 26, pp. 381–388, 1990.

[28] J. Gertler and M. Kunert, "Optimal residual decoupling for robust fault diagnosis," *Int. J. Control*, vol. 61, pp. 395–421, 1995.

[29] G. Delmaire, J. P. Cassar, and M. Staroswiecki, "Comparision of identification and parity space approach for failure detection in single-input single-output systems," in *Proc. IEEE Conf. Contr. App.*, (Glasgow, UK), pp. 865–870, 1994.

[30] M. Staroswiecki, J. P. Cassar, and V. Cocquempot, "Generation of optimal structured residuals in the parity space," in *Proc. 12th IFAC world congress*, (Sydney, Australia), pp. 535–542, 1993.

[31] J. Wuennenberg, *Observer-based fault detection in dynamic systems.* PhD thesis, University of Duisburg-Essen, 1990.

[32] C. Christophe, V. Cocquempot, and B. Jiang, "Link between high-gain observer-based and parity space residuals for fdi," *Trans. Inst. Measur. Contr.*, vol. 26, pp. 325–337, 2004.

[33] S. K. Nguang, P. Zhang, and S. X. Ding, "Parity relation based fault estimation for nonlinear systems: An lmi approach," *Int. J. Automation & Computing*, vol. 04, pp. 164–168, April 2007.

[34] S. K. Nguang, P. Zhang, and S. X. Ding, "Parity based fault estimation for nonlinear systems: An lmi approach," in *Proc. American Cont. Conf.*, (Minneapolis, Minnesota), June 2006.

[35] B. Halder and N. Sarkar, "Robust fault detection of robotic manipulator," *Int. J. Robotic Research*, vol. 26, pp. 273–285, March 2007.

[36] B. Halder and N. Sarkar, "Robust nonlinear analytic redundancy for fault detection and isolation in mobile robot," *Int. J. Automation & Computing*, vol. 2, pp. 177–182, April 2007.

[37] B. Halder and N. Sarkar, "Robust fault detection of robotic systems: New results and experiments," in *Proc. ICRA*, (Orlando, Florida), May 15-19, 2006.

[38] B. Halder and N. Sarkar, "Robust fault detection and isolation in mobile robot," in *Proc. IFAC SafeProcess*, (Beijing, China), August 30-September 01, 2006.

[39] P. M. Frank and L. Keller, "Sensitivity discrimination observer design for instrument failure detection," *IEEE trans. Aero. Electron. Syst.*, vol. 16/4, pp. 460–467, 1980.

[40] J. Wuennenberg and P. M. Frank, "sensor fault detection via robust observers," in *First European Workshop On Fault Diagnostics. Reliability and Related Knowledge-Based Approaches*, (Rhodes, Greece), 1986.

[41] W. Ge and C. Z. Fang, "Detection of faulty components via robust observation," *Int. J. Control*, vol. 47:2, pp. 581–599, 1988.

[42] W. Ge and C. Z. Fang, "Extended robust observation approach for failure isolation," *Int. J. Control*, vol. 49:5, pp. 1537–1553, 1989.

[43] P. M. Frank and J. Wuennenberg, *Fault Diagnosis in Dynamic Systems: Theory and Application*, ch. Robust fault diagnosis using unknown input schemes, pp. 47–98. Prentice Hall, 1989.

[44] X. Ding and P. M. Frank, "Fault detection via factorization approach," *System & Control Letters*, vol. 14, pp. 431–436, 1990.

[45] P. M. Frank and X. Ding, "Frequency domain approach to optimally robust residual generation and evaluation for model-based fault diagnosis," *Automatica*, vol. 30/5, pp. 789–804, 1994.

[46] M. Hou and P. C. Müller, "Fault detection and isolation observers," *Int. J. Control*, vol. 60:5, pp. 857–846, 1994.

[47] D. Chu, "Matrix pencil characterizations of disturbance decoupling for systems with direct feed-through matrices," *Int. J. Control*, vol. 73:11, pp. 1042–1050, 2000.

[48] R. J. Patton and M. Hou, "Design of fault detection and isolation observers: A matrix pencil approach," *Automatica*, vol. 34, pp. 1135–1140, 1998.

[49] M. A. Massoumia, "A geometric approach to the synthesis of failure detection filters," *IEEE Trans. Automat. Contr.*, vol. 31, pp. 839–845, September 1986.

[50] T. Kailath, *Linear Systems*. Printice Hall, 1980.

[51] S. X. Ding, **A. Q. Khan**, Y. Q. Wang, and M. Abid, "A note on unknown input fault detection filter," in *17th IFAC World Congress*, (Seoul, Korea), pp. 5523–5528, July 6-11, 2008.

[52] F. Hamelin, C. Defranoux, and D. Sauter, "Geometric-based approach to fault detection for interval systems," in *Proc. 41st IEEE Conf. Deci. Contr.*, (Las vagas, Nevada, USA), pp. 4365–4370, December 2002.

[53] H. Gao, T. Chen, and L. Wang, "Robust fault detection with missing measurements," *Int. J. Control*, vol. 81, pp. 804–819, 2008.

[54] L. H. Mutuel and J. L. Speyer, "A discrete-time game-theoretic fault detection filter," in *Proc.of American Contr. Conf.*, (Chicago, illinois, USA), June 2000.

[55] E. Mazars, I. Jaimoukha, and Z. Li, "Computation of reference model for robust fault detection and isolation residual generation," *J. Contr. Sci. Engg*, vol. 2008, pp. 1–12, 2008.

[56] N. Liu and K. Zhou, "Optimal robust fault detection for linear discrete time systems," *J. Cont. Sci. Engg.*, vol. 2008, pp. 1–16, 2008.

[57] N. Liu and K. Zhou, "Optimal robust fault detection for linear discrete time systems," in *Proc. 46th IEEE Conf. Decis. Contr.(CDC)*, (New Orleans, LA, USA), pp. 981–988, Dec 12-14, 2007.

[58] L. Bai, Z. Tian, and S. Shi, "Robust fault detection for a class of nonlinear time-delay systems," *J. Franklin Institute*, vol. 344(6), pp. 873–888, 2007.

[59] X. Li and K. Zhou, "A time domain approach to robust fault detection of linear time-varying systems," *Automatica*, vol. 45, pp. 94–102, 2009.

[60] H. Wang and G. H. Yang, "A finite frequency domain approach to fault detection for linear discrete-time system," *Int. J. Control*, vol. 81:7, pp. 1162–1171, 2008.

[61] Y. Cui, X. Huang, and M. Wang, "Multi-objective robust fault detection filter design in a finite frequency range," in *Proc. Int. Symp. on Neural Networks: Advances in Neural Networks-PartIII*, (Wuhan, China), pp. 733–743, 2009.

[62] D. Henry and A. Zolghadri, "Design of fault diagnosis filters: A multi-objective approach," *J. Franklin Institute*, vol. 342, pp. 421–446, 2005.

[63] M. Hou and R. J. Patton, "An lmi approach to h_-/h_∞ fault detection observers," in *UKACC Int. Conf. Control*, pp. 305–310, 1996.

[64] X. Ding, L. Guo, and P. M. Frank, "A frequency domain approach to fault detection of uncertain dynamic systems," in *Proc. 32nd IEEE Conf. Decis. Contr.(CDC)*, pp. 1722–1727, 1993.

[65] S. X. Ding, T. Jeinsch, P. M. Frank, and E. L. Ding, "A unified approach to the optimization of fault detection systems," *Int. J. of Adapt. Control Signal Proces.*, vol. 14, pp. 725–745, 2000.

[66] J. L. Wang, G. H. Yang, and J. Liu, "An lmi approach to h_- index and mixed h_-/h_∞ fault detection observer design," *Automatica*, vol. 43, pp. 1656–1665, 2007.

[67] A. E. Naini, M. M. Akhter, and S. R. Rock, "Effect of model uncertainty on failure detection: The threshold selector," *IEEE Trans. Automat. Contr.*, vol. 33, pp. 1106–1115, 1988.

[68] F. Rambeaux, F. Hamelin, and D. Sauter, "Optimal thresholding for robust fault detection of uncertain systems," *Int. J. Robust Nonlinear Control*, vol. 10, pp. 1155–1173, 2000.

[69] S. X. Ding, P. Zhang, and P. M. Frank, "Threshold computation using lmi technique and its integration in the designing of fault detection systems," in *Proc. 42nd IEEE Conf. Decis. Contr.(CDC)*, (Maui, Hawaii, USA), December 2003.

[70] M. G. Perhinschi, M. R. Napolitano, G. Campa, B. Seanor, J. Bruken, and R. Larson, "An adaptive threshold approach for the design of an actuator failure detection and identification scheme," *IEEE trans. Contr. Sys. Tech.*, vol. 14(3), pp. 519–525, 2006.

[71] A. Johansson, M. Bask, and T. Norlander, "Dynamic threshold generator for robust fault detection in linear systems with parameter uncertainty," *Automatica*, vol. 42, pp. 1095–1106, 2006.

[72] Y. E. Faitakis, S. Thapliyal, and J. C. Kantor, "An lmi approach to the evaluation of alarm thresholds," *Int. J. Robust Nonlinear Control*, vol. 8, pp. 659–667, 1998.

[73] Z. Shi, G. Gu, B. Lennox, and A. D. Ball, "The development of an adaptive threshold for model based fault detection of nonlinear electro-hydraulic systems," *Control Engg. Practice*, vol. 13, pp. 1357–1367, 2005.

[74] R. Isermann, "Process fault detection on modeling and estimation methods - a survey," *Automatica*, vol. 20, pp. 387–404, 1984.

[75] D. Brie, D. Sauter, and T. Cecchin, "Robust fault detection in a welding process using parametric estimation," in *Proc. Int. Conf. Syst., Man and Cyber.*, (Le Touquet , France), pp. 412–417, October 1993.

[76] T. Jiang, K. Khorasani, and S. Tafazoli, "Parameter estimation-based fault detection, isolation and recovery for nonlinear satellite models," *IEEE Trans. Automat. Contr.*, vol. 16, pp. 799–808, 2008.

[77] P. M. Frank and X. Ding, "Survey of robust residual generation and evaluation methods in observer based fault detection systems," *J. Proc. Control*, vol. 7, pp. 403–424, 1997.

[78] E. A. Garcia and P. M. Frank, "Deterministic Nonlinear observer-based approaches to fault diagnosis," *Contr. Engg. Pract.*, vol. 5, pp. 663–670, 1997.

[79] M. Witczak, *Modelling and Estimation Strategies for Fault Diagnosis of Non-Linear Systems: From Analytical to Soft Computing Approaches*. Springer, 2007.

[80] H. A. Talebi, F. Abdollahi, R. V. Patel, and K. Khorasani, *Neural Network-Based State Estimation of Nonlinear Systems: Application to Fault Detection and Isolation*. Springer, 2009.

[81] H. A. Talebi and K. Khorasani, "An intelligent sensor and actuator fault detection and isolation scheme for nonlinear systems," in *Proc. 46th IEEE Conf. Decis. Contr.(CDC)*, (New Orleans, LA, USA), pp. 2620–2625, Dec 12-14, 2007.

[82] M. E. M. El-ghatwary, *Robust Fuzzy observer-based fault detection for nonlinear systems*. PhD thesis, University of Duisburg-Essen, 2007.

[83] M. Zeitz, "The extended luenberger observer for nonlinear systems," *Syst. Control Lett.*, vol. 9, pp. 149–156, 1987.

[84] K. Adjallah, D. Maquin, and J. Ragot, "Nonlinear observer-based fault detection," in *Proc. 3rd IEEE Conf. Contr. App.(CCA)*, (Glasgow, UK), pp. 1115–1120, August 1994.

[85] D. Hengy and P. M. Frank, "Component failure detection via nonlinear observers," in *Proc. IFAC Workshop on Fault detection and safety of chemical plants*, (Kyoto, Japan), pp. 153–157, 1986.

[86] P. M. Frank, "Enhancement of robustness in observer-based fault detection," *International Journal of Control*, vol. 59, pp. 955–981, 1994.

[87] P. M. Frank, G. Schreier, and E. A. Garcia, *New direction in nonlinear observer design*, ch. Nonlinear observers for fault detection and isolation, pp. 401–422. Springer-Verlag, 1999.

[88] R. Seliger and P. M. Frank, *Issues of Fault diagnosis for dynamic systems*, ch. Robust observer based fault diagnosis in nonlinear uncertain systems, pp. 145–185. Springer-Verlag, 2000.

[89] R. Seliger and P. M. Frank, "Fault diagnosis by disturbance decoupled nonlinear observers," in *Proc. IEEE Conf. Decis. Contr.*, (England), pp. 2248–2253, 1991.

[90] R. Seliger and P. M. Frank, "Robust component fault detection and isolation in nonlinear dynamic systems," in *Proc. IFAC Symposium on Fault Detection, Supervision and Safety of Technical Process*, (Baden-Baden, Germany), pp. 313–318, 1991.

[91] X. Ding and P. M. Frank, "An adaptive observer based fault detection scheme for nonlinear dynamic systems," in *Proc. of IFAC WC'93*, 1993.

[92] Q. Zhang, "A new residual generation and evaluation method for detection and isolation of faults in nonlinear systems," *Int. J. Adapt. Control Signal Process*, vol. 14, pp. 759–773, 2000.

[93] J. P. Gauthier, H. Hammouri, and S. Othman, "A simple observer for nonlinear systems application to biorectors," *IEEE Trans. Automat. Contr.*, vol. 37(6), pp. 875–880, 1992.

[94] R. M. Guerra, R. Garrido, and A. O. Miron, "The fault detection problem in nonlinear systems using residual generators," *IMA J. Math. Contr. Infor.*, vol. 22, pp. 119–136, 2005.

[95] H. Hammouri, M. Kinnaert, and E. H. E. Yaagoubi, "Observer-based approach to fault detection and isolation for nonlinear systems," *IEEE Trans. Automat. Contr.*, vol. 44(10), pp. 1879–1884, 1999.

[96] G. Besancon, "High-gain observation with disturbance attenuation and application to fault detection and isolation for nonlinear systems," *Automatica*, vol. 39, pp. 1095–1102, 2003.

[97] H. Hammouri, M. Kinnaert, and E. E. Yaagoubi, *New direction in nonlinear observer design*, ch. Application of nonlinear observers to fault detection and isolation, pp. 423–443. Springer-Verlag, 1999.

[98] H. K. Khalil, *Nonlinear Systems*. Prentice Hall, 3rd ed., 1996.

[99] X. G. Yan and C. Edwards, "Sensor fault detection and isolation for nonlinear systems based on sliding mode observer," vol. 21, pp. 657–673, 2007.

[100] X. G. Yan and C. Edwards, "Nonlinear robust fault reconstructive and estimation using a sliding mode observers," vol. 43, pp. 1605–1614, 2007.

[101] X. G. Yan and C. Edwards, "Robust sliding mode observer-based actuator fault detection and isolation for a class for nonlinear systems," vol. 39, pp. 1605–1614, 2008.

[102] C. D. Persis and A. Isidori, "A geometric approach to nonlinear fault detection and isolation," *IEEE Trans. Automat. Contr*, vol. 46, pp. 853–865, 2001.

[103] C. D. Persis and A. Isidori, *Nonlinear Control in the Year 2000*, ch. An $H_\infty-$optimal Fault Detection Filter for Bilinear Systems, pp. 331–3393. Springer-Verlag, 2000.

[104] H. Hammouri, P. Kabore, and M. Kinnaert, "A Geometric Approach to Fault detection and Isolation for Bilinear Systems," *IEEE Trans. Automat. Contr.*, vol. 46(9), pp. 1451–1455, 2001.

[105] C. E. de Souza, U. Shaked, and M. Fu, "Robust H_∞ filtering for continuous-time varying uncertain systems with deterministic input signals," *IEEE Trans. Autom. Contr.*, vol. 43, pp. 709–719, 1995.

[106] D. J. N. Limebeer, B. D. O. Anderson, and B. Handel, "A nash game approach to mixed h_2/h_∞ control," *IEEE Trans. Automat. Contr.*, vol. 39(1), pp. 69–82, 1994.

[107] Y. Theodor and U. Shaked, "A dynamic game approach to mixed h_∞/h_2 estimation," *Int. J. Robust Nonlinear Control*, vol. 6, pp. 331–345, 1996.

[108] M. D. S. Aliyu and E. K. Boukas, "Discrete-time mixed h_2/h_∞ nonlinear filtering," in *Proc. American Contr. Conf.*, (Seattle, Washington, USA), pp. 5230–5235, June 11-13, 2008.

[109] M. D. S. Aliyu and E. K. Boukas, "Mixed h_2/h_∞ nonlinear filtering," *Int. J. Robust Nonlinear Control*, vol. 19, pp. 394–417, 2009.

[110] N. Berman and U. Shaked, "h_∞ nonlinear filtering," *Int. J. Robust Nonlinear Control*, vol. 6, pp. 281–296, 1996.

[111] M. Shergei, U. Shaked, and C. E. D. Souza, "Robust H_∞ nonlinear estimation," *Int. J. Adapt. Control Signal Process*, vol. 10, pp. 395–408, 1996.

[112] W. H. Chung and J. L. Speyer, "A game theoretic fault detection filter," *IEEE Trans. Automat. Contr*, vol. 43, pp. 143–161, 1998.

[113] C. D. Persis and A. Isidori, "On the design of fault detection filter with game-theoretic-optimal sensitivity," *Int. J. Robust Nonlinear Control*, vol. 12, pp. 729–747, 2002.

[114] F. E. Thau, "Observing the state of nonlinear dynamic systems," *Int. J. Control*, vol. 17:3, pp. 471–479, 1973.

[115] R. Rajmani and Y. M. Cho, "Existence and design of observers for nonlinear systems: relation to distance unobservability," *Int. J. Control*, vol. 69(5), pp. 717–731, 1998.

[116] C. Aboky, G. Sallet, and J. C. Vivalda, "Observers for lipschitz non-linear systems," *Int. J. Control*, vol. 75:3, pp. 204–212, 2002.

[117] R. Rajmani, "Observer Design for Lipschitz Nonlinear Systems," *IEEE Trans. Automat. Contr.*, vol. 43(3), pp. 397–401, 1998.

[118] G. D. Hu, "Observers for one-sided lipschitz non-linear systems," *IMA Journal of Math. Contr. and Infor.*, vol. 23, pp. 395–401, 2006.

[119] S. Ibrir, "Circle-criterion approach to discrete-time nonlinear observer design," *Automatica*, vol. 40, pp. 1931–1938, 2004.

[120] A. M. Pertew, H. J. Marquez, and Q. Zhao, "h_∞ synthesis of unknown input observers for non-linear lipschitz systems," *Int. J. Control*, vol. 78:15, pp. 1155–1165, 2005.

[121] A. M. Pertew, H. J. Marquez, and Q. Zhao, "h_∞ observer design for lipschitz nonlinear systems," *IEEE Trans. Automat. Contr.*, vol. 51(7), pp. 1211–1216, 2006.

[122] M. Abbaszadeh and H. J. Marquez, "Robust h_∞ observer design for sampled-data Lipschitz nonlinear systems with exact and euler approximate models," *Automatica*, vol. 44, pp. 799–806, 2008.

[123] F. Zhu and Z. Han, "A note on observer for lipschitz nonlinear systems," *IEEE Trans. Automat. Contr.*, vol. 47(10), pp. 1751–1754, 2002.

[124] M. Chen and C. Chen, "Robust nonlinear observer for lipschitz nonlinear systems subject to disturbance," *IEEE Trans. Automat. Contr.*, vol. 52(12), pp. 2365–2368, 2007.

[125] G. Schreier, J. Ragot, R. J. Patton, and P. M. Frank, "Observer design for a class of nonlinear systems," in *Proc. IFAC SAFEPROCESS*, (Hull, England), pp. 498–503, 1997.

[126] A. M. Pertew, H. J. Marquez, and Q. Zhao, "Lmi based sensor fault diagnosis for nonlinear lipschitz systems," *Automatica*, vol. 43, pp. 1464–1469, 2007.

[127] X. Zhang, M. M. Polycarpou, and T. Parisini, "Fault diagnosis of a class of uncertain nonlinear systems with lipschitz nonlinearities," in *Proc. of IFAC SafeProcess'09*, (Barcelona, Spain), June 30- July 3, 2009.

[128] S. Mondal, G. Chakraborty, and K. Bhattacharyya, "Robust unknown input observer for nonlinear systems and its application to fault detection and isolation," *J. Dyn. Sys. Meas. & Control*, vol. 130, July 2008.

[129] M. Witczak, J. Korbicz, and V. Puig, "An lmi approach to designing observers and unknown input observers for nonlinear systems," in *Proc. IFAC SAFEPROCESS*, 2006.

[130] X. Zhang, M. M. Polycarpou, and T. Parisini, "Fault diagnosis of a class of uncertain nonlinear systems with lipschitz nonlinearities," *Automatica*, vol. 46, pp. 290–299, 2010.

[131] B. Lei-shi, H. Li-ming, T. Zuo-hua, and S. Song-jiao, "Design of h_∞ robust fault detection filter for nonlinear time-delay systems," *J. Zhejiang Univ Science A*, vol. 7, pp. 1733–1741, 2006.

[132] R. M. G. Ferrari, T. Parisini, and M. M. Polycarpou, "A fault detection and isolation scheme for nonlinear uncertain discrete time systems," in *Proc. 46th IEEE Conf. Decis. Contr.(CDC)*, (New Orleans, LA, USA), December 2007.

[133] X. D. Zhang, M. M. Polycarpou, and T. Parisini, "A robust detection and isolation scheme for abrupt and incipient faults in nonlinear systems," *IEEE Trans. Automat. Contr.*, vol. 47, pp. 576–593, 2002.

[134] M. Basseville and I. Nikiforove, *Detection of abrupt changes: Theory and Applications*. Information & System Science Series, Prentice-Hall, Englewood Cliffs, N.J, 1993.

[135] M. Kinnaert, "Model-based statistical signal processing and decision theoretical approach to monitoring," in *Proc. IFAC SAFEPROCESS*, (Washingten, USA), pp. 1–12, 2003.

[136] A. M. Pertew, H. J. Marquez, and Q. Zhao, "Sampled-data stabilization of a class of nonlinear systems with application in robotics," *J. Dyn. Sys. Measur. & Control*, vol. 131, p. 021008, 2009.

[137] H. J. Marquez, *Nonlinear Control Systems: Analysis and Design*. New York: Wiley, 2003.

[138] G. R. Wood and B. P. Zhang, "Estimation of the lipschitz constant of a function," *J. Global Optimization*, vol. 8, pp. 91–103, 1996.

[139] E. Sobhani-Tehrani and K. Khorasani, *Fault Diagnosis of Nonlinear Systems Using a Hybrid Approach*. Springer, 2009.

[140] G. J. J. Ducard, *Fault-tolerant Flight Control and Guidance Systems: Practical Methods for Small Unmanned Aerial Vehicles*. Springer, 2009.

[141] "Ds1102-board, user's guide," tech. rep., Paderborn, 1995.

[142] J. Liu, J. L. Wang, and G. H. Yang, "An lmi approach to minimum sensitivity analysis with application to fault detection," *Automatica*, vol. 41, pp. 1995–2004, 2005.

[143] Y. Chen, Z. Weng, and S. Shi, "Robust fault diagnosis for nonlinear difference-algebraic systems," *Int. J. Control*, vol. 76:15, pp. 1560–1569, 2003.

[144] M. Z. Chen, Q. Zhao, and D. H. Zhou, "A robust fault detection approach for nonlinear systems," *Int. J. Autom. Compt*, vol. 1, pp. 23–28, 2006.

[145] T. Basar and P. Bernhard, *H^∞-Optimal Control and Related Minimax Design Problems: A Dynamic Game Approach*. Birkhäuser, 2nd ed., 1995.

[146] T. Basar, *Dynamic Non-cooperative Game Theory*. Academic Press, 2nd ed., 1995.

[147] U. Shaked and N. Berman, "H_∞ nonlinear filtering of discrete-time process," *IEEE Trans. Signal Process.*, vol. 43(9), pp. 2205–2209, 1995.

[148] Z. Wang and H. Unbehauen, "A class of nonlinear observers for discrete time systems with parametric uncertainty," *Int. J. System Sci.*, vol. 31(1), pp. 19–26, 2000.

[149] M. Arcak and D. Nešić, "A framework for nonlinear sampled-data observer design via approximate discrete-time models and emulation," *Automatica*, vol. 40, pp. 1931–1938, 2004.

[150] A. Zemouche and M. Boutayeb, "Observer design for lipschitz nonlinear systems: The discrete time case," *IEEE Trans. Automat. Contr.*, vol. 53(8), pp. 777–781, 2006.

[151] I. Karafyllis and C. Kravaris, "On the observer problem for discrete-time control systems," *IEEE Trans. Automat. Contr*, vol. 52, pp. 12–25, 2007.

[152] M. Abbaszadeh and H. J. Marquez, "Robust H_∞ observer design for a class of nonlinear uncertain systems via convex optimization," in *Proc. American Contr. Conf.*, (USA), July 2007.

[153] H. Ye, S. X. Ding, and G. Wang, "Integrated design of fault detection systems in time-frequency domain," *IEEE Trans. Automat. Contr.*, vol. 47, pp. 384–390, February 2002.

[154] J. Abedor, K. Nagpal, and K. Poolla, "A linear matrix inequality approach to peak-to-peak minimization," *Int. J. Robust Nonlinear Control*, vol. 6, pp. 899–927, 1996.

[155] J. X. Fu, S. H. Ye, and C. Jian, "Peak-to-peak gain minimization for uncertain linear discrete systems: A linear matrix inequality approach," *ACTA Automatica SINICA*, vol. 33, pp. 753–756, 2007.

[156] J. Aubrecht and P. G. Voulgaris, "Minimization of the peak-to-peak gain in periodic systems under full state feedback," *J. Dyn. Sys. Meas. & Control*, vol. 123, pp. 10–20, 2001.

[157] N. Elia and M. A. Dahleh, "Minimization of worst case peak-to-peak gain via dynamic programming: State feedback case," *IEEE Trans. Automat. Contr.*, vol. 45, pp. 687–701, 2000.

[158] C. Scherer, P. Gahinet, and M. Chilali, "Multiobjective output-feedback control via lmi optimization," *IEEE trans. Automat. Contr.*, vol. 42, pp. 896–910, 1997.

[159] H. Gao, J. Lam, L. Xie, and C. Wang, "New approach to mixed $\mathcal{H}_2/\mathcal{H}_\infty$ filtering for polytopic discrete-time systems," *IEEE Tran. Signal Process.*, vol. 53, pp. 3183–3192, 2005.

[160] K. M. Grigoriadis and J. T. Watson, "Reduced-order h_∞ and $l_2 - l_\infty$ filtering via linear matrix inequalities," *IEEE Trans Aerosp. Electron. Syst.*, vol. 33, pp. 1326–1338, 1997.

[161] D. Du, S. Zhou, and B. Zhang, "Generalized h_2 output feedback controller design for uncertain discrete-time switched systems via switched lyapunov functions," *Nonlinear Analysis*, vol. 65, pp. 2135–2146, 2006.

[162] G. Zhu and R. Skelton, "Mixed l_2 and l problems by weight selection in quadratic optimal control," *Int. J. Control*, vol. 53:5, pp. 1161–1176, 1991.

[163] D. A. Wilson and J. E. Rubio, "Computation of generalized h_2 optimal controller," *Int. J. Control*, vol. 61:5, pp. 999–1012, 1995.

[164] R. M. Palhares and P. L. D. Peres, "Robust filtering with guaranteed energy-to-peak performance-an lmi approach," *Automatica*, vol. 36, pp. 851–858, 2000.

[165] X. Zhang, M. Polycarpou, and T. Parisini, "Robust fault isolation for a class of non-linear input-output systems," *Int. J. Control*, vol. 74:13, pp. 1295–1310, 2001.

[166] L. Li and D. Zhou, "Fast and robust fault diagnosis for a class of nonlinear systems: detectability analysis," *Computers and chemical engineering*, vol. 28, no. 12, pp. 2635–2646, 2004.

[167] M. Fliess, C. Join, and H. Sira-Ramirez, *Control and Observer Design for Nonlinear Finite and Infinite Dimensional Systems*, ch. Closed-loop fault-tolerant control for uncertain nonlinear systems, pp. 217–233. Springer-Verlag, 2005.

[168] C. Join, H. Sira-Ramirez, and M. Fliess, "Control of an uncertain three-tank system via on-line parameter identification and fault detection," in *16th IFAC World Congress*, Prague, 2005.

[169] R. Galindo, "Mixed sensivity h-infinity control of a three tank system," in *American Control Conference*, 2005.

[170] K. Tsuda, D. Mignone, G. Ferrari-Trecate, and M. Morari, "Reconfiguration strategies for hybrid systems," in *American Control Conference*, June 2001.

[171] S. X. Ding, T. Jeinsch, E. L. Ding, D. Zhou, and G. Wang, "Application of observer based fdi schemes to the three tank system," in *Proc. Europ. Contr. Conf.*, Karlsruhe, August 31 September 3, 1999.

[172] C. Join, J. C. Ponsart, D. Sauter, and D. Theilliol, "Nonlinear filter design for fault diagnosis: application to the three-tank system," *IEE Proc. Control Theory Appl.*, vol. 152(1), pp. 55–64, January 2005.

[173] Amira, "Lab manual dts200 three tank system," tech. rep., Bismarckstr. 67, 47057 Duisburg, Germany, 1992.

[174] C. I. Chihaia, O. Bredtmann, E. Goldschmidt, W. Li, S. Ding, and A. Czylwik, "Winc-advanced experimentation platform for wireless networked control," in *Proc. 7th IFAC SAFEPROCESS*, (Barcelona), 2009.

[175] P. R. Pagilla and Y. Zhu, "Controller and observer design for lipschitz nonlinear systems," in *Proc. of ACC*, (Boston, USA), pp. 2379–2384, June 30-July 2, 2004.

[176] K. Ogata, *Modern Control Engineering.* Prentice Hall, 2002.

[177] S. C. Bengea, X. Li, and R. A. DeCarlo, "Combined controller observer design for uncertain time delay systems with application to engine idle speed control," *J. Dyn. Sys. Meas. & Control*, vol. 126, pp. 772–780, 2004.

[178] Y. Wang, L. Xie, and C. E. de Souza, "Robsut control of a class of uncertain nonlinear systems," *Syst. Control Lett.*, vol. 19, pp. 139–149, 1992.

[179] M. Abid, S. X. Ding, and **A. Q. Khan**, "Dynamic threshold for fault detection in lipschitz nonlinear systems," in *Proc. of 7th IFAC SAFEPROCESS*, (Barcelona, Spain), pp. 36–40, June 30 - July 3, 2009.

About the Author

The author of this dissertation was born on February 18, 1979. He received his secondary education from Islamia College Peshawar in 1997 with distinguished grades. Then he joined Department of Electrical Engineering at N.W.F.P University of Engineering & Technology Peshawar in 1998 and graduated as B.Sc. Electrical Engineer in 2002 with honors. In 2002, he joined Department of Electrical Engineering for M.Sc. Systems Engineering under the fellowship grant awarded by Pakistan Institute of Engineering & Applied Sciences (PIEAS), Islamabad, Pakistan. He completed his Master degree in September 2004. The title of his Master thesis was, "Robust controller design for nonlinear systems", and was graded as excellent. After then, he joined the same department as a Assistant Engineer. In 2007, he was promoted to the post of Senior Engineer. In April 2007, he joined Institute of Automatic Control and Complex Systems, University of Duisburg-Essen Germany for pursuing PhD degree under the joint scholarship scheme from Higher Education Commission (HEC) of Pakistan and Deutscher Akademischer Austausch Dienst (DAAD) Germany. He defended his PhD thesis with excellent grads in December 2010. His research interest include fault diagnosis and process monitoring for technical systems, linear and nonlinear observer design, nonlinear control of dynamical systems.